ENVIRONMENTAL DESIGN AND OPTIMIZATION OF MODULAR HYDROPOWER PLANTS

A Dissertation Presented for the
Doctor of Philosophy
Degree
The University of Tennessee, Knoxville

Colin M. Sasthav
May 2022

Draft. Final version will be available on https://trace.tennessee.edu/ during Summer 2022.

ACKNOWLEDGEMENTS

Thank you to
Erika Baldwin
Gbadebo Oladosu
The SMH Team
Mohan, Jody, and Derek Sasthav
G.V. Loganathan and family

This dissertation is a testament to the love and support of many family and friends who have taught me the value of education and creative thinking.

ABSTRACT

This research aimed to understand the pathways to cost-effective and sustainable low-head hydropower. Designing viable hydropower projects requires optimization across many economic, environmental, and social outcomes. However, existing run-of-river hydropower design models often focus on economic performance and customizing technologies for high-head diversion schemes. Standard modular hydropower is a new design approach that uses standardized rather than custom-designed technologies to achieve economies of scale. Oak Ridge National Laboratory established a conceptual outline for module classes based on functions, such as generation modules and fish passage modules, but further research was needed to identify how modules should be selected and operated for a site. Therefore, a new hydropower design model, called the waterSHED model, was created to incorporate multi-objective optimization strategies and design considerations specific to standard modular hydropower. The waterSHED model uses an object-oriented approach, heuristic optimization techniques, and a system of inter-disciplinary models to assess project feasibility and design tradeoffs. The model quantifies the non-power benefits of fish passage, sediment passage, and recreation passage by integrating existing and novel modeling approaches into an operation simulation. Two case studies were conducted to validate the model and help answer research questions related to 1) the cost-benefit tradeoffs of non-power modules, 2) the economic drivers of modular designs, and 3) the value of fish-safe designs. These case studies highlighted the potential of several technologies, such as fish-safe turbines and sediment sluice gates, to improve the environmental performance of projects with minimal impacts on generation. However, cost reductions are needed to overcome the economic and regulatory challenges of low-head projects, particularly for foundation and generation technologies. The object-oriented approach facilitates rapid integration of the innovations that will emerge to meet these challenges. This research helped modernize hydropower design thinking and provided valuable tools to the industry that will enable communities to meet clean electricity goals and protect riverine ecosystems.

TABLE OF CONTENTS

LIST OF TABLES

LIST OF FIGURES

ACRONYMS

AEG – Annual energy generation
DOE – Department of Energy
EDES – Exemplary design envelope specification
FEMA – Federal Emergency Management Agency
FOA – Funding opportunity announcement
FS – Fish-safe turbine
GIS – Geographic Information System
GUI – Graphical user interface
ICC – Initial capital costs
LCOE – Levelized cost of energy
LIR – Low-head, instream, run-of-river
NOL -Normal operating headwater level
NPV – Net present value
NSD – New stream-reach development
O&M – Operation and maintenance
OOP – Object-oriented programming
ORNL – Oak Ridge National Laboratory
RHDP – Run-of-river hydropower design problem
ROR – Run-of-river
RR – Rock ramp
SMH – Standard Modular Hydropower
US – United States
USGS – United States Geological Survey
VS – Vertical-slot fishway
waterSHED – Water allocation tool enabling rapid small hydropower environmental design
WPTO – Water Power Technologies Office
WW – Whitewater park

CHAPTER ONE

INTRODUCTION

Background

Hydropower is a unique renewable energy resource in many ways. First, hydropower plants are highly integrated into the local riverine ecosystem, so plants often provide many social and environmental services in conjunction with electricity production. Second, due to this integration, hydropower plant designs vary widely as structures and technologies must often be custom designed for site-specific conditions, leading to long development timelines and a lack of scalability. Third, hydropower's operational characteristics are different from intermittent renewables, thus enabling baseload, distributed generation, and storage capabilities depending on the license constraints.

For these reasons, hydropower will play an essential role in the US transition to a 100% clean energy system by 2050 [1]. Hydropower is currently the backbone of all countries with high penetrations of clean electricity, like Norway and Canada [2]. The US supports approximately 80GW of hydropower capacity [3]. In 2019, this capacity produced about 6.7% of all US electricity and 38% of all US renewable electricity. Studies from Oak Ridge National Laboratory (ORNL) show that the US has the potential to more than double existing hydropower capacity with 84GW of technical potential from new stream-reach developments (NSD) and 12GW from non-powered dam (NPD) retrofits [4], [5].

Hydropower infrastructure will also play an important role in mitigating existing and future climate-related social and environmental changes. Storage dams will help communities adapt to more frequent severe weather patterns while providing water supply for drinking water and irrigation. Innovative fish passage technologies will help alleviate ecosystem fragmentation caused by existing dams. Sediment passage measures will remediate the current sediment deposition and transport imbalance that has altered riverine and coastal ecosystems [6]. Dams and recreational features will enable fishing and boating experiences that are a staple of many communities. Hybrid systems with the co-location of wind, solar, or storage can support the resilience of energy systems in black-start conditions. Increased deployment of distributed hydropower resources can facilitate energy access to under-represented and energy impoverished communities [7]. Advantages like these are termed **non-power benefits** and are defined as the monetary and non-monetary rewards of hydropower development that are not electricity generation revenues.

The academic conversation surrounding hydropower development in the US revolves around the three "R's": remove, rehabilitate, and retrofit [8]. These include the removal of obsolete dam infrastructure, the rehabilitation of worthwhile projects, and the retrofit of generation capabilities onto non-powered dams (NPDs). These options were identified by a consortium of industry, environmental, and regulatory stakeholders. Aging dam

infrastructure, the significant number of upcoming hydropower relicenses, the need for clean energy, and the environmental impacts of water infrastructure are all clear motivations to these stakeholders. However, the three R's underlying message is that new stream-reach development in the US is not a priority for the hydropower community, at least not in the current state of practice. New stream-reach development (NSD) is the construction of hydropower infrastructure at greenfield sites or sites that do not have existing civil structures like non-powered dams or irrigation canals. The current consensus on NSD in the US stems from several challenges that impact its costs and benefits.

First, NSD projects typically have higher unit costs than previous hydropower projects and other renewable resources. As illustrated in Figure 1, the majority (75%) of NSD potential stems from low-head sites, defined as having a hydraulic height difference (headwater elevation minus the tailwater elevation) of less than 30ft. Head represents the potential energy change across the facility, so higher head projects can extract more power per unit of water. Thus, lower head projects are less energy-dense resources and are typically more expensive per kilowatt. For example, hydropower cost models determine initial capital costs (ICC) as a function of plant capacity and plant head [9]. The estimated unit costs of NSD compared to other energy sources are described in Table 1 below.

Second, conventional hydropower plants are often custom-designed for each site, thus increasing development times and costs. Turbines, foundations, and structures have required careful site assessment, engineering design, and testing to ensure durability over the 30 or 50 license periods. However, dams typically are designed for much longer lives. These long license periods can be beneficial for the value proposition of the asset in comparison to other resources, but they can also detract from the ability to innovate. Long development timelines make NSD particularly difficult because the low-head nature requires the development of multiple sites to build the same capacity as higher-head projects. Long timelines can also lead to sunk costs spent in site assessment and engineering for unsuccessful projects. For example, a recent review of non-powered dam development showed that 36 NPD retrofits were successfully licensed between 2000 and 2020, while 120 proposed retrofits were not successful [10].

Third, high regulatory standards require new hydropower projects to mitigate many social and environmental impacts. These standards can have an outsized effect on the cost of small projects due to the fixed cost nature of environmental mitigation measures [11]. In practice, this has limited hydropower development to sites with negligible or previously incurred impacts, such as at non-powered dams [12]. The potential benefits of hydropower are also affected by operational requirements. For example, it is increasingly more common for projects to be operated in run-of-river (ROR) mode, meaning that plants have little to no storage (i.e., flows into the plant equal flows out of the plant in a short time scale) [13]. Run-of-river constraints help maintain natural flow regimes leading to improved habitat, water quality, and social outcomes [13]. However,

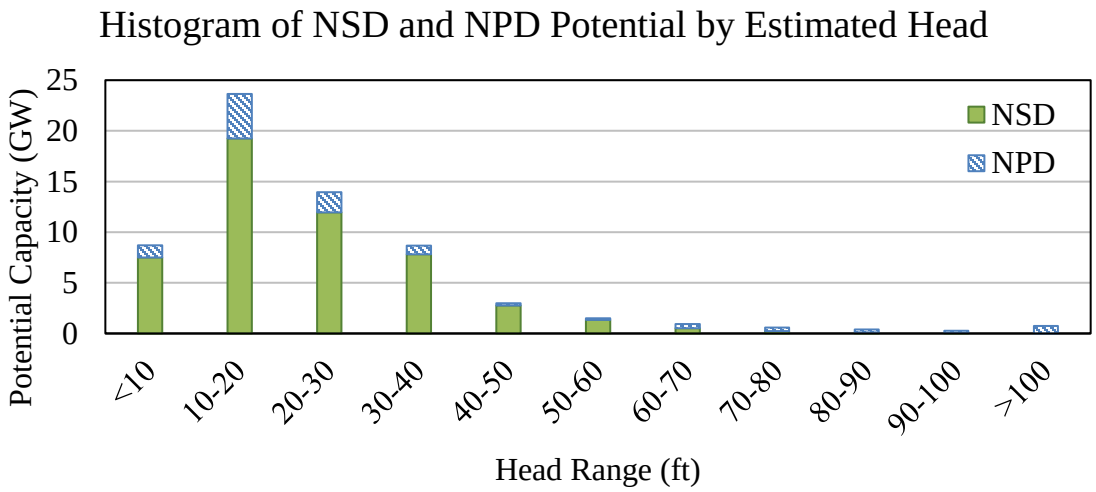

Figure 1. Histogram of new stream-reach development (NSD) potential by average head in the watershed and non-powered dam (NPD) cumulative potential for sites with >1MW of estimated capacity. Uses data from Kao et al. [5] and Hadjerioua et al. [4]. Published with author permission [14].

Table 1. Levelized cost of energy comparison for select generation technologies.

Technology	**Levelized Cost of Energy (2019$/MWh)**	**Source**
New-stream reach development hydropower	145	Baseline Cost Model [9][1]
Non-powered dam	126	Baseline Cost Model [9][1]
Utility-scale offshore wind	122.25	EIA [15][2]
Conventional hydropower with seasonal storage	52.79	EIA [15][2]
Utility-scale onshore wind	39.95	EIA [15][2]
Combined cycle natural gas plants	38.07	EIA [15][2]
Utility-scale solar PV	35.74	EIA [15][2]

[1] Converted from 2014$ to 2019$ using an inflation rate of 8%

[2] Unweighted LCOE, excluding tax credits, for new generation sources entering service in 2025 from the Energy Information Administration (EIA)

stakeholders often assume ROR operation reduces annual energy generation and decreases the value of hydropower by converting it from a storage resource to an intermittent renewable. Regardless, future hydropower development must design for environmental and social outcomes and understand how these design choices affect project costs and benefits.

The Standard Modular Hydropower Technology Acceleration Project at Oak Ridge National Laboratory (ORNL) was created to help the industry combat these challenges. The Standard Modular Hydropower (SMH) concept is a reflection of industry technology trends and has the following goals: "*(a) cost reduction through standardization and modularity, (b) ecological compatibility through eco-functional design, and (c) stakeholder acceptance*" [16]. Standardization of technologies allows them to be mass-produced and improves construction efficiencies, enabling economies of scale. Modularity describes the principle of functional decomposition, which separates system functions, like energy generation and fish passage, into separate modules so that facilities can be designed by selecting the module types that meet the project's needs. In the early conceptualization of SMH, these principles also applied to the modular form of the technologies, as illustrated in Figure 2 below, although modules can look very different in practice.

The US needs as many energy solutions as possible to meet climate goals and decarbonize the electricity system by 2050. Low-head hydropower can play a major role in expanding hydropower capacity and providing infrastructure capable of mitigating hydrologic changes and climate impacts on aquatic ecosystems. However, many stakeholders do not view low-head NSD and NPD projects as viable investments in the current state of technology. As innovative modular hydropower technologies and development techniques continue to enter the market, the value proposition of low-head hydropower will change, becoming more attractive as a climate solution. Stakeholders need the tools to understand how these innovations affect the costs and the power and non-power benefits of the project. Design optimization is a key component of understanding these interactions and quantifying the maximum potential of development. As hydropower technologies evolve, design thinking should also evolve to address the emergence of modular technologies and multi-objective performance requirements.

Objectives

The purpose of this research effort was to identify and quantify the design tradeoffs between economic, environmental, and social outcomes at low-head, modular hydropower facilities. Non-power benefits, like fish passage and recreation, will be key drivers for new development, so it is important to have the methods and metrics for stakeholders to evaluate the monetary and non-monetary costs and benefits. Innovative modular technologies are changing how developers think about hydropower design, so new strategies are also needed to integrate modularity into the design process. Standardized technologies aim to reduce change the costs through economies of

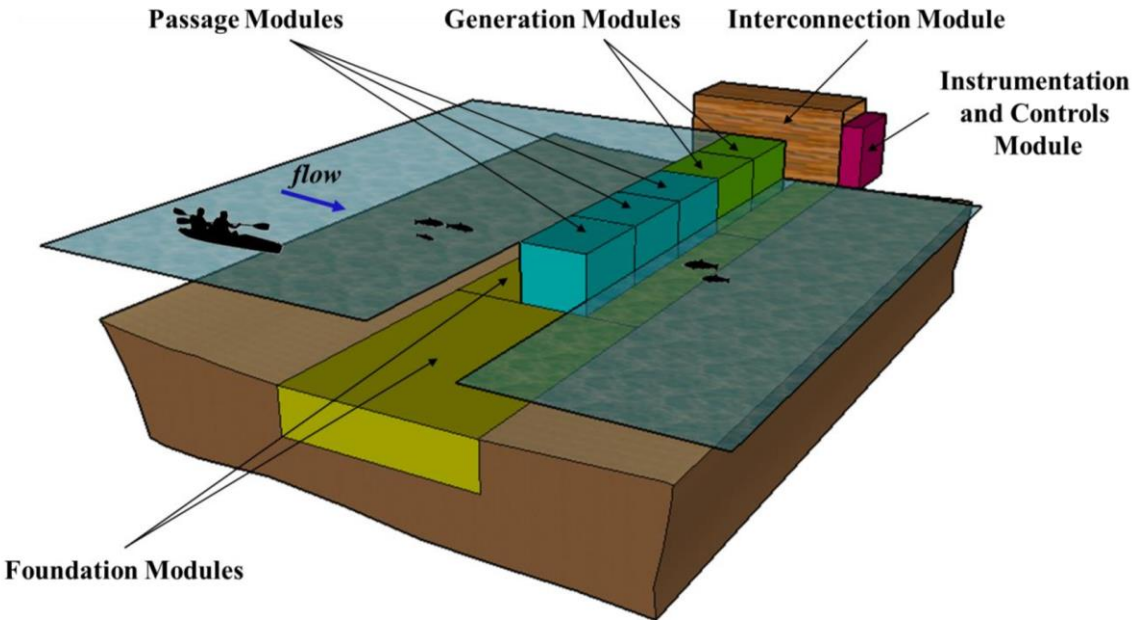

Figure 2. Conceptual schematic of a Standard Modular Hydropower facility with modules represented as "black boxes." Reprinted from Witt, Smith, et al. [16]

scale on a plant and multi-plant level, so new cost estimate methods are needed to incorporate new technologies and the effects of standardization into feasibility assessments.

A new hydropower design model, called the waterSHED model, was created to help accomplish these goals. The name waterSHED stands for the *water allocation tool enabling rapid small hydropower environmental design*. The tool is based on previous ORNL research documented in the SMH Case Study Report [17]. The waterSHED model uses a graphical user interface (GUI) to virtually represent a modular hydropower facility, simulate the facility's operation, and optimize the facility's design across multiple objectives. The waterSHED model specializes in technology selection (which modules should be included in the facility) and flow allocation (how the modules should be operated). The desired research insights were generated by applying the tool to case study sites and using sensitivity analysis to evaluate tradeoffs between performance metrics. Two case studies were selected in accordance with the industry stakeholders and the goals of the SMH team. These cases helped answer the following research questions:

Case Study A – Reference Sites

- Cost reduction scenarios – what are the technology areas and site conditions that are most critical for project cost and economic performance?
- Headwater level tradeoffs – what are the cost, generation, and sedimentation tradeoffs related to the selection of headwater elevation?
- Sediment sluicing analysis – what are the relationships between operation parameters and the sediment passage performance metrics?

Case Study B – Bosher Dam

- Value of fish-safe turbines – what are the cost, generation, and downstream fish passage tradeoffs for fish-safe turbine designs compared to conventional fish exclusion designs?
- Value of nature-like rock ramps – what are the cost, generation, and upstream fish passage tradeoffs for nature-like rock ramp designs compared to technical fishway designs?
- Value of recreation modules – what are the cost, generation, and recreation availability tradeoffs for recreation passage modules?

Scope

The scope of this research was informed by the Standard Modular Hydropower project's goals and related sponsors, the research gaps illustrated in the literature review, and the available data and modeling capabilities. The SMH concept was primarily meant for new stream-reach development (NSD), but it can also apply to NPD retrofits, as exemplified by Case Study B. As described earlier in the introduction, most NSD potential is located at low-head sites, defined as having a hydraulic head of less than 30ft. These sites are also classified as small hydropower sites with nominal capacities of less than 30MW. However, these numeric limits of less than 30ft and 30MW are not strict limits for applying this research. As described in the literature review in Chapter Two, a common

trend for new hydropower developments is to require run-of-river (ROR) operating constraints, which limit the amount of allowed storage and prohibit peaking power releases. Additionally, Chapter Two highlights that existing literature on ROR hydropower design tends to assume the use of diversion schemes that route water through long penstocks to obtain higher heads. These schemes are less cost-effective at low-head sites, so it is important to consider instream schemes with no diversions or relatively short diversions of water from the primary channel. Instream schemes also exclude trans-basin schemes where water is routed between channels. Taken together, the type of site studied in this research is classified as low-head, instream, run-of-river (LIR) hydropower.

Although hydropower is a well-established industry, the development of LIR hydropower is still relatively novel. Companies and developers targeting these sites are typically in prototyping or pilot scale deployment stages (technology readiness levels 6-9) [18]. An important part of increasing deployment is finding sites that are cost-effective and suitable for given technologies. Feasibility and pre-feasibility studies determine whether a given site has enough potential to warrant further site investigation. This step occurs after site selection and before any in-person site reconnaissance. Hydropower design models provide tools to help quantify the potential at the pre-feasibility stage. Since this stage happens before site investigations, design models are limited to desktop-level data, meaning all required inputs should be publicly available online or based on user preferences and assumptions. This scope constrained the model to high-level insights about site design but enabled faster implementation and broader application. Additionally, as described in Chapter Three, the waterSHED model optimizes designs by simulating the operation of different facility designs. To limit runtimes, the models involved in simulating operation must be relatively efficient and flexible for simulating various technologies. The waterSHED model was limited to simple one-dimensional hydraulics models, but improved models could be added in future versions. Finally, component-level cost information for modular technologies and facilities is rarely publicly available. However, empirical estimations for conventional designs and construction practices are well documented [9], [17]. In addition to empirical models, this project leveraged high-level cost estimates and reference designs provided by industry stakeholders.

Significance

As two criteria for a successful dissertation, this research must illustrate intellectual merit and a broader impact. Intellectual merit describes the originality and academic rigor of the research. This criterion ensures that the research extends the frontier of scientific knowledge and that the candidate can lead research projects. The broader impact describes the value of the research to academic, industry, and regulatory stakeholders. Broader impact ensures that the research informs real-world decision-making and achieves the sponsor's goals. The following sections clearly describe how the research presented meets these two criteria.

Intellectual Merit

Hydropower research is inherently inter-disciplinary because of the interaction between hydrologic, hydraulic, biological, social, structural, and economic components. Developing a multi-objective hydropower design model showcased the ability to conduct inter-disciplinary research, which is a tenet of the Energy Science and Engineering Ph.D. program in the Bredesen Center for Inter-disciplinary Research and Graduate Education. For example, the waterSHED model includes techno-economic analysis, flood frequency analysis, sediment transport equations, a novel fish passage performance model, and turbine engineering. The waterSHED tool also highlights the technical coding and optimization skills required to create an object-oriented framework for modular design, a graphical user interface, turbine dispatch algorithms, and a custom genetic algorithm for multi-objective optimization.

Regarding the extension of the academic knowledge base, the literature review in Chapter Two compares the capabilities of existing hydropower design models to the capabilities presented in the waterSHED model. First, existing models use conventional hydropower design assumptions for high-head diversion schemes. These models are outdated, so the waterSHED model provides an updated scope given the need for LIR hydropower designs. Second, almost all existing models focus on singular economic objectives rather than the multi-objective environmental and social outcomes that must be addressed for NSD projects. The case studies quantify the tradeoffs between power and non-power benefits, a much-needed research gap [18]. Finally, this research extends the conceptual framework of SMH, as described in the Exemplary Design Envelope Specification [19], to an applied design process using an object-oriented approach to capture the inputs, outputs, and process outlined in the framework. The waterSHED model and related research will be an important outcome of the SMH Technology Acceleration project. This work will provide a platform for future education and coordination of modular design practices.

Broader Impact

The SMH Technology Acceleration project is sponsored by the Department of Energy's (DOE's) Water Power Technologies Office (WPTO). The SMH project and this research effort are meant to support the current trends toward modularity and standardization in the industry. The target stakeholders for the waterSHED model and related research are hydropower developers, technology developers, and energy researchers. The waterSHED model will be made available to the public so these stakeholders can learn about modular design practices, utilize helpful tools for pre-feasibility assessments, and quickly identify high-potential projects. Furthermore, research into the primary cost components will help investors identify the target areas for innovation and help regulators validate the value of policy initiatives. As one example, regulators typically require fish exclusion measures for turbine installations, but fish-safe turbine technologies may limit the need for these measures. Removing the standards for fish exclusion presents a risk to fish populations if the turbines do not perform as intended and cost savings for developers. To help evaluate this decision, Case Study B examined the costs of fish exclusion, including capital costs

and changes in operation that lead to reduced generation. The application of the research can also expand outside of the US to developing economies that are interested in utilizing their low-head hydropower potential [20], [21]. Overall, this research produced a flexible and user-friendly tool that can support a host of academic and commercial interests, improving decision-making across the small hydropower development industry.

CHAPTER TWO

ENVIRONMENTAL DESIGN OF LOW-HEAD RUN-OF-RIVER HYDROPOWER IN THE UNITED STATES: A REVIEW OF FACILITY DESIGN MODELS

A version of this chapter was published as a peer-reviewed journal article in *Renewable and Sustainable Energy Reviews* [14]. Colin Sasthav was the primary author in charge of conceptualization, methods, literature review, analysis, and manuscript writing. Dr. Gbadebo Oladosu supported conceptualization and provided written comments and edits throughout the writing process. The original version was modified to fit the dissertation formatting requirements and integrate with the introductory material in Chapter One. Figure 1 was relocated to Chapter One.

Abstract

The goal of run-of-river hydropower is to produce cost-competitive renewable electricity with minimal disruption of the natural riverine ecosystem. Modeling and feasibility analysis of alternative design options are crucial for developing new run-of-river hydropower projects. Our review shows that existing run-of-river hydropower design models focus on maximizing economic potential at high-head diversion schemes with limited consideration of environmental outcomes. Since nearly three-quarters of new hydropower potential in the United States is found at low-head sites and environmental performance standards are imperative to project success, new models are needed to address the multi-dimensional design challenges at these sites. To aid in formulating holistic models, we synthesize the performance objectives and design variables related to early-stage run-of-river facility design. The objectives span six potential impact areas, including hydrologic alteration, sediment continuity, water quality, aquatic species passage, social, and economic. Based on these reviews, we identify three key areas to enhance the capabilities of run-of-river hydropower design models. These are 1) expanded model formulations, 2) assessment of barrier effects, and 3) explicit environmental objectives. The resulting modeling improvements would accelerate the identification of run-of-river hydropower designs that minimize environmental impacts, promote economic competitiveness, and incorporate the value of non-power benefits.

1. Introduction

The state of hydropower development in the United States (US) today has changed drastically from the era of rapid construction of dams in the mid-20th century and will continue to evolve in the face of grid modernization and decarbonization. Over the last two centuries, the US built over 91,000 dams and supporting structures, which provide multiple purposes, including hydropower, navigation, flood control, water supply, and irrigation [10]. These dams support approximately 2,200 hydropower facilities with a total generation capacity of about 81GW [1]. Many of these facilities have large dams and reservoirs that enable the production of low-cost, reliable power. Until the recent acceleration in wind and solar power development, hydropower was the largest renewable energy resource in the US [22], and pumped storage hydropower remains the largest commercial electricity storage resource in the US [23].

Despite the large amount of already developed resources, the potential for new hydropower in the US is substantial. New stream-reach developments (NSD), hydropower at sites without existing infrastructure, are estimated to have about 84.7GW

of potential [5]. In addition, the potential from retrofitting the remaining 80,000+ non-powered dams (NPDs) to generate hydropower has been estimated at 12GW [4]. Figure 3 compares the NSD and NPD potentials (in blue) to existing hydropower assets (EHA in green) capacity for each basin in the contiguous US. Except for the Great Lakes (Basin 4) and the Tennessee (Basin 6) basins, all basins have an estimated unbuilt capacity of at least 25% of the total potential. However, new hydropower development has slowed considerably in recent decades. Instead, the hydropower industry has focused on upgrading and maintaining current facilities, with about 75% of new capacity (2010-2019) coming from capacity additions at existing projects [23]. Expansion of hydropower through the retrofit of NPDs and canals/conduits contributed 445MW of capacity from 35 NPD projects and 88.6MW from 78 conduit facilities between 2010-2019 [23]. In contrast, only six NSD hydropower projects contributing a total of 27.7MW have been completed in the same period [23].

The slow growth of US new stream reach development in recent decades reflects several challenges. For one, the environmental impacts of damming rivers, such as adverse water quality changes and blocked fish migration routes resulting in large declines in migratory fish populations, have become a major public concern [24]. These impacts led to stricter environmental regulations concerning endangered species, properties with historical or cultural importance, and equal consideration of power and non-power benefits [25]. While increases in hydropower environmental performance have accompanied more stringent environmental regulations, they have also led to increased time and costs associated with hydropower licensing and construction [12]. Thus, original hydropower licenses have largely been limited to projects in already impacted areas (e.g., NPDs, canals, and conduits) or at sites with low environmental complexity where endangered species or migratory fish are less prevalent [12]. Concurrently, the removal of small dams in the U.S has surged in the last several decades, with almost 1,200 total removals [26]. A recent stakeholder group brought together by the Stanford Woods Institute for the Environment drafted a joint statement highlighting the three “R’s” – retrofit, rehabilitate, and remove, as three key strategies for addressing the role of dams in US climate resilience [8]. These options are complex, and outcomes depend heavily on site-specific conditions, so stakeholders carefully assess the risks and tradeoffs to inform decision-making [27], [28]. The same care must be applied to new hydropower development.

Future NSD and NPD hydropower expansion in the US requires comprehensive methods to assess project costs and benefits. Hydropower design models are used to determine the high-level design variables (e.g., capacity and spillway size) that will optimize predicted project outcomes. These models are tasked with selecting the design variables, quantifying stakeholder objectives, and modeling the relationships among these variables. Given the evolving nature of US hydropower development and the expansion of small hydropower globally [29], design models must also evolve to capture the outcomes relevant to modern stakeholders. Without the proper representation of economic, social, and environmental outcomes, stakeholders may over- or under-value the construction of

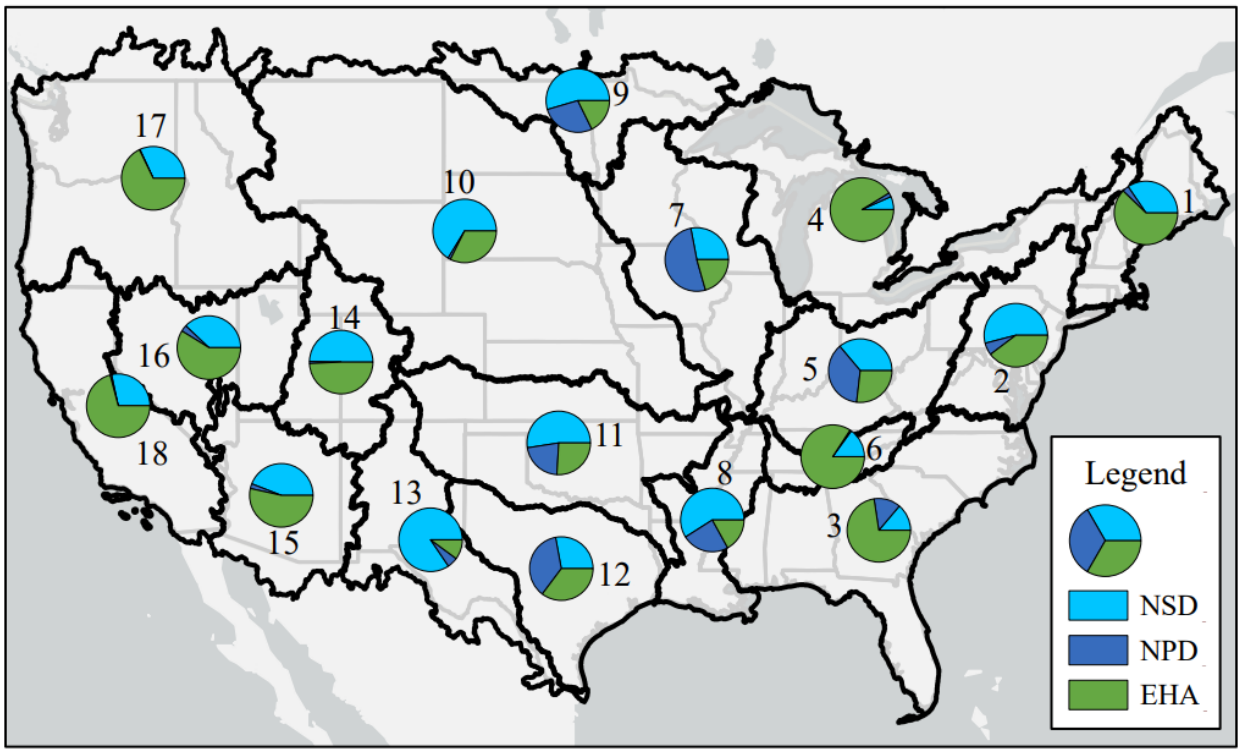

Figure 3. Map of US hydropower capacity and potential by basin. Numbers indicate the hydrologic unit code for the basin. The existing hydropower assets (EHA - green) represent the built capacity in the basin, while new stream-reach development (NSD – light blue) and non-powered dam development (NPD – dark blue) represent estimated potential for plants >1MW. Uses data from Kao et al. [5], Hadjerioua et al. [4], and Johnson et al. [30].

new hydropower infrastructure, limiting the potential contribution of hydropower to meeting future energy challenges.

The purpose of this paper is to review existing run-of-river hydropower design models (RHDMs) and identify how gaps in these models may be addressed to enable better economic, environmental, and social outcomes of future hydropower decision-making in the US**.** To accomplish this objective, Section 2 describes the commonalities across potential NSD sites and the relevant design trends. Section 3 reviews the performance objectives, design variables, and models used in existing run-of-river hydropower design studies to illustrate the scope of current design thinking. Section 4 then synthesizes these reviews to identify potential enhancements in hydropower design models. The paper ends with conclusions.

2. Toward Low-head, Instream, Run-of-river (LIR) Hydropower

Future hydropower infrastructure designs will likely look different from existing facilities. Many existing hydropower plants in the US are characterized as medium-to-high head projects, meaning the nominal height difference between the upper reservoir and lower tailwater is greater than 30ft (9.1m). Power output is a function of head and flow (see Section 3 for a full equation), so higher head projects can produce more power per unit of water. Higher heads and larger capacities lead to lower costs per kilowatt, so large projects benefit greatly from economies of scale [9]. In contrast, 74% of potential NPD and NSD capacity have expected head levels below 30ft (9.1m), as shown in Figure 1[1]. Not only are these low-head projects challenged by economics of scale at each site, but also multiple projects are needed to build a given total capacity. Public, private, and academic research efforts aim to decrease the costs of small hydropower through innovations, such as modularity (e.g., the Standard Modular Hydropower [19] and "Hydropower-by-Design" frameworks [31]) and new low-head designs [32]. Modular designs, for example, may use an "off-the-shelf" approach to reduce costs rather than the conventional custom-design approach that has been used for existing large hydropower plants.

The need to minimize each site's environmental and social impacts and their cumulative impacts across the fleet will be a major driver of new hydropower facility designs. Hydropower plants, even small run-of-river plants, can significantly impact the upstream, downstream, and local ecology by changing natural flow conditions and creating a physical barrier. Kuriqi et al. [33] reviewed 146 studies on the ecological impacts of hydropower plants globally across several domains, including biota, hydrologic alteration, water quality, and geomorphology. The most common impacts identified are habitat and water quality degradation, reductions in connectivity and downstream water quantity, and a loss of diversity [33]. Structural mitigation measures, such as fish passageways and aerating turbines, and non-structural measures, like minimum flow

[1] Figure 1 located in Chapter One

requirements, can have significant impacts on a projects' economic and environmental performance.

An increasingly common licensing requirement to minimize environmental impacts in the US is to operate hydropower facilities in run-of-river (ROR) mode [13]. ROR mode means plants have little to no active storage (the allowable change in reservoir volume). Run-of-river constraints are incorporated into licenses for many reasons, including improving aquatic habitat, meeting state water quality requirements, and improving aesthetics or other social outcomes [13]. Since ROR projects have limited active storage and dispatchability, they are assumed to provide less generation revenue than peaking plants. However, a study of plants that switched from peaking to ROR operation showed that these assumptions are not true in all cases and that the costs and benefits of ROR operation are project-specific [13].

There seems to be ambiguity around the definitions and implications of "run-of-river" in the hydropower literature. The Federal Energy Regulatory Commission's definition includes "limited storage capacity" and "water is released at roughly the same flow rate as the natural flow of the river" [34]. In contrast, other definitions specify the limit in headpond level variation. Annandale, Morris, and Karki [35] state that, in some cases, ROR projects may store water during off-peak hours and generate at full power during peak demand for about six hours. However, the amount of allowable storage is rarely defined. Also, the term run-of-river hydropower is often conflated with high-head diversion schemes, which may have long penstocks that dewater long stream reaches. For design modeling, the term "run-of-river" means that, for a specified timestep, the average inflow entering a facility equals the average outflow exiting the facility. The length of that timestep, herein called the ROR timescale, is determined by the available site data and the environmental requirements considered in the model. In practice, the ROR timescale is constrained by the ability of the facility to monitor and regulate headwater levels in real-time.

Another strategy for reducing the environmental impacts of new hydropower is through instream (or dam-toe) designs rather than diversion schemes [33]. Both schemes require a dam that creates a headpond to provide consistent depth for the turbine intakes. However, instream designs generate power at the dam rather than at a powerhouse downstream. The key differences between instream and diversion schemes are illustrated in Figure 4. Instream schemes limit changes in the flow regime and dewatering of the downstream reach, which can have significant social [36], geomorphic[37], and ecological implications [38]. Given the trend towards ROR licensing requirements, hydropower capacity expansion in the US, particularly at NSD sites, would likely be increasingly based on low-head, instream, run-of-river (LIR) hydropower designs. By minimizing the storage and diversion of water, LIR schemes limit flow regime change, which is a major driver of environmental impacts. By limiting the construction footprint, instream schemes may reduce land and conveyance costs and enable modular construction practices. While multiple low-head facilities may be difficult to license and develop (compared to single

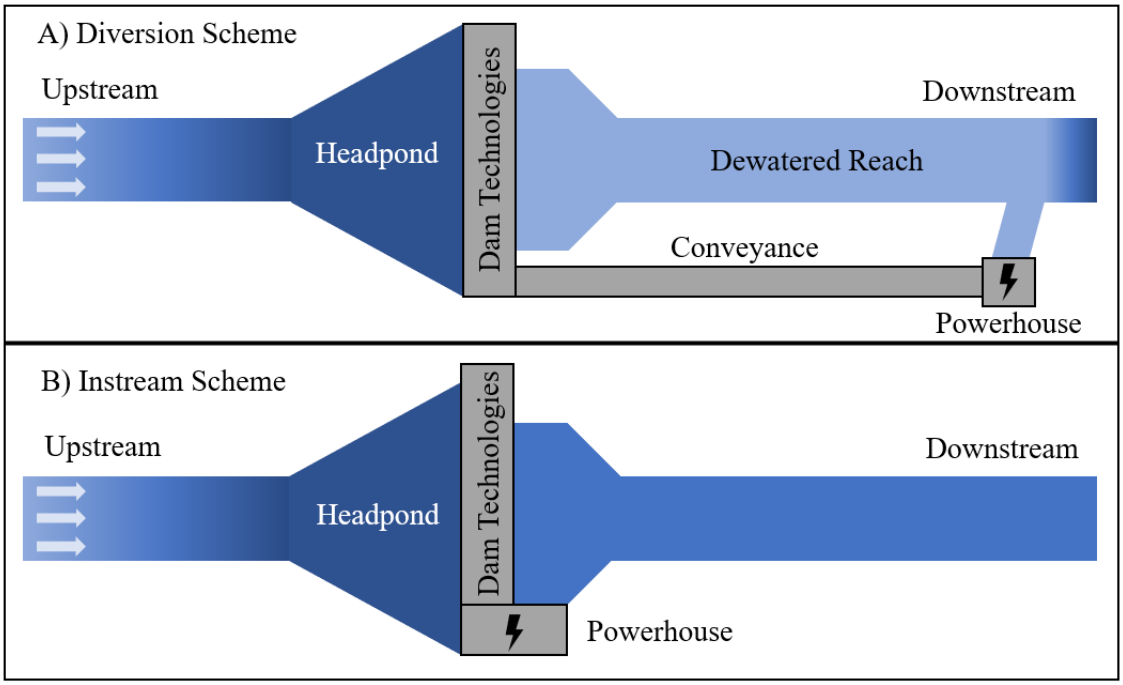

Figure 4. Comparison of run-of-river design schemes. A) a diversion scheme suited to high-head sites. B) instream scheme suited to low-head sites.

high-head facilities), the distribution of the hydropower potential (Figure 1), the need for distributed hydropower [7], modular design approaches [19], and the emergence of connected hydropower networks [39] incentivize the investment in LIR projects. Instream schemes may also be more cost-effective than diversions at low-head sites since low-head sites are typically characterized by small stream slopes [40]. Penstocks or other conveyances are used in diversion schemes to increase the head across the turbine by taking advantage of high terrain slopes. Adding length to a penstock is advantageous when the benefits of the head increase outweigh the costs of additional conveyance. Since low-head sites tend to have smaller terrain slopes [40], the head gain per length of conveyance is likely smaller and thus less cost-effective to build long diversions.

However, expected hydropower outcomes are highly site-specific, determined by the river conditions and the selected technologies. The quantity and timing of flows, the prevalence of migratory fish species, the stream geometry, and stage-discharge relationships are some of the important site considerations. These conditions drive the costs of civil works (e.g., foundations, dams, cofferdams, etc.), the costs of mitigation measures, and the potential hydropower capacity. Existing studies identify feasible hydropower sites via classification and other analysis techniques. For example, Bevelhimer, DeRolph, and Witt [41] classified stream reaches to help identify the need for mitigation measures. Additionally, a study found that generation from plants in pluvial stable flow regimes was less sensitive to environmental flows than in pluvial-nival regimes [42]. Although these classification efforts are useful for initial site assessments, they are insufficient for project design and technology decisions, which require more detailed site-specific data and analysis.

3. Review of Run-of-river Hydropower Design Studies

Due to the site-specific nature of hydropower, run-of-river hydropower design models (RHDMs) are used early in the development process to determine high-level design features and predict whether a project is worth exploring further. These models enable plant design optimization by quantifying the relationships between the design variables and objectives. As illustrated in Figure 5 below, RHDMs are tasked with 1) selecting a set of relevant design variables, 2) identifying and quantifying the stakeholder's objective(s), and 3) applying models to define the relationships between design variables and objectives. The design parameters, site inputs, and assumptions in the RHDM depend on the study's goals.

RHDMs can be considered a reflection of stakeholders' design thinking and interests at the time of publication. As the focus of new hydropower innovation and development moves towards LIR hydropower, RHDMs must be updated to account for the differences in design assumptions and objective priorities. LIR projects are typically smaller and have higher costs per kilowatt than high head projects, so greater resolution and accuracy are needed to estimate profitability. For example, fixed-cost mitigation measures will have much larger impacts on project costs for a 1MW project than a 30MW project.

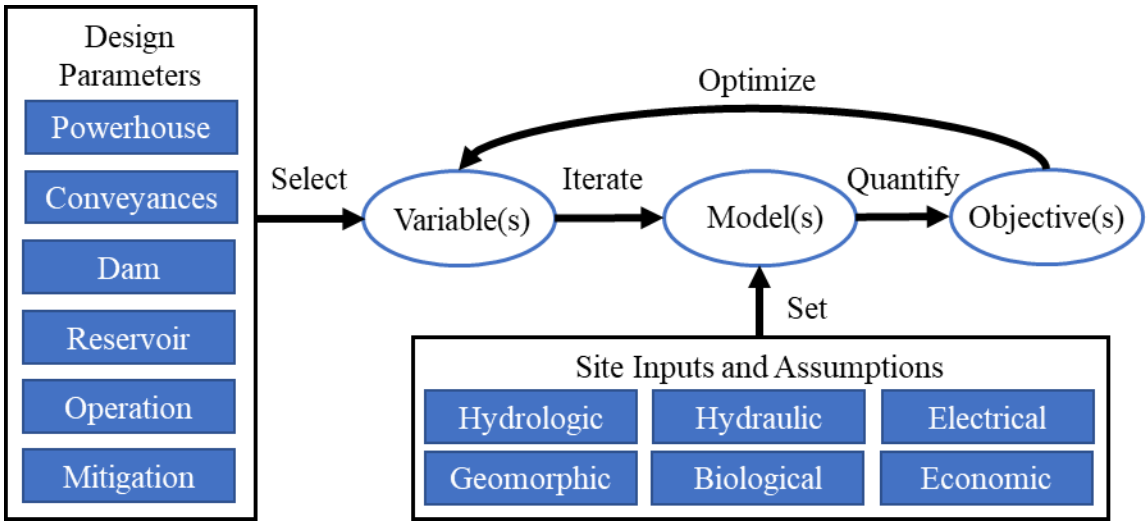

Figure 5. High-level hydropower design model schematic.

Project success also requires designs that meet the often-conflicting objectives of multiple stakeholders (developers, regulators, local communities, etc.). To support future hydropower decision-making, new RHDMs must quantify and assess the relationships among design variables and objectives to support the economic and environmental sustainability of modern LIR hydropower.

3.1 Materials and Methods

This review consisted of two main efforts, including 1) a review of the emerging economic, social, and environmental objectives important to hydropower developers, and 2) a review and analysis of existing RHDMs studies (articles presenting RHDMs). The following sections present the results of this review according to the design objectives, variables, and model formulations as described conceptually in Figure 5. These reviews represent the modeling needs of stakeholders and the current capabilities of RHDMs. Areas for improvement and future research in RHDMs were determined by comparing these capabilities to the desired stakeholder objectives.

Regarding the review of hydropower objectives, several systematic literature reviews already exist for hydropower-related performance metrics. Rather than conduct an overlapping systematic literature review or meta-analysis, this review compiled existing reviews from relevant fields, categorized impacts based on those suggested in these reviews, and used snowballing to identify additional articles relevant to this scope. The primary review articles included Parish et al. [43], who created a comprehensive database of hydropower-related environmental metrics, Pracheil et al. [44], who created a checklist of river function indicators, Anderson et al. [45], who synthesized the literature on the impacts of ROR hydropower, and Trussart et al. [46] who cataloged effective mitigation measures for hydropower. In addition, reviews of the social externalities [47], economic value [48], and water quality impacts of hydropower [49] were also helpful in identifying objective categories. The resulting objective categories that apply to LIR hydropower are described in Section 3.

The scope of RHDMs was an important factor in selecting the article collection methods for this study. The variables, objectives, and specifications used in RHDMs depend considerably on the modeler's available information, which is often limited. Since RHDMs are often used to determine the feasibility of a project before investing in site exploration, they are often based on "desktop-level" information publicly available online, such as maps or gauged flow data. Additionally, RHDMs can be used to evaluate the potential of a site, but they are typically not built for site selection purposes. As such, the objectives of interest to this review are those driven by design decisions rather than objectives related primarily to site selection or construction practices. For example, some impacts on terrestrial habitat are driven by the construction of roads and site clearing that depend on the site's location rather than the design of the dam or powerhouse. Finally, this review is limited to the modeling considerations related to LIR hydropower. These models assume ROR operating constraints, which precludes an expansive branch of dispatch optimization literature that pertains mainly to large storage hydropower.

Given this limited scope, the expected number of studies presenting RHDMs was low, so a simple literature search and snowballing (i.e., searching each source's references) approach was used to identify RHDM studies. The review was conducted using Google Scholar. The terms "low head dam," "run of river hydropower," "low head hydropower," and "small hydropower" were used in combination with the following terms "design optimization," "design model," "optimal design," and "capacity sizing." Articles with only an abstract and no available text were excluded, such as older papers (published before 1990) or those behind paywalls. Additionally, only peer-reviewed scientific articles and conference proceedings written in English were collected, thus neglecting articles in other languages and other formats, such as technical reports or licensing documents. Twenty-three RHDM studies published between 1992-2020 were identified using this method. Section 3.4 details the RHDMs according to the relevant objectives, variables, and model formulations.

3.2 Review of ROR hydropower performance objectives

Performance objectives are quantifiable representations of the environmental, economic, and social outcomes important to project stakeholders. Selecting metrics to represent these objectives can be challenging because non-power benefits, like fish passage, are often difficult to model with available information and are difficult to quantify with concise metrics. However, improved representation of these objectives early in the design process may lead to more optimal designs. The results of the hydropower objective review are captured in the metrics and qualitative objectives described in Table 2. Based on existing systematic reviews and filtered to the LIR scope, the broad objective categories are social, economic, hydrologic alteration, sediment continuity, aquatic species passage, and water quality.

This review highlights two underlying objectives 1) to maintain the "natural" or desired river functions and 2) to maximize the net benefit of development. Following Anderson et al. [45], the environmental impacts can be categorized into barrier effects (interruptions to ecosystem functions through the physical blockage at the dam) and effects from hydrologic alteration (the change of flow patterns within a stream-reach). Regarding barrier effects, the objective for a facility is to be "transparent" [50]. Aquatic species must be able to successively traverse upstream and downstream across the facility with minimal fitness costs or time delays [50]. Similarly, sediment continuity means no considerable change from natural conditions in the quantity, quality, or timing of sediment flows [51]. Continuity requires considerations for reservoir sedimentation, passage modes through the facility, and downstream geomorphic changes. Regarding hydrologic alteration, the natural flow regime paradigm asserts that the ecological functions of a water system are driven by the change in magnitude, frequency, duration, timing, and rate of change of the water flow [38]. Hydropower plants can change these flow patterns through the storage and diversion of water, leading to numerous environmental and social impacts such as reductions in fish populations [52], water quality impairments [53], [54], and conflicts around agricultural water availability [55].

Table 2. Examples of run-of-river hydropower impacts and performance metrics

Objective	Potential performance metrics
Economic: Create a beneficial and competitive value proposition by	
Maximizing the expected net benefit of the project.	Levelized cost of energy [56]; Internal rate of return [57]; Net present value [58]; Benefit-cost ratio; Operation and maintenance costs
Minimizing the risks and costs of dam/component failure.	Design flood; Cost of failure [59]; Dam failure probability [59]; Project life
Minimizing the initial cost, risk, and time requirements for construction	Initial cost of capital; Probability of project failure; Lead time
Maximizing the value of generation to the grid.	Capacity; Ancillary service value [60]; Capacity factor [61]; Annual generation [62]
Hydrologic Alteration: Maintain natural flow conditions by	
Minimizing the difference between pre- and post-development flow characteristics.	Indicators of Hydrologic Alteration [63]; Downstream diversion index [64]; ROR timescale [65]; Degree of regulation [66]; River regulation index [67]; Minimum/Environmental flows [36], [55]
Minimizing the spatial extent of hydrologic alteration.	Length of the dewatered reach; Length of the reservoir; River connectivity index [67]
Sediment Continuity: Maintain sediment continuity by	
Minimizing reservoir sedimentation.	Volume of accumulated sediment; Changes in grain size distribution; Capacity-Inflow ratio [68]; Trap efficiency [68]; Sedimentation index [68];
Maximizing sediment passage across the facility.	Sediment flux; Flushing efficiency [51]; Flushing frequency [51]; Flushing time [69]; Sediment reduction index [70];
Minimizing downstream geomorphic changes.	Sediment surplus/deficit [71]; Shields number [71]; Magnitude of flood reduction [71]; Sediment transport capacity [72]; Change in channel form [73]; Ratio of critical flow frequency [74]
Aquatic Species: Enable "transparent" passage of aquatic species by	
Maximizing upstream passage success rates and minimizing fitness losses and delays.	Fish attraction efficiency [75]; Fish entrance efficiency [75]; Fish passage efficiency [76]; Fallback rate [77]; Average delay [50]
Maximizing downstream passage success and minimizing mortality rates.	Fish mortality rate [78], [79]; Rate of refusal [80]; Fish guidance/collection efficiency [80], [81]
Water Quality: Create safe water quality conditions by	
Minimizing negative limnological effects on water quality and resident species.	Reservoir volume; Reservoir area; Densimetric Froude number [82]; Weighted usable area [83]
Maximizing water quality improvements.	Aeration efficiency [84], [85]; Rate of pollution removal/treatment
Social: Promote community acceptance by	
Maximizing the value and availability of recreational features.	Value of recreation [25]; Recreation availability; Rafting hydro-suitability index [86]

Water quality is closely tied to sediment continuity and hydrologic alteration, but this review identified safe water quality conditions as a separate goal to better highlight the potential of water quality improvement measures, like aerating turbines and weirs [84], [85]. Additionally, water quality impacts from stratification are not expected for small hydropower reservoirs, although further research is needed to identify the conditions where stratification will occur [49].

Hydropower facilities must be profitable, economically competitive with other electricity sources, and socially acceptable. Economic indices of performance, like net present value (NPV) and levelized cost of energy, are well understood in existing design models. However, decision-making requires a complete understanding of the power and non-power cost-benefit tradeoffs. The value of hydropower to the grid has multiple components, including energy generation, capacity, and ancillary services [48]. Non-power benefits, such as recreation features or water quality improvements, can provide monetary value (e.g., park entry fees) and non-monetary value (e.g., increased social acceptance). The costs to provide these services come in many forms, including capital costs, operating costs, the risk of dam failure, the time required for construction/licensing, and any environmental or social consequences. Valuation methods exist to monetize certain non-power benefits, such as the travel cost and stated preference method, although they typically require surveys of local stakeholders [25]. It is difficult to represent economic potential with a single metric, even for economic-focused models. For example, RHDMs often ignore start-stop costs, which are the indirect costs of increased maintenance due to additional turbine start-ups that can cause abrasion [87]. Future design models should systematically quantify and optimize multiple objectives, similar to the cost-benefit and decision analysis valuation framework developed by several US national laboratories for pumped storage hydropower [88].

The selection of performance metrics is a critical part of design models. Metrics must represent all outcomes and tradeoffs of interest and must be measurable given the available information and modeling tools. Creating metrics can be challenging when defining the “natural” state of the river, especially in streams that are already regulated and experience anthropogenic disturbances. For existing hydropower facilities, environmental performance can be viewed through river functions, which are outcomes produced by the design and operation of the facility [43], [44]. However, design models have limited ability to predict these complex physical or biological processes reliably. Alternatives to using predicted outcomes as performance metrics are technical specifications and intermediate variables. For example, it is common practice to use turbine specifications (e.g., capacity and efficiency) to predict future power production. However, the same cannot be said for environmental technology specifications. Fish passageways, for instance, have been studied to assess their fish attraction, entrance, and passage efficiencies [75]. Still, models are needed to apply these metrics to facility-wide performance over time, where the operation may impact passage performance. Intermediate variables can be modeled using design variables that have known qualitative relationships with the objectives of interest. For example, Trussart et al. [46] suggest

minimizing the impoundment area (an intermediate variable dependent on the dam height and normal operating level) to reduce technical, economic, and environmental concerns. These strategies can facilitate the integration of non-power benefits into future design models.

3.3 Review of ROR hydropower design variables

Design variables represent the alternatives available to stakeholders to meet their goals. The primary ROR design decisions are site selection, technology selection, and flow allocation. Although site selection is an important driver of hydropower potential [6], foundation costs [18], and fish connectivity impacts [19], it is typically outside the scope of RHDMs and acts as an input. Technology selection is the combination and design of components such as turbines, water conveyance structures, gates, spillways, and fishways. Flow allocation pertains to how the flow resource is distributed across those technologies over time. Technology selection and flow allocation decisions are typically determined simultaneously in design optimization models since technology performance depends on the operation and vice versa.

Table 3 documents a variety of potential design variables included in existing design models (described later in Table 4), hydropower and dam engineering guidebooks [35], [89], [90], new modular design specifications [19], and papers identified in the previous review of objectives.

As illustrated by the review of existing models in Section 3.4, powerhouse design and water conveyance design are the most studied design variables since they directly impact electricity sales. In addition, the impacts of minimum flows on generation and environmental performance are studied in recent design models through the lens of environmental flow methods [64], [91]. However, mitigation measures, such as those reviewed by Trussart et al. [46], are often ignored. With smaller economies of scale, mitigation measures tend to represent a higher share of costs for low-head NSD and NPD projects relative to relicensed projects [92]. As such, design models require greater accuracy in predicting performance, and the costs and benefits of these mitigation measures can play a pivotal role.

Design variables should be included in the formulation if they can significantly affect the objectives important to stakeholders. While there are too many tradeoffs between each possible variable and objective to describe in detail, it is helpful to highlight how mitigation measures commonly excluded from models can influence common objectives. For example, fish guidance structures, such as bar racks or louvers, reduce the flow velocity into powerhouse intakes to prevent fish entrainment, thus creating a head loss to the turbine inflows. By altering the dimensions of the bars, designers can increase the fish guidance efficiency at the expense of increased head loss [80]. Light, acoustic, bubble, and electric technologies have been investigated as sensory stimuli to guide fish without considerable head losses, but their effectiveness is unclear [78], [93]. As another example, drawdown flushing is a common way to pass bedload sediments through

Table 3. Potential run-of-river hydropower design model variables by design category.

Category	Potential Design Variables
Powerhouse Design	**Turbine**: type, number, size (design flow or rated capacity), number, design head, runner diameter, elevation setting **Generator**: type, number, voltage, speed, frequency **Transmission**: voltage, capacity, length
Water Conveyance Design	**Penstock**: design flow, length, diameter, number, transitions, material, intake location **Spillway**: design flood, length, material, head control capabilities
Operation Design	**Operating Rules**: minimum flow rates, the timing of minimum flow requirements, run-of-river timescale
Dam Design	**Dam**: height, length, shape, volume, material
Headpond Design	**Reservoir**: normal elevation, minimum elevation, maximum elevation
Mitigation Measures	**Sediment Passage**: passage mode, operating conditions, design flow, gate/structure design **Fish Passage**: design flow, operating conditions, structure design **Fish Guidance**: type, dimensions **Recreation Passage**: design craft(s), operating conditions, design flow, structure design **Recreation Feature**: type, availability conditions

low-level outlets. Studies found that smaller and more frequent flushings are preferred to improve sediment continuity [51], [94]. However, frequent flushing may impact the availability of the powerhouse due to decreased heads and increased sediment fluxes. As a final example, voluntary fishways provide safe and attractive hydraulic regimes for migratory fish. While the passage efficiencies of fishways depend on many variables, studies found that lower slopes and larger resting pools can lead to improved passage efficiency [75], [95]. However, these designs likely require longer structures and higher design flows, increasing capital costs and the opportunity cost of generation.

3.4 Review of existing ROR hydropower design models (RHDMs)

Table 4 summarizes the features of 23 RHDM studies obtained through the review process described in Section 3.1. The following sections further break down the trends in RHDMs according to their formulations, assumptions, objectives, and solution strategies.

3.4.1 Formulations

RHDM formulations describe the combinations of design variables, objectives, and constraints and depend on the study's purpose. Ibrahim, Imam, and Ghanem [96] differentiated planning models (used for site selection and capacity estimation) from design models (used to determine powerhouse configurations). Site selection and investment timing models, for example, focus on decision variables for overall plant capacity [97], while engineering design models include detailed dam, water conveyance, and powerhouse design variables [98]. The most common design decision studied in this literature is the selection of powerhouse design flow. For this problem, models must determine the number and size of turbines and any operating rules for those turbines that maximize expected generation on a given set of inflows (often historical inflows). In addition, some formulations set an environmental flow requirement, which is the minimum flow that must be met in the main channel to support ecological functions before spinning any turbines. A basic powerhouse flow optimization problem is described below.

This basic formulation highlights the non-linear properties of ROR design decisions, including the interdependence of technology selection and operation. This formulation also has non-linearities expressed through the generation efficiency term, $\eta(Q_i, Q_{i,t})$ and the turbine operating flow constraint. Formulations can include discrete variables (e.g., turbine type) and continuous variables (e.g., penstock length). For example, multiple turbine types (Kaplan, Francis, Pelton, etc.) were included in 52% of design models reviewed in this paper. In addition, some models limit the design scope to single turbine configurations [99], while others allow for parallel turbine schemes [61]. Therefore, formulations vary across studies in the level of detail, assumptions, and design scope.

Table 4. Summary of run-of-river hydropower design models.

Source	Year	Optimization Type (Method)	Objective Metric(s)	Decision Variable Descriptions	Environmental Considerations	Timescale	(D)iversion or (I)nstream
Najmaii and Movaghar [100]	1992	Simulation (Lagrange relaxation)	Net benefit	Turbine design flow, type, and number	None	15 FDC increments	D
Voros, Kiranoudis, and Maroulis [62]	2000	Analytical	AEG	Turbine design flow	None	Daily	D
Montanari [58]	2003	Analytical	NPV	Turbine design flow and type	None	Daily	D/I
Hosseini, Forouzbakhsh, and Rahimpoor [101]	2005	Analytical	NPV	Turbine design flow; Headpond volume	None	Daily	D
Lopes de Almeida et al. [98]	2006	Simulation (Non-linear programming)	NPV	Dam design; Powerhouse design; Water conveyance design	None	4 timesteps/day	D
Andaroodi and Schleiss [102]	2006	Simulation (Custom)	Annual net benefit	Plant capacity; Water conveyance design	None	Daily	D
Anagnostopoulos and Papantonis [61]	2007	Simulation (Stochastic evolutionary algorithm)	NPV and Capacity factor	Turbine design flow; Penstock diameter and length	None	100 timesteps/year	D
Bøckman et al. [97]	2008	Simulation (Real Options Analysis)	NPV	Plant capacity; Investment timing	None	Weekly	D/I
Niadas and Mentzelopoulos [57]	2008	Analytical (Probabilistic flow duration curves)	IRR	Turbine design flow	Minimum flow (static)	Daily	D
Pena et al. [103]	2009	Simulation (Time-series forecasting)	AEG	Turbine design flow	None	Monthly	D

Table 4 continued.

Source	Year	Optimization Type (Method)	Objective Metric(s)	Decision Variable Descriptions	Environmental Considerations	Timescale	(D)iversion or (I)nstream
Santolin et al.[104]	2011	Analytical (Techno-economic Analysis)	NPV, IRR, AEG, Machine cost	Turbine type, dimensions, and installation height	Minimum flow (static)	Daily	D/I
Basso and Botter [99]	2012	Analytical	IRR	Turbine design flow and type	Minimum flow (static)	Monthly	D/I
Adejumobi and Shobayo [105]	2015	Analytical	AEG	Turbine design flow and type	Minimum flow (static)	Daily	D/I
Munir, Shakir, and Khan [106]	2015	Analytical (Graphical)	IRR	Turbine design flow, type, and number	None	10-day timestep	D/I
Razurel et al. [107]	2016	Simulation (Hydrologic and Eco-hydraulic modeling)	AEG, IHAs, Habitat availability	Environmental flow method	Minimum flow (dynamic)	Daily	D
Yousuf, Ghumman, and Hashmi [108]	2017	Simulation (Multi-objective Decision Making)	Design flow, AEG, ICC, Payback period, Turbine technology	Turbine design flow	None	Daily	D
Sarzaeim et al. [109]	2018	Simulation (NSGA-II)	AEG, Plant factor	Plant capacity	None	Monthly	D
Mamo et al. [56]	2018	Simulation (Sequential Least-Squares Programming)	Specific cost ($/kWh)	Turbine design flow and number; Operating rules	None	Daily	D/I
Yildiz and Vrugt [110]	2019	Simulation (Differential Evolution Algorithm)	NPV	Turbine design flow, type, and number; Water conveyance design	Minimum flow (static)	Daily	D

Table 4 continued.

Source	Year	Optimization Type (Method)	Objective Metric(s)	Decision Variable Descriptions	Environmental Considerations	Timescale	(D)iversion or (I)nstream
Ibrahim, Imam, and Ghanem [96]	2019	Simulation (Genetic Algorithm)	Annual net benefit	Intake location; Penstock diameter and length; Turbine design flow, type, and number; Project #	Minimum flow (static)	Hourly	D
Kuriqi et al. [64]	2019	Simulation (Tradeoff analysis)	NPV, Custom IHAs	Environmental flow method	Minimum flow (dynamic)	Daily	D
Kuriqi et al. [83]	2020	Simulation (Hydrologic and Eco-hydraulic modeling)	Seasonal energy generation, IHAs, Habitat availability	Turbine design flow; Environmental flow method	Minimum flow (dynamic), Habitat suitability	Daily	D
Basso et al. [111]	2020	Simulation (Multi-objective opt. methods)	NPV, Hydrological connectivity	Turbine design flow; Minimum flow discharge	Minimum flow (static), Fish passage	Daily	D

Decision Variables: $Q_i, Q_{i,t}$

Maximize: $$\sum_t \sum_i \gamma H Q_{i,t} \eta(Q_i, Q_{i,t})$$

Such that: $$Q_{i,min}(Q_i) < Q_{i,t} < Q_{i,max}(Q_i) \quad \forall\, i$$

$$\sum_i Q_{i,t} \leq Q_t - Q_{env} \quad \forall t$$

Where: Q_i – Turbine design flow for turbine i
$Q_{i,t}$ – Flow allocation to turbine i at time t
Q_t – Total facility inflow at time t
Q_{env} – Minimum instream environmental flow
$Q_{i,min}$ – Minimum turbine flow for turbine i
$Q_{i,max}$ – Maximum turbine flow for turbine i
γ – Specific weight of water
H – Gross head on the turbine
$\eta(Q_i, Q_{i,t})$ – Turbine efficiency as a function of turbine design flow and allocated flow

3.4.2 Assumptions

The studies often did not set an explicit scope for the models, i.e., the range of site conditions in which their models apply. The formulations and discussions of the models were used to identify whether they apply to diversion schemes, instream schemes, or both. For example, models that select penstock length and minimum flow requirements indicated diversion schemes. Sixteen models (70%) target diversion schemes, while the remaining seven use generalized methods that could apply to either diversion or instream schemes. No models explicitly target low-head instream designs, meaning these models' application to low-head sites is uncertain.

The treatment of head variation is also an important model component. For high-head projects, head variation may be relatively small compared to the gross head under normal flow scenarios; however, this may not be the case for low-head projects. Engineering design models [61], [98], [110] typically calculate net head as three components: a constant gross head (the nominal difference between headwater and tailwater elevations), hydraulic losses (head loss from friction in conveyance structures), and tailwater losses (adjustments in the gross head due to changing tailwater elevations). At a given timestep, the tailwater losses are a function of total outflow, and the hydraulic losses are a function of flow allocated through the conveyances. Ignoring head variation can reduce non-linearities [112] and account for the fact that the impact of head on turbine efficiency is not captured in most empirical models [113]. Sixteen models (70%) ignore tailrace losses, often assuming constant head throughout the analysis. Nine models (57%) do not explicitly calculate hydraulic losses and those that do typically use design flow rather than allocated flow at a given timestep.

Another inherent assumption in most models is that historical flows will represent future flows. Using historical flow data alone to estimate plant capacity can ignore the risks of wet or dry years and increased variability in the future, which is a potential outcome of climate change [108]. Yousuf et al. [108] and Sarzaeim et al. [109] use climate models to consider the impacts of climate change scenarios on plant design. Niadas and Mentzelopoulos [57] use a probabilistic flow duration curve method, and Peña et al. [103] use various time series forecasting methods to account for long-term hydrologic changes. Validating design assumptions, accounting for flow and head variability, and incorporating risk into design models will be important for evaluating the feasibility at low-head sites.

The timescale of the ROR constraint is important, particularly for hydrologic alteration and power generation. Often the ROR timescale is determined by the data timestep, which is daily for most US gages. During the timestep, flow out equals the average flow in, and any storage changes during the timestep are often ignored. Fourteen (61%) models used a daily timestep, and two used sub-daily timesteps. Others used larger steps, typically in the form of flow duration curves (FDCs), which describe flow exceedance probabilities rather than a time series. FDCs can effectively analyze the tradeoff between capacity and availability at a high level but may ignore flow variability and flood events depending on the timescale of the data. Sub-daily timesteps are necessary to capture the full scale of hydrologic alteration impacts [65] and to model the ability of the plant (or a network of plants) to provide generation flexibility and ancillary services [60], [114]. Future models should employ greater temporal granularity and balance the tradeoffs between ROR timescale and performance.

3.4.3 Objectives

Table 4 highlights the primary objective function metrics in the ROR design studies. Studies with more than one objective function value indicate multi-objective techniques. Most models were designed to optimize economic indices, like the initial cost of capital (ICC), net present value (NPV), and internal rate of return (IRR), even for multi-objective studies. For example, Sarzaeim et al. [109] simultaneously optimized annual generation and plant factor (the ratio of energy generated to the time that theoretical maximum generation), which are both economic indices. These economic indices are well established in the literature; however, future models should ensure that cost and electricity price models are up-to-date and relevant to low-head hydropower.

Several models (43%) optimize environmental performance, all of which do so through the lens of environmental flow methods (EFMs). These models aim to determine the minimum flow discharges within the dewatered reach that can support river functions without significant losses to generation [115]. For example, Basso et al. [111] used a probabilistic model to relate minimum flows to fish passage and then co-optimized fish connectivity and NPV by setting minimum flow discharge as a decision variable. Minimum flow discharges can be static (a constant value) or dynamic (changes each timestep). They can also be set using a variety of EFMs, such as those in Kuriqi et al. [83]. Most (70%) of these minimum flow constraints were static values, while the others

[64], [83], [107] used dynamic EFMs. Additionally, dynamic EFMs can be proportional (a constant percent of total inflow) or non-proportional, which were shown to lead to more optimal flow allocation policies [107]. These multi-objective studies conclude that, with proper planning, it is possible to improve environmental performance without significant losses to generation.

3.4.4 Solution strategies

As formulations increase in complexity, improved strategies are needed to identify optimal solutions quickly. In the existing RHDMs, the two main strategies are simulation-based and analytical models. Mishra, Singal, and Khatod [116] similarly categorized these models into simulation models, economic analysis models, and cost optimization models. Analytical models use governing equations to provide a closed-form solution by simplifying the scope of the problem, such as via flow duration curves [58], [106]. These models can find globally optimal solutions but sacrifice detail such as the impacts of seasonal or daily flow variation on the operation. Simulation-based models maintain the complexity of the design problem and often use heuristic algorithms to search the design space efficiently. These algorithms, such as differential evolution [110] or stochastic evolution [61], programmatically select design solutions and then use operation models to evaluate each possible solution. Simulation models can also use sequential optimization procedures. For example, the OPAH model breaks down the problem into five modules that analyze the dam, the hydraulic circuit, the power station, the budget, and the project finances [98]. By maintaining the complexity of the problem, simulation models can expand the number of decision variables and may use more detailed cost and operation models; however, heuristic strategies cannot guarantee globally optimal solutions.

4. Discussion

RHDMs are used early in the project evaluation process to optimize the objectives important to stakeholders, so they must adapt as the objectives and project characteristics evolve. Table 4 (ordered by ascending publication years) shows that environmental considerations in RHDMs have become increasingly common in recent years. Section 2 shows that future hydropower development in the US will likely be driven by stricter environmental standards that LIR project designs and modular technologies could address. Based on the reviews in this study, potential enhancements to future RHDMs can be grouped into three primary areas, as discussed below.

4.1 Expanded model formulations

Almost all design variables affect how water is routed through the system, directly or indirectly impacting project performance. Figure 6 illustrates these inter-dependencies and highlights the relationships studied in existing models with the darker lines. Numerous design considerations are often ignored, such as mitigation measures and headpond design. Similarly, performance objectives are limited to economic and hydrologic alteration indicators. These limited scopes are likely due to 1) stakeholders

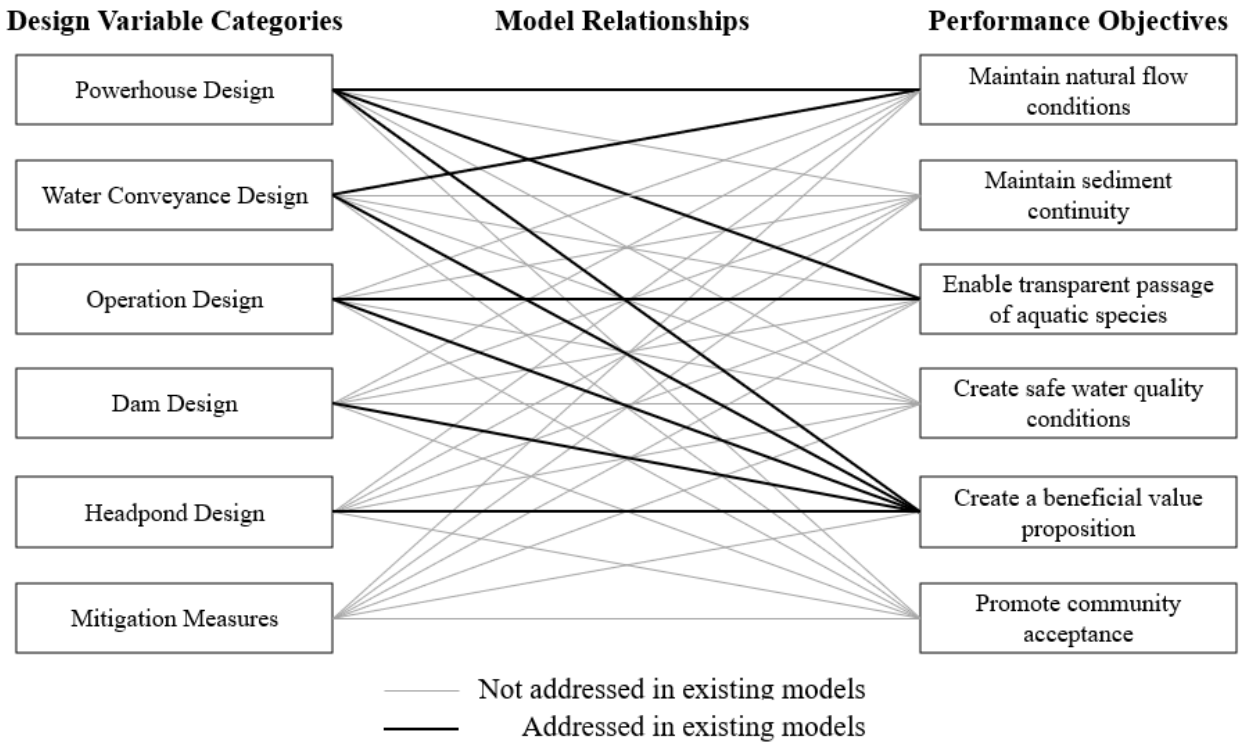

Figure 6. Summary of run-of-river design model decisions and how well they are addressed in existing models.

prioritizing economic outcomes, 2) the added modeling complexity of additional relationships, and 3) a lack of research to quantify certain relationships. Expanding model scopes to include non-power benefits and more detailed design variables can not only improve accuracy but can also lead to improved designs [64], [83], [111], so research into expanded models is beneficial.

Moving from high-diversion projects to LIR hydropower, models must study the time scale of ROR operation and incorporate low-head technologies. Assuming a daily timescale may ignore the sub-daily hydrologic impacts [65] and the value gained through ancillary services or peaking capabilities [48], [60], [114]. Larger operating timescales require more active storage to manage flow variation, which could negatively impact sedimentation and water quality. However, more research is needed to understand the pond size and conditions at which significant sedimentation or stratification occurs. The timescale also affects the head variability across the turbines, which is more important to consider at lower head sites. Various technologies, such as Archimedes Screw turbines, are emerging to address the abundance of low-head potential [117]–[119]. These turbines tend to focus on cost and operational flexibility at the expense of efficiency [89]. Holistic design models should include these technologies and study the tradeoffs between technology selection, head variation, operational constraints, generation, and the associated operation and maintenance costs. Additionally, a consistent definition of run-of-river operation across literature and regulators would help set standards for future developments.

4.2 Assessment of the barrier effects of hydropower infrastructure

As discussed in Section 3, barrier design is important for environmental performance across all impact areas, although barrier effects are not widely considered in RHDMs. The selection of technologies along the dam axis (e.g., fishways, sediment sluice gates, and spillways) should be considered in addition to the selection of powerhouse configuration because they have distinct economic and environmental tradeoffs. Section 3 identified a variety of metrics, like fish passage efficiency, that can be used to measure a technology's ability to mitigate barrier effects. However, these metrics are often technology-specific and require new models for connecting technology-specific functions to facility performance and overall river function. For example, fish passage studies help predict the passage efficiency through a given fishway, but it is unclear how to apply these metrics to innovative facilities with more than one fishway. Instead of aggregating technology-specific metrics, new holistic metrics describing the overall performance of a facility could provide a framework for technology-specific metrics. These metrics should reflect how the performance scales with the flow, river width, number of technologies, and operation over time.

4.3 Explicit environmental performance objective functions

Environmental performance of ROR projects is increasingly important for project success due to increased stakeholder engagement and the cumulative effects of small dams [120]. Arguably these environmental interactions are complex and are likely seen as outside the

scope of the original ROR design problem. However, with smaller power potentials for low-head projects, it is important to understand mitigation costs and the value of non-power benefits early in the design process. Existing models focus primarily on economic performance indices. Even in papers that study economic and environmental objectives [83], [111], the tradeoffs are limited to objectives that revolve around environmental flows methods, which are less applicable for instream schemes since downstream reaches are not dewatered. Nevertheless, these multi-objective papers did highlight the ability to identify beneficial scenarios in which environmental performance improves with minimal generation losses. Setting environmental performance as an objective requires quantifying non-power impacts like recreation, fish passage, and water quality enhancement. Section 3 identifies numerous ways to quantify performance in each impact area. However, adequate data and reliable models are needed to represent the associated tradeoffs in design tools. Once non-power benefits can be reliably represented in design models, several optimization approaches exist to co-optimize monetized and non-monetized metrics [121].

4.4 Future research recommendations

In addition to improved hydropower design models, many other research efforts could support hydropower decision-making. First, research into the water quality costs and benefits of small hydropower could support alternative opportunities for hydropower, like irrigation modernization and environmental restoration. Studies expect limited negative impacts from stratification, with proper sediment management, but quantifying the value of potential water quality improvements could provide additional revenue into models [49]. Second, studies should explore the tradeoffs between sub-daily storage, hydrologic alteration, and generation value for small hydropower in practice. Studies have shown that dynamic environmental flow methods can improve hydrologic alteration outcomes with limited generation losses [91] and that small hydro can flexibly support grids with high solar penetrations [122]. However, this flexibility requires validated powertrain and control system technologies to handle variable operations over extended periods. Thus, research into variable speed technologies, cascaded/networked systems, or innovative operation regulations could improve the value of small hydropower. Finally, research into standardized environmental performance metrics and measurement techniques that apply on a facility level instead of a technology level would support modeling and design efforts.

5. Conclusion

Evolving economic and environmental contexts are changing the value propositions for new hydropower. Stakeholders must decide to remove, maintain, or expand existing hydropower infrastructure. The costs and benefits of expanding hydropower depend largely on the chosen design. An emerging area of interest for new stream-reach development within the US is low-head, instream, and run-of-river designs, which have different economic, social, and environmental implications than large storage hydropower and high-head diversion schemes. This review identified a multi-disciplinary set of hydropower objectives and compiled a comprehensive number of RHDM studies

that can inform modeling efforts for LIR hydropower. However, several factors may have limited the breadth of articles captured in this review. Relying on snowballing, existing review studies, and a single search engine limited the ability to conduct quantitative meta-analysis and may ascribe the limitations of the existing reviews. Limiting the scope to LIR hydropower designs in the US required manual processing of articles and may have excluded impact areas relevant to site selection, medium-sized projects, innovative plant designs, and other countries. However, this review is still the most holistic assessment of RHDMs to the authors' knowledge, but future reviews can expand the scope to include these other design considerations.

The review showed that ROR hydropower design models have largely been used to optimize the economic potential of projects, so there is a need to expand the scope of design models to incorporate barrier effects, low-head designs and technologies, and the tradeoffs related to the run-of-river timescale. Additionally, the explicit incorporation of environmental performance into objective functions could lead to win-win design scenarios and additional non-power benefits. Innovative hydropower environmental design frameworks could employ multi-objective design models to improve designs and project outcomes. The development of sustainable run-of-river hydropower could be an attractive option for providing renewable electricity along with non-power benefits. Modernizing design thinking through improved design models is a crucial step toward this goal.

CHAPTER THREE

METHODOLOGY

The first two chapters highlight the need for an improved hydropower design model to facilitate modern hydropower decision-making. The methodology for constructing the model is instrumental in the accuracy of the model, the applicability of the model to various situations, and the usefulness of generated results. For example, computational fluid dynamics models and other 2D and 3D hydraulic/hydrodynamic models are used to assess the performance of turbines, conveyances, and structures [18]. However, these high-resolution models can be difficult to quickly adapt to different designs or site conditions with limited data, reducing their use for feasibility assessments. Alternatively, as described in Chapter Two, analytical hydropower design models employ high-level flow data and turbine assumptions to roughly approximate generation for feasibility assessments, but they neglect important environmental outcomes and operational relationships. The waterSHED model was constructed to balance these tradeoffs and address the areas for improvement outlined in the first two sections. These improvements include the expansion of model applicability to low-head, instream, run-of-river sites with a modular design framework and the integration of barrier effects into the simulation and performance metrics. In addition, the waterSHED model compiles a variety of empirical and conceptual models to capture the economic, social, and environmental processes outlined in Figure 7 below.

While the model components described in Figure 7 cover many linkages between hydropower design variables and hydropower performance objectives described in Figure 6, two performance objectives are excluded from this research due to the limited scope. First, hydrologic alteration is not a performance objective because the model is limited to LIR sites. These sites are expected to have a limited impact on hydrologic variability because there are little to no dewatered reaches, and the run-of-river timescale is assumed to be daily or sub-daily. The potential for small plants to create value from small storage volumes through plant aggregation or reregulation operation is being investigated [39], but these practices currently face little to no deployment. Modeling small-scale storage would require high-resolution stage-storage information and added complexity to operation processes, so hydrologic alteration was deemed out of scope. However, as exemplified in Case Study B, the model can include minimum spillway flows, which is an important consideration in the field of environmental flows [123]. Water quality was also excluded as an explicit performance objective because the primary cited water quality impacts, like aeration and temperature changes, stem from stratification at large reservoirs, which is less likely at LIR sites [124]. Temperature or aeration models require detailed information on the reservoir size and shape and the intake/outlet locations, which is not available during feasibility assessments. However, water quality is also closely tied to sediment transport, which is included as a model component.

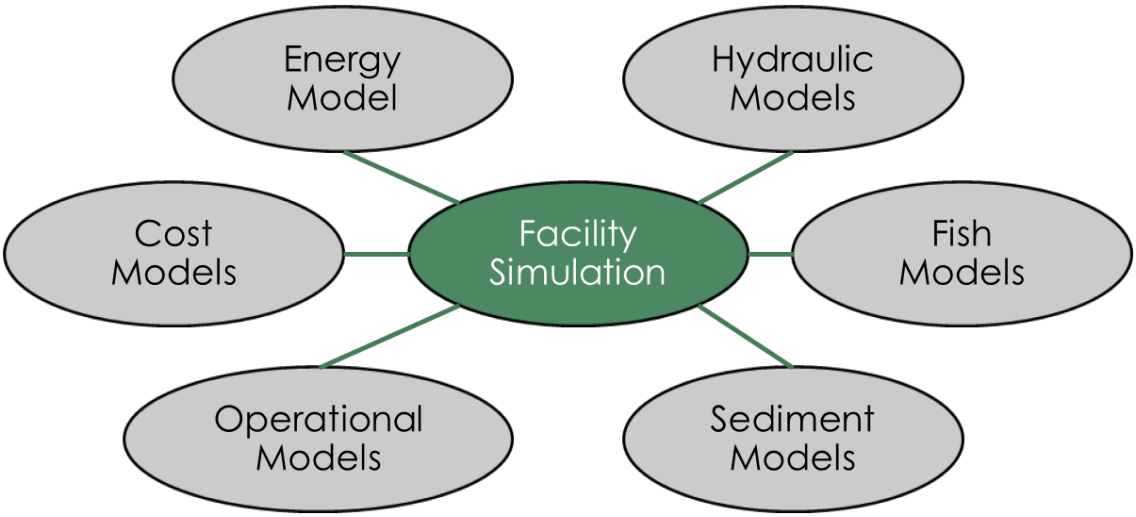

Figure 7. Overview of modeling components needed for improved hydropower design modeling.

There were three main challenges when constructing the model, including 1) the formulation and selection of component models, 2) the parameterization of inputs, and 3) the selection of a solution algorithm. The first challenge targeted how high-level environmental, social, and economic outcomes could be quantified in a meaningful way to stakeholders. The Model Specifications: System of Models section explains the empirical and conceptual models used to represent the processes illustrated in Figure 7. The second challenge addressed how diverse technologies and site conditions could be represented consistently with limited data availability. The Modeling LIR Hydropower using an Object-Oriented Approach section describes how the module classes from the SMH literature are implemented in the model to characterize conventional and emerging technologies. The Object-Oriented Class Attribute Definitions section in the Appendix documents the module parameterizations and can serve as a glossary for the object-oriented approach. The third challenge addressed how to efficiently search the design space for optimal designs and incorporate multiple types of performance metrics in analyses. The Solution Methods describes the enumeration and genetic algorithm optimization procedures created for the tool and their benefits.

Modeling LIR Hydropower using an Object-Oriented Approach

The SMH Exemplary Design Envelope Specification (EDES) report outlines each module class's objectives, requirements, inputs, functional relationships, and performance measures [19]. The SMH project has taken a “black-box” approach to characterize modular technologies, meaning that general relationships between module inputs and outputs are represented rather than the internal processes. The first step toward implementing the waterSHED model was adapting the EDES into a “language” to describe a diverse set of hydropower technologies as black-box SMH modules.

Object-oriented programming (OOP) is a way of structuring information in computer science and was used to structure the characteristics of hydropower technologies according to module class. In OOP, classes are created by defining a set of attributes. For example, the generation module class has attributes such as a design flow, a design head, and an efficiency curve. Then, objects are created by inputting values for those attributes. For instance, a Kaplan turbine object can be created by inputting a design flow of 300cfs, a design head of 12ft, and an efficiency curve equation. The same class could create a Pelton turbine object that operates very differently from Kaplan turbines but can be parameterized similarly. The objects have functions that can run computations using the attribute values, like calculating power output for a generation module.

The black-box approach from the EDES has clear parallels to object-oriented programming. Thus, the waterSHED model was created using OOP to represent the module classes from the SMH framework. The EDES, the literature review in Chapter Two, and a review of existing technology specifications were used to inform the structure of classes used in waterSHED [19]. The object-oriented approach toward hydropower technologies is an actionable research insight that can inform future research efforts, such as the environmental performance metrics work at ORNL [44].

This type of OOP approach for hydropower is not new, but it is not widely used in existing hydropower design models (Table 4). Garrido et al. [125] created an object-oriented simulation model for small run-of-river plants; however, the tool acts as a digital twin that can represent the operation of an existing plant under a variety of conditions rather than optimizing the design for a particular set of conditions. In addition, the types of technologies are more narrowly defined to represent the control system. For example, the Garrido et al. [125] tool can represent either Kaplan or Francis turbines with various speed settings so that the model can simulate the interactions between the turbine speed, controllers, generator, and converters. The waterSHED model has a higher level of abstraction that incorporates internal functions, like turbine speed control and generator losses, as part of module characteristics, like a turbine flow efficiency curve. This approach enables greater flexibility for representing and optimizing a wide variety of technologies, which is important due to the need for innovations to reduce development costs. Other simulation and analytical models assume a particular plant design and hard-code design variables according to the preset design, making it difficult to adapt the model to new design configurations. The waterSHED model's OOP allows the decision variables to change depending on the desired technologies for a given site.

The classes used in the waterSHED model can be categorized as Module classes, Simulation classes, and Backend classes. The Module classes describe the suite of user-defined hydropower technologies that can be included in an SMH facility as outlined by the EDES [19]. The Simulation classes describe the other user-defined project conditions, including the Site, Cost Tables, Preferences, and Species classes. The Backend classes are internally created classes that facilitate the simulation and optimization processes and include the Module Library, SMH Project, Facility, and Results classes. The classes and their attributes are detailed in the Object-Oriented Class Attribute Definitions in the Appendix. The following sections provide a brief overview and highlight the reasons behind the formulation of each class.

Module Classes

One of the features of OOP is inheritance, which means that "child" objects can inherit the attributes and functions of "parent" objects. Inheritance simplifies the construction of hierarchical classes and is used in Figure 8 below to illustrate the module classes. Every SMH module, as illustrated by the parent module at the top, has a capital cost, an annual operating cost, a width, and a length. Given the tool's scope, which is limited to simple 1D or 2D hydraulics models, module heights are not required unless the height is relevant to the module function, and any instream modules are assumed tall enough to limit overflow up to the maximum spillway design flood.

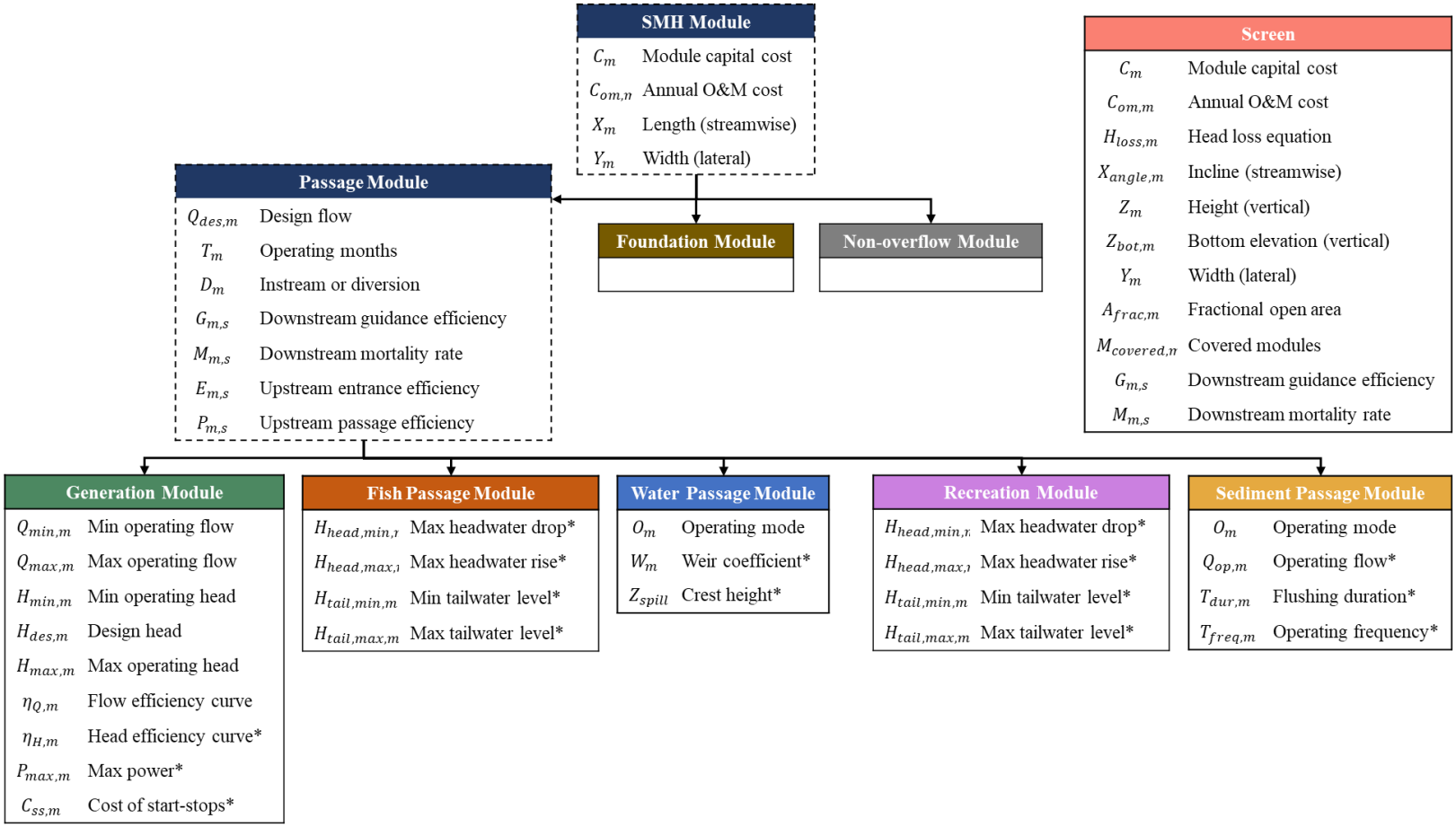

Figure 8. Hierarchical structure of SMH module classes.

Foundation and Non-overflow modules are basic SMH modules that do not have attributes outside these SMH module parameters. Foundation modules provide structural support and are an important driver of project costs [40]. Modular foundations, including prefabricated and 3D printed concrete structures, are still in the early innovation stages [126]. Further research is needed to understand how these technologies adapt to diverse riverine sub-surfaces. In the waterSHED model, foundation modules are characterized into discrete rectangular units that cover a specified area of the facility footprint. The model assumes that all instream modules must be supported by a foundation module. So, when creating a facility, the number of foundation modules is determined by dividing the footprint of all instream modules by the area of one foundation module (rounding up). Non-overflow modules act like a typical dam and provide a water-tight barrier between the upstream and downstream sides to create sufficient headwater levels of module intakes. Conventionally, low-head dams use spillways that span most of the river or earthen dams that must be custom designed for each site [40]. Modular dam designs and installation practices are still in the early innovation stages, and the Non-overflow class was not included in the original EDES [19]. The concept of non-overflow modules was derived during the reference design work described in Case Study A to account for facility abutments, the space between passage modules, and the need for vehicle access. As such, non-overflow modules were characterized as discrete units that fill in any remaining river width that is not covered by other passage modules. In the model, the number of non-overflow modules is calculated by dividing the river width minus the sum of the passage module widths by the width of the non-overflow module. Currently, only one type of foundation module and one type of non-overflow module can be used to create a facility because the numbers of each module are automatically calculated to complete the facility.

Passage modules are any module that passes water, which will impact flow allocation and fish passage. Each passage module has a design flow, which generally means the flow allocated to the module during normal operation. However, the definition does change for spillway modules, representing the maximum design flow for the spillway. Modules may be operated seasonally, which is often the case for fish bypasses and sediment sluicing measures that operate during migration seasons and floods. Additionally, four metrics describing their ability to pass fish safely upstream and downstream can parameterize each passage module, including the mortality rate, guidance efficiency, entrance efficiency, and passage efficiency. As illustrated in Chapter Two, these metrics are commonly used for fish passage studies and are used in the novel fish passage models (described in the Fish Models section).

Generation modules represent hydropower turbine systems (including generators, conveyances, and accessory electric equipment) and provide power generation capabilities. Literature on turbine conceptual design is rich, and this parameterization largely leveraged Gordon (2001) and Gulliver and Arndt (1994) [89], [113]. Generation modules have a range of head and flow conditions in which they can operate safely without significant cavitation that can damage turbines. The power generation

efficiencies vary across these ranges depending on the turbine type, with a peak efficiency occurring at the design head and flow. Kaplan turbines, for example, have adjustable propeller blades that extend the operational flow and head ranges and increase the efficiency across this range [127]. Oppositely, propeller turbines are only actuated by wicket gates, so the design range is limited but can be much cheaper than dual-regulated Kaplan's [128]. These cost-efficiency tradeoffs are common in existing design models, per Chapter Two. Hill charts are often used to parameterize turbine efficiency for a range of flows and speeds [89]. However, these charts are difficult to parameterize in a format compatible with the user interface, and they may not be widely available for new turbine types. The turbine efficiencies are parameterized in waterSHED as a flow efficiency curve and a head efficiency curve. Flow efficiency curves are common in the literature, whereas head efficiency curves are not, so a typical curve from Gordon (2001) is provided as a default (see Equation 4) [113].

Fish Passage and Recreation modules are parameterized and operated similarly but evaluated differently in performance calculations. Fish passage modules, also referred to as Aquatic Species Passage modules, provide safe pathways for aquatic species across the dam. Volitional fishways, such as Denil, vertical slot, and nature-like designs provide attractive hydraulic conditions for target species to swim upstream and downstream across more gradual slopes [129]. Volitional fishways are typically more common at low-head sites than non-volitional measures, like trap-and-truck, because lower-head sites require shorter fishways, which can be cheaper than labor-intensive measures [130]. The fish passage metrics (guidance efficiency, mortality rate, passage efficiency, and attraction efficiency) depend on many factors for fishways, including slope, design flow, species, and fishway type [75]. Recreation modules provide safe passage for vessels and recreationalists. Whitewater parks at low-head dams are an emerging feature for new developments, although there is limited research on the practicality of co-development for recreation and hydropower [131]. Both module types have optional parameters describing the headwater and tailwater deviation limits. Whenever the modeled headwater or tailwater elevations leave these ranges, the modules are turned off because they represent unsafe conditions for the recreationalist or species. For example, if the tailwater is too low, kayakers may contact the riverbed when exiting drop structures, leading to injury [131]. Similarly, fishways may require headwater and tailwater elevations to provide suitable depth and velocity for the target species [17]. The specific parameters described in Figure 8 were selected for ease of input because tailwater requirements can be set in reference to the bed elevation. At the same time, the normal operating headwater level (NOL) may change during design, so headwater constraints were set in reference to the NOL.

Water passage modules are a general class of SMH modules whose main role is to pass water. Spillways are the typical example of water passage modules, which have the hydraulic capacity to pass flood flows safely without overtopping that can erode embankment materials or damage equipment [40]. However, water passage modules can also represent minimum flow or aesthetic features. Spillways play a very important role

in dam safety and operation for hydropower plants, so the waterSHED model requires at least one spillway in every facility. There are two main types of spillways, controlled and uncontrolled, which describe their ability to regulate flow, so the operating mode attribute was created to represent these distinctions. Controlled spillways, such as overshot gates and overflow structures with radial gates, can regulate the flow of water, which allows the plant operator to maintain desired headwater levels [89]. Uncontrolled spillways, often weirs, pass flow according to the head across the weir and the weir shape [132]. The typical weir equation (Equation 1) is solved in the simulation process to determine the resultant headwater level for a given flow allocation (Equation 2). Uncontrolled spillways, while cheaper and simpler to operate, can cause head fluctuations that can limit the operation of other modules with head constraints.

Sediment modules describe technologies used to pass accumulated sediments across the facility. Dams increase the water depth and reduce velocities upstream, which causes sediments to accumulate over time in the upper reservoir. Accumulated sediments can cause problems for intakes, plant operation, and downstream environmental health [133]. Riverine sediments can be broadly categorized as suspended loads, typically lighter/smaller particles transported in normal river flows, or bed loads, heavier/larger particles that settle into the riverbed and move along the bed [35]. Particles on the riverbed can be re-suspended when exposed to high shear forces. Most dam designs assume that suspended loads can be transported as part of the flow through spillways and other technologies, although de-sanding basins may be needed to remove sediments from turbine flows [134]. Thus, dedicated sediment technologies often focus on passing bed loads by creating high shear conditions at the bed. Annandale, Morris, and Karki [35] identify three methods of sediment passage that were incorporated into the sediment classes and operating modes: continuous bypass, sluicing, and flushing. The default Sediment Passage module with continuous operation represents a sediment bypass that continuously passes flow through a canal, culvert, tunnel, or siphon to transport sediments around the dam. Sluicing operation represents technologies, typically low-level gates, that pass flow only when inflow meets a certain threshold called the operating flow. Sediments typically pass in the highest quantity during flood events when rain and high velocities entrain bed load sediments and runoff sediments [35]. Sediment sluice gates thus limit the amount of flow required to mitigate accumulation by only opening during those flow events. Flushing operation was created to represent technologies with scheduled reservoir drawdowns where low-level gates are opened, and the reservoir is evacuated through the gates to scour accumulated sediments. The frequency and duration of the flushing events are set by the class attributes. When flushing occurs in the simulation, all other modules are turned off, because it is assumed that headwater elevations significantly decrease during flushing.

Screens are a special type of module class that can represent fish screens, trash racks, log booms, and other technologies that interact with the flow before that flow enters modules. These screens are important considerations for cost and barrier effects. For example, fish screens exclude fish from unsafe passageways and can be a prohibitively expensive

mitigation measure [135]. Trash racks are also required in many designs to prevent large objects, like branches, from entering and damaging turbines. In addition, these screens can cause head losses based on the flow velocity and dimensions of the screen, which can decrease generation [136]. These screens are placed upstream of SMH modules and were not included in the SMH EDES, so they are not parameterized as an SMH module but as a separate object. The Screen class has several attributes, including downstream fish passage metrics, capital and operating costs, a head loss function, a screen area, and related dimensions. The modules can be parameterized in waterSHED to scale based on the width of the modules "covered" by the screen and the angle of the screen so that the screen cost, size, and head loss can be adjusted between design iterations.

An additional feature of waterSHED is the ability to create either static or dynamic modules. Static modules maintain the same design parameters throughout the simulation and can represent off-the-shelf technologies. **Dynamic modules** can be created to automatically calculate certain attributes based on one or more **design variables**. These modules rely on customizing modules for a given site design, reflecting trends toward additive manufacturing and 3D printing [16]. For example, a precast concrete non-overflow module could be designed based on the normal operating headwater level. If the NOL was altered in a sensitivity analysis, then the size of the non-overflow module would change accordingly. The dynamic modules require known relationships between attributes and design variables, which were relatively common for hydraulic turbines [89], but not for the other module classes. The design variables can represent select module attributes or conditions of the site, like the NOL. The relationships were hard coded into the tool, so the available design variables were limited to those particularly relevant to each module class, as described in Table 23 in the Appendix. For ease of entry, intermediate variables were also specified to allow parameterization of attributes based on these values; however, the intermediate variables could not be directly specified. For example, a dynamic generation module could parameterize capital cost based on the design power, but the design power would have to be calculated based on the design head and flow. Full descriptions of the variable relationships for the dynamic modules used in Case Study A are included in the Appendix.

Simulation Classes

The simulation classes include all the additional variables needed to turn a collection of modules into an SMH project. These include the Site, Cost Table, Preferences, and Species classes. Rather than combining all the attributes into one class, the attributes were subdivided into these classes to help conceptualize the development processes like site investigation and cost modeling. The following paragraphs provide an overview of each class. The attribute definitions are compiled in the Object-Oriented Class Attribute Definitions section in the Appendix.

The **Site class** describes the river system's physical, hydraulic, and hydrologic characteristics. The stream width attribute sets the minimum instream distance that modules must cover to create a water-tight barrier. The stream slope is used in the

sediment entrainment model and the geometric reservoir model. The trap efficiency parameter is a dimensionless parameter between 0-1 that describes the risk of storage reduction due to sedimentation in the average trap efficiency model [137]. A key input for the Site is the inflow data, a time series of mean daily inflows used to simulate the operation of the plant (each time step is one day) and can be used to create flow duration curves and other analyses during the design process. While shorter timescales (e.g., hourly) enable higher resolution results, mean daily flow data is the most common type of data available from the US Geological Surveys (USGS) vast network of stream gages [138]. Daily data adequately represent the scale of hydraulic variability for small ROR plants to preclude the need for extrapolation to a smaller timescale. Peak flow data can also be provided to inform a flood frequency analysis process that quantifies the efficacy of the spillway design flood according to the expected flood years (described in the Flood Frequency Analysis section in the Appendix). The stage-discharge equation attribute is also key because it represents the relationship between flow and tailwater elevation, influencing head across turbines and module availability. Stage-discharge data is relatively common at USGS sites and can be directly input into the model, assuming that pre-development and post-development stage-discharge relationships are similar [138]. Finally, the stage-storage curve quantifies the reservoir size for headwater elevations provided by the simulation process. The reservoir size is used to calculate average sediment trap efficiency and is used qualitatively to illustrate potential impacts on local communities and hydrologic alteration.

The **Preferences class** describes the operational and simulation preferences of the user. The normal operating headwater level (NOL) attribute controls the gross head of the facility, along with the stage-discharge tailwater curve. As discussed in Chapter Two, existing design models often assume a constant head value because head variation creates a non-linear dispatch problem, and it is difficult to size technologies for different heads. Several features, including the Site class, the dynamic modules, and supporting models, enable SMH facilities to be evaluated at different NOLs and under controlled spillway (constant headwater) or uncontrolled spillway (variable headwater) operation. The Preferences class also enables the selection of inflow data that is used in the simulation. Flows should represent normal, wet, and dry conditions to evaluate the facility's performance in various conditions. The operational priorities, which describe the ranking of module classes in the flow allocation processes (outlined in the Model Specifications: System of Models section), are also set in the Preferences class. The turbine over-run attribute allows the simulation to ramp turbines past the set design flow once all turbines have been turned on to their design flows. This allows the plant to generate more power at the expense of generation efficiency and increased wear on the turbines, which is a tradeoff experienced by existing plant operators [48]. Minimum spillway flows can ensure that aesthetic or environmental flow requirements, which are often imposed during licensing, are being met during the simulation [91]. The minimum flow can be set as a constant value (static) or as a percent of inflow (dynamic), which have been shown to provide benefits for both power generation and environmental performance [91]. Additionally, the notch flow attribute reflects a feature of some spillway designs that help

ensure minimum flows by providing cut-out sections below the NOL. In the model, the notch flow is allocated with high priority to the spillway but does not affect the headwater elevation.

The **Cost Table class** describes the economic assumptions used for cost modeling and includes common economic modeling variables like the average energy price, the discount rate, and the project life. A variety of options are also available to include capital (related to the cost of physical assets), non-capital (non-fungible costs), and operational (annually recurring) costs that are not captured on a module level, such as transmission, parking, licensing, overhead, engineering, and contingency costs. These cost attributes are used according to the cost models described in the Economic Models section. Two tools for optimizing facility design are the value of recreation and flood cost attributes. The value of recreation represents the hourly revenue from recreational assets, like whitewater parks. The business models for recreational features may vary; however, setting a dollar value based on module availability enables economic valuation studies similar to revealed preference models [25]. For example, through a sensitivity analysis process, the waterSHED model can evaluate the value of recreation that makes the recreation module worthwhile and a net positive to project LCOE. Similarly, the flood cost attribute sets a value per unit of flow that exceeds the plant's hydraulic capacity at a given timestep, which can be used in optimization or sensitivity analyses to determine the optimal spillway capacity.

The **Species class** is used to index species of interest for the fish passage performance models (described in the Fish Models section). Fish passageways are often designed for a select number of species. For example, Denil fishways are volitional fishways with relatively steep slopes that are hydraulically designed for strong burst swimmers like salmonids [139]. So, the fishway may have high passage efficiencies for salmon but low passage efficiencies for juvenile sturgeon with lower burst speeds [140]. The cross-species effective mortality and effective passage metrics help describe the average fish passage performance across several species. The attributes include the upstream and downstream migratory months that help represent the seasonal nature of fish passage and focus on the critical times of the year. For example, if fish passage is highly seasonal for certain species, then fish passage modules can be operated only during those months to provide reliable fish passage with minimal generation losses during the other months. The Species object is also parameterized by two factors that influence the attraction efficiency model (see the Fish Models section) called the relative discharge parameter (a) and the attraction sensitivity parameter (b). These parameters shape the species-specific attraction efficiency curve that is a function of the relative discharge of the module (i.e., module flow divided by total inflow). The higher the relative discharge parameter, the higher the module relative discharge must be to attract fish. The attraction sensitivity parameters affect how quickly the efficiency drops off at the relative discharge threshold.

Backend Classes

The **Module Library class** is the collection of modules that can be selected when creating a facility. The genetic algorithm (described in the Appendix) will automatically generate random facilities by selecting feasible combinations of modules from the Module Library. The library can have two kinds of modules, including static and dynamic modules. Static modules have constant attribute values that do not change during the optimization processes and represent standardization because modular technology vendors will tend to sell units of consistent dimensions. On the other hand, dynamic modules allow another level of optimization by setting attribute values as relations to design variables rather than fixed values. For example, a dynamic turbine module can change the operating head and flow ranges by setting the limits as a percentage of the design head and flow, which are the design variables. Then the design head can then be linked to the normal operating level, and the design flow can become a decision variable in the optimization process to allow turbine optimization over two degrees of freedom. This type of optimization reflects emerging construction techniques like additive manufacturing/3D printing of runner molds and concrete structures that can custom design modular technologies cost-effectively [16]. Standardization is still involved when using dynamic module optimization because it is assumed that all dynamic modules within the same facility are designed to the same design variables.

The **SMH Project class** is the umbrella structure that collects the Module Library, Species, Cost Table, Preferences, and Site objects to create and optimize a facility. It is meant to reflect the starting point for developers when conceptually designing a site. As outlined in Figure 9, the SMH project combines all the user-defined inputs and uses either the enumeration or the genetic algorithm optimization processes to create facilities.

The **Facility class** represents the collection of modules that can simulate operation. When a facility is initialized, the number of Non-overflow and Foundation modules are computed using the uncovered stream width dimension and the footprint of instream modules. The facility also combines all spillways modules into a single structure because the operation model assumes that the spillway modules are operated as one unit. For example, a prefabricated weir would not control whether flow travels over one module section versus the entire weir length. Controlled spillways may control modules separately, but this does not impact operation since the headwater level is assumed constant. The Facility class also handles internal functionalities like calculating the plant nameplate capacity, establishing the operating rule curve, and plotting the conceptual layout.

The **Results class** computes the performance of a Facility object for a simulation run. A facility is simulated using the flow allocation process described in the next section and creates a Results object. The Results object then computes the economic, social, and environmental performance metrics for that simulation. A facility may have different simulation results for different inputs, so a separate class was needed to save multiple runs. The Results class also provides figures and tables to illustrate model runs.

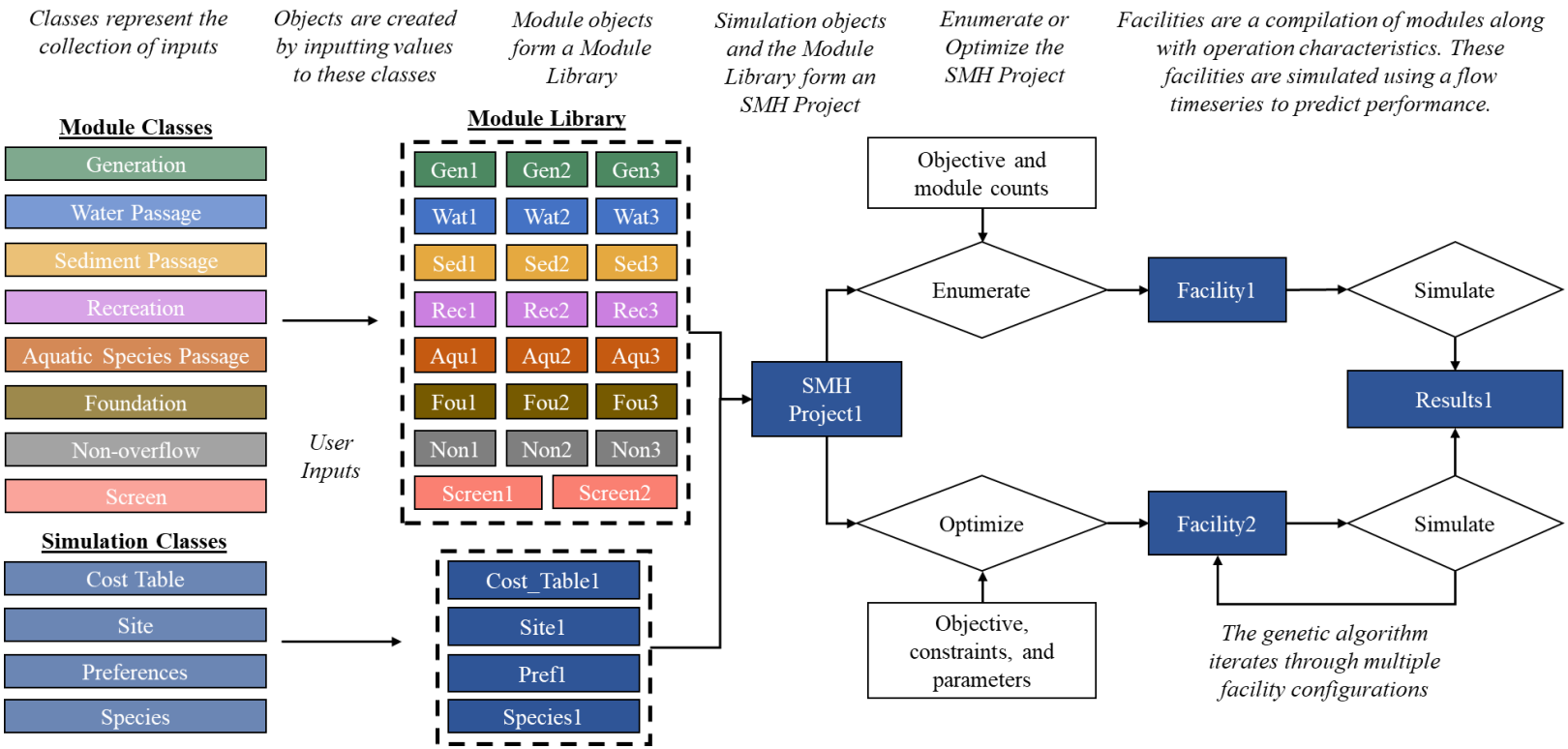

Figure 9. Flow diagram of waterSHED model processes. The numbers indicate instances of the class, also known as objects.

Model Specifications: System of Models

Design models are only valuable if they provide actionable insights into plant design and operation, so the model's outputs are critical. The primary outputs of waterSHED are high-level estimates of the performance metrics listed in Table 5 below, recommendations for module selection and design parameters, and quantitative tradeoff curves between variables. The performance metrics are used within the optimization process as objective functions and constraints and as tradeoff variables within the sensitivity analysis process. The performance metrics described in this section were formulated given the data and modeling limitations defined in the scope and the goal of representing the major economic, social, and environmental outcomes. When possible, the metrics were formulated as percentages between 0-100% to provide intuition about the quality of results between good (100%) and bad (0%). The performance metrics are calculated using a simulation process that represents an SMH facility using the OOP framework, simulates the daily operation of the model with provided mean daily inflows, and then translates the operation into quantifiable metrics. Compared to the performance metrics captured in existing models (Table 4), the waterSHED model encompasses far more metrics specifically related to social and environmental performance. Additionally, the environmental performance metrics are not focused on environmental flow methods, which are the most common measure of environmental performance, but are not necessarily relevant to LIR hydropower since flow is not stored or taken out of the main reach.

The simulation requires a system of models to represent the network of related physical, hydraulic, biological, economic, and social factors, as described in Figure 10. The following sections document the formulations and reasonings for each of the models in waterSHED. The following notation in Table 7 helps describe the model mathematically throughout the following sections. In addition, any model-specific variables are presented along with the corresponding equation.

Operational Models

The operational models are used to simulate the hydraulic conditions of the site throughout the simulation and allocate the mean daily inflow across the modules in the facility. Although many factors affect plant operation, including climate, forced/unforced outages, and electricity prices, the main drivers of operation for run-of-river plants are inflow and its relationships with headwater and tailwater elevations. Three models are used in this study to represent these relationships, including the stage-discharge model, a weir model for uncontrolled spillways, and rule-based operation.

The **stage-discharge model** is an equation that represents the relationship between the tailwater elevation and the flow through the facility. For run-of-river facilities, greater inflows can enable greater flows for generation modules; however, greater inflows also increase the tailwater elevation, which decreases the gross head across the facility.

Table 5. Performance metrics calculated in the waterSHED model.

Category	Performance Metric	Description (unit – suggested goal, i.e., maximize or minimize)
Economic	Annual energy generation	The annualized sum of energy generation for all generation modules in the simulation. (MWh/year - maximize)
	Initial capital costs	The one-time expenses used to purchase or construct capital assets, such as buildings, land, and equipment. ($ - minimize)
	Total cost	All the one-time costs required to begin operation. ($ - minimize)
	Net present value	The current value of the project based on the total cost, expected revenue, annual maintenance expenditures, and discount rate assumptions. ($ - maximize)
	Levelized cost of energy	The average net present cost to produce energy over the life of the project. ($/kWh - minimize)
Aquatic Species passage	Effective downstream mortality	A novel metric describing the expected time-averaged mortality rates for a species over the simulation. (0-100% - minimize)
	Effective upstream passage	A novel metric describing the expected time-averaged upstream passage success rates. (0-100% - maximize)
Sediment	Sediment flow ratio	The average ratio of flow allocated to sediment modules compared to the total inflow at each timestep. (0-100% - maximize)
	Sediment passage frequency	The number of timesteps in which sediment modules are operating divided by the total number of timesteps. (0-100% - maximize)
	Average trap efficiency	The average percentage of incoming sediment that accumulates in the reservoir. (0-100% - minimize)
Social	Recreation availability	The percentage of simulation time in which recreation features are available. (0-100% - maximize)
	Spillway flood return period	The flood year capable of being passed through the spillway. (years - maximize)
	Average impoundment volume	The average volume of the reservoir over the simulation period. (ft^3 - minimize)
Operational	Module availability factor	The number of timesteps that the module is operating divided by the total time that the module could be on given operating months. (% - maximize or minimize)
	Module flow ratio	The percent of total simulation inflow allocated to the module. (% - maximize or minimize)

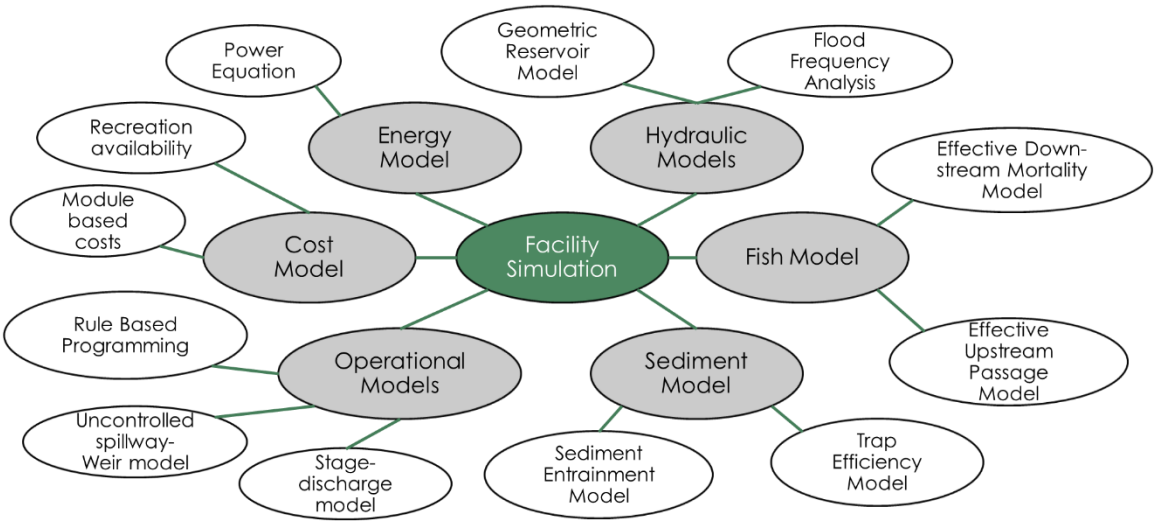

Figure 10. System of model diagram.

Table 6. Summary of common mathematical notation variables.

Notation	Description
t	Index used to represent a timestep.
T	The set of timesteps in the simulation. Used to represent the total number of timesteps (days).
s	Index used to represent a species.
Sp	The set of species included in the simulation. Used to represent the total number of species.
m	Index used to represent a module.
Fa	The set of modules in the facility.
Gn	The set of Generation modules in the facility.
Rc	The set of Recreation modules in the facility.
Sd	The set of Sediment Passage modules in the facility.

The tailwater elevation can also control the ability of Recreation and Fish Passage modules to operate, so proper evaluation of the stage-discharge curve is important. Based on the Case Study Report [17] approach, the stage-discharge models used in case studies were generated by downloading and regressing either daily or 15min stage and discharge data for at least the previous ten years of available data. Power curves were often the best approximation for the relationship at low flows, but the curves often developed linear trends at high flows. Therefore, a piecewise equation was generated to represent the two components in these cases. The methodology for determining the piecewise equations is described in the Regression Analysis section in the Appendix. An example piecewise stage-discharge curve for the Housatonic case study site is illustrated in Figure 11. The curves could be manually adjusted to reflect changes in the downstream geometry and roughness post-development. However, the case studies assumed that the downstream pre-development stage-discharge relation persisted after development.

The **headwater elevation model** depends on the operating mode of the spillway. Controlled spillways can regulate flow, so the headwater elevation is assumed constant and equal to the normal operating headwater level. Uncontrolled spillways cannot regulate flow, so a weir equation, Equation 1, is included to describe the relationship between headwater and spillway flow. Spillways are often the primary hydraulic feature at low head sites, so the impacts of other modules on headwater are not considered in the model. The weir equation depends on the shape of the weir, which can be classified as sharp-crested, broad-crested, trapezoidal, and many others. The form, exponents, and coefficient (*C*) can vary for these different weir shapes. The rectangular weir equation (Equation 1) is used throughout this study to standardize the input process and reflect the modular design concept, while the weir coefficient is varied to reflect differences in crest shape. The head provided in the weir equation describes the head over the weir rather than the headwater elevation, as described in Figure 12. The rule-based process allocates flows before calculating headwater elevations, so the weir equation was transformed into Equation 2 to calculate the headwater elevation (with respect to the bed elevation).

Weir equation

$$Q = CLH^{\frac{3}{2}} \qquad \text{Equation 1}$$

Headwater equation

$$Z_{head,t} = \left(\frac{Q}{C_{spill}L}\right)^{\frac{2}{3}} + Z_{spill} \qquad \text{Equation 2}$$

$\boldsymbol{Q}$ Flow over the weir (cfs)

L Length of the weir (ft)

H Head over the weir (ft)

C_{spill} Weir coefficient ($\frac{ft^{\frac{1}{2}}}{s}$)

$Z_{head,t}$ Headwater elevation (ft)

Z_{spill} Spillway crest height (ft)

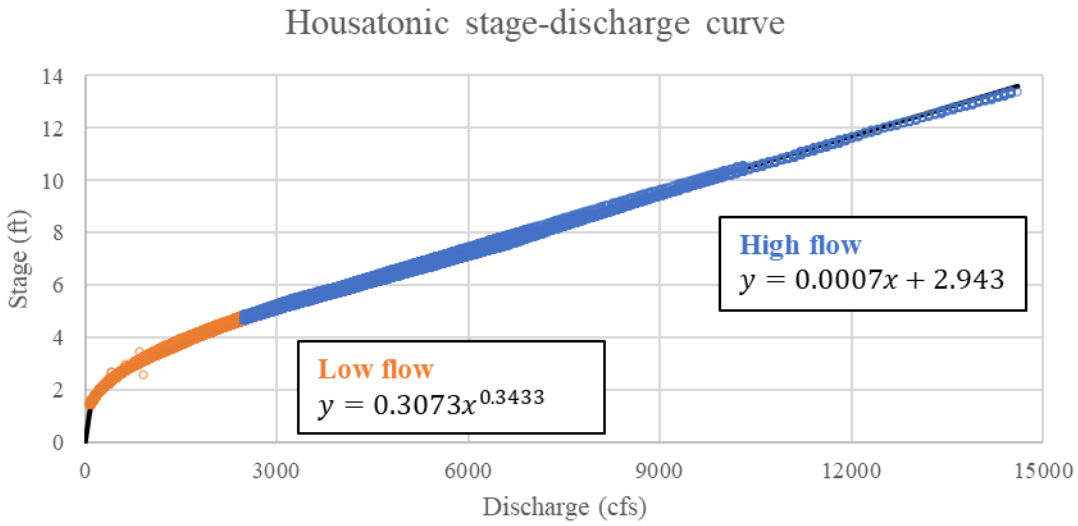

Figure 11. Example piecewise stage-discharge curve for the Housatonic case study site.

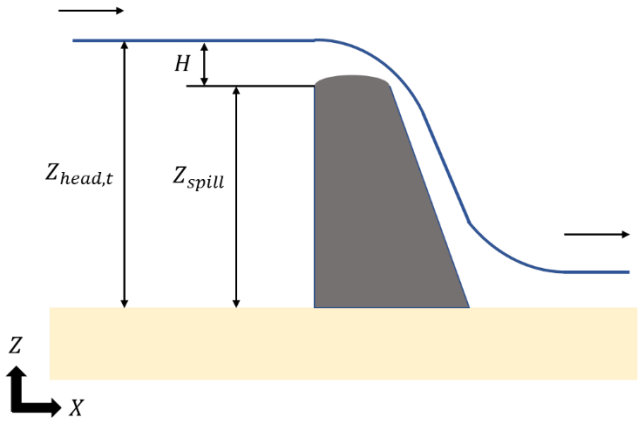

Figure 12. Profile view of weir with notations for head over the weir (H), the headwater elevation ($Z_{head,t}$), and the height of the spillway (Z_{spill}).

The rule-based programming model determines the flow allocation according to the module class priorities set in the Preferences object. A basic example of the process is illustrated in Figure 13. Inflow is allocated to the modules in order of priority if there is flow remaining and the modules are on. The generation modules are treated as a singular powerhouse, and a dispatch model (described in the following subsection) is used to distribute powerhouse flows across the generation modules. Any flow remaining after all modules are turned on is spilled over the spillway. The rule-based programming method is representative of rule curves used by storage dams to partition sections of the reservoir volume for different purposes like conservation and flood control [141]. Optimized dispatch schemes are common in the literature for storage reservoirs [142] but, in practice, are used to create rules for operating certain units. When allocating flow between non-power modules within the same class, the smallest modules are turned on first. This is like a greedy approach because the program turns on the smallest module, which can reach its design flow first. Priority orders may differ between stakeholders; however, Fish Passage modules are typically high priority due to regulatory requirements, and sediment passage is often last because sediment accumulation can take several years, and flows largely occur during flood events when there is sufficient flow to operate all modules.

Several other processes are needed to simulate operation, as described in Figure 14. First, if there is a scheduled sediment flushing event, all modules except the sediment flush gate are turned off, the reservoir is evacuated, and all flow is allocated to the sediment module. Next, since certain module classes have headwater and tailwater limitations, the model must predict elevations. In the case of controlled spillways, these elevations are known. However, in the case of uncontrolled spillways, the headwater elevation relies on the flow over the spillway, and the flow over the spillway relies on flow allocations to other modules, which also rely on the headwater elevation. This creates a non-linear problem that is solved using an iteration process illustrated in Figure 14. For the first iteration, flow is allocated to the modules with rule-based programming without head constraints. The headwater and tailwater elevations are estimated with this initial run. The simulation is run again with the estimated headwater and tailwater elevations. If the calculated elevations match the estimated elevations, the flow allocations match, and the iteration stops. Otherwise, the modules with head constraints are turned off and iterated again until the flow allocation is successful, or all modules are turned off, and an error is raised. Errors only occur when head constraints are very narrow. Additional operation considerations are minimum spillway flows, which are often regulatory requirements for aesthetic or environmental purposes, and spillway notch flows, which are features of some weirs that help meet minimum flow requirements. Weirs built with cuts or notches will discharge flow below the crest elevation, so these flows are allocated to the weir before any other rule-based allocation, and these flows do not contribute to the head water elevation. The notch flows are considered part of the minimum spillway flows, so if the minimum spillway flow requirement is not fulfilled after allocating the notch flows, then flow is allocated to the spillway before rule-based allocation. The flow allocation to the spillway is important for the fish passage models in Case Study B.

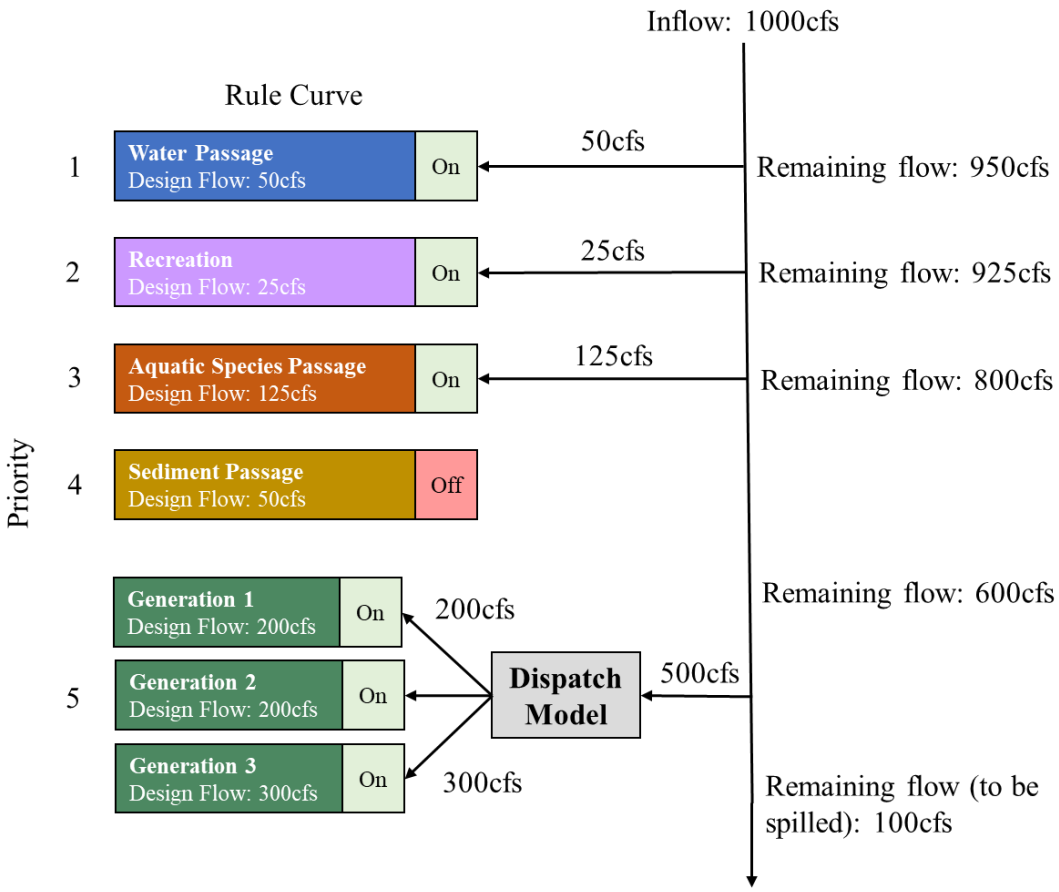

Figure 13. Example of rule-based programming for module flow allocation and operation.

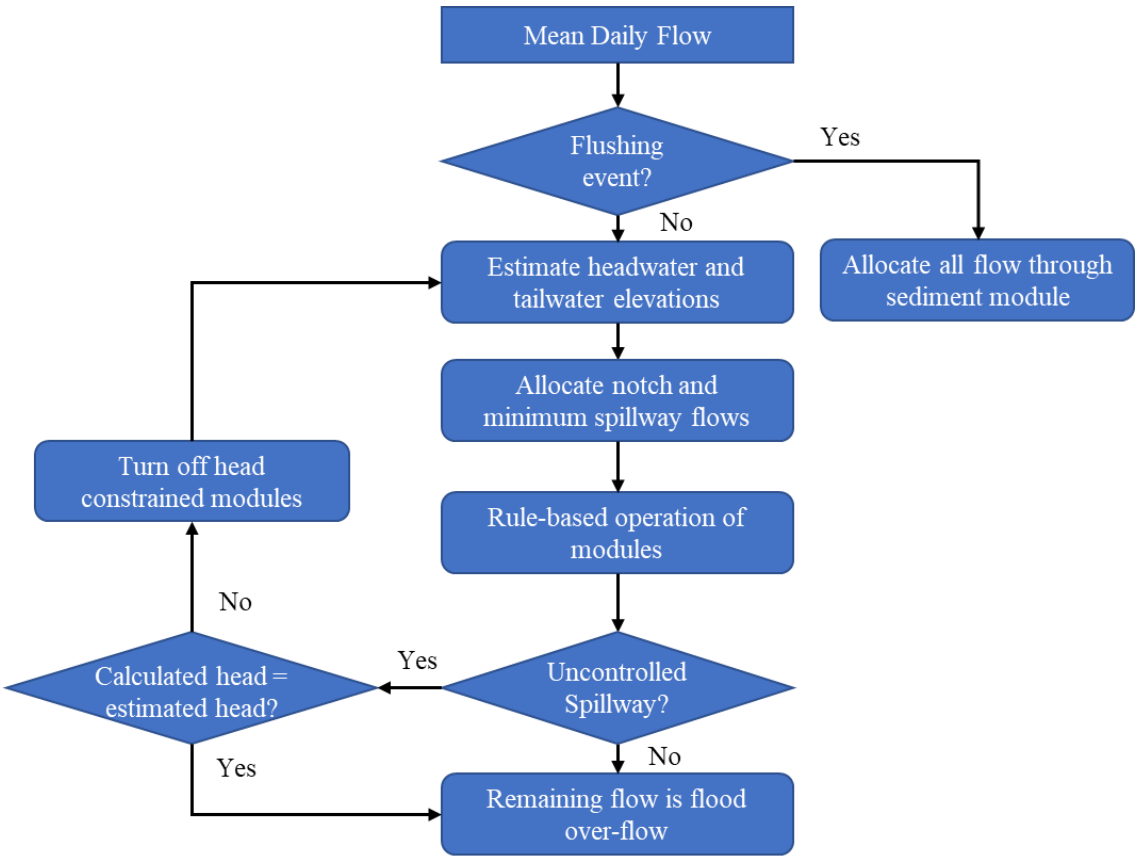

Figure 14. Operational flow chart.

Generation Dispatch Models

As illustrated in the literature review, optimal operation of hydropower turbines is a large field of research; however, the scopes of the problems studied varied significantly. The goal of the generation dispatch models in waterSHED is to quickly allocate flows between generation modules to provide the largest annual energy generation within realistic operating regimes. As described in Figure 13, the amount of flow available for generation is determined by the rule-based allocation method, and the dispatch model must allocate that flow across the modules that are operational at each timestep (not turned off based on the time of year or head constraints). The main constraint for this daily dispatch model is termed a ramping constraint, which means that once a turbine has been turned on at a given amount of flow, it should not be turned off at higher generation flows. Turning on and off turbines can damage the units because off-design hydraulic conditions can lead to cavitation and other forms of wear [48]. Ramping turbines too quickly can also be damaging; however, given the daily timescale of operation, it is assumed that the turbines can be ramped safely within the operating flow range. Algorithms must balance accuracy and computation time since dispatch is required at every timestep within the simulation, and multiple simulations may be needed for analyses in waterSHED. The context of SMH may provide benefits for simplifying dispatch. For example, the turbines will often have the same operating flows and efficiency characteristics. Given this problem statement, four dispatch models were created in waterSHED for different use cases with tradeoffs regarding computation time and performance. These methods are Design Ramping, Peak Ramping, Simple Greedy, and Advanced Greedy.

Before introducing the algorithms, it is important to establish the conceptual approach for this dispatch problem. The goal of dispatch optimization is to maximize power or $\rho g Q H \eta$. As previously described, the head across the facility depends on the inflow and the spillway characteristics. Within the context of the dispatch problem, a certain flow is allocated to the turbines, and the dispatch model should allocate as much of that flow as possible. If the dispatch model does not allocate all the flow and leftover flow is allocated to a weir, then the dispatch can affect the head across the turbines. However, the impact on head from the dispatch model is likely insignificant since the model will aim to maximize generation, so head can be assumed constant when dispatching. The power equation can thus be reduced to $Q\eta$. The flow and the flow efficiency are input attributes for the generation module, so waterSHED must handle a variety of efficiency curves. However, typically several principles apply to most efficiency curves. Figure 15 is an example of the reference Kaplan turbine efficiency curve used for Case Study A and highlights four major points on the curve: the minimum operating flow, the peak efficiency flow, the design flow, and the maximum operating flow. These points also correlate to the marked points in Figure 16, which illustrate the product of design flow percentage and efficiency ($Q\eta$). The Kaplan efficiency curve was adapted from Gordon [113] and the Case Study Report [17] to have a maximum $Q\eta$ at the design flow. This curve highlights that while the efficiency at the design flow is less than the peak efficiency for Kaplan turbines, the design flow still outputs the most power, because the

$Q\eta$ is higher. Turbines should only be ramped if the $Q\eta$ increases when additional flow is added. For example, the $Q\eta$ decreases after the design flow in Figure 16, so this unit should not be operated above the design flow. The optimization procedures can leverage $Q\eta$ to search for the allocation that will provide the greatest power output.

The first dispatch method is called Design Ramping. This method is the simplest and the fastest computationally. When provided a powerhouse flow, the algorithm ramps the turbines up to their design flows in order from smallest to largest design flow. Once a turbine is ramped to the design flow, the next turbine is turned on if there is enough flow to meet the minimum flow requirements. When turbine overrun is allowed and all modules are ramped to their design flows, the modules are ramped to the max design flow, from smallest to largest. Ramping in this order ensures that low flows can be captured by operating the smallest module first. However, turbines in an SMH design are often the same size, so the size order may be arbitrary. This method is effective when the peak efficiency occurs at the design flow and the $Q\eta$ is increasing across the operating flow range. Each dispatch method was evaluated in terms of speed and optimality in the case studies.

The second dispatch method is called Peak Ramping and is similar to the Design Ramping method, except that the modules are all ramped to the peak efficiency flow before ramping to the design flow. So, in order of smallest to largest, the modules are ramped to the peak efficiency flow if possible. If the remaining flow is sufficient to turn on another module, then the module is turned on and allocated the rest of the flow. Otherwise, the remaining flow is used to ramp the modules to their design flow from the peak efficiency flow. When turbine overrun is allowed and all modules are ramped to their design flows, the modules are ramped to the max design flow, from smallest to largest. This method is effective when the peak efficiency flow occurs below the design flow and the $Q\eta$ is increasing across the operating flow range. Case Study A shows that this method performs better than the Design Ramping and Simply Greedy methods with similar computation times.

The third dispatch method is Simple Greedy, which uses a greedy algorithm to simulate the ramping process. The process starts with the minimum turbine flow and iterates by 1cfs until the maximum powerhouse flow (the sum of max operating flows for all modules). For each flow increment, the algorithm calculates the increase in $Q\eta$ for each possible flow allocation and then chooses the allocation with the maximum increase in $Q\eta$. The flow unit is not allocated to any modules above their design flow (max operating flow if turbine overrun is allowed), and new modules are not turned on unless the flow unit exceeds the minimum operating flow. If the unit of flow cannot be allocated at an iteration, it is accumulated for the next iteration until it is large enough to turn on the next turbine. Additionally, if there is no increase in $Q\eta$, then the flow is not allocated and is accumulated for the next iteration. The flow allocation is saved between runs so that the dispatch of the next unit of flow is dependent on the previous dispatch. This process simulates the real-world scenario where turbines are online, and operators must allocate

incremental changes in flow. This method is slightly slower than the Design and Peak Ramping methods but faster than the Advanced Greedy method. This method performs similarly to the Design Ramping method because the incremental increase in $Q\eta$ is always higher for a turbine that is on for small increments of flow; however, it is more effective than the Design Ramping when there are different generation module types in the facility. The computational speed depends on the powerhouse flow range and the number of generation modules. This method is primarily used to compare a naïve greedy method to the other methods.

The last method is called the Advanced Greedy method, which improves upon the Simple Greedy's limitations by making better decisions about when to turn on turbines. The algorithm operates similarly to the Simple Greedy by iterating between the minimum and maximum powerhouse flows by 1cfs. However, the algorithm keeps track of which turbines have been turned on rather than the previous allocation. Once a module is turned on, it cannot be turned off. During each iteration, the algorithm decides between turning on a new module or allocating the available flow to modules that are already on. The greedy algorithm used for the Simple Greedy method is run for each case (one run for each module that is not turned on plus one for the allocation to the already ramped modules). Running multiple greedy algorithms is computationally expensive but does lead to improved dispatch, as illustrated in the case studies. Unlike the Design and Peak Ramping methods, this method can essentially ramp down turbines that are already on to bring another turbine online. For Kaplan turbines (Figure 15) with a flat and wide peak efficiency range, there are limited efficiency losses when ramping down a turbine to help another turbine turn on. The performance and behaviors of each method are described in the case studies.

Energy Model

Energy generation is an important part of any hydropower design model because electricity sales are the main source of revenue. A version of the hydropower equation, shown in Equation 3, is used to calculate the power produced by a Generation module for a given inflow. As described in the Module Classes section, the turbine performance is quantified by the flow and head efficiency equations. Both equations are parameterized in relation to the design parameter. While head efficiency equations are not widely used, they provide a useful alternative to Hill charts, and head losses are expected to be a relatively small part of generation losses compared to the role of head changes. An example head efficiency curve used for the case studies and adapted by Gordon (2001) is shown in Equation 4 [113]. The flow allocated to a generation module ($Q_{m,t}$) is determined by the flow allocation and dispatch models. The net head across the module ($H_{m,t}$) is calculated using Equation 5, which represents the gross head (headwater and tailwater difference) minus head losses ($H_{loss,m}$) from any relevant screen objects. The screen head losses can be a function of the flow through the screen and or the screen area, although only flow is shown in Equation 5. Case Study B provides an example of a screen head loss equation in Equation 31.

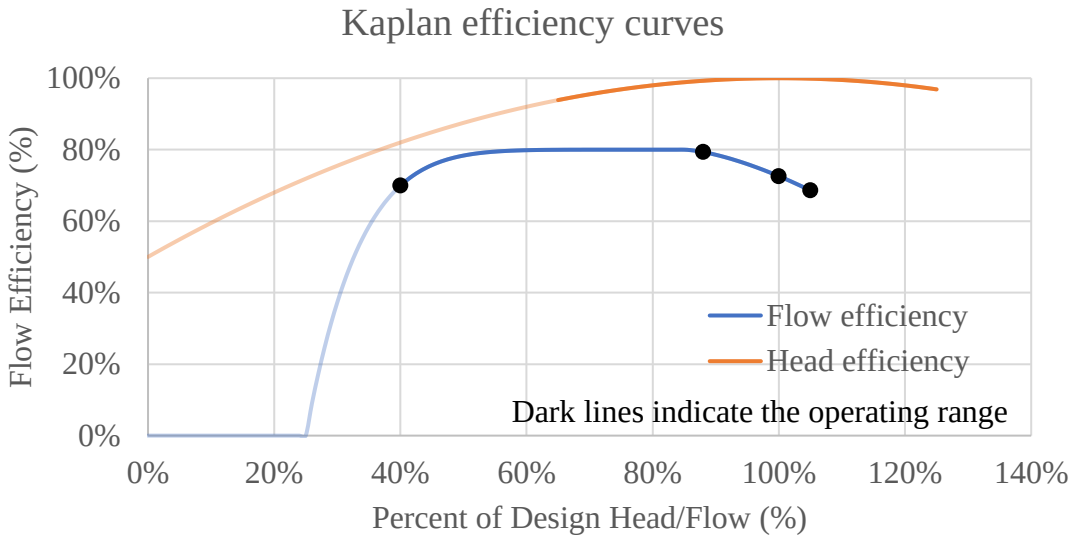

Figure 15. Flow and head efficiency curves for the reference Kaplan turbines used in Case Study A.

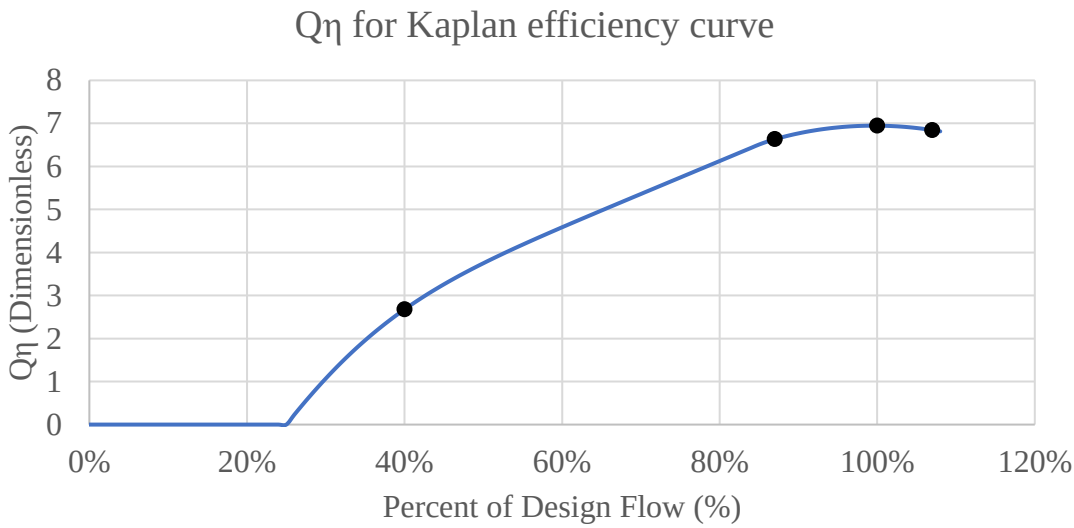

Figure 16. Efficiency flow product curve for the reference Kaplan turbine.

Power output (kW)

$$P_{m,t} = \left(\frac{1kW}{737\frac{lb_f ft}{s}}\right)\gamma\left(Q_{m,t}\right)\left(H_{m,t}\right)\eta_{Q,m}\left(\frac{Q_{m,t}}{Q_{m,des}}\right)\eta_{H,m}\left(\frac{H_{m,t}}{H_{des,m}}\right) \quad \text{Equation 3}$$

$Q_{m,t}$ The flow allocated to module *m* at time *t*. (cfs)

$Q_{m,des}$ The design flow of module *m*. (cfs)

$\eta_{Q,m}$ The flow efficiency curve of module *m*. (%)

$H_{m,t}$ The net head across module *m* at time *t*. (ft)

$H_{des,m}$ The design head of module *m*. (ft)

$\eta_{H,m}$ The head efficiency curve of module *m*. (%)

γ Specific weight of water (assumed 62.4 lb_f/ft^3).

Default head efficiency equation (%)

$$\eta_{H,m}\left(\frac{H_{m,t}}{H_{des,m}}\right) = -0.5x^2 + x + 0.5 \quad \text{Equation 4}$$

Net head across turbine (ft)

$$H_{m,t} = Z_{head,t} - Z_{tail,t} - H_{loss,m}\left(Q_{m,t}\right) \quad \text{Equation 5}$$

Given the daily time step, the module is assumed to generate the same power for the entire day, so daily energy production is calculated by multiplying the power by 24 hours. Finally, the annual energy generation is computed by annualizing the sum of the daily energy production for each module for the entire simulation, as illustrated in Equation 6.

Annual energy generation (MWh/year)

$$E_{ann} = \left(\sum_{t}^{T}\sum_{m}^{Gn} P_{m,t} * 24hrs\right)\left(\frac{T}{365}\right)\left(\frac{1MWh}{1000kWh}\right) \quad \text{Equation 6}$$

Fish Models

Chapter Two finds that it is important to understand the barrier effects of run-of-river hydropower plants. Fish passage is critically important to hydropower stakeholders and regulators, so literature has worked to quantify the complex nature of fish passage behavior [143]. The success of upstream and downstream fish passage measures vary widely between projects and depends on many factors, including climate, water quality, location, hydraulics, species preferences and capabilities, and even lighting [50]. The purposes of the fish passage models proposed in this section are not to predict technology-specific performance but to provide first-order approximations of facility-level performance from studied technology-level performance metrics and to quantify the expected tradeoffs between design decisions and fish passage performance. A downstream effective mortality model and an upstream effective fish passage model were

created for these purposes. Both models are novel and need to be validated with field data in future research but are informed largely by literature on fish passageways and fish behavior and accurately capture the conceptual linkages between design considerations [143].

Effective Downstream Mortality

Effective downstream mortality is a novel metric describing the expected time-averaged mortality rates for a species over the simulation. This value is based on the flow allocation, module guidance efficiencies, and module mortality rates. These metrics are common in the literature but are typically used with different technology classes. For example, mortality rates are measured for turbines and sometimes spillways [79], while guidance efficiencies are measured for fish guidance structures (e.g., bar racks, louvers, bubble screens) [80]. Mortality rate and guidance efficiency represent the two main factors in downstream fish passage. First, fish are guided by physical barriers or behavioral devices away from undesirable pathways and toward safe bypasses. These deterrents are rarely 100% effective for all species, so some individuals may still travel through undesirable pathways (i.e., modules). The percentage of fish that are successfully guided away from the module is the guidance efficiency, where 100% means that all fish are deterred from the module. Then, fish must pass through the modules. Turbines and other conveyances can injure fish via several modes, including rapid decompression, blade strike, cavitation, turbulence, and shear forces [79]. The risk of injury is often quantified by the mortality rate because it provides a clearer distinction than other measures of trauma [79]. A 100% mortality rate indicates that all fish entering the module are killed. Fish bypasses are designed for low mortality rates by providing gradual descents. The rate of refusal, the impacts of delayed migration and predation, and delayed mortality are more difficult to determine from empirical evidence, so this model assumes that any factor that creates an inability to pass safely and reach suitable habitat should be included in the mortality rate. Impingement can also occur where fish contact intakes or screens and cannot flee due to high velocities, which can be captured in the mortality rates for modules or screens.

In addition to the mortality and guidance metrics, flow allocation plays a role in the likelihood of an individual approaching a given technology. Migratory fish aim to minimize energy expenditure while swimming downstream, so they tend to follow the bulk flow [143]. Although swimming behavior is species-specific, this formulation (Equation 7) assumes that the proportion of fish approaching a given module is proportional to the module's relative discharge (module flow divided by total flow). With this assumption, each module's expected “fish flow” is computed by multiplying the module flows by the inverse of the guidance efficiency, representing the percent of fish entering a module despite guidance structures. Each module should have a guidance efficiency for each species. This formulation is lossless, meaning that all fish that enter the facility will go through one of the modules (since refusals are incorporated as mortalities). As such, the model considers that if a fish is initially guided away from module A, it may return after being excluded from module B. Thus, the probability of fish going through a given module is calculated as the proportion of the module’s fish

flow to the sum of fish flow across the facility. This captures the desired behavior because although module A has a 60% guidance efficiency, if module B has an 80% guidance efficiency, then more fish will likely go through module A despite high guidance efficiencies. Fish bypasses with 0% guidance efficiency will collect most of the fish excluded from other modules. Then, multiplying the mortality rates of each module by the percentage of fish flow through that module gives the amount of fish flow through each module. This enables the calculation of the effective mortality across the facility at a given timestep for a given species, shown below.

Effective mortality at a timestep (%)

$$\mathrm{M}_{\mathrm{eff,s,t}} = \sum_{m}^{Fa} \frac{(1 - G_{m,s})Q_{m,t}M_{m,s}}{\sum_{m}^{Fa}(1 - G_{m,s})Q_{m,t}} \qquad \text{Equation 7}$$

$G_{m,s}$ Guidance efficiency of module *m* for species *s*. (%)

$M_{m,s}$ Mortality rate of module *m* for species *s*. (%)

$Q_{m,t}$ Flow allocation to module *m* at time *t*. (cfs)

The effective mortality across the simulation and across multiple species is calculated by taking the average across the simulation time and the number of species, as shown in Equation 8 below. The facility's goal should be to minimize this value in coordination with the other objectives and create a “transparent” facility.

Cross-species effective downstream mortality (%)

$$\mathrm{M}_{\mathrm{eff}} = \sum_{t}^{T} \sum_{s}^{Sp} \frac{M_{eff,s,t}}{SpT} \qquad \text{Equation 8}$$

In addition, Screen objects add another layer of complexity to implementing this model. The effective mortality model allocates fish flow across modules at the same “level” of the facility. However, screens create separate levels since lateral mobility is limited. For example, if a fish passes a fish screen, it is assumed that the hydraulic and physical barriers limit the ability of the fish to leave the facility upstream. Therefore, the fish that pass the screen can only be distributed across modules within the screen. This process resembles a decision tree where the fish make a series of choices as they encounter screens and modules. To solve this problem, when a facility has a screen object, it is turned into a tree structure, which creates a hierarchy with the most upstream screens/modules at the top and branches to indicate modules within the screen coverage. The model is then applied iteratively through each branch to allocate fish within the same branch level. An example tree structure for an example facility is illustrated in Figure 17.

This mortality model simplifies an extremely complex process; however, it considers the tradeoffs between flow allocation over time and technology selection, which are not considered in existing studies. In addition, the proportional approach to fish flow should be validated using real-world data and facilities with multiple pathways. Despite the lack

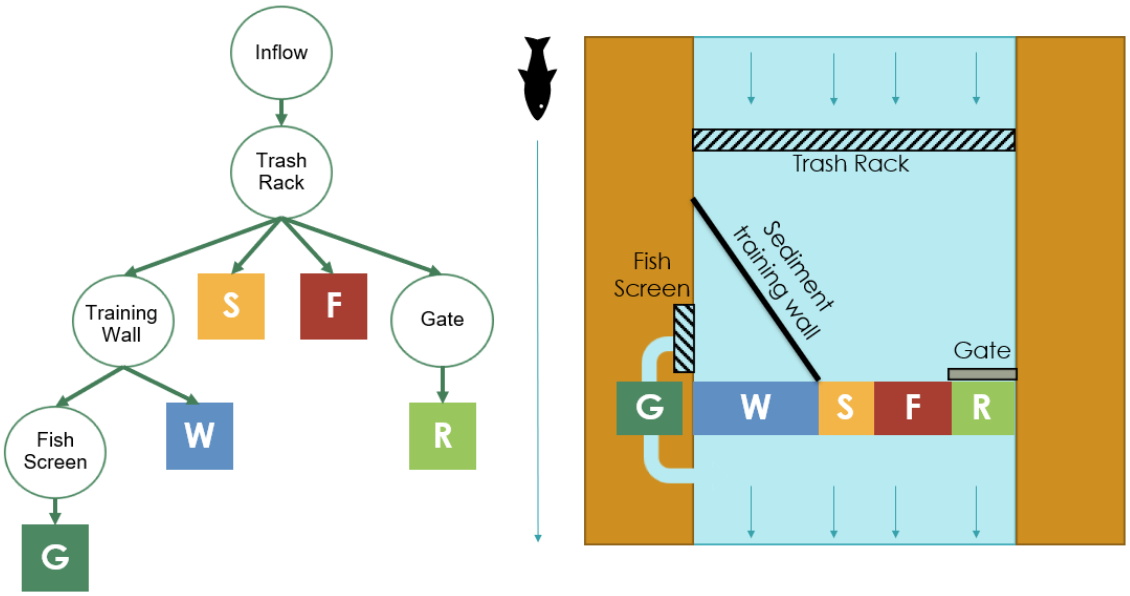

Figure 17. Example screen tree implementation for an example facility layout.

of real-world validation, this formulation captures the expected tradeoffs, including modules without exclusion measures and larger flows will attract more fish, and turbine mortality rates can be reduced with exclusion measures but are rarely zero, especially for modules with high relative discharges.

Effective Upstream Passage

The effective upstream fish passage efficiency model was formulated similarly to the effective downstream mortality model. This model was designed for volitional fishways, which are increasingly common for low-head projects where the aim is to provide passage with minimal delay, injury, or energetic losses. Volitional structures are designed to create hydraulic conditions that attract and pass different species that move on their own accord, but they require flow to create these conditions [77]. While numerous technology-specific studies examine the effectiveness of a particular fishway, there are no existing approaches for modeling multi-species passage across a facility with more than one passage structure. The proposed model pulls technology-specific metrics and general knowledge about fish passage into a novel approach for predicting fish passage effectiveness and the tradeoffs between flow allocation and technology selection.

Upstream aquatic species passage effectiveness is typically measured by total passage efficiency or the number of fish that can successfully ascend a facility compared to the number of migratory fish that approach the facility. Total passage efficiency is widely considered the product of three efficiencies related to the steps during passage [50]: the attraction, entrance, and passage. These efficiencies have been computed for various fishway types and vary widely depending on factors like species physiology and flow conditions [95]. Fishways are designed to accommodate the swimming behavior of a target species, so the entrance and passage efficiencies are parameterized as species-dependent attributes. The upstream entrance efficiency is the percentage of individuals that can successfully enter the module after being attracted to the entrance. An entrance efficiency of 0% means that no fish can enter the module, while an entrance efficiency of 100% means that all fish can enter safely. The entrance efficiency depends on the velocity, area, location, species, and many design-dependent parameters, so it is considered a module attribute. Upstream passage efficiency is the percentage of individuals that can successfully ascend the module after entering. A passage efficiency of 0% means that no fish can ascend, while a passage efficiency of 100% means that all fish can ascend safely. Like entrance efficiency, passage efficiency is determined by the internal hydraulics of the structure, namely slope, so it is incorporated as a module attribute. For example, pool and weir fishways have large, slow pools that allow fish to rest between jumps, while others, like Denil fishways, aim to create attractive velocities for strong swimmers [130].

Attraction efficiency is the percent of migratory fish within the project boundary that approach a given module within a certain distance. Swimming behavior is not often random because migratory fish follow signals that lead to suitable habitats [143]. Fish tend to follow the mainstem river, so they are signaled by flow allocation. The flow through fish passage structures must be sufficient compared to the total inflow to attract

fish to the entrance [144]. The ratio of module flow to the total inflow is called the module relative discharge. Several cases have shown low passage efficiencies are related to insufficient attraction flows [95]. The higher the attraction flow, the better, but industry standard says that 10% of the total inflow is recommended; however, 1-5% can be sufficient if entrances are properly placed and the total flow is relatively high [144], [145]. Although attraction efficiency is a function of the relative discharge, studies often record an average attraction efficiency for a given technology rather than model attraction as a function of relative discharge.

The formulation in this study relies on the conceptual understanding of attraction, entrance, and passage efficiencies to create an effective upstream aquatic species passage metric that captures technology selection and flow allocation tradeoffs. The first step is to estimate attraction efficiency. There is limited literature on quantitative methods for assessing attraction separately from entrance efficiency. As a novel approach, the attraction efficiency was formulated as a sigmoid function that depends on the module relative discharge and two species-specific parameters. In Equation 9 below, the attraction efficiency is modeled using a logistic curve ("S-Curve") that acts as a step function so that once a user-defined relative discharge threshold is met, the attraction efficiency is near 100%. The parameter a_s is called the relative discharge parameter and is used to establish where the threshold starts for a given Species object. Equation 9 uses the inverse of a_s so that larger values of a_s relate to a higher relative discharge threshold. The b_s is called the attraction sensitivity parameter and determines how steep the step function is for a given Species object. Higher values of b_s indicate a steeper step function, which will more drastically lower attraction if the relative discharge threshold is not met. The product $a_s \times b_s$ determines the relative discharge where the 50% attraction efficiency will occur. As illustrated in Figure 18, an a_s value of 0.3 and a b_s value of 0.03 (the baseline condition for Case Study B) creates a curve that reaches an efficiency of 99% at relative discharges of around 2% and an efficiency close to 0% at relative discharges less than 0.1%. The a_s and b_s parameters, as well as, the shape of the curve should be validated using real data, but the estimated form does represent qualitative expectations from the literature.

Attraction efficiency factor

$$A_{m,s,t} = \frac{1}{1 + e^{-100\left(\left(\frac{1}{a_s}\right)Q_{m,t}/\sum_m^{Fa} Q_{m,t} - b_s\right)}} \qquad \text{Equation 9}$$

a_s, b_s Species attributes used to shape the sigmoid function (dimensionless)

$Q_{m,t}$ The flow allocated to module *m* at time *t*. (cfs)

Like the downstream passage model, the next step is to estimate the probability of fish entering a given module. The model (Equation 10) assumes that fish can only make one attempt to pass through the facility to simplify the calculation. Energy used in unsuccessful attempts may preclude fish from making second attempts. Based on this assumption and the fact that fish can only enter one module at a given time, the entrance probability is lossless, meaning that the sum of probabilities to enter each module is

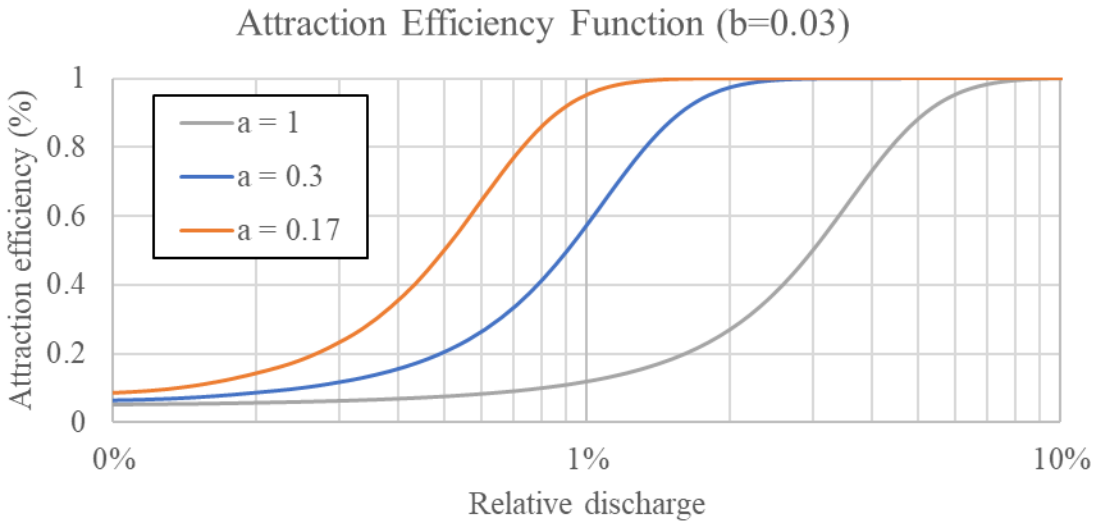

Figure 18. Attraction efficiency function for upstream fish passage.

100%. So, the probability of a fish selecting a given module is calculated by multiplying the module's entrance and attraction efficiency and dividing it by the sum of these products for all modules. Thus, modules with high attraction and entrance efficiencies will attract the most fish but competing flows from other modules with non-zero entrance efficiencies can detract from entrance probabilities. The resulting proportion of fish flow is multiplied by the entrance, attraction, and passage efficiencies. Summing the effective passage for each module gives the percentage of a species that can ascend the facility at a given timestep. These values can then be averaged over the simulation time and across species to get a metric (Equation 11) that describes the facility's performance over the simulation time.

Effective upstream passage at a timestep (%)

$$U_{m,s,t} = \frac{E_{m,s}A_{m,s,t}}{\sum_{m}^{Fa} E_{m,s}A_{m,s,t}} E_{m,s}A_{m,s,t}P_{m,s} \quad \text{Equation 10}$$

$E_{m,s}$ The entrance efficiency of module *m* for species *s*. (%)

$P_{m,s}$ The passage efficiency of module *m* for species *s*. (%)

Cross-species effective upstream passage (%)

$$U_{eff} = \sum_{t}^{T}\sum_{s}^{Sp} \frac{\sum_{m}^{Fa} U_{m,s,t}}{SpT} \quad \text{Equation 11}$$

Attraction and entrance efficiencies are also significantly influenced by the location of the entrance. Fish tend to swim along the banks of the rivers where considerable velocity gradients exist and proceed as far upstream before entering structures, although the behavior is species-dependent [143]. The spatial component of fish attraction is outside the modeling capabilities of waterSHED, so the proposed model assumes that aquatic species modules are placed in appropriate locations along banks at the most upstream point. Thus, the losses in attraction and entrance efficiency from placement are negligible. Other factors can also influence overall passage effectiveness, such as fallback rate, delay, and trauma resulting from passage. These factors are not widely quantified in existing studies and are not considered in mortality metrics, so they are excluded from the proposed formulation.

Sediment Models

Modeling the passage of sediment presents several challenges for hydropower design models. First, information about the stream morphology and the local sediment composition is limited without in-person site assessments. Downstream scouring and upstream accumulation will also change the bedforms and sediment composition after development, so additional analysis is needed to extrapolate future conditions from site assessments [71]. Second, sediment accumulation on the scale that would impact dam operation typically occurs over decades, whereas design models typically focus on daily timescales for generation operation. Third, there is limited information about the efficacy

of sediment passage technologies. Sluices, siphons, and gates rely on water to pass sediment. The amount of sediment passed per unit of water depends on the amount of sediment accumulation and the design/placement of the technology. Several studies question whether low-head dams are effective sediment traps [51], [146]. Additionally, sediment may accumulate in ramps and pass safely over spillways without low-level outlets, reducing the need for dedicated sediment modules [134].

Performance Metrics

Nonetheless, sediment continuity is an important goal for operational and ecological health, so understanding the tradeoffs for SMH projects at least at a high level is critical. Several performance metrics were created to quantify high-level sediment performance, including the sediment module flow ratio, sediment passage frequency, and average trap efficiency. These models are not meant to model volumetric sediment flows but rather to track the operational characteristics of the reservoir and sediment passage modules that are correlated with improved sediment passage.

The sediment module flow ratio is the average ratio of flow allocated to sediment modules to the total inflow at each timestep. Assuming sediment passage technologies work as intended, the more flow allocated to sediment modules, the better the sediment continuity performance. The formulation (Equation 12) below is a simple ratio of the total flow allocated to sediment modules divided by the total inflow. The sediment module flow ratio is a percentage (0-100%) that should be maximized. The primary disadvantage of this approach is that the ratio between sediment module flow and volumetric sediment flow is rarely constant. Different passage technologies may pass more (or less) sediment per unit of flow than others. In addition, sediment transport can become supply-limited, particularly at high flows, so transport rates may change based on inflow and the amount of accumulated sediment [146]. Volumetric models would require in-depth data on the sediment inflow, the bedforms, and the hydraulics during passage. The model only considers bed loads passed by sediment modules rather than suspended loads through other modules like turbines or spillways. Thus, this metric should be used in conjunction with the other two sediment performance metrics to judge qualitatively whether the facility is likely to accumulate sediment.

Sediment module flow ratio (%)

$$P_{sed,mfr} = \sum_{t}^{T} \sum_{m}^{Sd} \frac{Q_{m,t}}{Q_{in,t}} \qquad \text{Equation 12}$$

$Q_{in,t}$ The inflow into the facility at time *t*. (cfs)

Sediment passage frequency is the ratio of sediment passage events to total timesteps. The timing of sediment passage is important to consider, along with the quantity of sediment flows. The goal of sediment continuity means that the sediment passage frequency is 100%, assuming sufficient transport capacity. Studies have shown that more frequent but smaller flushing events are environmentally preferred to larger flushing

events less frequently [51], [94]. As such, facilities should aim to maximize sediment passage frequency if sediment continuity is desired. However, continuous sediment flows are not needed to limit sediment accumulation since sediment inflows are often caused by seasonal high flow events [147]. Therefore, acceptable frequencies must be determined in accordance with any available sediment inflow data and the other sediment performance metrics. This metric is particularly helpful when using sluicing operation, in which the frequency of operation is not explicitly defined. The probability of entrainment model (described later in this section) provides some insight into the operating flow that should be used based on the median sediment size class, the river slope, and the preferred probability of entrainment. The formulation below is a simple approach that counts the number of timesteps where the flow allocated to all sediment modules is greater than zero and divides this by the number of total timesteps. If there is more than one sediment module, then only one of the sediment modules must be on to count as sediment passage.

Sediment passage frequency (%)

$$P_{sed,freq} = \frac{1}{T}\sum_{t}^{T} f_{on}\left(\sum_{m}^{Sd} Q_{m,t}\right) \qquad \text{Equation 13}$$

On function

$$f_{on}(Q) = \begin{cases} 1\ ;\ Q > 0 \\ 0\ ;\ Q \leq 0 \end{cases}$$

The average trap efficiency is the average percentage of incoming sediment that accumulates in the reservoir. The metric can be a percentage based on volume or weight, but that distinction is not needed in this formulation. Over the project's life, accumulated sediments can reduce storage capacity, impact water quality, and lead to service interruptions [35]. Smaller ROR impoundments have been shown to have limited sediment trapping [146], so this metric may not apply well to low-head projects with small headponds and minimal sediment inflow. In these cases, the estimated trap efficiency will be negligible. The true trap efficiency is based on the sediment composition, the reservoir shape, the modes of sediment passage, climate, and several other variables [148]. Therefore, this metric is only a first-order approximation, and further investigation is required to determine the likelihood of significant sediment accumulation.

The model for trap efficiency (Equation 14) is based on the trap efficiency equation from Siyam [137] as reported in Eizel-Din [149]. Siyam [137] created the equation using empirical evidence to generalize the Brune model [68], which asserts that the trap efficiency is a function of the capacity-inflow ratio (i.e., the reservoir volume divided by the average annual inflow). The Brune model was selected for its simplicity, accuracy compared to other models [135], and compatibility with the variables defined in waterSHED. The sedimentation parameter β used in this model captures the reduction in reservoir storage due to sedimentation [150]. Higher β values (range between 0 and 1) indicate that the reservoir is less likely to deposit sediment for a given capacity-inflow ratio, like in the case of semi-arid reservoirs with small particle sizes. According to Siyam [137], the β values of 0.0055, 0.0079, and 0.015 are related to the upper, median, and lower curves on the Brune model. The final metric (Equation 15) is adjusted per the

procedure in Lewis [151] to calculate daily trap efficiencies by annualizing daily inflows (converting $Q_{in,t}$ from cfs to ft^3/yr) and then summing the daily trap efficiencies using a flow weighted summation. According to Lewis [151], the flow weighting accounts for the fact that the majority of sediment is transported during higher inflows.

Annualized daily trap efficiency (%)

$$P_{trap,t} = 100e^{-\frac{365x60x60x24\beta Q_{in,t}}{V_{res}(Z_{head,t})}} \quad \text{Equation 14}$$

Average Trap Efficiency (%)

$$P_{trap,ave} = \frac{\sum_t^T P_{trap,t} Q_{in,t}}{\sum_t^T Q_{in,t}} \quad \text{Equation 15}$$

β The sedimentation parameter.

$V_{res}(Z_{head,t})$ The reservoir volume as a function of the headwater elevation at time *t*. (ft^3)

It should be noted that this model does not reflect the effects of sediment modules and only quantifies the expected effects of reservoir sedimentation on sediment continuity. Reservoir sedimentation allows suspended sediments to settle and become part of the bed, which are typically more difficult to pass. Smaller reservoirs have lower hydraulic residence times, which increases the likelihood of particles passing downstream before settling. The geometric reservoir volume model (described in the following section) can estimate reservoir volume when digital elevation models are unavailable. In addition, this trap efficiency model has been shown to overpredict sediment trapping in certain climates [151]. Therefore, designs should aim to minimize the trap efficiency of the reservoir, which is primarily determined by design decisions affecting reservoir size (i.e., normal operating level and spillway type). To achieve better sediment passage performance, the operation should either allocate more flow to sediment modules in cases of high trap efficiencies or decrease the normal operating level to decrease trap efficiency.

Reservoir Model

Reservoir volume is an important factor in sedimentation, water quality changes, and flood risk. The reservoir volume is a function of the normal operating level and the site's topography. For typical site investigations, digital elevation models can be used to digitize the topography and evaluate the volume and surface area relationships for a given site. However, elevation models may not be available with sufficient resolution for the small reservoirs involved. Instead, this relationship is parameterized through a stage-storage equation ($V_{res}(Z)$) that is an attribute of the Site object. Models for the storage (volume) estimation have been created specifically for small dams where GIS tools may be limited, such as through the geometric approach based on Lawrence and Cascio [152]. The reservoir volume is leveraged within the trap efficiency model described previously. Additionally, reservoir size is qualitatively associated with several negative environmental and social outcomes, so it is generally recommended to minimize the impoundment size [46]. For example, larger reservoirs can be correlated with more displaced communities, greater chances for lacustrine water quality conditions, and more significant modification of the flow regime [46].

For Case Study A, the geometric approach from Lawrence and Cascio [152] is used as a direct method of estimating small reservoir capacity [153]. This approach represents the reservoir valley cross-section as a pyramid with the base as the dam cross-section that extends upstream. The model described in Lawrence and Cascio [152] uses two constants (k_1 and k_2) that describe the shape of the valley-cross section, the maximum water depth at the dam, the width of the dam, and the throwback (distance from the dam to the entrance of the reservoir). All terms are multiplied together to determine the volume of the pyramid. Lawrence and Cascio [152] reviewed four different methods for identifying the k_1 and k_2 constants and compared to nine surveyed reservoir volumes, as summarized in Table 7. This formulation (Equation 16) combines the two constant terms into k_{res} to simplify the inputs and assumes that the throwback length is the headwater level divided by the stream slope. Figure 19 below illustrates how these parameters represent the reservoir control volume for different values of k_{res}. As described in Table 7, k_{res} should range between 0.5 to 0.16 with a recommended value of 0.26. Larger coefficients represent larger volume to stage ratios. The formulation below creates a function that determines the reservoir volume for a given headwater level. Through the course of the simulation, the reservoir volume and length may change depending on the headwater elevation, in which case Z_{op} is replaced by $Z_{head,t}$.

Reservoir volume (ft^3)	$V_{res} = k_{res} Z_{op} Y_s L_{res}$	Equation 16
Reservoir length/ throwback (ft)	$L_{res} = \frac{Z_{op}}{S_{river}}$	
Reservoir size factor	$k_{res} \sim \left[\frac{1}{6}, \frac{1}{2}\right]$	

Sediment Entrainment Probability Model

The Modeling LIR Hydropower using an Object-Oriented Approach section identified three operating modes for sediment modules, one of which is sluicing, in which the modules are only operated if the inflow exceeds an operating flow threshold ($Q_{op,m}$). Identification of the operating flow threshold is key for balancing sediment module flow ratio and frequency with the plant generation. A lower flow threshold will increase sediment passage frequency, but decrease flows available for generation. The probability of entrainment model from Elhakeem et al. [154] was used to provide insights from physical sediment modeling studies to select the operating flow threshold. This model aims to identify the likelihood that a particle size class in the bed will be mobilized for given flow conditions. To prevent sediment accumulation, sediment sluice gates should be operated whenever there is significant sediment mobilization that would otherwise deposit in the reservoir. The entrainment model uses information about the target sediment size, stream slope, and stage-discharge curve to determine the operating flow

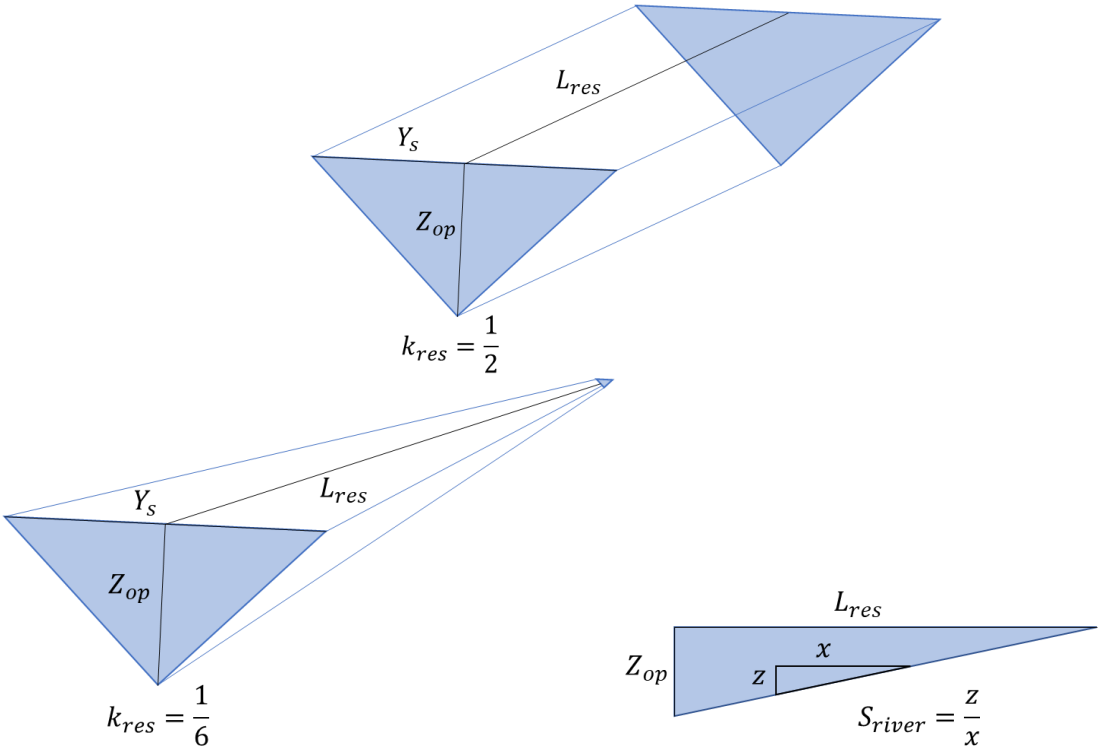

Figure 19. Illustrations of geometric reservoir approach with representative dimensions.

Table 7. Results of reservoir capacity estimation models from Lawrence and Cascio [152].

Method	k_1	k_2	k_{res}	**Ratio of predicted to surveyed volume**
USAID (1982)	0.4	1	0.4	1.36
Fowler (1977)	0.25	1	0.25	0.86
1/6 Rule	0.167	1	0.167	0.57
Nelson (1986)*	0.22	1.22	0.26	0.9

* In the Nelson method, k_2 is dependent on the valley cross-section. Lawrence and Cascio [152] assumed a value of 1.22 in their comparison.

for a user input probability of entrainment. This model has been used in the previous SMH Case Study Report [17], the system dynamics model by Sarah Dowda [134], and Case Study A.

In this approach, particles have a condition of incipient motion that is probabilistic and depends on the bed shear forces [17]. By estimating the bed shear force at a given timestep, the probability of entrainment for a representative particle size can be estimated, which is the likelihood that the particle is mobilized, separating from the active bed layer and moving downstream. The shear force can be estimated using the stage-discharge relationship of the upstream reach. The resulting probability vs. flow curve can be used to provide information about the sediment transport properties of the stream to aid in the selection of a design flow. The use of this model requires two additional inputs: a representative particle size (d_{50}) in millimeters and a probability of entrainment threshold $(P_{op,m})$. In this notation, d_{50} indicates the particle size in which 50% of bed material is finer, however, other particle sizes may be used as allowed by the Elhakeem et al. [154] model. Larger particle sizes would lead to higher operating flow triggers since larger flows are needed to mobilize the larger particles. Similarly, a higher probability of entrainment thresholds would lead to higher operating triggers since the probability threshold indicates the minimum probability of entrainment that must be met to open the sluice gate. Higher operating triggers would lead to less frequent operation, higher sediment accumulation between events, and less cumulative flow for the same design flow.

The Elhakeem et al. [154] model improves existing probabilistic models in several ways, like considering both bed surface irregularity and near-bed turbulence. The model was derived analytically and validated/calibrated using several lab-scale datasets that studied various sediment types. The following formulation has been adapted to use the variables in this model. This formulation requires five main steps.

Step 1. Determine the minimum critical shear stress

First, the model must determine the minimum critical shear stress required to mobilize the target particle class. Any shear stresses below this threshold have a 0% probability of mobilizing the target particle size class. Following the methodology of the SMH Case Study Report [17], two methods are used for calculating the critical shear stress, one for fine (sand) beds (Equation 17) and one for coarse (gravel) beds (Equation 18). The bed is assumed fine if the representative grain size (d_{50}) is less than 2mm, and coarse otherwise. For fine (sand) beds, the formula for critical shear stress is provided by Brownlie [155].

Minimum critical shear stress – fine beds

$$\tau_{*c} = 0.22R_p^{-0.6} + 0.06 \times 10^{-7.7R_p^{-0.6}} \qquad \text{Equation 17}$$

Particle Reynolds number	$R_p = \frac{d_{50}}{\upsilon}\left(\left(\frac{\gamma_s}{\gamma_w}-1\right)g d_{50}\right)^{0.5}$
Kinematic viscosity of water at 10˚C	$\upsilon = 1.31e^{-6}\frac{m^2}{s}$
Specific weight of sediment	$\gamma_s = 2650g\frac{N}{m^3}$
Specific weight of water	$\gamma_w = 1000g\frac{N}{m^3}$

For coarse beds, the equation for the critical shear stress is derived from Elhakeem [154] and based on the assumptions used in the SMH Case Study Report [17]. Per the recommendations in Elhakeem [154], several coefficients are assumed for fine and coarse beds, as summarized in Table 24 in the Appendix. $\beta = 15$ describes particle-flow interaction and accounts for the effects of particle protrusion and packing density. $C_D = 0.4$ is the drag coefficient and $C_L = 0.12$ is the lift coefficient. $R_r = 1.5$ is the relative roughness of the bed compared to a value of 1 for fine beds. By inserting the assumed coefficients, the model is simplified into a simple equation using the stream slope.

Minimum critical shear stress – coarse beds

$$\tau_{*c} = \frac{\cos(S_s)}{0.75(r_m C_D + C_L)f^2} = \frac{\cos(S_s)}{0.75(3.84 \times 0.4 + 0.12)8.50^2} = \frac{\cos(S_s)}{89.8}$$

$$r_m = \sqrt{3(R_r+1)^2 - 4} = \sqrt{3(1.5+1)^2 - 4} = 3.84$$

$$f = 2.5\ln(\beta R_r + 7.5) = 2.5\ln(15 \times 1.5 + 7.5) = 8.50$$

Equation 18

Step 2. Determine the maximum critical bed shear stress

The next step is to identify the maximum critical bed shear stress with a 100% probability of entrainment for the representative particle. Again based on Elhakeem [154], the form of the equation is the same for both fine (Equation 19) and coarse beds (Equation 20), but the assumed coefficients are different, as illustrated in Step 3. The model can compute max dimensionless shear stresses for fine and coarse beds by incorporating these assumed coefficients into the equation.

Maximum critical shear stress – fine beds

$$\tau_{*max,fine} = nCa((R_r+1)^2 - 1.333)^{-0.5} = 5 \times 0.6 \times 0.94((1+1)^2 - 1.333)^{-0.5} = 1.727$$

Equation 19

Maximum critical shear stress – coarse beds

$$\tau_{*max,coarse} = nCa((R_r + 1)^2 - 1.333)^{-0.5}$$
$$= 3 \times 0.4 \times 0.94((1.5 + 1)^2 - 1.333)^{-0.5}$$
$$= 0.509$$

Equation 20

Step 3. Define a probability function between the minimum and maximum critical shear stresses

Equation 21 from Elhakeem [154] defines the probability of entraining the target particle size class as a function of the bed shear stress. The formula uses the minimum critical shear stress value to determine m_c and applies to the range of shear stresses between the minimum and maximum critical shear stresses.

Probability of Entrainment (%)

$$P = \left[1 + e^{-0.07056m^3 - 1.5976m}\right]^{-1} - \left[1 + e^{-0.07056m_c^3 - 1.5976m_c}\right]^{-1}$$

Equation 21

$$m = \frac{X - \bar{X}}{\sigma_x};\ m_c = \frac{X_c - \bar{X}}{\sigma_x}$$
$$X = \ln(\tau_*);\ X_c = \ln(\tau_{*c})$$
$$\bar{X} = \frac{1}{2}(\tau_{*c}\tau_{*max});\ \sigma_x = \frac{1}{6}\ln(\tau_{*max}/\tau_{*c})$$

Step 4. Determine the bed shear stress for a given flow value

The previous equations set the dimensionless shear stresses corresponding to the minimum and maximum shear stresses. Now, the model must connect shear stress to river flow to identify the probability of entrainment for the range of inflows. Equation 22 below is a basic particle shear stress equation that uses the user input stage-discharge curve to determine the water depth.

Bed shear stress

$$\tau_* = \frac{\tau}{(\gamma_s - \gamma_w)d_{50}} = \frac{\gamma S_s Z_{stage}(Q)}{(\gamma_s - \gamma_w)d_{50}}$$

Equation 22

Step 5. Solve for the recommended flow given a probability of entrainment

Equation 21 in Step 3 describes the probability of entrainment as a function of shear stress, and Equation 22 in Step 4 describes the shear stress as a function of flow. Given the complex form of the probability of entrainment equation, linear interpolation was used to relate the probabilities to flow values. This is done by iterating through flow

values, calculating the shear stresses for each flow value, and then using the calculated shear stress to a corresponding list of probabilities. Finally, the user-defined probability of entrainment is compared to the list of probabilities and computed using linear interpolation between the nearest two probabilities in the list. The resulting model provides a flow value for a given entrainment probability and particle size, which can determine the sediment operating flow. The model is applied in Case Study A.

Social Performance Models

Social performance in the waterSHED model is described through the availability of recreation modules and the spillway design flood. As previously addressed, reservoir volume is also a measure of social performance that can impact displaced communities, upstream flood risk, and fishing/boating availability. For the case studies, the social performance focuses on recreation availability, and the spillway return period is established as an input.

Recreation modules must be designed with hydraulics that ensure the safe passage of recreationalists. Proper design includes safe drop heights, large recovery pools, and the exclusion of hydraulic rollers that can entrain passengers [131]. The internal module hydraulics often depend on the headwater and tailwater elevations, represented by minimum and maximum headwater and tailwater elevation limits that turn off the module whenever the hydraulic conditions become dangerous. These operating limits impact the availability of the passage module, which is the primary performance metric of recreation modules, as defined in Equation 23 below. The on function is used to determine the number of timesteps that the module is on and is allocated flow. Given the daily timestep, the model currently assumes that recreation modules are operated all day. Operation during daylight hours would require sub-daily dispatch, which is out of scope for this study but could be implemented in future research efforts.

Annual recreation hours (hrs)

$$P_{rec,hrs} = \left(\sum_{t}^{T}\sum_{m}^{Rc} f_{on}(Q_{m,t}) * 24\right) * \left(\frac{T}{365}\right) \qquad \text{Equation 23}$$

On function

$$f_{on}(Q) = \begin{cases} 1\ ;\ Q > 0 \\ 0\ ;\ Q \leq 0 \end{cases}$$

In addition to the annual recreation hours, the model calculates an average recreation availability factor that measures the ratio of the timesteps that the recreation modules are on to the timesteps that the modules should be on. This metric helps determine the effect of head limitations on the module operation. In Equation 24 below, the availability function is used to determine the number of timesteps that the module should be on, given the operating months set by the user.

Recreation availability factor (%)

$$P_{rec,avail} = \frac{\sum_{m}^{Rc}\sum_{t}^{T} f_{on}(Q_{m,t})}{\sum_{m}^{Rc}\sum_{t}^{T} f_{avail}(Q_{m,t})} \qquad \text{Equation 24}$$

On function $$f_{on}(Q) = \begin{cases} 1\ ;\ Q > 0 \\ 0\ ;\ Q \leq 0 \end{cases}$$

Availability function $$f_{avail}(Q_t) = \begin{cases} 1\ ;\ t\ \in\ T_m \\ 0\ ;\ else \end{cases}$$

T_m The set of operating months for module m.

The spillway return period is the flood year capable of being passed through the spillway. Hydropower facilities are typically required to have spillways to pass excess flows in case of flooding or outages. When designing the spillway, designers must balance the cost of the spillway with the risk of flooding. This tradeoff is often discussed using the design flood of the spillway, which describes the maximum flow that can safely pass through the spillway. The design flood can also be described by its return period, the expected time between flood events. Standards suggest that small hydropower facilities should design for at least the 50-year flood, although up to the 100-year flood is recommended [89]. This design flood also depends on the cost of flood damages, which is different for earthen versus concrete dams. New modular designs, like the reference designs used in Case Study A, may be designed for overtopping to reduce spillway costs by using a smaller design flood.

Calculating the return period requires conducting a flood frequency analysis that uses historical peak flow data to estimate a curve relating flows to the likelihood of occurrence. The analysis used in this study follows the same method used in the previous SMH Case Study Report [17], which can be referenced at the Oregon State University website [156]. This method uses a Log Pearson Type-III distribution, recommended by the USGS Bulletin 17B [157], to fit the sorted historical data. Detailed equations are provided in the Flood Frequency Analysis section in the Appendix. The estimated curve is only as accurate as the flood data available, which differs between sites. In addition, this method only outputs the return period for a discrete set of flood years, so linear interpolation was used to interpret the flow values between these flood years to create a flood frequency function.

Economic Models

Project costs, both capital and operating, are key considerations when estimating feasibility and optimizing facility design. In conventional hydropower designs, the costs of civil works are largely site-specific, depending on site conditions, the selected dam type, the turbine sizes, and required environmental mitigation measures. Studies of hydropower costs typically use “top-down” empirical models to predict total costs as a function of plant capacity and the design head and then determine component costs based on the relative portions of the total costs [9]. Oppositely, itemized cost models use a “bottom-up” approach to determine total costs based on the sum of equipment costs. Itemized costs models can be more accurate, but estimates from equipment vendors are often customized for specific design or site conditions. Standard modular hydropower may change the development process from custom designs and pricing to off-the-shelf products with standard prices or even prices that decrease with the number of orders due

to economies of scale. Given these considerations, the waterSHED model employs an itemized cost module where each module has a cost, and the capital cost equals the cost of each module times the number of modules. However, several other factors like licensing and engineering costs are not module-based, so they must be included separately. The following models described how the waterSHED model uses module-based costs to calculate initial capital costs (ICC), net present value (NPV), and levelized cost of energy (LCOE) from simulation runs.

Initial capital costs (ICC) represent the one-time expenses used to purchase or construct capital assets, such as buildings, land, and equipment. These are also known as "hard costs" because they are associated with tangible physical infrastructure. The main components are the module capital costs, the one-time costs to prepare a module for operation, such as material, equipment, installation, and transportation. Capital costs not tied to a particular module, like land, interconnection infrastructure, or signage, are also included through the additional capital costs attribute of the Cost Table object. The ICC is different from the total initial cost of the project because it does not include "soft costs," such as the overhead, engineering, contingency, and any additional non-capital costs. The soft costs can be even harder to estimate than equipment costs, so if lump-sum costs are unknown, they are estimated as a percentage of the ICC. Equation 25 below shows the ICC as the sum of module capital costs and the Cost Table's additional capital costs. The summation includes the module capital costs times the number of modules in the facility. The number of passage modules set in the optimization process and the number of non-overflow and foundation modules are automatically calculated based on the additional stream width that must be covered and the facility footprint.

Initial capital costs ($)

$$C_{icc} = C_{cap} + \sum_{m}^{Fa} C_m \qquad \text{Equation 25}$$

C_{cap} The additional capital cost attribute of the Cost Table object. ($)

C_m The capital cost of module *m*. ($)

The total cost of the project describes all the one-time costs required to begin operation. This value does not include any operating or maintenance costs incurred after commissioning. As shown in Equation 26, the total cost sums the initial capital costs and the soft costs from the Cost Table object. In addition, several soft costs, including overhead, engineering, and contingency costs, can be input as either a lump sum or a percentage of ICC. Both methods are shown below.

Total Cost – all input as lump sums ($)

$$C_{tot} = C_{icc} + C_{over} + C_{eng} + C_{cont} + C_{non} \qquad \text{Equation 26}$$

Total – all input as % of ICC ($)

$$C_{tot} = C_{icc}\left(1 + C_{over} + C_{eng} + C_{cont}\right) + C_{non}$$

C_{over}	The cost of overhead described as either a lump sum or a percent of initial capital cost. ($ or %)
C_{eng}	The cost of engineering described as either a lump sum or a percent of initial capital cost. ($ or %)
C_{cont}	The contingency costs described as either a lump sum or a percent of initial capital cost. ($ or %)
C_{non}	The additional non-capital cost attribute of the Cost Table object. ($ or %)

Net present value (NPV) is the current value of the project based on the total cost, expected revenue, annual maintenance expenditures, and discount rate assumptions. The goal of the simulation process is to estimate the annual benefits and annual costs that are incorporated into the NPV calculations. There are two sources of benefits in the model (Equation 27), including energy generation, which uses the average energy price times the total annual generation to determine revenue, and recreation availability, which uses the total recreation hours and the value of recreation parameter.

Annual Benefits ($/yr)

$$B_{ann} = E_{tot}R_{MWh} + P_{rec,hrs}R_{rec} \quad \text{Equation 27}$$

E_{tot}	The total annual energy generation calculated from the simulation. (MWh/year)
R_{MWh}	The energy price from the Cost Table object. ($/MWh)
$P_{rec,hrs}$	The total annual recreation availability. (Hours)
R_{rec}	The value of recreation from the Cost Table object. ($/hour)

There are also two unique sources of costs that require further calculation based on the simulation performance, the flooding cost, and the start-stop cost. The flood cost (C_{flood}) is included to penalize facility designs that do not have enough flood capacity and are overtopped during high floods. Often earthen dams cannot be overtopped safely, so the flood cost should be high, whereas concrete dams may be designed for overtopping, in which case the flood cost may be relatively low. The annualized total over-flow volume ($Q_{flood,ann}$) is calculated by summing the total over-flow from the simulation, which occurs when inflows cannot be distributed through active modules. The cost of start-stops (C_{ss}) is an alternate way of accounting for the damages caused by ramping turbines. Implementation of start-stop costs is growing but not yet standardized [87]. The number of start-stops ($P_{ss,m}$) is calculated by counting the number of timesteps where each generation module is ramped from zero to non-zero flow. The maintenance costs can be set on either a module level or at the plant level as a lump sum or a percentage of ICC, as shown in Equation 28.

Annual Costs – input as a lump sum ($/yr)

$$C_{ann} = C_{om} + C_{flood}Q_{flood,ann} + \sum_{m}^{Gn} C_{ss,m}P_{ss,m} + \sum_{m}^{Fa} C_{om,m}$$

Equation 28

Annual Costs – input as % of ICC ($/yr)

$$C_{ann} = C_{om}C_{icc} + C_{flood}Q_{flood,ann} + \sum_{m}^{Gn} C_{ss,m}P_{ss,m} + \sum_{m}^{Fa} C_{om,m}$$

$Q_{flood,ann}$	The annualized total over-flow volume during the simulation. Over-flow occurs when operating modules cannot pass the inflow. (cfs)
$P_{ss,m}$	The annualized number of start-stops for module *m* counted as the number of instances the module ramped up from zero to non-zero flow.
C_{om}	The annual operation and maintenance costs from the Cost Table object. ($/year or %/year)
C_{flood}	The cost of damages for flood over-flows. ($/cfs)
$C_{ss,m}$	The cost of a start-stop cycle for module *m*. ($)

The calculation of NPV is standard across the literature and uses the annual costs and benefits from the previous equations, as illustrated in Equation 29 below.

Net Present Value ($)

$$P_{npv} = \sum_{y}^{T_{life}} \frac{(B_{ann} - C_{ann})}{(1+d)^{y}}$$

Equation 29

T_{life}	The life of the project from the Cost Tables object (indexed by *y* for each year). (Years)
d	The discount rate from the Cost Table object. (%)

The levelized cost of energy (LCOE) is the average net present cost to produce energy over the life of the project. LCOE is a useful metric for comparing the project to other energy sources. The formulation takes the ratio of the net present costs of the project and the discounted energy generation over the life of the project. Equation 30 below leverages the annual costs and the annual energy generation calculated from the simulation process.

Levelized cost of energy ($/MWh)

$$P_{LCOE} = \frac{\left(C_{icc} + \sum_{y}^{T_{life}} \frac{C_{ann}}{(1+d)^{y}}\right)}{\sum_{y}^{T_{life}} \frac{E_{ann}}{(1+d)^{y}}}$$

Equation 30

Solution Methods

The object-oriented approach provides structure to the design variables, and the system of models employs that structure to simulate operation and determine performance objectives. Optimization tools were needed to take the results of each simulation and determine the optimal configuration and design of modules for the project based on the designer's goals. Two optimization methods, an enumeration method and a genetic algorithm, were created to meet this need. Before describing the details of each method, it is important to describe why these methods were selected.

Chapter Two highlights two basic classes of hydropower design models, analytical models and simulation models. Analytical models simplify the design problem into a system of equations that can be solved using pre-packaged linear or non-linear solvers. The most common assumptions include a constant head across the powerhouse to reduce nonlinearities and a focus only on the powerhouse design (number and size of turbines). However, a constant head assumption is not valid for low-head hydropower projects because small changes in head represent a larger portion of the total head than high-head projects. Additionally, non-power modules are crucial for project feasibility, so optimization cannot rely solely on powerhouse optimization. Simulation models maintain the complexity of the model operation and use heuristics to find the optimal design iteratively. These methods do not guarantee optimality and can require long solution times but are effective for large design spaces. These models must also carefully consider the flows and conditions used to simulate operation, which should represent the expected future hydrologic conditions. A simulation model was selected to maintain the complexity of the operational model and enable more detailed insights into the operational relationships between modules.

The next step was to identify the optimization method or simulation process methods. When selecting an optimization method, the key considerations were optimality (reliability of the method to identify the global optima) and runtime (how long the method took to find the optima). These considerations relied on the size of the design space or the number of possible design options. The main design decisions were the number of each class of modules and the design variables of the dynamic modules, as described in Table 23 in the Appendix. Each module object and design variable represented an axis of the design space. In some cases, the design variables were continuous. Other variables, like the module counts and turbine design flow, were discrete variables, assuming that standardization will lead to off-the-shelf module sizes. So, the size of the design space could vary significantly based on the number of module classes, the allowed number of modules for each class, and the structure of the design variables in the analysis. The time for each simulation run also depended on the length of the simulation, the dispatch method, and the number of modules. Two optimization methods were created for small design spaces (enumeration) and large design spaces (a custom genetic algorithm) to facilitate different problem compositions and enable the comparison of each method.

Enumeration procedures simulate all possible configurations of design variables and rank the resulting objective functions. This method is best used for small design spaces and reflects the standardization (or discretization) of technologies. The enumeration process used in waterSHED is based on the design variables of interest to the analysis. The main steps included 1) selecting the required modules (non-overflow, foundation, and spillway), 2) identifying the range of module counts (including a minimum, maximum, and step size), and 3) choosing the range of any design variables for dynamic modules (also including a minimum, maximum, and step size). The total number of iterations depended on the product of the number of possibilities in each range. During the optimization, each combination of the design variables was created as a facility, simulated, and recorded. After iterations were complete, the objective functions were ranked, and the facility with the best-recorded objective function was reported.

However, more flexible optimization methods are needed as the number of modules in the market increases and customizable technologies add continuous design variables. Several heuristic methods exist for intelligently searching large design spaces, such as simulated annealing, tabu search, genetic algorithms, and swarm approaches. Each method has advantages and disadvantages in terms of speed and optimality. Still, the main consideration for this research was how well the method could be integrated into the object-oriented approach. The modular hydropower design problem can be considered a version of the Knapsack problem where modules must be selected from the module library (the knapsack) to optimize an objective function according to spacing and other constraints (like the weights in the Knapsack problem). However, several considerations make the problem unique and complex. First, the design space included a mix of continuous variables and discrete variables. Second, the constraints and treatment of the modules changed depending on the selected modules. For example, the model only allowed one type of spillway module, so adding one type of module excluded the ability to add other types, but the model could add multiple modules of the same type. Third, these constraints required flexibility in the implementation, making it more difficult to use out-of-the-box optimization packages. Finally, existing hydropower design knowledge provided some guidance that could allow the tool to identify feasible paths through the design space. For example, it is common to design facilities for the 30% exceedance flow, which could be used to initialize facilities. Thus, the selected algorithm must provide methods for customizing the search procedure accordingly.

A custom genetic algorithm (GA) was selected as the heuristic method because it met the flexibility requirements needed for the implementation. The GA creates a population of potential solutions (facilities), evaluates all of them, and then creates a new population based on principles of natural selection. The evolution process is represented using a series of mutation and evolution functions that creates new facilities for the population based on the best facilities of the previous population. The evolution process also limits the number of iterations by learning from the previous generations. Conventional GA's view individuals (potential solutions) as bitstrings, and the mutation process changes the bits (1's and 0's within the string). This process conceptually parallels the selection of

modules within a linear facility. Creating custom mutation functions enabled the integration of several built-in constraints, like limiting the facility to only one type of spillway module. The methods used in the GA are described in detail in the Custom Genetic Algorithm section in the Appendix. Several heuristics could perform similarly to the GA, but it is not within the scope of this research to determine the best performing heuristic method.

When building the optimization problem for the case studies in the next section, it was clear that the design spaces were relatively small (less than approximately 200 options). This fact stems from several factors, including limited module technologies in the market, standardization enabling the discretization of variables, and analyses that often focused on optimizing generation given non-power constraints. Given the limited number of configurations, it was reasonable to simulate all possible configurations of the facility, so the enumeration option was used. In the case studies, the configuration of non-power modules was often held constant, and the optimization problem focused on selecting the number and design flows of the generation modules. The specific enumeration parameters used in each case study are presented in the respective sections. Generally, the best objective function metric for generation optimization was the LCOE ($/MWh) because it factored in the initial costs, the annual costs, and the annual generation without consideration for the energy price, which is a source of uncertainty. Net present value (NPV) includes the value of generation but can lead to optimal designs with no generation modules if NPVs are negative and the marginal benefit of additional generation modules is negative, which can be the case with expensive conventional designs. Unit costs ($/kW), ICC, and total cost do not incorporate energy generation, so these metrics need capacity constraints.

CHAPTER FOUR

RESULTS AND DISCUSSION

Chapter Three described the construction of an improved hydropower design model called waterSHED that employs a system of novel conceptual models and empirical models from the literature. Testing the waterSHED model was necessary to validate proper construction and to illustrate potential applications that could extend the frontier of hydropower design research. To this end, two case study analyses were developed to answer research questions important to industry stakeholders, exemplify the innovative features of waterSHED, and help identify pathways to sustainable and cost-effective small hydropower development. These case studies and their respective research questions are:

Case Study A – Reference Sites

- Cost reduction scenarios – what are the technology areas and site conditions that are most critical for project cost and economic performance?
- Headwater level tradeoffs – what are the cost, generation, and sedimentation tradeoffs related to the selection of headwater elevation?
- Sediment sluicing analysis – what are the relationships between operation parameters and the sediment passage performance metrics?

Case Study B – Bosher Dam

- Value of fish-safe turbines – what are the cost, generation, and downstream fish passage tradeoffs for fish-safe turbine designs compared to conventional fish exclusion designs?
- Value of nature-like rock ramps – what are the cost, generation, and upstream fish passage tradeoffs for nature-like rock ramp designs compared to technical fishway designs?
- Value of recreation modules – what are the cost, generation, and recreation availability tradeoffs for recreation passage modules?

These case studies served several purposes. First, they validated and tested the waterSHED model's functionalities. Case Study A is an extension of the previous SMH Case Study Report [17], and Case Study B was conducted in parallel with similar site assessment efforts by Natel Energy, a hydropower developer. The results of waterSHED were validated by comparing them to the results of the other research efforts. Second, they helped answer the aforementioned research questions from the other research efforts by using the innovative optimization and environmental modeling functions within waterSHED. Third, the case studies help quantify the cost-benefit tradeoffs for environmental modules, which is a major field of interest in hydropower design but has not been adequately addressed, particularly in a modular framework. The inclusion of non-power modules (NPMs) in this study addresses ecological compatibility and stakeholder acceptance, which are key principles for SMH development. These modules have a variety of tradeoffs related to capital costs, operating costs, environmental

performance, generation losses, and operational impacts that have not been well addressed in existing models. The case studies examine these tradeoffs for recreation, sediment, and fish passage modules at several sites to exemplify the possible insights with the waterSHED modeling approach. Some results may be relevant for the general population of low-head sites, but this population of sites is diverse, and further applications of the tool are needed to identify broader themes.

The following sections discuss the purpose, background information, case-specific sensitivity analysis methods, and quantitative results of each case study. The Baseline Conditions section below describes the methods that are consistent across both cases. Case Study A leveraged previous research from ORNL on three reference sites on the Deerfield, Housatonic, and Schuylkill rivers and focused on the cost-benefit sensitivities for a set of reference technologies that were custom designed using dynamic modules. Case Study B built on work with Natel Energy that evaluated a modular design concept for repowering a non-powered dam on the James River. This case compares fish-friendly and conventional designs and evaluates the costs and benefits of a modular whitewater rafting park. These case studies are for research purposes only and do not imply that development is recommended at these sites or is under consideration. Further stakeholder engagement and site assessment would be needed to evaluate feasibility.

Baseline Conditions

These case studies relied on runs of the waterSHED model for various sites, which provided insight into project design and performance tradeoffs. The inputs to the model varied for different sites and technologies, so standardized processes for determining the inputs were needed to ensure comparability between model runs. The baseline conditions and assumptions, listed in Table 8, describe the default inputs and processes for determining inputs used whenever the input was not part of a sensitivity analysis. Some inputs differ slightly between the two case studies, as marked by the italic text in Table 8. Summaries of the technologies used for each case study are provided in the respective sections, and in-depth details about the object-oriented attributes are provided in the Appendix. These include cost and dimensioning equations and assumptions.

Case study A relied on conceptual reference technologies and procedures developed under the original SMH Case Study report [17]. These technologies are based on existing literature and technology specifications but are conceptual and are not exact reflections of products on the market. For example, foundation, non-overflow, recreation, and sediment modules are not yet widely available on the market. Fortunately, the object-oriented approach allows the model to characterize general module processes rather than detailed designs so that the reference technologies can apply across several technology types. Costs were gathered for these conceptual technologies by an engineering contractor using existing cost data and industry quotes. However, as Case Study A shows, the costs are very conservative and reflect the first-of-its-kind nature of the modular reference facilities. Case Study B leveraged technologies and assumptions provided by industry partners, but these are conceptual and do not reflect the products from industry partners.

Table 8. List of baseline conditions and assumptions for case studies.

Model Input	**Baseline Condition** *(Case Study B specific conditions)*
Simulation time period (years)	Simulations used ten years of flow data, which is commonly used in industry and provides reasonable solution times for enumeration. This range is expected to capture a range of wet and dry years without biasing towards historical flows that may not reflect current hydraulic conditions and hydrologic impacts from climate change. *(Twenty years of data were used because there were fewer iterations).*
Energy price ($/MWh)	The energy price was assumed to be a constant $60/MWh. This value reflects trends for power purchase agreement prices for small hydropower plants, which are typically higher than the average price across the hydropower fleet of 40-50 $/MWh [23]. This price did not account for renewable energy credits (RECs), which can add approximately 20-60 $/MWh.
Discount rate	A discount rate of 7% was used for cost metrics, like LCOE and NPV, commonly used for hydropower cost modeling.
Project life	A project life of 40 years was used for cost metrics, like LCOE and NPV. This reflects typical hydropower licenses from FERC, either 30 or 50 years.
Annual O&M Cost	The plant's annual operating and maintenance costs were assumed to be 6% of initial capital costs. This value was based on cost modeling research at ORNL that examined O&M and capital cost data from FERC's Electric Utility Report [158]. As illustrated by Figure 50 in the Appendix, the ratio of operating to capital cost has declined over the last two decades, particularly for small projects. The capacity weighted annual average ratio for 2020 was approximately 6%. *(O&M costs were specified for each module).*
Overhead cost	The overhead cost (licensing, administration, insurance, etc.) was assumed to be 4% of the initial capital costs. This is the assumption provided by the engineering consultants for the SMH reference design cost estimates. *(Assumed a fixed $200,000 overhead cost).*
Engineering Cost	The engineering cost (skilled labor, site assessment, etc.) was assumed to be 6% of the initial capital costs. This is the assumption provided by the engineering consultants for the SMH reference design cost estimates. *(Assumed a fixed $200,000 engineering cost).*
Contingency allowance	The contingency allowance, which accounts for unexpected cost overruns, was assumed to be 10% of the initial capital costs. This is the assumption provided by the engineering consultants for the SMH reference design cost estimates. *(Assumed a 5% contingency).*

Table 8 continued.

Model Input	**Baseline Condition** *(Case Study B specific conditions)*
Stream width	The stream width was measured as the distance from the top of each riverbank for the selected project site using publicly available geographic information system (GIS) tools (Google Earth).
Stream slopes	Stream slopes were gathered from the National Hydrography Dataset Plus for the selected stream reach [159], per the methodology in the NSD Resource Assessment [5].
Stage-discharge curves	The stage-discharge curve was generated by conducting linear regression on stage-discharge data from the selected USGS gage to create a power curve (with a piecewise linear or power component for high flows as needed), as discussed in the Regression Analysis section in the Appendix.
Inflow data	Inflow data was gathered from the closest upstream USGS gage and was not adjusted by catchment area because sites were selected near flow gages.
Peak flow data	When necessary, available peak flow data was gathered from the USGS REST database [138] and analyzed using the flood frequency analysis methodology discussed in the Flood Frequency Analysis section in the Appendix.
Normal operating headwater level	When the NOL was not otherwise specified, the NOL was set to the 100-year flood elevation from the Federal Emergency Management Agency (FEMA) flood maps, which was used as the default headwater in the NSD Resource Assessment because it represents the area of land less likely to be developed due to flooding concerns [5].
Operation priority rankings	The default operation priority rankings from highest priority (turned on first) to lowest priority module class were Water Passage (minimum flows), Recreation, Fish Passage, Generation, and Sediment. This reflects a prioritization of human and animal health, which is typically required by licenses. *(Recreation was moved to the fourth priority because the powerplant operation is meant to supersede the whitewater park and sediment is the last priority).*
Other	Any additional features, such as minimum spillway flows, turbine over-run, recreation value, stage-storage curve, or flood costs, were assumed zero (not incorporated in the model) unless otherwise specified.

Case Study A. Reference Sites

As described in Chapter One, one of the primary challenges for conventional small hydropower development are high costs per kilowatt. The Department of Energy's Water Power Technologies Office and ORNL have invested significant time and money to reduce technology costs through programs like the Groundbreaking Hydro Prize [126]. Technology-level capital cost reductions may lead to proportional reductions in facility-level capital costs. However, in addition to technology costs, several other factors, such as site conditions and changes to the optimal design, project life, and maintenance costs, affect the overall project cost. In addition, a key principle of SMH is achieving economies of scale through standardization, so models need to evaluate how costs per unit may change with the number of module units. Thus, this case study uses sensitivity analyses on technology costs and site parameters for three reference sites to evaluate the innovation areas and site characteristics that offer the highest cost reduction potential.

This case study extended previous unpublished research from ORNL and was formulated under the previous work's constraints, assumptions, and goals. During the initial research efforts within SMH, an early version of waterSHED was used to create a reference design for a low-head project on the Deerfield River [17]. The reference design used modular technologies that were conceptualized based on models from the literature and optimized specifically for the case study site. The early version of waterSHED was used to select module designs for the anticipated hydraulic conditions and to test multiple configurations of modules to determine the impacts on generation. However, this design did not have itemized cost information, so ORNL obtained cost estimates from an engineering contractor along with engineering drawings for the Deerfield site and two similar sites on the Housatonic and Schuylkill Rivers. These sites all had similar gross heads of approximately 10ft (13.5ft headwater elevation) since the reference modules were designed for this head. The cost estimates were conservative given the unknown site conditions and novelty of the design, which resulted in costs much higher than the typical industry target of $3,500/kW. These estimates also highlighted the conventional nature of the module designs, which used large concrete structures for several modules. A cost-effective design for this class of sites would greatly benefit from further investment and research in low-head hydropower. Early attempts to conduct cost sensitivity analysis were useful but were limited to high-level scenarios involving capital costs because of the limitations of the early waterSHED model version. Redoing the cost sensitivity analysis in waterSHED allowed a more detailed assessment of cost-benefit relationships. It also provided an opportunity to validate the cost modeling functionalities of waterSHED.

Model Setup

The three reference sites on the Deerfield, Housatonic, and Schuylkill rivers are informative because they have approximately 10ft of head, the most common head class of NSD sites, as illustrated in Figure 1. These heads were estimated based on FEMA 100-year floodplain elevation data and assumptions from the NSD Resource Assessment [5]. For the original research effort, similar heads enabled consistent use of the same

generation module without consideration for changes in runner diameter or speed, which can change module dimensions and costs.

Although the design heads were similar, the hydraulic and site conditions differed slightly, as illustrated in Table 9. The stream widths, which refer to the distance across the top of the dam as opposed to the width of the riverbed, varied considerably and impacted the number of non-overflow structures required to span the river. The inflow characteristics also varied between the three sites, with Schuylkill having the highest average inflow, followed by Deerfield and Housatonic. The inflows impacted the baseline generation designs and operation of the facility. The seasonality of inflows can play a major role in hydropower design models because facilities must balance the size of turbines and the capacity factor. However, the flow duration curves, shown in Figure 20, reflect very similar shapes meaning the hydrological conditions are similar for the three sites. Additionally, the stage-discharge relationships differ among the sites owing to differences in the stream bathymetry, stream roughness, vegetation, floodplain elevations, and several other factors. The curves illustrated in Figure 21 are empirical equations generated from USGS gage data using the methods described in the Regression Analysis section in the Appendix. These curves comprise two piecewise equations that model high and low flow conditions separately. The low flow equations were power curves, while the high flow conditions were linear or power curves.

The reference technologies used for these three sites are summarized in Table 10. These technologies were included as dynamic modules in waterSHED, meaning that technologies could be optimized for various conditions. For example, the Kaplan turbine generation module could be redesigned for different design flows and heads, automatically recalculating the runner diameter, costs, and operating ranges based on these design variables. However, the ability to redesign modules depended on the availability of cost and design information that enabled the technology to be properly scaled. For example, little information was available for the sediment sluice gate module, so it was assumed to have a constant width throughout the simulations, and the design flow could be varied by changing the gate opening. Full documentation of the module attribute determinations is provided in the Module Attributes section in the Appendix.

The baseline module configurations for each of the three sites are summarized in Table 11. These configurations were selected during the SMH Case Study Report and interactions with the engineering consultants; however, the designs were not explicitly optimized for Housatonic or Schuylkill [17]. The baseline designs were used to validate costs and compare results; however, optimized designs are included later in this analysis. The optimized designs are used for the sensitivity analyses, as indicated in the respective sections.

Table 9. Summary of Case Study A site conditions.

Attribute	Deerfield	Housatonic	Schuylkill
Stream width (top of dam)	400ft	302ft	328ft
Mean daily flow	1489cfs	1237cfs	1765cfs
30% exceedance flow	1680cfs	1360cfs	1880cfs
95% exceedance flow	296cfs	178cfs	386cfs
Normal operating level	13.5ft	13.5ft	13.5ft
Generation design head	10.5ft	10.5ft	10.5ft
Stream slope	0.0012	0.0012	0.0012
100yr flood flow	69070cfs	21050cfs	60790cfs
10yr flood flow	33000cfs	11710cfs	32650

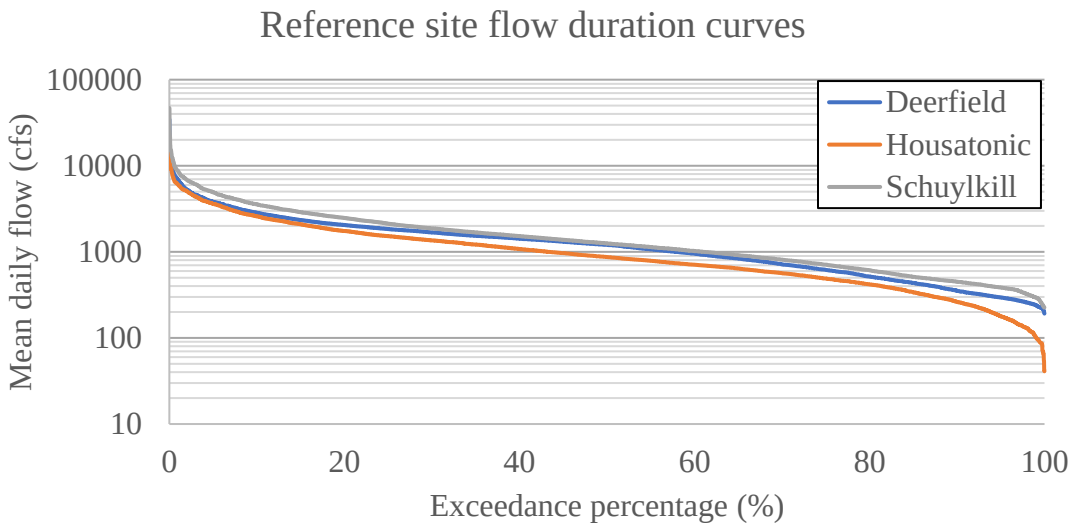

Figure 20. Flow duration curves for Case Study A, including USGS gage data from 2000-2020.

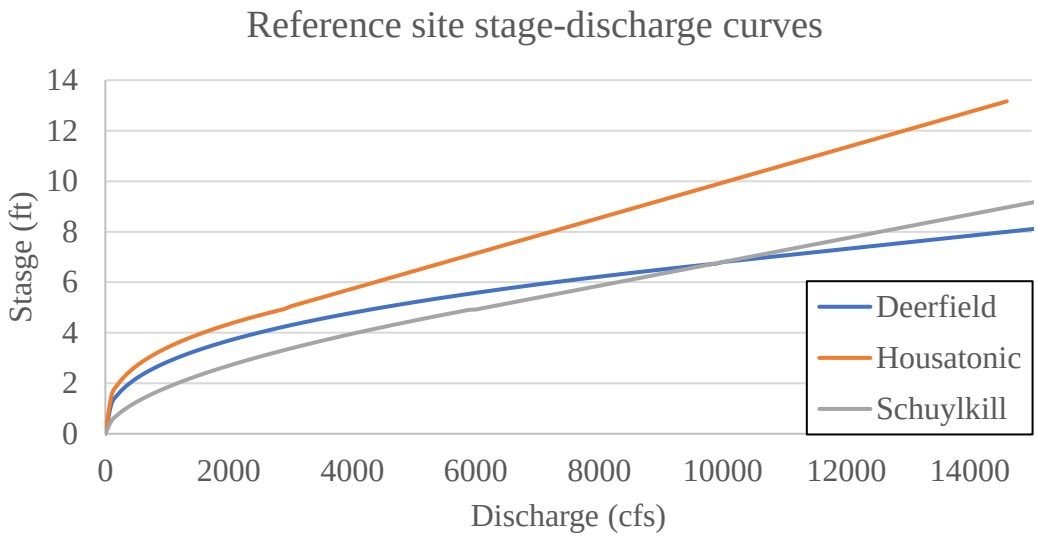

Figure 21. Stage-discharge curves for Case Study A sites using USGS gage data from 2000-2020.

Table 10. Summary descriptions of reference modular technologies.

Technology	Description
Modular Kaplan (Generation)	The Kaplan turbine is a dual regulated turbine, meaning it can adjust both wicket gates and the blade angle to operate at high efficiencies for a range of flows. All necessary electrical equipment to prepare power for interconnection is included in the module, such as generators and control systems.
Sediment Gate (Sediment)	The sediment gate is a low-level vertical lift sluice gate that can be raised to pass bedload sediments under the dam.
Obermeyer Spillway (Water Passage)	The Obermeyer spillway gate is a pneumatically actuated overshot gate that inflates and deflates a bladder to raise and lower the structure's height.
Boat Chute (Recreation)	The boat chute is designed for standard kayaks and canoes and allows recreationalists to descend the facility through a series of drop structures. Each step has a drop structure and a recovery pool for recreationalists to safely turn in case of a fall. The number of steps is determined by the height of the facility and the maximum allowable drop, as described in the Appendix.
Vertical Slot Fishway (Fish Passage)	The vertical slot fishway is a volitional passage structure with a series of resting pools for fish to regain energy before passing through vertical slots designed to attract upstream migrants. Each step in the module contains one pool and a slot for entry and exit. The number of steps is determined by the height of the facility and the maximum slope that can facilitate effective passage, as described in the Appendix.
Precast Concrete Foundation (Foundation)	The precast foundation module is made of concrete blocks anchored to the riverbed after excavation, leveling, and treatment. The cost of all foundation treatment, except for the care of water (cofferdams and dewatering), is included in the foundation module costs. The module is parameterized by the depth to competent bedrock, which differs between sites and is difficult to estimate without in-person site assessment.
Precast Concrete Non-overflow (Non-overflow)	The precast non-overflow modules are precast concrete molds filled with cheaper “filling” concrete to create a block structure. The structure is designed to have a 0.5ft freeboard over the expected normal operating level. The module dimensions are proportionally scaled based on this height, and costs are determined based on the volumes of concrete.

Table 11. Summary of baseline module configurations for Case Study A.

Module	Deerfield Module Count	Housatonic Module Count	Schuylkill Module Count	Module design flow (cfs)	Module width (ft)
Kaplan module	4	3	5	338	13.8
Vertical slot fishway	1	1	1	34.5	21
Sediment sluice gate	1	1	1	1355	15
Obermeyer spillway	6	3	6	5500	20
Precast concrete non-overflow modules	55	47	45	NA	3.28
Precast concrete foundation	1365 (14,684 ft^2)	1133 (12182 ft^2)	1370 (14,734 ft^2)	NA	NA

Cost Model Validation

The engineering consultants provided itemized costs for the reference designs. The first challenge of this case study was parameterizing the modules to allow customization for different design points while leveraging the itemized cost data. For example, the non-overflow modules were designed for headwater elevations of 13.5ft, making them 14ft with 0.5ft of freeboard. The headwater level sensitivity analysis varied the headwater levels for these sites, so the model must be able to scale the costs of the non-overflow module with height. In the case of the pre-cast concrete non-overflow modules, the length-to-height ratio of 0.86 was maintained, and the costs were determined based on the volumetric amounts of pre-cast and filling concrete. The design considerations for the other modules are included in the Case Study A section in the Appendix.

There were several cases where the itemized cost strategy did not pair well with the functionalities in waterSHED, so scaling factors were used to match the cost models with the reference costs. For one, the number of foundation modules in waterSHED is computed by dividing the total surface area of the modules by the surface area of one foundation module, which is a $1m^2$ pre-cast concrete slab. However, the reference designs included foundations outside the module footprint to provide stability and erosion protection. Accordingly, the costs of the foundation modules were scaled using factors of 1.82, 1.2, and 1.4 for Deerfield, Housatonic, and Schuylkill, respectively. The itemized non-overflow module capital costs were higher than the reference designs, accounting for the concrete that is not needed for the abutments. The non-overflow module costs were tuned to the Deerfield site using a scaling factor of 0.87, which was also used for the other two sites. Finally, the cost of the generation module was parameterized using an empirical model from the Small Hydropower Cost Reference Model [128], which used nominal power and head as inputs and only costed the electro-mechanical equipment. The empirical equation was scaled using a factor of 3.7 to account for the additional module structure components, like the gates, draft tube, and freeboard.

The resulting itemized costs for the baseline module configurations (
Table 11) for the three sites are provided in Table 12. The Deerfield modeled cost estimate for the baseline design is within 0.05% of the reference cost estimate from the engineering contractor. The modeled Housatonic cost estimate is 1.4% (~$170,000) higher than the reference, and the Schuylkill estimate is 0.8% ($130,000) lower. These deviations are well within the expected accuracy range for high-level cost estimates, which can differ from real values on the scale of millions in cases with unexpected costs overruns. This trend may indicate that these itemized models over-predict for small sites and under-predict for larger sites, but more data is needed to validate this trend. The differences in cost, reflected by the percentages in Table 12, may result from several factors, including rounding differences and the distribution of cost components. The reference costs included separate items for the switchyard/interconnection costs and financing. The modeled costs were separated into fixed and variable costs components so that modules could be properly scaled. For example, the switchyard & interconnection cost item was broken into a $695,000 fixed cost component for the electrical and control

Table 12. Cost breakdown for the three reference sites.

Cost Summary	Calculated Costs			Comparison to Reference Costs		
Item	Deerfield	Housatonic	Schuylkill	Deerfield	Housatonic	Schuylkill
ICC	**$13,861,039**	**$9,420,522**	**$13,494,967**	**-6.8%**	**-6.1%**	**-6.3%**
Boat Chute	$910,000	$910,000	$910,000	0.0%	4.4%	0.0%
Vertical Slot Fishway	$303,500	$303,500	$303,500	-0.2%	-0.2%	-0.2%
Kaplan	$3,575,478	$2,681,609	$4,469,348	2.4%	1.7%	3.7%
Sediment Sluice Gate	$288,000	$288,000	$288,000	0.0%	0.0%	0.0%
Precast Foundation	$5,086,498	$2,783,723	$3,927,023	-0.1%	0.3%	-0.1%
Precast Concrete	$552,564	$472,191	$452,098	0.3%	-2.9%	1.8%
Obermeyer Spillway	$2,326,998	$1,163,499	$2,326,998	0.0%	3.5%	0.0%
Electrical and Controls	$818,000	$818,000	$818,000	-25.2%	-17.8%	-30.1%
Other	**$4,040,608**	**$2,841,746**	**$3,739,081**	**23.1%**	**26.1%**	**19.4%**
Care of Water and Financing	$1,268,400	$957,642	$1,040,088	0.4%	17.6%	-18.1%
Overhead	$554,442	$376,821	$539,799	-17.4%	-15.2%	-16.9%
Engineering	$831,662	$565,231	$809,698	-17.5%	-15.2%	-17.0%
Contingency	$1,386,104	$942,052	$1,349,497	-6.8%	-4.7%	-6.3%
Total	**$17,901,646**	**$12,262,268**	**$17,234,048**	**-0.035%**	**1.4%**	**-0.8%**
Annual O&M (6% ICC)	**$831,662**	**$565,231**	**$809,698**	-	-	-

building and a $50,000 variable cost component that was integrated into the generation module cost to account for scalable transmission and controls costs. In addition, the care of water, which includes the cofferdam and dewatering costs, was separated from the foundation costs and included as a non-capital cost along with the financing. Since the engineering, O&M, and contingency costs were a function of the initial cost of capital, which only includes capital/physical assets, it was important to differentiate these non-capital cost components from the capital components, like the concrete foundation modules.

Overall, the comparison in Table 12 shows that the modeled costs accurately replicated the reference costs. However, this does not mean that the reference costs are necessarily realistic development costs. During the initial Case Study Report [17], the nominal capacities for Deerfield, Housatonic, and Schuylkill were 1MW, 0.75MW, and 1.25MW[2], which relate to unit costs of approximately $17,900/kW, $16,350/kW, and 13,790/kW, respectively. These costs are much higher than the target costs of $3,500/kW for several reasons. First, the engineering contractors used conservative estimates, particularly for the foundation depth, because of the limited site-specific information. As shown in Figure 22, foundations represent about 28% of the total project costs, which was determined assuming a depth to bedrock of 5ft. This depth is a critical factor in foundation costs, but there was limited available data, representing considerable uncertainty. Second, the cost estimates from vendors were indicative of a first-of-its-kind pilot project since module technologies are not widely available. One principle of SMH is to drive down costs through economies of scale, which were not apparent in this pilot-like project. Third, the baseline designs include a boat chute, a vertical slot fishway, and a sediment sluice gate, which may not be needed or cost-effective for these sites. Finally, the reference technologies were modularized versions of conventional technologies and did not reflect technological innovations outside of the modular form. For example, nature-like rock ramps (described in Case Study B) could act as a spillway and a fish passageway, removing the need for large concrete structures. Although the cost estimates throughout this case study are high, they provided useful validation for the waterSHED functionalities and enabled analyses that identified cost reduction areas.

Generation Optimization

The baseline designs were initially selected using the methods in the Case Study Report [17]. However, the costs were not estimated, and the powerhouse optimization methodology was not applied to the Housatonic and Schuylkill sites. As such, this study examines the optimality of the baseline designs and validates the functionalities of waterSHED. This process aimed to identify the configuration of generation modules

[2] The method for calculating nominal capacity differs between the Case Study Report [17], which used the peak turbine efficiency, and this research, which used the turbine efficiency at the design flow. The efficiency curves are similar in shape because they use the same model from Gordon [113], but have different peak and design efficiencies. So, for design flows of 1352cfs (338cfs across four modules) and design heads of 10.4ft, the Case Study Report [17] used a peak efficiency of 83% to get a nominal capacity of 1MW, while this research used the design efficiency of 73% to get a nominal capacity of 864kW.

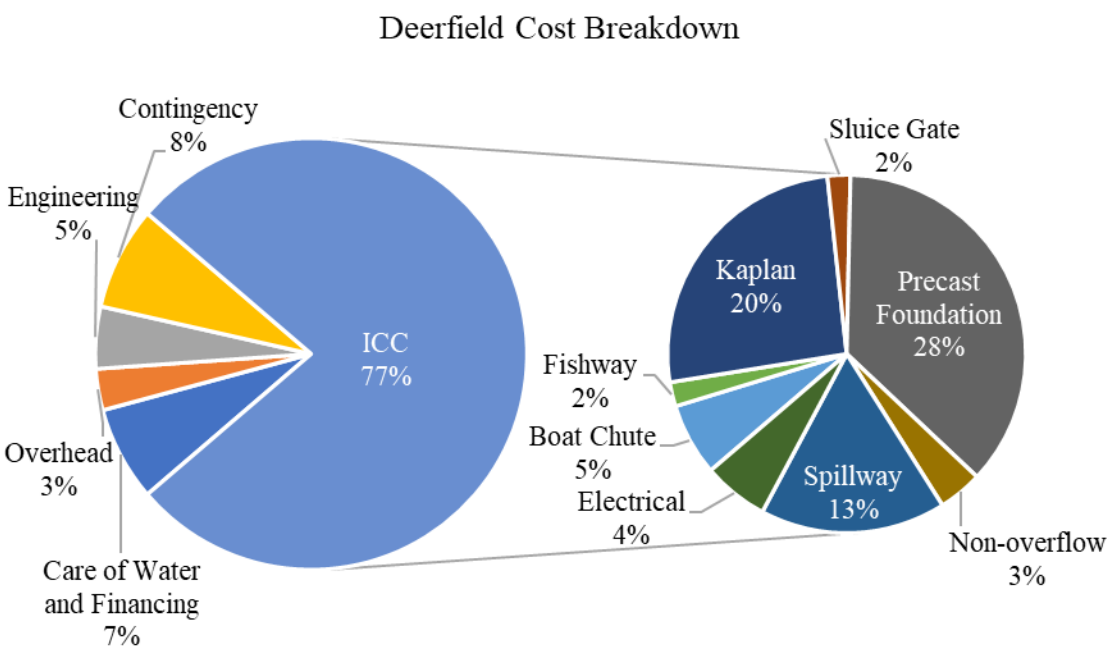

Figure 22. Cost breakdown of Deerfield baseline reference design.

that provided the lowest levelized cost of energy (LCOE). This metric was selected because it factors in the project's capital costs, operating costs, and energy generation without consideration of the energy price, which is an area of uncertainty. The configuration design variables included the design head, design flow, and the number of modules. Based on the principles of SMH, it is assumed that all the generation modules were the same size.

The first step was to identify which dispatch model to use and their tradeoffs. The four dispatch methods described in the Operational Models section are Design Ramping, Peak Ramping, Simple Greedy, and Advanced Greedy. These dispatch models were run three times for each reference site to determine the average computation run for one simulation. The simulations were run on a Dell XPS 13 with a 2.3GHz Intel Core i5-6200U CPU and 8GB of RAM. The simulations were run with ten years of flow data and the computation time includes the time required for the dispatch optimization, the flow allocation, and the calculation of results.

The results are illustrated in Figure 23 and Figure 24. The Advanced Greedy dispatch model provided the highest annual energy generation in each case but required significantly longer runtimes than the other methods. This difference between the Advanced Greedy computation times for the three sites is driven by the number of generation modules and the powerhouse design flow. The Design Ramping and Simple Greedy methods perform very similarly in terms of optimality and computation time because they behave very similarly when modules are the same size. Both methods ramp the generation modules to the design flow one by one, which led to annual energy generation estimates about 5% lower than the Advanced Greedy method. The Peak Ramping method was similar in speed to the Design Ramping method but only performed about 1.4% worse than the Advanced Greedy method. The plant efficiency curves in Figure 24 reflect the difference in performance. The turbine efficiency curve for the Kaplan turbine generation modules (illustrated in Figure 15) has a flat peak efficiency for a wide flow range that drops around the minimum operating flow and the design flow. The plant efficiency curve for the Advanced Greedy model is flat because the model ramps down modules that are already on to help bring new turbines up to the flat efficiency range. On the other hand, the Peak Ramping method leaves turbines at the peak efficiency point and ramps the other modules one at a time, leading to more distinct peaks in the plant efficiency curve. In addition, when all modules are at the peak efficiency flow, the Advanced Greedy method allocates flow evenly across all modules to maintain higher efficiencies than ramping modules to the design flow one at a time. Although the Advanced Greedy method performed the best, it took 10-30 times longer for only a 1.4% improvement, which is well within the margin for error in pre-feasibility estimates. The Advanced Greedy model was used for single runs, and the Peak Ramping model was used for analyses with multiple runs, as indicated in the respective sections.

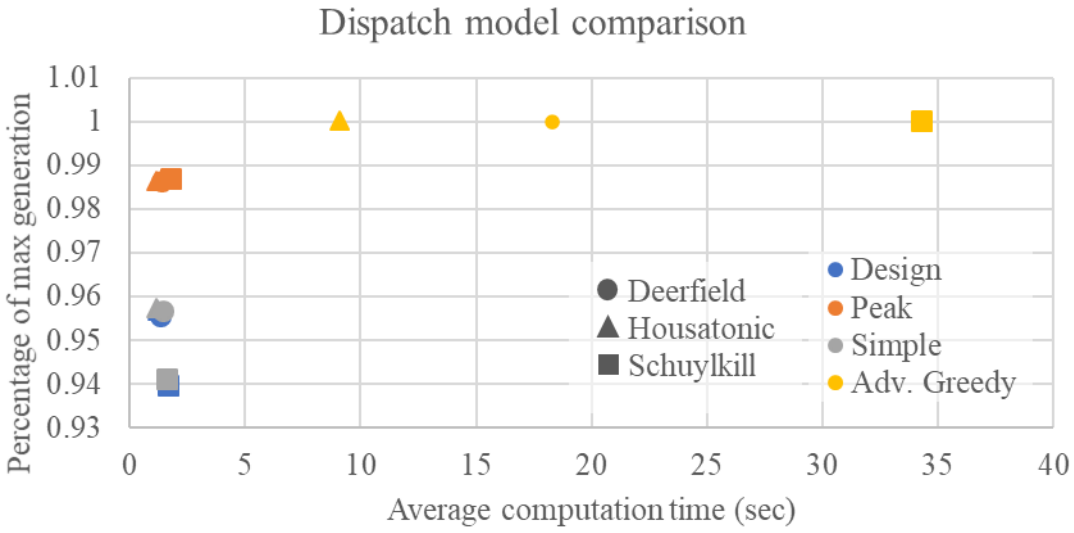

Figure 23. Comparison of dispatch models by computation time and optimality.

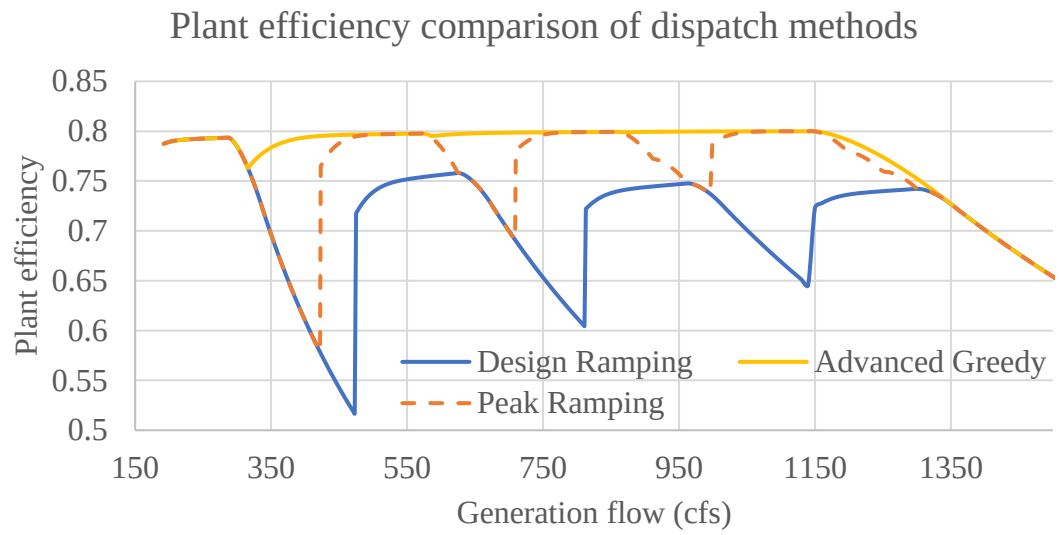

Figure 24. Comparison of plant efficiency for each dispatch model (the Simple Greedy model performs the same as the Design Ramping curve, so it is not shown).

The next step was to narrow down the possible design configurations. There were three dimensions of the powerhouse configurations: the design flow, the design head, and the number of turbines. Typical RHDMs, like those in Table 4, typically assume a turbine design head and a set number of turbines and then aim to optimize the design flow. For example, the Case Study Report [17] assumed that the design head for the Deerfield Kaplan turbines was 95% of the gross head associated with the 50% exceedance flow or 10.4ft. The design head of the turbines depends on the expected gross heads, the turbine setting, and the operating head range. The number of modules depends on cost differences between adding another module versus increasing the size of one module and the optimal powerhouse design flow. The goal of this analysis was to get within 10cfs of the optimal design flow and 0.1ft of the optimal design head. Additionally, the analysis used the enumeration method rather than the genetic algorithm to visualize the shape of the design space. As such, the enumeration process would require significant runtimes if optimizing all three variables simultaneously. Instead, the design head and the number of units were identified with a separate enumeration process and held constant through a more granular design flow optimization process.

The selection of design head and turbine number was conducted for the three reference sites using a coarse enumeration process with the Peak Ramping dispatch model. The powerhouse design flows (total design flows for all equally sized modules) were iterated between the Q_{50} and the Q_{10} (the 50% and 10% flow exceedance values) in 10 equally sized intervals. The design heads were iterated between the expected gross heads at the Q_{50} and the Q_{10} in 0.1ft increments. The number of modules was incremented between 2 and 5 modules for each site. The optimal configuration was identified via the lowest LCOE. Heat maps of the LCOE results for the optimal module count for each site are shown in Table 13, Table 14, and Table 15. The black borders highlight the design heads for the minimum LCOE in each row.

The optimal design heads for the Deerfield and Schuylkill rivers stay relatively constant (within a 0.2ft range) across the design flows, while the design heads for the Housatonic site change more significantly across the flows ranging between 9.0ft and 9.6ft. This trend may reflect the relative sizes of the projects since Housatonic is the smallest site in terms of annual flow, and 0.1ft changes may be more impactful to the total generation. The optimal design head decreased as the design flow increased for all three sites. In the cost model for the Kaplan turbines, increases in design head decrease the cost of the module (illustrated by a negative exponent) because higher head technologies typically have economies of scale. So, as the design flow increases, the relative value of the cost savings from a higher head decreases, so the optimal design head decreases to capture high flow events with lower gross heads. At this level of granularity, the heatmaps also reflect a smooth design space that converges to a single optimal point rather than local minima. While this doesn't fully disprove the existence of local minima at smaller resolutions, it helps narrow down the location of the global minima.

Table 13. LCOE heatmap of the head and flow enumeration for Deerfield with four generation modules.

LCOE ($/MWh)	Powerhouse Design Flow (cfs)										
Design Head (ft)	1210	1374	1538	1702	1866	2030	2194	2358	2522	2686	2850
9.0	477.3	447.7	428.3	415.8	407.4	402.7	399.8	399.5	400.4	402.3	405.7
9.1	463.1	436.6	419.4	407.2	398.7	394.1	391.4	391.4	392.4	394.5	397.9
9.2	451.7	427.4	410.3	398.2	390.3	386.0	383.7	384.0	385.2	387.4	391.0
9.3	444.1	420.1	403.4	392.0	384.5	380.6	378.5	378.9	380.4	382.8	386.5
9.4	434.7	411.3	395.5	384.7	377.7	374.2	372.4	373.1	374.7	377.3	382.0
9.5	428.8	406.2	391.0	380.7	374.0	370.8	**369.2**	370.6	373.3	377.3	382.7
9.6	428.3	405.8	390.7	380.5	374.0	370.9	369.7	371.4	374.3	378.3	383.8
9.7	428.6	406.1	391.1	381.0	374.5	371.5	370.3	372.1	374.9	379.1	384.6
9.8	429.1	406.7	391.8	381.7	375.2	372.3	371.2	373.0	375.9	380.2	385.8
9.9	429.5	407.1	392.2	382.2	375.8	372.9	371.9	373.7	376.8	381.1	386.7
10.0	429.9	407.6	392.8	382.8	376.4	373.6	372.6	374.5	377.6	381.9	387.6
10.1	430.5	408.3	393.4	383.5	377.2	374.5	373.5	375.5	378.6	383.0	388.8
10.2	431.1	408.9	394.2	384.3	378.0	375.3	374.4	376.4	379.7	384.1	389.9
10.3	431.7	409.5	394.8	385.0	378.7	376.1	375.2	377.3	380.6	385.1	391.0
10.4	432.3	410.2	395.5	385.7	379.5	377.0	376.1	378.2	381.5	386.1	392.1
10.5	433.0	411.0	396.3	386.6	380.4	377.9	377.1	379.3	382.7	387.3	393.4
10.6	433.9	411.9	397.3	387.6	381.5	379.0	378.3	380.5	384.0	388.7	394.8
10.7	434.7	412.6	398.1	388.4	382.4	379.9	379.3	381.5	385.0	389.8	396.0
10.8	435.5	413.6	399.0	389.4	383.3	381.0	380.4	382.7	386.2	391.1	397.3
10.9	436.2	414.2	399.7	390.1	384.2	381.8	381.3	383.6	387.2	392.1	398.4
11.0	436.9	415.1	400.6	391.1	385.0	382.8	382.3	384.7	388.4	393.3	399.7
Min	428.3	405.8	390.7	380.5	374.0	370.8	369.2	370.6	373.3	377.3	382.0

Table 14. LCOE heatmap of the head and flow enumeration for Housatonic with four generation modules.

LCOE ($/MWh)	Powerhouse Design Flow (cfs)										
Design Head (ft)	872	1045	1218	1391	1564	1737	1910	2083	2256	2429	2602
8.6	481.7	439.2	413.0	395.5	385.3	381.5	379.9	380.8	383.5	386.6	389.8
8.7	465.3	425.9	401.4	386.0	377.7	374.0	372.1	372.9	375.7	379.0	382.2
8.8	449.4	412.8	391.3	377.8	369.5	365.8	364.0	365.1	368.1	371.5	374.9
8.9	438.7	405.0	384.9	371.6	363.5	360.1	358.7	360.0	363.1	366.7	370.3
9	432.3	400.0	380.1	367.2	359.6	356.5	355.3	356.8	360.1	363.9	368.2
9.1	427.0	395.0	375.9	363.5	356.3	353.4	352.6	354.5	358.8	364.1	369.2
9.2	422.8	391.6	373.1	361.2	354.3	**352.3**	352.6	355.6	360.0	365.3	370.6
9.3	419.8	389.4	371.3	360.0	354.0	352.6	353.4	356.5	361.0	366.4	371.7
9.4	417.3	387.4	369.7	358.7	353.4	353.2	354.5	357.6	362.2	367.7	373.1
9.5	416.9	387.4	369.9	359.3	354.3	354.1	355.6	358.8	363.5	369.1	374.6
9.6	416.6	387.7	370.7	360.2	355.3	355.3	356.8	360.1	364.9	370.6	376.2
9.7	417.0	388.5	371.5	361.1	356.3	356.3	357.9	361.3	366.2	372.0	377.7
9.8	417.6	389.2	372.4	362.0	357.3	357.4	359.2	362.6	367.6	373.5	379.4
9.9	418.3	390.1	373.3	363.0	358.3	358.6	360.4	363.9	369.0	375.0	381.0
10	419.3	391.0	374.3	364.1	359.5	359.9	361.7	365.4	370.7	376.7	382.8
10.1	419.9	391.7	375.0	364.9	360.4	360.8	362.8	366.5	371.8	378.0	384.1
10.2	420.5	392.5	375.8	365.8	361.4	361.8	363.9	367.7	373.0	379.3	385.5
Min	416.6	387.4	369.7	358.7	353.4	352.3	352.6	354.5	358.8	363.9	368.2

Table 15. LCOE heatmap of the head and flow enumeration for Schuylkill with three generation modules.

LCOE ($/MWh)	Powerhouse Design Flow (cfs)										
Design Head (ft)	1260	1490	1720	1950	2180	2410	2640	2870	3100	3330	3560
9.7	345.1	324.0	312.4	305.3	301.4	300.4	301.2	302.2	305.0	307.8	311.2
9.8	334.3	315.8	304.0	297.2	293.9	293.3	294.3	295.6	298.6	301.6	305.3
9.9	322.8	304.5	293.7	287.7	285.0	284.8	286.2	287.9	291.4	296.9	303.7
10	317.1	299.6	289.3	283.8	**281.4**	281.5	283.6	287.0	292.0	297.6	304.4
10.1	317.1	299.7	289.6	284.1	281.8	282.0	284.2	287.7	292.8	298.4	305.4
10.2	317.3	299.9	289.9	284.5	282.2	282.5	284.8	288.3	293.4	299.2	306.2
10.3	317.6	300.3	290.3	285.0	282.8	283.1	285.4	289.0	294.2	300.0	307.2
10.4	317.8	300.6	290.6	285.4	283.3	283.6	286.0	289.7	295.0	300.8	308.0
10.5	318.1	300.9	291.0	285.8	283.8	284.2	286.7	290.4	295.7	301.6	308.8
10.6	318.5	301.4	291.6	286.4	284.4	284.9	287.4	291.2	296.6	302.6	309.9
10.7	318.9	301.9	292.1	287.0	285.0	285.6	288.2	292.0	297.5	303.5	310.9
10.8	319.3	302.4	292.7	287.6	285.7	286.3	289.0	292.9	298.4	304.5	312.0
10.9	318.9	302.1	292.3	287.3	285.4	286.0	288.6	292.5	298.0	304.1	311.5
11	319.5	302.7	293.0	288.1	286.2	286.9	289.6	293.5	299.1	305.3	312.8
11.1	320.3	303.5	293.9	289.0	287.2	288.0	290.7	294.8	300.4	306.7	314.3
11.2	321.1	304.3	294.8	290.0	288.3	289.1	292.0	296.1	301.8	308.2	316.0
11.3	321.8	305.0	295.6	290.8	289.2	290.0	293.0	297.2	303.0	309.4	317.3
11.4	322.4	305.8	296.3	291.6	290.1	291.0	294.0	298.3	304.2	310.7	318.6
11.5	323.1	306.5	297.2	292.5	291.0	292.0	295.0	299.4	305.4	312.0	320.0
Min	317.1	299.6	289.3	283.8	281.4	281.5	283.6	287.0	291.4	296.9	303.7

The optimal configurations for each module count are presented in Table 16. The differences in minimum LCOE between the module counts are relatively small between several configurations, such as between three and four module configurations for Housatonic ($352.64/MWh vs. $352.33/MWh). In general, more modules would enable greater generation flexibility and efficiency, while fewer modules would reduce the total powerhouse footprint. The optimal module counts also differ from the baseline designs. For example, the Schuylkill baseline has five generation modules, while the enumeration process identified three modules. The Housatonic baseline has three modules, while the enumeration identified four, indicating that the design capacity is a larger driver of LCOE than the number of modules. In these cases, the difference between multiple smaller modules and fewer larger modules is relatively small compared to the total costs. As innovation and modularity drive down the costs of each module, this distinction may become a larger percentage of total costs. However, based on SMH principles, the number of modules will be based on standardized sizes to meet a desired optimal capacity and additional engineering and supply chain factors.

The design heads and module counts were assumed to be the identified optimal values based on the coarse enumeration process. For example, Deerfield had four modules with a design head of 9.5ft. Housatonic had four modules with a design head of 9.2ft. Schuylkill had three modules with a design head of 10ft. The next step was to identify the optimal design flow by enumerating the design flow by 10cfs increments between the upper and lower bounds of the optimal design flow range from the coarse enumeration. For example, as illustrated in Table 13, the optimal design flow for the coarse enumeration was 2194cfs, so the design flow was enumerated between 2030cfs and 2360cfs in 10cfs increments, which were the design flows iterations on either side of the optimal value.

The results of design flow enumeration for each site are illustrated in Figure 25 as a plot of capacity versus normalized LCOE. The differences between the maximum and minimum LCOEs within this range were very small (<1.5%) for all three sites, so the normalization helps identify the shape of the design space. The normalized curves show local minima and a non-smooth design space reflective of the model's modular nature. Discrete thresholds, like the footprint needed to add another $1m^2$ foundation module or the stream width needed to add another non-overflow unit, created these abrupt changes in the objective functions. The existence of local minima that were not the global minima precludes convex optimization techniques. Although the differences in LCOE between these flow values were very small, this may result from the high overall project costs since higher total costs would make small changes in turbine costs and revenues less significant. Nonetheless, there was a wide range of capacities that could achieve similar LCOEs. The generation optimization in Case Study B exemplifies this as well. The underlying tradeoff within hydropower design optimization is that higher capacities lead to lower capacity factors, which risk under-utilizing the technologies. The selection of turbine capacity in practice will be affected by supply chain limitations, standardized product SKUs (stock-keeping units), transmission limits, and the needs of the

Table 16. Coarse enumeration results by module count for each reference site.

Site	Module Count	Min LCOE ($/MWh)	Design Capacity (kW)	Design Head (ft)	Design Flow (cfs)
Deerfield	2	388.1	1054	9.2	1866
	3	372.091	1185	9.5	2030
	4	369.245	1280	9.5	2194
	5	372.161	1280	9.5	2194
Housatonic	2	356.583	950	8.9	1737
	3	352.64	971	9.1	1737
	4	352.334	982	9.2	1737
	5	354.041	1003	9.4	1737
Schuylkill	2	285.722	1198	10	1950
	3	281.429	1339	10	2180
	4	282.856	1480	10	2410
	5	285.179	1480	10	2410

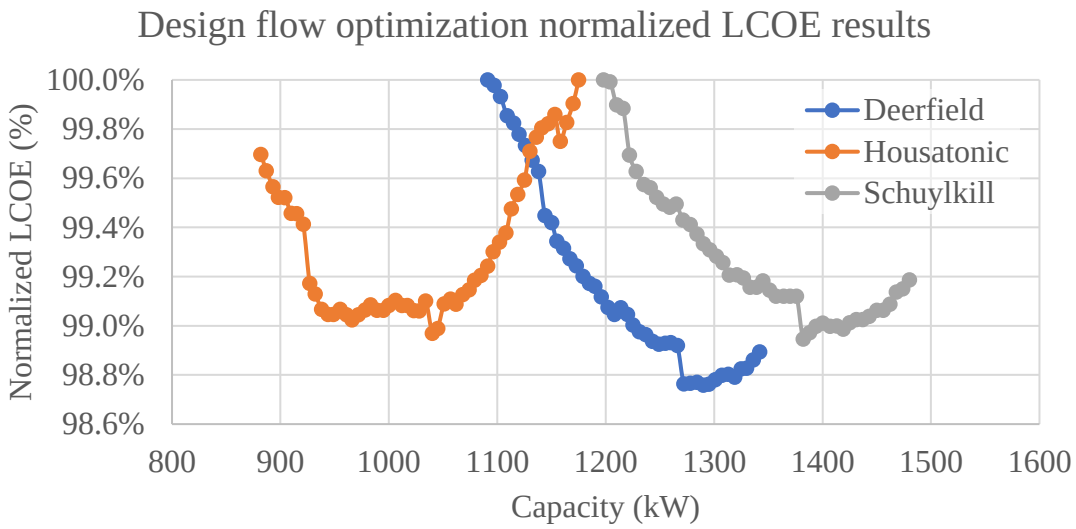

Figure 25. Results of design flow enumeration for reference sites (LCOE values normalized with respect to the highest value in each enumeration sample).

local electricity system. Although there is limited data to inform constraints like transmission capacities, the object-oriented approach helps integrate standardized technologies into design modeling.

The optimal designs were selected by taking the optimal design flow values from the flow enumeration and the design heads and module counts from the coarse enumeration. These enumeration procedures used the Peak Ramping dispatch method to facilitate faster runtimes. The final optimized designs, described in Table 17, were re-run with the Advanced Greedy method to obtain better LCOEs. There was a chance that the dispatch method would affect the optimal design through higher generation estimates. However, this increase would be relatively equal across design flows and was assumed to be marginal given the small differences in LCOE from the design flow enumeration. Table 17 highlights significant improvements in LCOE between the baseline and optimized designs (11% for Deerfield and Housatonic and 6% for Schuylkill). The optimal LCOE occurred at higher capacities and higher costs than the baseline designs in each case. Only the Deerfield design was optimized in prior research; however, that optimization did not have itemized cost data. The differences in LCOE could also stem from the slightly different inputs, assumptions, and modeling/dispatch approaches, which include the ability to custom design the turbine modules. The baseline designs used the same generation module across the three sites, whereas the generation module design heads and flows were optimized for each site in this approach. Using standard module sizes may limit generation optimality to reduce development costs. Advanced manufacturing approaches, like 3D printed runners, could help support custom-designed components within a modular framework to help address this loss.

Cost sensitivity analysis

As previously discussed in the Cost Model Validation section, the reference costs were conservative and reflective of pilot-type projects, whereas modular projects are assumed to gain economies of scale through mass deployment. This section uses the itemized cost model to evaluate the effect of various cost scenarios on project economics. These scenarios assess the impacts of the foundation depth, the non-powered modules, and the turbine price on project feasibility. The optimized designs identified in the previous section are used for the sensitivity analyses throughout this section.

Foundation depth uncertainty

Foundations represent one of the largest cost components and areas of uncertainty in hydropower projects [40]. For example, in the baseline Deerfield design (Figure 22), the foundation represents 28% of the total project cost. Foundations are designed to connect the specific superstructure and subsurface conditions at the site, so they vary based on the type of bed material and the design of the superstructure[40]. The goals are to provide stability and a water-tight barrier for the superstructure (the dam or modules) to limit potential dam failure modes like sliding, overturning, and others caused by water infiltration [40]. Foundations and foundation construction practices can include excavation of bed material, leveling existing rock formations, grouting to fill cracks,

Table 17. Simulation results for the baseline and optimized designs for the three reference sites.

Metric	Deerfield		Housatonic		Schuylkill	
	Baseline	Optimized	Baseline	Optimized	Baseline	Optimized
LCOE ($/MWh)	$408	$363	$389	$345	$293	$275
Capacity (kW)	864	1290	648	1040	1080	1382
Annual generation (MWh)	5332	6689	3819	5019	7176	8081
Total Cost ($M)	$17.9	$19.9	$12.3	$14.2	$17.2	$18.2
ICC ($M)	$13.9	$15.5	$9.4	$0.8	$13.5	$14.3
Annual O&M ($M)	$0.83	$0.93	$0.57	$0.66	$0.81	$0.86

grout curtains to prevent seepage, anchors connecting to stable rock formations, and a variety of concretes [40].

The most stable foundation would be integrated into the existing bedrock at the site; however, the depth to the bedrock may differ greatly between sites, and there is limited data to understand the instream depth to bedrock without expensive, in-person geotechnical investigations. ORNL's report on the geotechnical state of practice highlights an underlying concept that valley regions (where the majority of NSD potential exists) are likely to be soil foundations with thicker overburden (bed material) layers due to lower stream gradients than mountainous regions [40]. As such, over 89% of low-head dams in the US are earthen dams that may be built on top of existing overburden material rather than integrated directly into the bedrock [160]. Earthen dams are larger in volume than concrete dams used for higher head projects but reduce costs by using local materials. Earthen dams are less dense and have wider footprints than concrete dams, allowing forces to be widely distributed across the subsurface [40]. Concrete dams must be placed on a stable subsurface material or bedrock because the forces during operation and material settling may cause movement of soil subsurfaces and result in dam failure. While modular technologies are still in development, it is expected that modules have limited footprints to enable transportation from manufacturing centers. As such, modular facilities may rely on foundations built into the bedrock rather than on soil subsurfaces, which presents a significant area of cost uncertainty.

The reference foundation technology used for this case study is based on pre-cast concrete blocks that sit flush with leveled and excavated bedrock and provide a flat surface for overlying modules. This design is conceptual, and no research has targeted how the modules connect with other modules. In addition, the foundation design was not optimized for the turbine setting (height in relation to the tailwater), which can impact cavitation and performance [89]. However, the simple design provided the opportunity to model costs volumetrically as a function of the facility footprint and the depth to bedrock. The primary cost components are excavation and leveling of the top 0.5m of the bed, precast concrete to fill the gap between the bedrock and the bed datum, and anchors to connect the concrete block to the bedrock. The module was parameterized as a function of the depth to bedrock to enable the following sensitivity analysis. The number of $1m^2$ modules is determined by dividing the footprint of all modules by the area of one foundation module. The assumed depth to bedrock was 5ft for the baseline condition, as suggested by the engineering contractors. As described in the Cost Model Validation section, scaling factors accounted for the difference between the modeled and reference costs. The module attributes are detailed in Table 29 – Table 35 in the Case Study A section in the Appendix.

A sensitivity analysis was conducted on the depth to bedrock for the three reference sites. Instead of a simple analysis of the total foundation cost, this approach allowed the model to separate the material/technology costs from the foundation depth, which is the primary

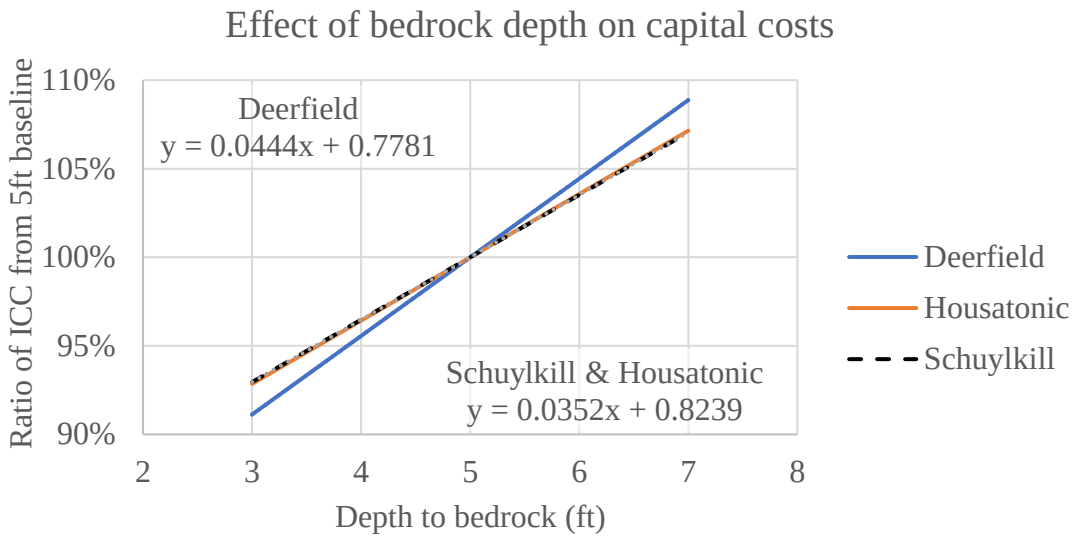

Figure 26. Sensitivity analysis results for depth to bedrock on initial capital costs.

area of uncertainty. Figure 26 presents the results as a function of the percent change in ICC. The results are linear trends (equations shown in Figure 26) resulting from the cost model used to parameterize the module. The primary takeaway is that, for these sites, a 1ft change in the assumed depth to bedrock can result in a 3-4% change in initial capital costs. To put this into perspective, for the Deerfield site, a 3ft foundation costs $3.86M while a 7ft foundation costs $6.32M, which is a 64% increase in foundation costs. The foundation cost uncertainty depends on several factors like the facility's footprint and the static and dynamic structural characteristics of the overlying modules. Cracks or instabilities in the foundation can also lead to considerable cost overruns through additional grouting and formwork [40]. These factors can lead to cost uncertainties well over the 3-4% per foot found in this sensitivity. These results highlight the need for research into cost-effective site investigation practices, modular earthen foundation technologies, and nationwide analyses of in-river subsurface conditions.

Module combinations

Another assumption within the baseline designs is that the facility must have the boat chute, sediment sluice gate, and vertical slot fishway modules. These non-power modules represent approximately 9% of the total costs for Deerfield and use flow that could be used for generation without providing explicit sources of revenue in the cost modeling. The recreation module may provide admission revenues, described further in Case Study B, but these revenues are not considered in this analysis. Instead, this analysis focused on the cost and generation tradeoffs associated with including these modules in the facility. Simulations were run for Deerfield without each non-power module and a case with only generation and spillway modules. One set of simulations was run while keeping the powerhouse design constant. The results for the constant powerhouse simulations are illustrated in Figure 27. The other set of simulations was run while reoptimizing the powerhouse design with each combination of modules, as represented in Figure 28. The Peak Ramping dispatch model was used to improve runtimes. While this increased LCOEs compared to the optimized baselines, the effect was assumed consistent across simulations, enabling fair comparisons between the runs.

The costs of the non-power modules drove changes in LCOE for the different module combinations, the design flows, and the operation interactions. The sediment sluice gate had a design flow of 1355cfs but was operated after the generation modules, so it did not directly affect generation. This is shown by equal energy generation for the baseline and “without sediment” runs in Figure 27. The boat chute and vertical slot fishways with design flows of 50.5cfs and 34.5cfs, respectively, were higher in the operating rule curve and directly affected the flow available for generation. The four generation modules for the optimized baseline design each have design flows around 552.5cfs, so the non-power design flows were small by comparison. The combined fishway and boat chute flows were about 3.8% of the total powerhouse design flow. Removing the recreation module led to a 1.9% increase in generation, and removing the fishway led to a 0.7% increase, leading to a combined increase of 2.5% in the generation-only scenario. The relationship between the non-power design flow ratio (3.8%) and generation loss (2.5%) is not 1:1 because excess flows during wet months did not lead to generation losses even though all

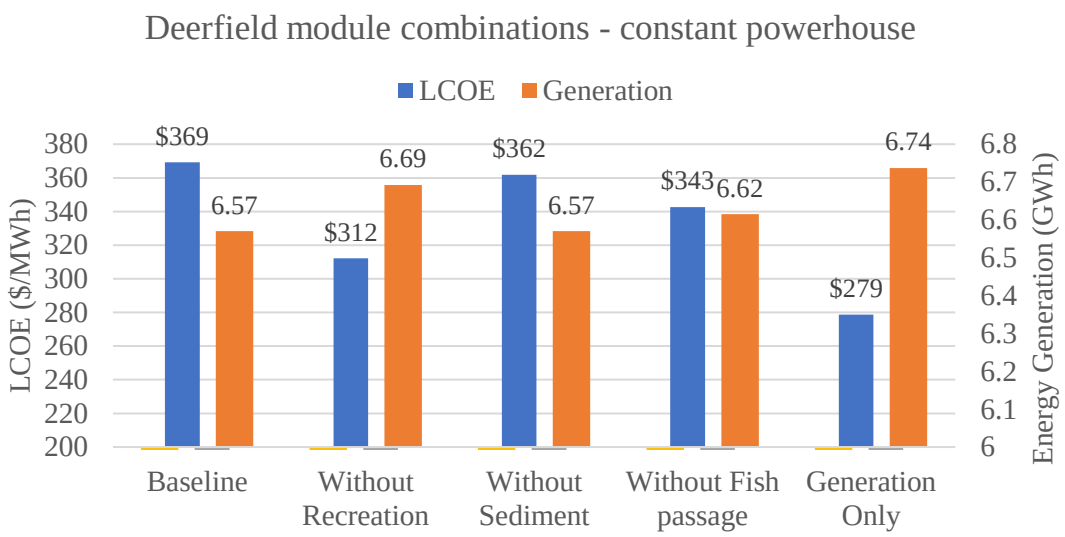

Figure 27. Comparison of levelized cost of energy (LCOE) and annual energy generation by module combination for the Deerfield site with a constant powerhouse design.

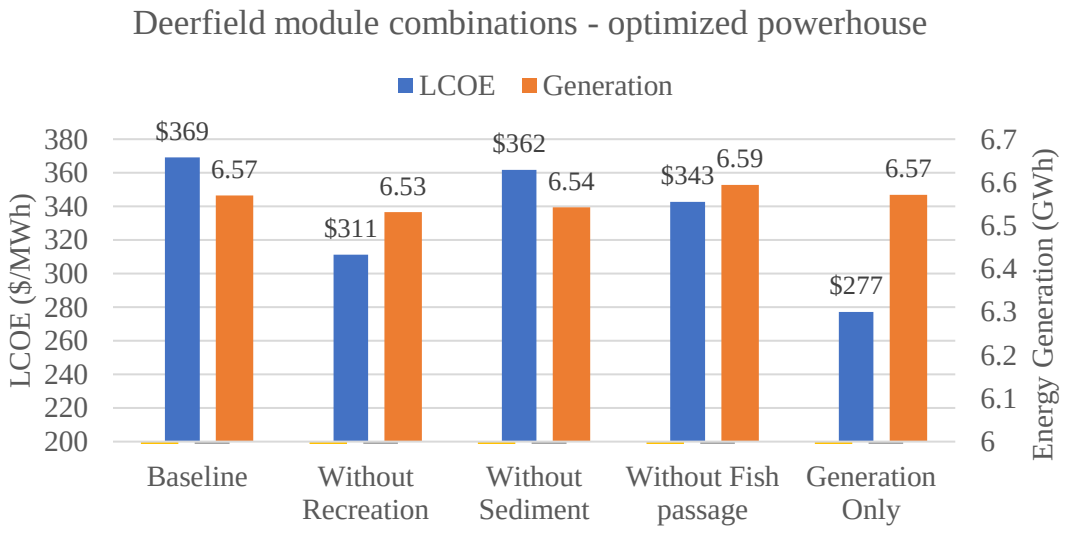

Figure 28. Comparison of levelized cost of energy (LCOE) and annual energy generation by module combination for the Deerfield site with re-optimized powerhouse designs.

modules were operational. In this scenario, the differences in LCOE were largely driven by module costs rather than generation losses.

The results of the optimized design scenarios (Figure 28) are interesting because the annual energy generation was similar across the module combinations and decreased in several cases. Generation would be expected to increase without the competing flow demands, like in the constant powerhouse results, but the optimized designs responded to lower costs by decreasing the powerhouse size slightly. The overall LCOE savings between the constant powerhouse and optimized powerhouse runs were small (1-2$/MWh). This reflected the small ratio of design flows between the non-power modules and the powerhouse. Different module designs, like the whitewater park in Case Study B, with higher design flows would have larger impacts on the optimal design, LCOE, and energy generation.

Nonetheless, the capital costs of the non-power modules were considerable ($1.3M) and increased the LCOE by about 25%, which could prohibit development in many cases. These modules can be valuable community resources and support ecosystem function, so further research is needed to decrease the costs of these technologies and monetize the value these technologies provide. For example, tax incentives for fish passage technologies or performance-based fish passage regulations could support low-head hydropower development and research into more effective technologies. Combined fish passage and recreation technologies could also reduce the civil works costs of constructing separate modules. Advanced operating strategies that leverage seasonal or optimized operation could reduce generation losses while maintaining environmental performance.

Generation economies of scale

The focus of hydropower innovation, particularly within the trends of standardization and modularity, often falls on turbines. Cost reductions for non-overflow modules, spillways, and other essential components are expected to have proportional decreases in total costs with some limited impacts on the optimal powerhouse design. This is reflected in the previous section because the costs reductions from removing the non-power modules did not significantly change the optimal annual energy generation. However, cost reductions for generation modules were expected to have more distinct effects on the optimal powerhouse design. Cost reductions could come from manufacturing economies of scale, additive manufacturing techniques, innovative runner materials, modular power electronic designs, and many other avenues. Lower-cost units would enable additional units to capture more energy at lower capacity factors to achieve break-even costs. This hypothesis was tested by sensitivity analysis of turbine costs on the optimal powerhouse design.

The analysis was run on the Deerfield site using the Peak Ramping dispatch method and an enumeration procedure to re-optimize the design flow and module count for each turbine cost iteration. The turbine costs were discounted from the original cost (0%) to half of the original cost (50%) in 5% increments. The enumeration method iterated

between 1700cfs and 2500cfs in 50cfs increments and between 2 and 7 modules. The design head of 9.5ft was held constant.

The results of this process are illustrated in Figure 29, which shows a positive relationship between the turbine discount (lower turbine costs) and both optimal capacity and annual energy generation. A 50% decrease in turbine cost led to a 13.6% increase in optimal capacity and a 3.8% increase in annual energy generation. The capacity factor, in this case, went from 58% at full turbine costs to 53% at half turbine costs. The relationships in Figure 29 exhibit a step-like function that may result from the discrete modular nature of the facility design. The optimal number of modules remained at four modules until the turbine discount hit 40%, at which point it increased to five modules. Lower module costs may incentivize using multiple smaller units rather than fewer larger units. The effect of turbine discount on the LCOE was linear with a relationship of $y = -117.6x + 369.6$ ($R^2 = 0.9998$). This means that a 50% decrease in turbine cost led to a $58.8/MWh or 16% reduction in LCOE.

Overall, the enumeration process validated the hypothesis that decreased turbine costs would lead to higher capacities and capacity factors along with significant reductions in LCOE. As such, investment in low-head turbine technologies to improve cost and performance can be worthwhile ventures. Research and development could target several areas of powerhouse design, including runner materials, module footprint, generator/converter efficacy improvements, and variable speed designs. For example, although the standardization principle of SMH implies the use of equally sized modules, there is considerable opportunity for modules of different types and sizes, as indicated in the RHDM study by Anagnostopoulis and Papantonis [61]. For example, having several propeller-type modules that operate in on/off mode and one variable speed turbine with greater flexibility to help capture intermittent flows could reduce the electro-mechanical costs while meeting generation goals. In addition to the direct capital costs of the generation modules, research could also target the indirect costs of the modules required to support the powerhouse. The Kaplan generation modules in this scenario only represented 20% of the total cost, while foundations, spillways, and non-capital cost components (engineering, overhead, care of water, etc.) also represented a large portion. Floating powerhouses, for example, could help reduce foundation costs and expedite construction, thus reducing non-capital costs. Partial dam designs or even hydrokinetic designs could allow in-river generation without the need for non-overflow modules, although research is needed to understand the generation and water level variability. The waterSHED model has the capabilities to support this research in the future.

Headwater level sensitivity

Head is a key driver of costs and performance for hydropower projects [9]. NSD sites can be developed for a wide range of head values, but the costs to create that head vary depending on the site's geomorphic, hydrologic, and hydraulic conditions. Increasing head requires creating taller structures to impound larger water volumes with larger impoundment footprints. As described in Chapter Two, reservoir creation and design

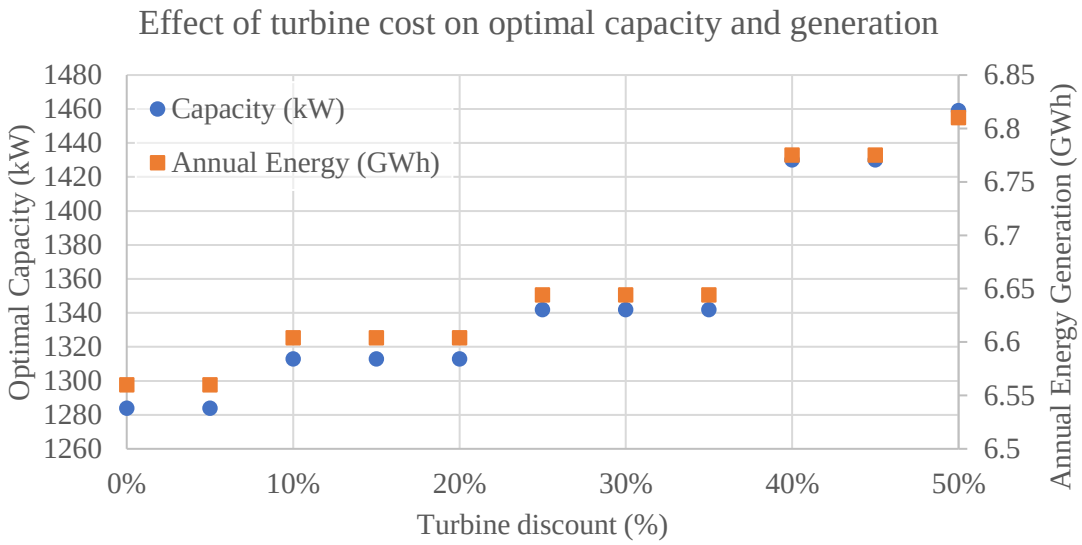

Figure 29. Results for the economies of scale sensitivity analysis examining the effect of turbine costs on optimal capacity and annual energy generation.

have numerous social and environmental impacts from the relocation of upstream communities, changes in flood risk for upstream and downstream stakeholders, increased sediment retention, implications on water rights and availability, and water quality changes, among others. The normal operating headwater level (NOL) of 13.5ft for the reference designs was based on the 100-year FEMA flood elevation for the Deerfield site. The same NOL was assumed for the Housatonic and Schuylkill sites, which were selected because they had similar head ranges. Per the NSD resource assessment [5], buildings are less likely to be constructed below the 100-year flood elevation, so the impoundment would have less chance of affecting buildings. In practice, hydropower developers would need to conduct geospatial analyses and surveys to identify how a new dam impacts upstream stakeholders. So, the selection of the NOL provides clear tradeoffs between multi-disciplinary objectives. The following analysis was designed to evaluate the effect of increasing NOL for the reference sites on economic outcomes and sedimentation. Increasing the NOL was expected to decrease LCOE and increase sediment trap efficiency. Future studies would be needed to evaluate the social impacts of the increased headwater elevations before selecting a final design NOL.

A sensitivity analysis was run for each of the three reference sites by changing NOLs between 13.5ft and 16ft in 0.25ft increments. At each iteration, the design flows and module counts were kept constant, and the design head was enumerated between the expected head ranges (9-12ft for Deerfield and Housatonic and 9.8-13ft for Schuylkill) in 0.1ft increments. This accounts for the change in optimal design head as the gross head changes. The simulations were run with the Peak Ramping dispatch model to expedite runtimes.

Many components of the design change as the NOL increases, which is why many RHDM studies assume a constant head. First, the non-overflow modules increased in height and length, maintaining a constant height to length ratio. The stream width was not adjusted for each NOL, so the cost of additional abutment modules was assumed to be part of the additional non-overflow cost. Second, the spillway modules were raised using pre-cast concrete blocks below the Obermeyer gate, which increased the crest elevation to match the NOL. Raising the Obermeyer gate may impact design flow or operational capabilities, but that assessment is outside the scope of this work, and the changes to spillway design flow were assumed to be minimal. Third, the recreation and fish passage modules increased in size by adding more steps once certain height thresholds were met. Fourth, the re-optimized design head for the turbines changed the cost and footprint of the modules. These design changes were associated with cost functions as described in Table 29 - Table 35 in the Appendix. Finally, the reservoir impoundment area changed based on the geometric reservoir volume model described in the Operational Models section. Since the Obermeyer spillway module regulates the headwater level as a controlled spillway, the reservoir volume was constant throughout the simulation. As the reservoir volume increased, the reservoir sedimentation was also expected to increase due to increased hydraulic residence times.

The effect of NOL on economic performance was relatively linear, as illustrated in Figure 30. For all three sites, each 0.25ft increase in NOL increased the optimal turbine design heads by 0.2ft, which was expected to be a 1:1 relationship with smaller design head increments. The relationships between NOL and LCOE were not exactly linear, given the discrete modular nature of the design. Increasing NOLs from 13.5ft to 16ft decreased LCOEs for Deerfield, Housatonic, and Schuylkill by 10%, 10.5%, and 8.9%, respectively. Annual energy generation increased linearly with NOL, and the increase from 13.5ft to 16ft resulted in generation increases of 23-26% for the three sites. Overall, these results were expected and followed conventional hydropower design knowledge, although the slopes of the linear relationships depended on site-specific factors.

The geometric reservoir volume model and the sediment trap efficiency models were used in conjunction to evaluate the expected effects of NOL on sedimentation. The geometric reservoir model computes the reservoir volume using the NOL, the stream width, the stream slope, and a dimensionless parameter (k_{res}) that describes the shape of the reservoir (larger k_{res} values indicate larger reservoir volumes). As shown in Table 7, the recommended k_{res} values range from 0.167 to 0.4. For this analysis, the largest recommended value of 0.4 was selected to represent an above-average scenario. The average trap efficiency model relies on a flow-weighted capacity-inflow ratio and a dimensionless sedimentation parameter β, which represents the reduction in storage capacity from sedimentation. Larger β values relate to better mixing capabilities and lower sedimentation. The lower bound parameter of the Brune model [68] of 0.0055 was used to represent an above-average scenario.

The results of the sedimentation analysis are illustrated in Figure 31 for the three reference sites. Each site had slight polynomial (almost linear) relationships between NOL and average trap efficiency driven by the polynomial changes in impoundment volume. The Deerfield reservoir, for example, increased from 557acre-ft to 783acre-ft with NOL changes from 13.5ft to 16ft. For comparison, Bosher Dam, the non-powered dam from Case Study B, has approximately 2,100acre-ft of storage capacity with an NOL of 16ft. These low-head reservoirs were quite small based on these parameters, which resulted in average trap efficiencies of less than 1.2%. This means that less than 1.2% of the incoming sediment was expected to accumulate in the reservoir, and the rest will be passed downstream as suspended loads. Larger reservoirs can have trap efficiencies of 79% depending on the sediment characteristics, reservoir geometry, and operating conditions [149]. Despite using above-average parameters, the trap efficiencies for these sites were low, indicating that the risk of sedimentation is low, which is corroborated by existing literature [146].

However, there are many limitations to this sediment modeling methodology. First, trap efficiency assessments are tuned to large impoundments, limiting their ability to model small headponds [161]. Second, the dimensionless parameters k_{res} and β are high-level approximations of physical processes that would require in-depth site assessments. Third, these models only address the sedimentation component of sediment continuity and

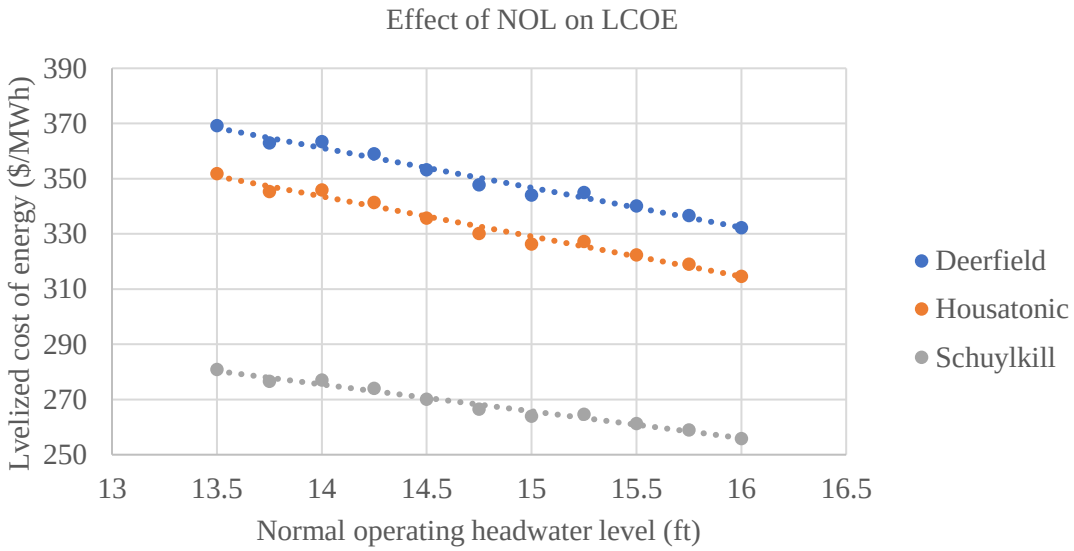

Figure 30. The relationships between normal operating headwater level and levelized cost of energy for the three reference sites.

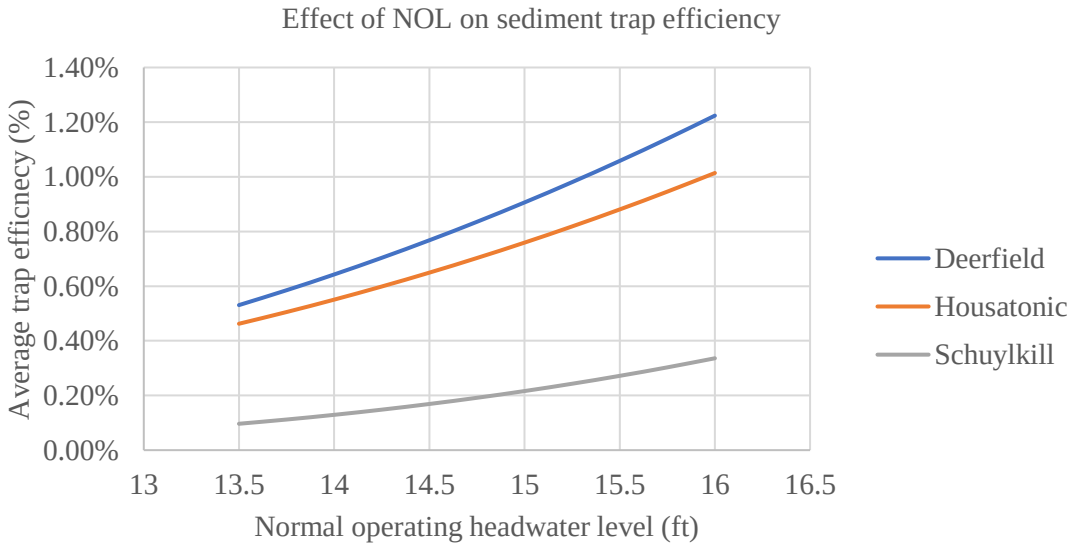

Figure 31. The relationships between normal operating headwater level and the average sediment trap efficiency for the three reference sites.

ignore downstream effects of armoring or scour that were determined to be outside of the scope of this research due to the need for high fidelity stream bathymetry data and hydraulics models. Fourth, this model only considers the risk of sedimentation and does not connect to the sediment module impacts on sedimentation, which is investigated in the following section. These results may indicate that the need for sediment module flows is minimal. Additionally, specific sediment modules may not be necessary if alternative bed load passage routes exist within current technologies, such as through sediment ramp flows over weirs [134] or by lowering Obermeyer spillway gates to the horizontal position that acts like a sluice gate. Overall, this combination of models helped establish high-level tradeoffs between NOL, sediment, and economic performance, but further research is needed to address these limitations and other social and flood risk impacts.

Sediment sluice gate tradeoffs

The previous section addressed the risk of sedimentation for different headwater levels, which determines the likelihood of incoming sediment to deposit in the riverbed. It is also important to consider how sediment that accumulates in the bed will be transported across the facility. Suspended sediments can be transported across the dam through spillways or other module flows, but bedload sediments can be difficult to pass since intakes for most modules are higher than the bed, and turbine modules, which can have low-level intakes, try to limit the amount of sediment flow to protect the blades from abrasion. As such, the SMH framework identified sediment modules as technologies that provide pathways for these bed-load sediments. The reference designs use a sediment sluice gate, which consists of a slide gate that is raised to create a low-level outlet that uses high velocity flows to entrain the local bed sediments. The Case Study Report [17] originally conceptualized the sluicing operation mode where the gate is opened when a given inflow threshold is met. The idea is to open the gate whenever inflows are likely to entrain upstream sediments into the reservoir so that incoming sediments pass through the facility without accumulation to meet the goal of 100% sediment continuity. The inflow threshold, called the sediment module operating flow in the object-oriented framework, was selected using the probability of entrainment model described in the Sediment Models section. The baseline operating flow of 6774cfs was identified by calculating the 50% probability of entrainment for a 24.6mm d_{50} particle size, the median particle size reported for the Deerfield site [17][3]. The 50% entrainment probability was arbitrarily selected since volumetric sediment flow models were not feasible with this level of data. The following analysis was used to put the selection of the sluice gate operating flow into perspective by identifying its relationship with the high-level sediment performance metrics in waterSHED.

A sensitivity analysis was conducted for the three reference sites by varying the entrainment probabilities through a range from 5-50% in 5% increments for the 24.6mm

[3] Modeling and input differences between this research and the Case Study Report [17] led to different entrainment probability calculations. The Case Study Report [17] determined the 50% probability of entrainment as 6774cfs, while this research determined a 50% probability as 16,044cfs. The entrainment model is relatively sensitive to model inputs, so this difference was expected.

particle size. The entrainment probability model also depends on the stage-discharge relationship, which differed between sites (Figure 21), and the stream slope, which was assumed to be the same for each site (0.0012ft/ft). The range of probabilities was used to calculate a range of operating flow values for each site (see Table 25 in the Appendix), which were iterated during the sensitivity analysis. The baseline flows of 6774cfs correspond to 28.5%, 44.7%, and 23.4% entrainment probabilities for Deerfield, Housatonic, and Schuylkill, respectively, highlighting the differences between the site conditions. The Case Study Report [17] assumed that the design flow of the module was 20% of the operating flow, so the design flow was also changed accordingly at each iteration. However, there was limited cost data to scale the sluice gate width to different design flows appropriately, so it was assumed that the gate cost was constant, and the design flows were met by raising the slide gate to different heights. The simulations were run with the Peak Ramping dispatch model and without the fish passage and recreation modules to focus only on the generation and sediment module tradeoffs. However, the sediment passage module was the last module class on the priority curve, so the sediment module was only allocated flow after the generation modules were ramped. Thus, the sediment design flows did not influence generation or the powerhouse design. Dam operators may prioritize sediment last since sediment accumulation can have large timescales, especially considering the low expected sedimentation rates at low-head dams. Additionally, it is important to note that the sluice gate was operated in an on/off fashion, meaning the gate was either fully open or fully closed. This limitation is an artifact of the design flow dispatch formulation, and partial gate opening could be explored in future assessments. So, to operate the sluice gate, the inflow had to exceed the operating flow threshold, and there had to be enough flow to ramp the other modules and meet the sluice gate design flow. Since sediment inflows occur during high flow events and the operating flow is varied in the analysis, this factor was not expected to affect the results significantly.

The analysis results in terms of the relationship between the entrainment probability and the sediment passage frequency are illustrated in Figure 32. The sediment passage frequency is the percentage of timesteps that the facility is operating the sediment module. Figure 32 shows a roughly polynomial relationship for each of the three sites that heads to zero at high entrainment probabilities. This trend was expected because higher entrainment probabilities mean higher operating flows, which lead to less frequent operation. The goal of sediment passage is to operate as frequently as possible, but 100% frequency is often not needed since sediment flows mostly occur during high flow events. The upper bound of the frequency at the 5% exceedance flows is driven by the availability of flow after allocation to the generation modules. Since the sediment passage modules were operated after the generation modules, opening the sluice gate after all other modules have been turned on rather than based on an operating flow threshold would be more effective. This would essentially use flows that would otherwise be allocated to the spillway. However, this assumes that the sluice gate has no local hydraulic effects on the other modules.

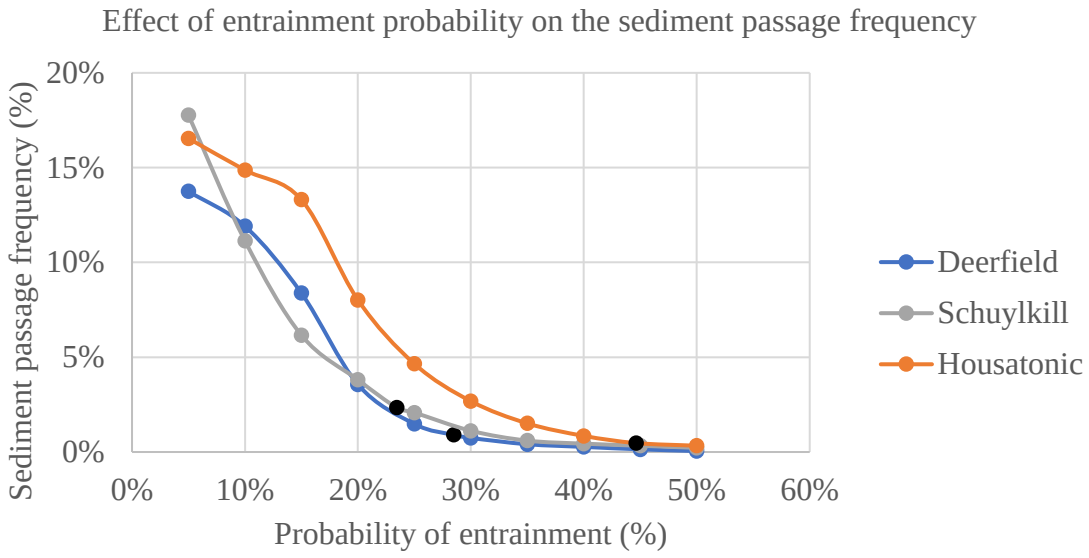

Figure 32. The relationship between entrainment probability and sediment passage frequency for the three reference sites. The black dots indicate the baseline condition (6774cfs of operating flow).

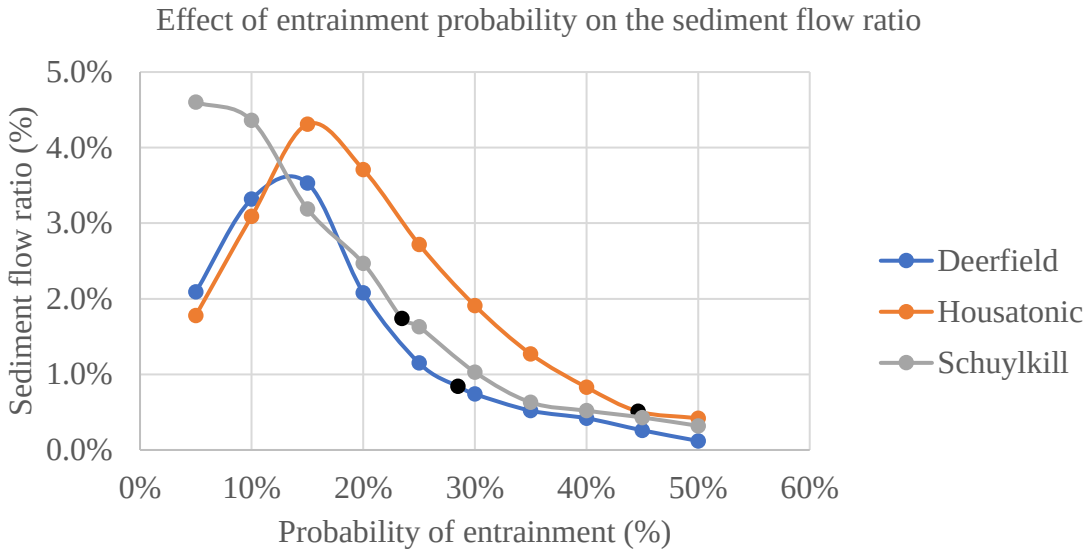

Figure 33. The relationship between entrainment probability and sediment flow ratio for the three reference sites. The black dots indicate the baseline condition (6774cfs of operating flow).

The relationship between entrainment probability and the sediment flow ratio, which is the ratio of sediment module flow to total inflow, is illustrated in Figure 33. Higher sediment flow ratios are linked to better sediment continuity because the model assumes that sediment module flows are correlated to bedload flow. Figure 33 shows an interesting relationship between the Deerfield and Housatonic sites as the sediment module flow ratio peaks at the 15% entrainment probability instead of the lowest probability like the Schuylkill site. This is a result of the design flows for the modules, which decreased as the entrainment probability decreased. The smaller design flows allow them to operate more frequently, but when they become too small (<15%), they become maxed out and miss out on leftover flows from the powerhouse that could be used for sediment passage. Given the higher operating flows at comparatively lower entrainment probabilities (Table 25), the Schuylkill site had large enough design flows to capture leftover flows, so iterations at lower design flows would reveal a similar peak. As such, if the goal is to utilize excess flows to pass sediments with the smallest possible sluice gate, the gates could be designed for these peak entrainment probabilities. For the Deerfield and Housatonic sites, the optimal operating flow is around the 15% entrainment probability, which relates to 3065cfs and 1989cfs (design flows of 613cfs and 398cfs), respectively. However, partially opening gates could facilitate better performance for larger gates.

Overall, these results validate the theme in the literature that smaller and more frequent sediment passage events are better for sediment continuity [51], [94]. In this sensitivity analysis, lower operating flows (lower entrainment probabilities) led to more frequent passage (Figure 32), which relates to improved sediment continuity. The highest sediment flow ratios also occurred at low entrainment probabilities due to the on/off limitation and assumed relationship between operating flow and design flow. Combining these results with the sedimentation model results indicates that sediment passage technologies will have minimal impact on optimal powerhouse design and generation since flow requirements are limited. With these operational assumptions (low sediment priority), the goal of sediment technologies should be to minimize capital costs rather than flow requirements. In practice, this means that sediment passage modules could leverage siphon or small low-level outlet type designs rather than larger sluicing gates currently used for larger plants to facilitate improved sediment continuity. Additionally, operational rather than structural solutions like flushing with Obermeyer gates could preclude the need for specific sediment modules. These results do not imply that sediment modules are unnecessary because prolonged periods without sediment passage can lead to accumulation that severely impacts structural safety, turbine health, and environmental performance. In addition, as with the sedimentation modeling limitations, more research is needed to understand better the relationships between the high-level performance metrics and volumetric sediment flows. For example, the relationship between sediment module flows and volumetric sediment flows needs to be studied over time for various sediment passage technologies to understand when sluicing gates should be operated. Future versions of waterSHED could explore partial gate openings and the hydraulic effects of opening sluice gates on other modules. Large gate openings could

lead to head drawdowns, which would decrease generation, and high sediment fluxes could lead to increased abrasion in the other passage modules. Improved data availability on US rivers' sediment flows and composition could also support holistic hydropower modeling. This sediment modeling approach provides a valuable first step toward integrating sediment performance in RHDMs and sets the stage for sediment passage performance metric research.

Discussion

This case study evaluated the cost, generation, and sediment passage tradeoffs for three NSD sites with around 10ft of gross head. Discussion of the results, limitations, and recommendations for future research are presented in the respective sections. This section summarizes how these separate analyses inform the research questions presented at the beginning of the section. The first question asked to identify the technology areas and site conditions that are critical for project cost and performance. The simulation results highlighted several well-identified areas in existing cost modeling literature, including headwater elevation (head), turbine costs, environmental mitigation costs, and foundation costs. Notably, the flow requirements for the non-power module design flows had minimal effect on economic performance since the flow requirements were small. Schuylkill consistently had the lowest LCOEs in each scenario because it had the highest flows on average with a smaller stream width than Deerfield. This corroborates existing design knowledge that larger projects benefit from economies of scale. However, costs across all sites were much higher than the target costs of $3,500/kW or LCOEs of other generation sources (Table 1). These high costs stem from the novelty of the modular technologies from cost estimates and the conventional reference designs, which primarily used large concrete structures. Although, as with all innovations, costs are expected to come down after high-cost, pilot and demonstration projects help stakeholders learn from deployment. Additionally, based on the sensitivity analyses, it may be beneficial to explore unconventional modular designs, such as:

- Modular earthen dams – that leverage local materials and existing expertise in low-head dam design to reduce costs.
- In-river hydrokinetic turbines – that reduce the costs associated with maintaining a pressurized hydropower conduit and consistent headwater elevations.
- Floating powerhouses – that reduce the foundation costs by anchoring generation units to soil subsurfaces.
- Combined modules – that support multiple functions like recreation and fish passage to reduce civil works costs.
- Hybrid systems – that combine hydropower with solar, wind, hydrogen storage, battery storage, or other energy resources to reduce costs by sharing electrical infrastructure.
- Advanced manufacturing for structures – that reduce development times by custom designing modules and potentially limiting the need for dewatering.

The second research question addressed the tradeoffs related to headwater level variation. The sensitivity analysis showed a negative linear relationship between LCOE and

headwater elevation, supporting existing knowledge that higher heads lead to more cost-effective projects. The sedimentation model showed a positive polynomial relationship between average sediment trap efficiency and headwater elevation, resulting from larger reservoir sizes and residence times. However, modeled trap efficiencies were very small for all three sites with above-average model parameters, which indicated that these low-head projects were not expected to be significant sediment traps. These results suggest that headwater elevation should be maximized given the social constraints of a given site, which can be assessed using additional geospatial analysis. Future resource assessments and tools could pair remote sensing techniques and other structure databases to identify the relationships between headwater elevation, reservoir volume, and affected structures.

Finally, the third question addressed the relationships between the sediment operation parameters and sediment passage performance metrics. Given the limited ability to conduct volumetric sediment modeling, it was important to evaluate the relationships between these high-level variables. The primary outcome of the analysis was that smaller and more frequent sediment passage events would better support sediment continuity than larger, less frequent operation. Since conventional high-head projects leverage large sluice gates for infrequent flushing, low-head modular technologies and operating strategies should investigate how this new paradigm can be applied cost-effectively. As described in the respective section, there were several modeling and design assumptions that could be improved with future research, including an efficacy assessment of modular technologies to understand the ratio of total module flow to sediment flow, partial gate opening modeling functionality, and validation of the hydraulic effects of sluice gates on other modules.

Overall, this case study successfully recreated the reference designs from the Case Study Report [17] and the subsequent cost estimation process. The model results align with design concepts in the literature which helped validate the system of models and construction of the software package. This case study also highlights the need for considerable investment and research into new modular technology designs to support cost reductions across the facility and development process.

Case Study B. Bosher Dam

As described in Chapter Two, the social and environmental outcomes of hydropower are increasingly important for project success. As part of the development process, plant designers must engage with stakeholders and resource agencies to assess the project's potential impacts according to several state and federal regulations, including the National Environmental Policy Act, the Federal Power Act, and the Endangered Species Act. Designers must then propose mitigation measures which often include a variety of fish exclusion and bypass measures, upstream fish passageways, and recreation features. The SMH framework addresses these measures through non-power modules, like fish passage and recreation modules. Understanding the associated cost-benefit tradeoffs and the relevant uncertainties of these non-power modules is critical for decision-making across stakeholder groups (developers, innovators, regulators, insurers, investors, etc.).

For example, developers must understand these tradeoffs when selecting the appropriate mitigation measures for their site, innovators must optimize technology designs for these tradeoffs, and regulators must understand the risks and rewards of adopting new mitigation standards. In addition, innovative environmental technologies face significant challenges because unproven technologies impart a level of risk to stakeholders, so the benefits of the technology must be justified as worth the risk of changing the state of practice. This case study aimed to evaluate the cost-benefit tradeoffs for several emerging modular technologies, including fish-safe turbines, nature-like rock ramps, and modular white-water parks.

As part of the Funding Opportunity Announcement (FOA) 1836, Natel Energy and ORNL have been investigating modular, fish-safe hydropower designs and the costs of fish exclusion systems. Part of the research has focused on conducting a feasibility assessment for an example modular facility at Bosher Dam, a low-head non-powered dam on the James River in Virginia. Their work was conducted for research purposes only, and the site is not recommended for development as further site-specific information would be needed to inform development decisions. This case study effort was conducted in parallel with FOA 1836 to leverage and validate the modeling capabilities of waterSHED. These design decisions involved 1) converting the existing concrete weir into a nature-like rock ramp, 2) adding fish-safe turbines without a fish exclusion screen, and 3) replacing the existing vertical-slot fishway with a modular whitewater park. The design tradeoffs were quantified by comparing the cost and performance metrics for the different facility configurations in waterSHED. These cases provided practical applications of the upstream and downstream fish passage models in waterSHED and provided an opportunity to validate the generation and screen head loss models. Given the level of uncertainty in the fish and cost model inputs, sensitivity analysis was used to characterize further the range of possible tradeoffs across economic and fish passage performance metrics.

Background

The existing Bosher dam consists of a 12ft tall, ~900ft long concrete gravity weir built in 1840 to provide water supply to Richmond, Virginia. A vertical-slot (VS) fishway, shown on the right in Figure 34, was added in 1999 to facilitate the passage of several migratory species, including American Eel and American Shad. The dam has been the cause of several recreation-related injuries and incidents because the weir has low visibility from the upstream side and can create hydraulic rollers just downstream. Several efforts have proposed the development of the site for hydropower purposes, but none have been successful to date. The Bosher site was selected as a case study for a modular hydropower facility because the existing dam was expected to help reduce costs. The ~12ft of gross head represents a common NSD size class, as illustrated in Figure 1.

The proposed modular facility design included several innovative modular components. Some design components are required in each configuration, while others are optional, so the waterSHED model facilitated testing of multiple configurations. The attributes for

Figure 34. Overhead view of the existing Bosher Dam site.

each module are described in detail in Table 36 – Table 41 in the Module Attributes section in the Appendix. Additional components, such as engineered log jams, trash racks, and signage, did not directly influence model performance, so the costs were included, but the features were not directly incorporated as modules. Forthcoming documentation from FOA 1836 will provide more detailed information about the design and costs. The proposed designs are highly innovative and meant to study the feasibility of environmental hydropower designs. These designs served to highlight the design tradeoffs and needs for technological or regulatory change.

The two required components were the powerhouse (generation modules) and the sluice gate. The powerhouse would be constructed in place of a portion of the existing concrete weir. The powerhouse may consist of either fish-safe generation modules (notated FS throughout this analysis) or conventional propeller turbines with a 0.75in fish exclusion screen (notated as Screen). The baseline design, determined by Natel Energy, consisted of 10 fish-safe generation modules, each with a design flow of 448 and a nominal capacity of 316kW for a total plant nameplate capacity of 3.16MW. A sluice gate was also required to pass sediments and large debris excluded from the powerhouse section. The sluice gate had a design flow of 500cfs and had an operating flow of 6,100cfs so that it operated after the higher priority flow requirements were met. Retrofitting Bosher dam with the sluice gate, conventional propeller turbines, and fish screen, along with the existing concrete weir (notated Weir) and vertical slot fishway (notated VS), would represent a **Conventional Unit Addition** (notated Screen + Weir + VS). This configuration was expected to be the design under the current state of practice because regulators would require fish screens to ensure fish safety. The screen and the non-power modules would drive up project costs. Using the fish-safe turbines instead of the conventional propeller plus fish screen design would represent a **Fish-safe Unit Addition** (notated FS + Weir + VS). This was expected to be the most cost-effective option because it would leverage the existing weir and VS fishway while disregarding the screen costs. However, this would require regulatory approval to include turbines without exclusion measures.

One of the optional components was a whitewater park built in place of the existing vertical slot fishway to provide a series of rapids for recreationalists. As described in Table 39 in the Appendix, the whitewater park was assumed to have a design flow of 300cfs, which is the minimum of the expected flow range of 300-600cfs and accounted for the fact that the waterSHED model assumes 24-hour operation, while the park would be operated during daylight hours. Richmond, Virginia, has about 12.2 hours of daylight per day on average (Table 26 in the Appendix), so the 300cfs design flow assumes a high average water usage as well as sufficient storage to mitigate the effects of variable water needs. Additionally, the whitewater park was assumed to operate year-round since recreationalists can be expected whenever the combined air and water temperature exceeds 80˚F, which occurs year-round on average (Table 26 in the Appendix). The analysis also explores seasonal recreation operation, which was assumed to occur from April to October, per the Case Study Report [17]. The whitewater park would only be

built in conjunction with the rock ramp because the park would be built in place of the VS fishway, and upstream fish passage would need to be provided.

The other optional component was a rock ramp that acts as an uncontrolled spillway and a nature-like fishway. The rock ramp is an engineered structure made of natural materials built into the existing weir spanning approximately 820ft, providing a gradual slope for upstream and downstream fish passage. The rock ramp would have a notch cut into it to provide a 250cfs minimum flow to the ramp but is otherwise assumed to behave similarly to the concrete weir with a spillway capacity of 280,000cfs. The minimum environmental flow, which is the flow that must be spilled before powerhouse ramping, was 1320cfs, so the 250cfs notch flow accounts for part of this minimum flow. In configurations with the existing weir and VS fishway, the fishway flows were included in the 1320cfs flow requirement. The natural design also improves the site's aesthetics and reduces the risks of recreation injury by providing shallower slopes over the weir. The baseline design, called **Eco-innovation** (notated FS + RR + WW), includes the fish-safe turbines, the sluice gate, the rock ramp, and the whitewater park. This design was expected to have the highest environmental and social performance due to the innovative non-power modules. For comparison purposes throughout the analysis, another configuration called **Eco-restoration** (notated Screen + RR + WW) was simulated to assess the case where the non-power modules are installed for environmental restoration purposes, and the regulators require fish exclusion measures. The following analyses leveraged the four configurations (summarized in Table 18) to understand the tradeoffs for the Bosher site.

The corresponding capital costs and annual operation and maintenance costs for each configuration are illustrated in Figure 35 and Figure 36. The costs were sourced from empirical models and engineering contractor estimates as described in Table 36 – Table 41 in the Module Attributes section in the Appendix. This model's costs and dimensions were high-level estimations for conceptual designs and should not be used for non-research applications. The rock ramp ($9.6M), the fish exclusion screen ($12.5M), and the generation modules ($10.3M) were the largest cost components. As such, the Eco-restoration configuration with all three components was the most expensive option, while the Fish-safe Unit Addition configuration with only the generation cost was the cheapest option. Several configurations leveraged existing structures at the non-powered dam (the concrete weir and vertical slot fishway), so these structures were incorporated as modules with zero capital costs. Fishways are not common at non-powered dams, so the following analyses also consider the cost of building a new vertical slot fishway. The original reported cost of the vertical slot fishway was $1.5M in 1999 [162], so after escalation (using a factor of 1.94 per the escalation methods in [158]), the estimated capital cost was $2.9M. The annual O&M costs (Figure 36) were defined on a module basis, resulting in similar values across the configurations. The O&M costs for the vertical slot fishway and the fish screen were based on average costs from relevant measures in the ORNL environmental mitigation cost database [92]. Overall, the costs reflected pilot-stage technologies, and the following analyses helped understand the relationships between cost and performance to highlight areas for future research and cost reduction.

Table 18. Summary of Case Study B module configurations.

Configuration name	Conventional Unit Addition	Fish-safe Unit Addition	Eco-restoration	Eco-innovation (Baseline)
Shorthand description	Screen + Weir + VS	Fish-safe + Weir + VS	Screen + RR + WW	Fish-safe + RR + WW
Included modules (Y=Yes, N=No)				
Rock ramp (RR)	N	N	Y	Y
Concrete weir (Weir)	Y	Y	N	N
Vertical-slot fishway (VS)	Y	Y	N	N
Whitewater park (WW)	N	N	Y	Y
Fish-safe turbine (FS)	N	Y	N	Y
Conventional propeller turbine (Screen)	Y	N	Y	N
Fish screen (Screen)	Y	N	Y	N
Sluice gate	Y	Y	Y	Y

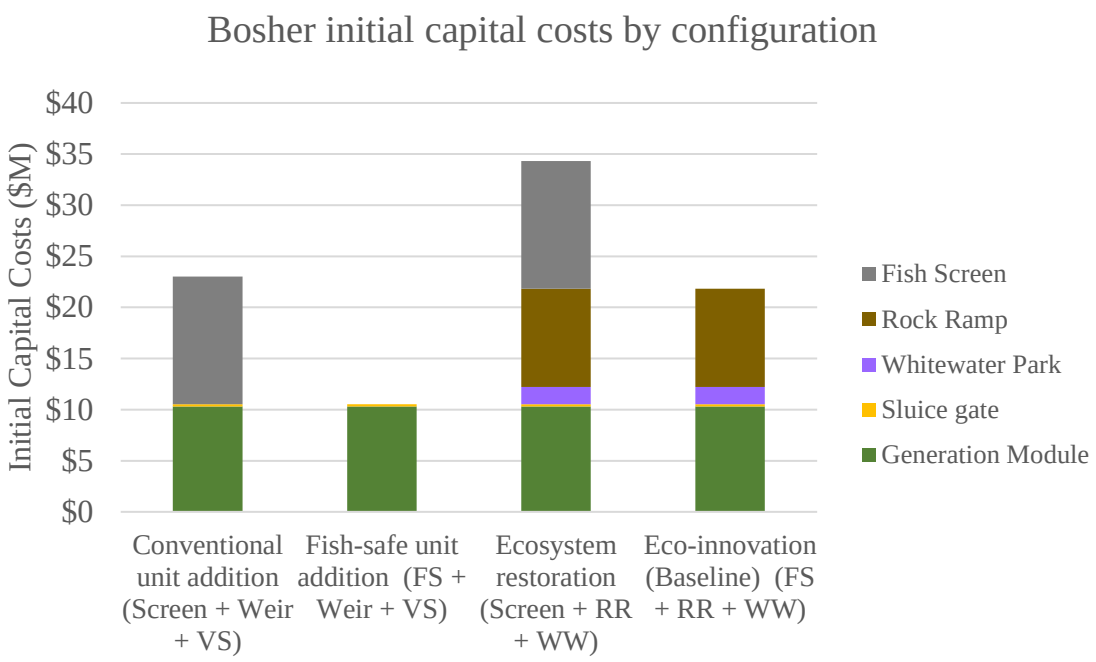

Figure 35. Capital cost breakdown for the Bosher module configurations.

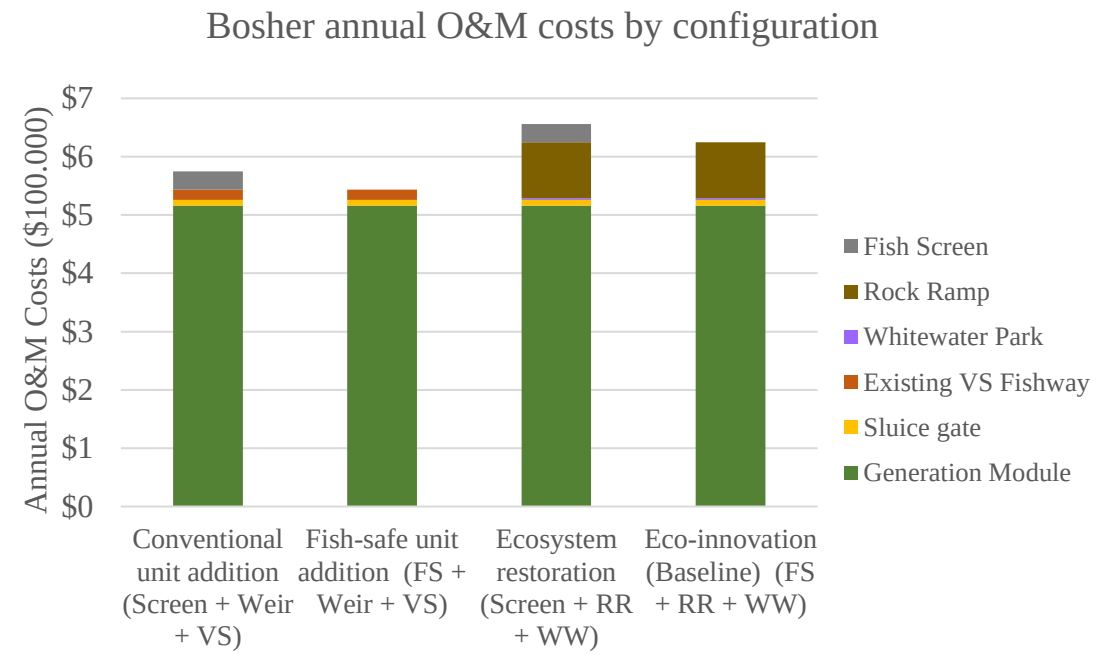

Figure 36. Annual operating and maintenance cost breakdown for the Bosher module configurations.

Model Setup

This section describes how the proposed designs and configurations were integrated into the object-oriented waterSHED framework. The baseline conditions for this case study are described in Table 8, with the italic sections highlighting the conditions specific to this case study. The main differences include a 20-year simulation time, fixed engineering and overhead costs of $200,000 each, module-specific O&M costs, and a 5% contingency. The primary module cost and dimension attributes are summarized in Table 19. Like the previous Case Study A, twenty years' worth of flow and stage data were gathered from an upstream USGS gage. The resulting flow duration curve is shown in Figure 37. The Q_{30} (30% exceedance flow) was 7630cfs, which was 4-6 times larger than the reference sites in Case Study A. The stage-discharge curve, illustrated in Figure 38, was regressed using piecewise power curves using the methodology described in the Regression Analysis section in the Appendix to address the distinct stage-discharge relationships at high and low flows. The normal operating headwater level was set at the weir crest elevation of 16.2ft, although the headwater level varied during the simulation because of the uncontrolled spillway operation. The assumed minimum flow requirement was 1320cfs, expressed through the spillway minimum flow attribute within the Preferences class. For configurations with the Rock Ramp, the spillway minimum flow was 1320cfs, and the spillway notch flow of 250cfs was automatically included in this flow. For configurations with the concrete weir and vertical slot fishway, the fishway flows of 225cfs were included in the minimum flow requirement by changing the spillway minimum flow to 1095cfs. As such, the spillway flows contributing to the headwater level were similar, but the flow allocations for the fish passage model differed.

The previously described technologies were parameterized according to Table 36 – Table 41 in the Module Attributes section in the Appendix. The module attributes were adapted from information and drawings provided by Natel Energy in collaboration with engineering contractors. Again, the costs and dimensions used in this model were high-level estimations for conceptual designs and should not be used for non-research applications. The Bosher configurations did not leverage non-overflow modules or foundation modules because the passage modules included these costs. As such, placeholder non-overflow and foundation modules were included were zero costs to satisfy model requirements without affecting the outcomes. The concrete weir and vertical slot fishways were implemented with zero capital costs to reflect the existing NPD structures.

This case study assessed the tradeoffs between cost and fish passage performance, so the fish-related baseline inputs were required, including the species and fish passage performance metrics for each module. Several migratory species exist in the James River, and American Eel was selected as the species of interest because considerable testing has been conducted on fish-safe turbine passage for American Eel. The upstream migratory months for American Eel were February to June and the downstream migratory months were September to December [163]. Upstream and downstream species passage effectiveness metrics were only calculated for these respective months, although the VS

Table 19. Attribute summary of modules used for Case Study B.

Module	Capital cost ($)	O&M cost ($)	Width (ft)	Design flow (cfs)
Rock ramp	$9,600,000	$96,000	820	280,000
Whitewater park	$1,700,000	$3,200	60	50
Sluice gate	$194,000	$9,700	20	500
Concrete weir	0	0	820	280,000
Fish-safe turbine	$650,000	$32,500	17	448
Conventional propeller turbine	$650,000	$32,500	17	448
Vertical-slot fishway	0	$18,000	56	225
Fish screen	$12,500,000	$31,000	224	4480
Foundation	$3,820,000	$38,200	NA	NA

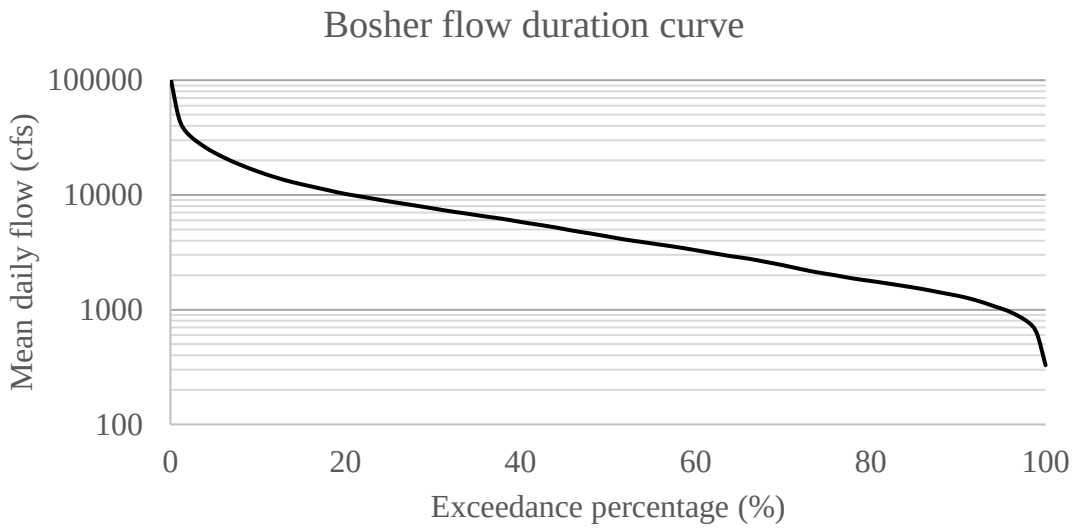

Figure 37. The flow duration curve for the Bosher case study site.

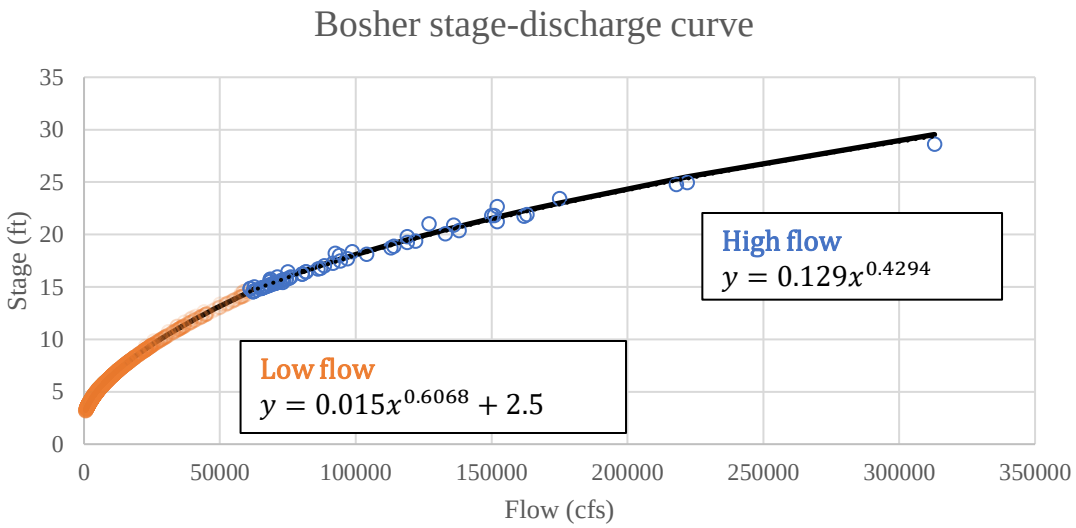

Figure 38. The stage-discharge curve for the Bosher case study site.

fishway and rock ramps were operated year-round because downstream passage can occur year-round [163]. The impact of seasonal operation of the VS fishway was evaluated as part of this analysis. Regarding fish passage performance, the scope of this research was to evaluate the range of possible outcomes rather than species-specific outcomes, which require detailed information about how species interact with specific technologies in certain environmental conditions. As such, American Eel was a useful representative species to illustrate the range of outcomes and associated tradeoffs, but more detailed hydraulic models and physical testing should be used in the final designs.

The upstream and downstream fish passage models required four metrics to be defined for each of the modules. Table 20 describes the four fish passage efficiency metrics for American Eel for each module in this case study. These efficiencies were baseline values determined from the literature (cited in the relevant sections) and assumptions about module operation. However, since the efficiencies depend heavily on the environmental conditions at the site, there were significant uncertainties. The following scenarios addressed this uncertainty by conducting sensitivity analysis on the highlighted values (*) in Table 20 to show the range of possible outcomes for different efficiencies. For the downstream metrics, zero values indicated that the modules had a negligible impact on fish mortality and all fish that passed through the module were unharmed. The rock ramp and VS fishways were designed for fish passage, so that is expected; however, the sluice gate and the whitewater park mortality rates were unknown. Therefore, the whitewater park was assumed to exclude fish from upstream and downstream passage (100% guidance and 0% entrance efficiencies). The sluice gate was assumed to provide safe downstream passage (0% mortality), and velocities were expected to be too high for upstream passage (0% entrance efficiency). Given the limited design flows, these modules were expected to have minimal effects on fish mortality. For upstream passage, modules without any modes for realistic upstream passage, like the 10ft concrete weir, were assumed to have entrance or passage efficiencies of zero. This allowed the model to focus on the effects of the rock ramp and VS fishway alternatives. Finally, the attraction efficiency model was tuned to provide minimal attraction efficiency losses for the VS fishway at the Q_{30}, a common design point for hydropower, and a moderate decline in attraction at higher flows. Given a fishway design flow of 225cfs and a Q_{30} of 7630cfs, the target relative discharge for the module was 2.3%, which related to a relative discharge parameter (*a*) value of 0.3 and an attraction sensitivity parameter (*b*) value of 0.03.

Generation Model Validation

To ensure proper construction of the waterSHED generation models, the results of waterSHED were compared to the reference results from Natel Energy and the engineering contractors. The validation steps were conducted using the baseline Eco-innovation design, whose primary components were the rock ramp, whitewater park, and array of ten fish-safe generation modules.

The first step was to validate the expected headwater and tailwater curves. Both

Table 20. Fish passage efficiencies for American Eel for each module in the Bosher case study site.

*Asterisks indicate values that are the subject of sensitivity analysis.

Module	Downstream Guidance Efficiency	Downstream Mortality Rate	Upstream Entrance Efficiency	Upstream Passage Efficiency
Rock ramp	0	0	80%*	70*
Whitewater park	100%	0	0	0
Sluice gate	0	0	0	0
Concrete weir	0	0*	0	0
Fish-safe turbine	0	0*	0	0
Conventional propeller turbine	0	85%*	0	0
Vertical-slot fishway	0	0	80%	45%
Fish screen	95%*	0%	NA	NA

waterSHED and the reference methods used stage-discharge equations to model the tailwater level and weir equations to model the headwater level based on the expected flow over the spillway. Figure 39 illustrates the comparison of the headwater and tailwater curves for different inflow values. The tailwater curves in blue are very similar, with slight differences owing to the piecewise approach used for the empirical stage-discharge models. The headwater curves in orange are relatively similar, although the waterSHED model is higher on average by about 0.27ft. One reason for this disparity is the difference in assumed weir coefficients. The reference model used an assumed discharge coefficient of 0.7, which relates to a weir coefficient of 3.74, while the waterSHED model used the weir coefficient of 3.087, which is the theoretical coefficient for a broad-crested weir [132]. The waterSHED model excludes notch flows from the flows that impact the headwater level, so the weir coefficient was selected to relate only to the flow above the notch. However, it is important to note that the weir coefficient for a nature-like rock ramp with complex hydraulic interactions represented an area of uncertainty in the model. Another possible reason for the headwater disparity is the difference in flow allocation methods. The waterSHED model used rule-based allocation, and the reference method used a flow duration curve, which is common practice for hydropower design models. The flow duration method determined the flow allocation for discrete exceedance values of the inflows. The exceedance flows were then used to determine annual generation by multiplying the expected power output at each exceedance by the percentage of time per year spent at that exceedance value. The waterSHED model specified differences between the notch flow, spillway flow, and other module flows, so the flow that affects the headwater differed for each inflow. This is reflected by the subtle peaks between 1500cfs and 4000cfs that reflect turbine ramping. These methodological and minor input differences (e.g., bed elevation and width) were exacerbated at high flows, but high flows were less common, so the impact on performance modeling was assumed within the expected range of accuracy for pre-feasibility models. Future research should identify the expected weir coefficient of the rock ramp for different flow values and evaluate its impact on generation.

The next step was to compare estimates for annual energy generation for the baseline design. Again, the waterSHED model used rule-based allocation to allocate powerhouse flows, while the reference method used a flow duration curve. The waterSHED model integrated the expected losses into the flow and head efficiency module attributes. The assumed efficiencies were a turbine efficiency curve (illustrated by the blue line in Figure 40), a variable speed drive efficiency of 96%, a generator efficiency of 95%, and an electrical loss of 2%. The head efficiency, which factored in any draft tube or intake head losses, was assumed to be a constant 96%, as shown by the orange curve in Figure 40. As described in Table 36 in the Appendix, the operating head range was 54% -118% of the design head (5.9ft to 13ft), and the operating flow range was 66%-100% of the design flow (300cfs to 448cfs) [164]. Using these inputs, the baseline Eco-innovation configuration was simulated for 20 years using the Advanced Greedy dispatch model. The Advanced Greedy model performed about 0.7% better than the other three methods, as illustrated in Figure 41. The Design Ramping, Peak Ramping, and Simple Greedy

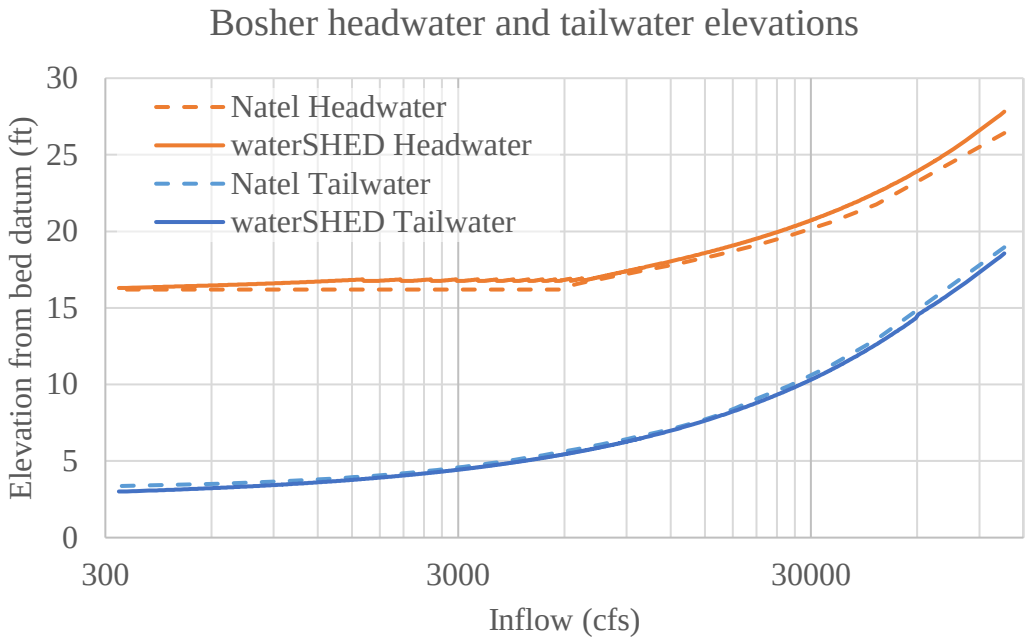

Figure 39. Comparison of headwater and tailwater curves between waterSHED and reference methods

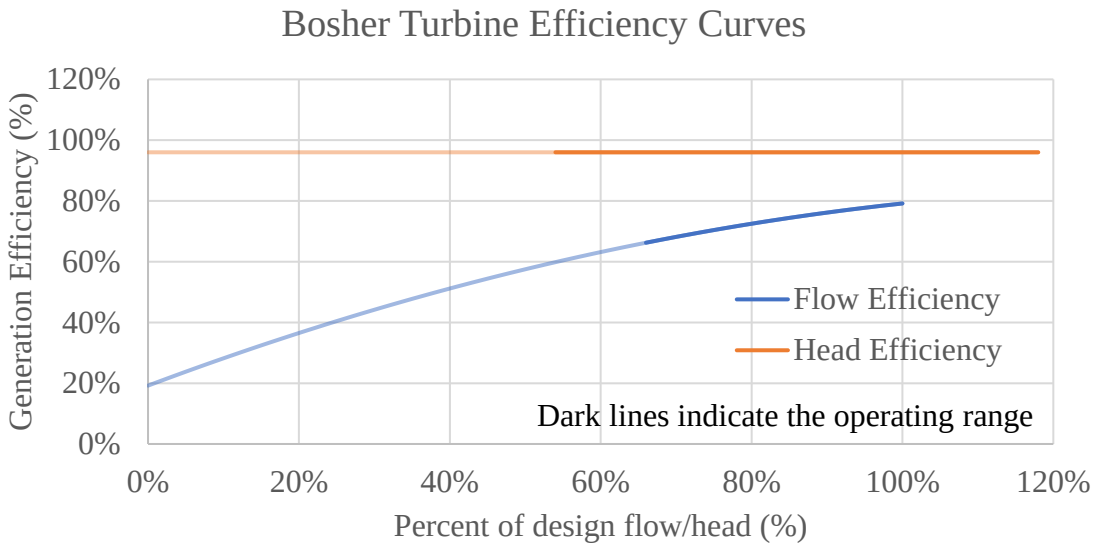

Figure 40. Bosher turbine head and flow efficiency curves.

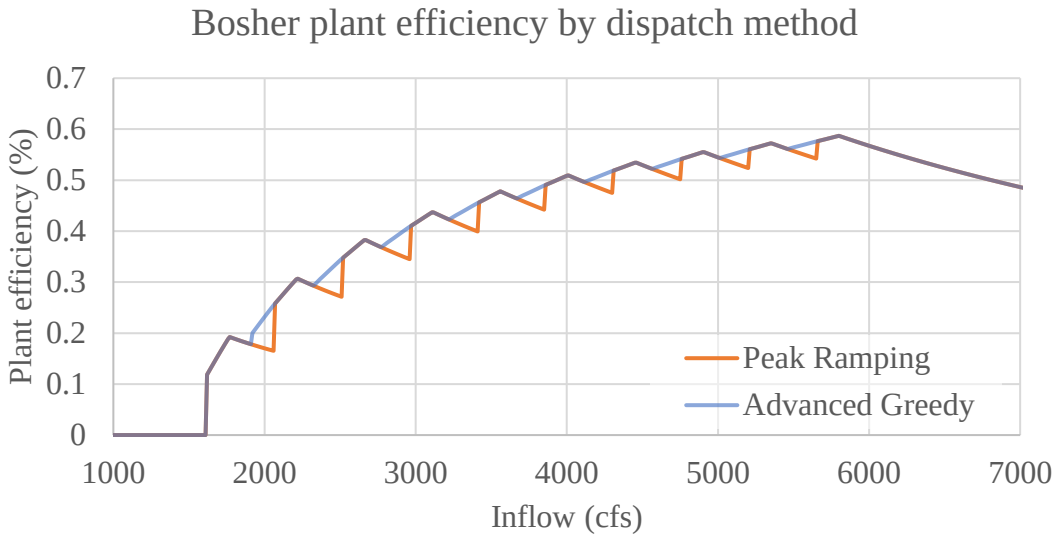

Figure 41. Comparison of plant efficiency by dispatch model for the Bosher case study sites.

models performed similarly since the $Q\eta$ curve (shown in Figure 51 in the Appendix) for the Bosher turbine increased linearly throughout the operating range.

The resulting annual energy generation from waterSHED was 16778MWh, about 5% higher than the flow duration curve estimate of 15986MWh. These relate to 60.6% and 57.8% capacity factors, respectively, which are high compared to the fleet-wide average hydropower capacity factor of 39% [3]. However, these models assume 100% availability, meaning there were no planned or unplanned turbine outages. Having multiple modules and low flow seasons to enable optimized maintenance practices may limit availability losses, but more information is needed to estimate the effect of outages. Run-of-river plants were shown to have higher capacity factors than peaking plants [3]. Additionally, recently small hydropower developers tend to select small powerhouse design flows with higher capacity factors to ensure utilization because smaller plants have less peaking capabilities [23]. The 5% difference in generation was expected to stem primarily from the difference in weir coefficients and headwater estimation, although differences in turbine dispatch methods and efficiency curves may also have played a role. Overall, the 5% difference was deemed within a reasonable limit but highlighted the fact that the waterSHED formulation represents a best-case scenario in terms of generation.

The last step was to model the effect of the fish screen on energy generation. The fish screen is a series of metal bars placed in front of the generation module intakes to exclude downstream migrants. However, the bars present a resistance to flow that creates a head loss for the modules covered by the screen. Per US Bureau of Reclamation guiding documents [136], the head loss can be estimated based on a head loss coefficient (*k*) and the velocity head at the screen. The head loss coefficient considers hydraulic factors like the geometry of the screen and the material roughness. The model was adapted into Equation 31 to calculate the head loss as a function of the flow through the screen (i.e., the modules covered by the screen). The flow divided by the active screen area provides the velocity through the screen. The active screen area is the submerged area of the screen times the fractional open area. The screen is 10ft tall, so the screen is assumed to be submerged throughout the simulation. Head loss models can be parameterized based on the approach flow velocity or the flow-through velocity by changing the head loss coefficient. Equation 31 was formulated based on the flow-through velocity so that the head loss calculation would change for different screen areas and different flow allocations. As such, the model calculates different head losses for each timestep based on the flow allocation.

Screen head loss

$$H_{loss,m}\left(Q_{covered,m}\right) = \frac{k}{2g}\frac{Q_{covered,m}^2}{A_{active,m}^2} \qquad \text{Equation 31}$$

k The head loss coefficient based on the flow-through velocity.

$Q_{covered,m}$	The flow through modules covered by the screen (cfs).
$A_{active,m}$	The screen's active area, which can be calculated by the submerged screen area times the fractional open area (ft^2).
g	Gravity (32.1 ft/s^2)

Based on the species of interest, the fish screen was designed by an engineering contractor with a 0.75in screen spacing and an assumed ratio of open to total area of 0.5. The screen was also designed for an approach velocity of 2ft/s, with an associated flow-through velocity of 4ft/s (2ft/s divided by the 0.5 fractional open area). If the approach velocity is too fast, fish can get pinned to the bars without sufficient swimming capabilities to escape, which is considered a mortality in the waterSHED model. The screen was designed to be 10ft tall, so to match the approach velocity and design flow (baseline of 4480cfs), the screen area was set as 2240 ft^2 (width of 224ft). The screen area was adjusted based on the number of generation modules using the width of the generation modules and a screen angle of 40 degrees. Based on the flow-through velocity, the head loss coefficient was assumed to be 0.975. Using these inputs, the estimated head loss through the screen at the baseline design flow was 0.243ft. The screen design assumptions and results are summarized in Table 27 in the Appendix.

The effect of the screen on generation was determined by running the model with and without the fish screen (i.e., the Eco-innovation and the Eco-restoration configurations). The simulations were run with the Advanced Greedy dispatch method. The scenario with the fish screen produced an annual energy generation of 16,483MWh, while the scenario without the fish screen produced 16,778MWh. This was a 1.76% reduction in generation from the screen head loss. In comparison, the design head of the generation modules was 11ft, so the screen design head loss (0.243ft) represented approximately 2.2% of the total head. Therefore, a reduction in energy generation of about 2.2% would be expected if the modules were operating the design flow year-round. Instead, the screen head loss decreased at lower velocities, so the head loss was lower when the powerhouse operated below the design flow. The 1.76% change in generation was reasonable but relatively small in context and may not greatly influence the design decisions.

Overall, the waterSHED model estimates of annual energy generation and screen head loss were consistent with expected values from the reference methods. The waterSHED model used a higher temporal resolution than the flow duration methods and simulated the roles of flow allocation and operational interactions on generation. However, the waterSHED method resulted in higher annual energy generation estimates and was interpreted as a best-case scenario because it assumed 100% availability and higher headwater elevations than the reference model.

Generation Optimization

A powerhouse enumeration procedure was conducted to understand the effects of the number of generation modules on facility performance. Unlike Case Study A, which had three degrees of freedom for the generation module designs, this analysis used a standardized turbine design, so only the number of modules could be changed. The analysis was conducted for the four main configurations with module counts between 1 and 30 using the Peak Ramping dispatch model to expedite the model runs. The model was parameterized so that increasing the generation modules increased the required screen and foundation costs, where applicable. However, the model assumed constant dimensions for the other modules, so the placement of generation modules and the spillway dimensions were not considered.

The enumeration results in terms of LCOE are shown in Figure 42. The Eco-innovation (FS + RR + WW) baseline design determined by Natel Energy was ten generation modules or 3.16MW, and the optimal number identified in this analysis was 11 or 3.49MW. The slope of the LCOE line for Eco-innovation was relatively flat for module counts greater than approximately eight, indicating that additional modules tended to pay for themselves during high flow periods. This is highlighted in the example flow allocation diagram in Figure 43, which includes a normalized plot of the inflow throughout the year. Bosher dam has a high flow season between approximately January to July and a low flow season during September and October. During the low flow season, none of the turbines were available. There were excess flows during the high flow season, as indicated by the low normalized flow percentage in green but high generation level. Thus, if generation modules can capture enough energy during the high flow seasons to break even in cost, their impact on LCOE will be minimal, leading to a flat LCOE curve. However, this highlights the principal tradeoff in generation optimization between total generation and capacity factor. This relationship is illustrated for the Eco-innovation case in Figure 44. Higher capacities lead to more generation with lower capacity factors. LCOE is meant to balance these factors by comparing the costs and generation benefits of additional units. However, numerous other factors play a role in capacity selection, including transmission limitations, the grid's needs, and the developer's goals, such as the desired level of risk and capital expenditure. The trend in hydropower development is towards smaller capacities with higher capacity factors [23]. However, more variable hydrologic conditions and higher peak electricity prices in the future may incentivize larger projects to capture peak flows.

The other module configurations, also shown in Figure 42, provide relevant insight into the optimization problem. The cheapest option, Fish-safe Unit Addition (FS + Weir + VS), had an optimal module count of three with a minimum LCOE of $68.79/MWh, approaching the target LCOEs of other renewable resources (Table 1). Since the cost of supporting structures was lower, additional turbine modules represented a larger percentage of total costs, making the slope of the line slightly steeper than the baseline configuration at higher module counts. Nonetheless, this capacity was lower than expected and reflected a limitation of LCOE as an objective metric.

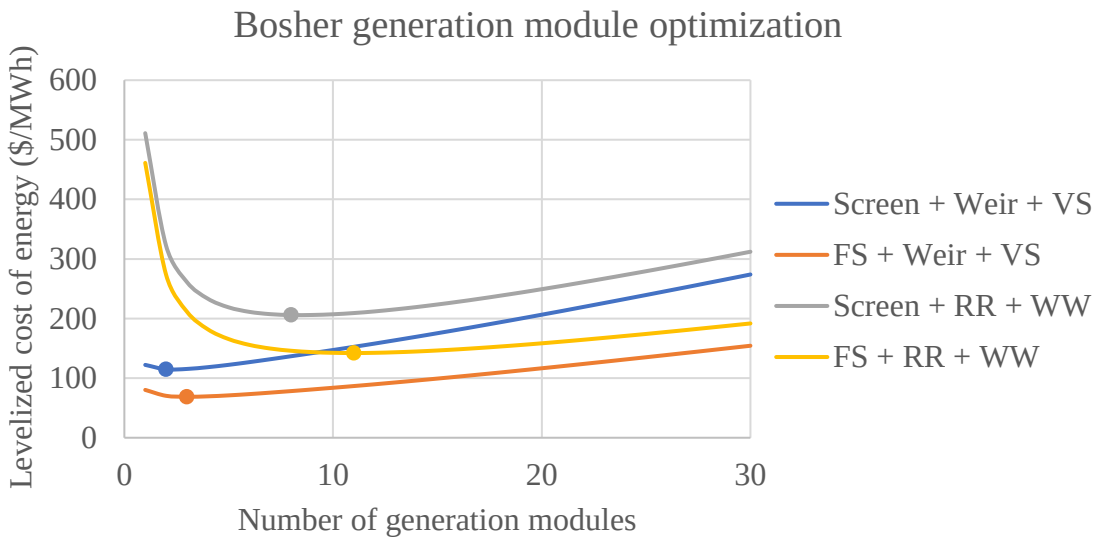

Figure 42. Results of the Bosher module count enumeration by levelized cost of energy. The dots indicate the minimum LCOE for each configuration.

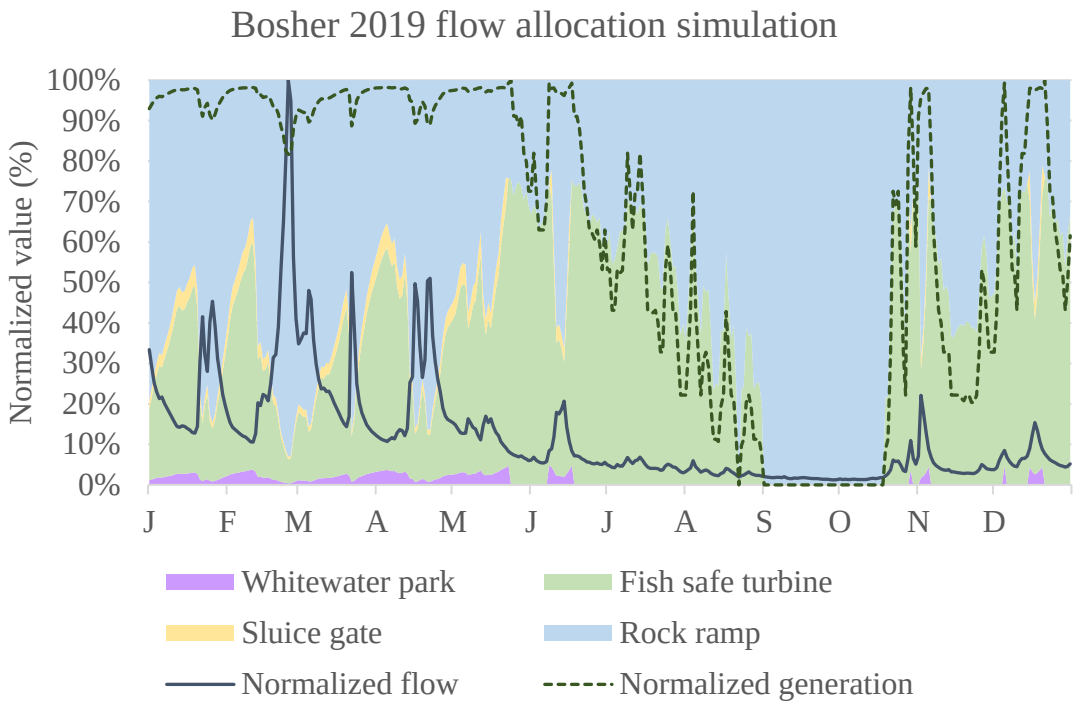

Figure 43. Normalized flow allocation, inflow, and generation for the 2019 simulation year with the Bosher Eco-innovation configuration. The x-axis is indexed by months.

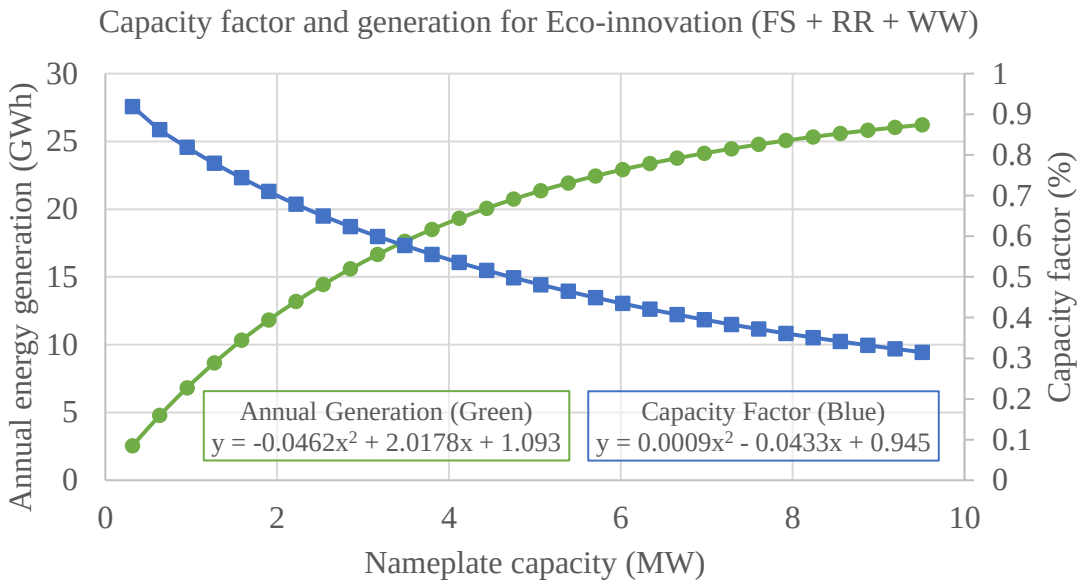

Figure 44. The capacity factor and generation tradeoffs for the Eco-innovation configuration of the Bosher case study. Annual energy generation is the increasing green line with circle markers and capacity factor is the decreasing blue line with square markers.

Although the three module configuration had the lowest LCOE based on the operational and cost interactions, developers are incentivized to build larger projects and provide more value to the grid, as long as LCOEs are similar. For example, the LCOE for the Fish-safe Unit Addition configuration with ten generation modules was $83.87. Both configurations with the fish screens (Conventional Unit Addition and Eco-restoration) had smaller optimal module counts than their fish-safe counterparts. The screens were parameterized on a per-module basis, so they increased the costs of each module and decreased the net benefit of additional modules. Additionally, for configurations with ten modules, the screen increased the LCOEs by approximately $64/MWh, most resulting from the capital cost rather than the generation loss, as illustrated by the previous analysis.

These results highlight the importance of stakeholder perspectives on the optimization process. LCOE and other economic metrics have limitations regarding the selection of realistic designs. For example, LCOE does not capture the incentive to provide maximum power from a project to help meet the growing electricity demand. Additionally, the net present values for each configuration were negative and decreased with module count, which would result in optimal designs with zero generation modules if used as the objective metric. These metrics were also sensitive to the high-level economic parameters like discount rate, project life, and cost of energy (in the case of NPV). The waterSHED model provides the opportunity to add constraints regarding design and performance requirements for the optimization process, like minimum capacity or maximum total cost. However, additional features could improve capacity selection, like setting a weighting factor that incentivizes larger projects. Additionally, the seasonality of the Bosher site highlights the potential of portable generation modules that could be incorporated seasonally. With modular designs that facilitate rapid deployment and decommissioning, it may be feasible to import modules for specific seasons at different sites, allowing one portable module to get considerable utilization. This type of design would be highly innovative and a long-term investment, whereas near-term investments should target cost reductions and performance improvements for standardized modules to increase their marginal net benefit.

Downstream passage - Fish screens vs. Fish-safe turbines

As discussed in Chapter Two, the protection of aquatic species is particularly important to economic and environmental outcomes. Hydropower facilities may deter, injure, or kill migratory fish and resident species, negatively impacting many animal populations. Conventional approaches to downstream fish passage focus on exclusion measures meant to deter fish from harmful downstream passage modes like turbine passage and towards safe passage modes like conduit bypasses. Recent research and investment have aimed to improve the safety and performance of mitigation measures [135]. “Fish-friendly” or “fish-safe” turbines have brought about the potential to turn turbine passage from a harmful to a safe passage mode. Fish-safe turbines would preclude the need for fish exclusion measures, like bar racks and louvers, which can be very expensive, especially for small projects, and contribute to head losses for generation [11]. However, positive

exclusion measures (e.g., fish screens) are the current state of practice and are commonly required by resource agencies. Like all innovations, fish-safe turbines present a risk to stakeholders because they lack wide-scale deployment. A large part of the value proposition for fish-safe turbines stems from the avoided costs of exclusion measures. As such, it is critical to illustrate the holistic value of fish-safe turbines to convince regulators to allow development without positive exclusion measures. Model testing of fish-safe turbines by Natel Energy has shown limited mortality (2%) for Rainbow Trout, a major stride toward validation [135]. The cost-saving component of the value proposition requires an understanding of the costs and performance of the alternative designs. By simulating the fish-safe and conventional designs, the waterSHED model enabled quantification of several factors, including the screen head losses, capital cost differences, operating cost differences, and changes to effective mortality.

The effective mortality model, described in Chapter Three, uses the flow allocation, the module guidance efficiencies, and the module mortality rates to estimate the facility-wide mortality at each timestep, which is then averaged over the downstream fish passage months. The primary assumption of this model is that the flow of fish across the modules is proportional to the flow allocation (i.e., more water equals more fish). The expected peak downstream passage months for American Eel (September to December) corresponds to the low flow season at the Bosher dam site, so flow allocation and minimum flow requirements could play an important role since there are limited excess flows. The baseline module guidance efficiencies and mortality rates, described in Table 20, were based on literary and anecdotal evidence to highlight the relative benefit of fish-safe designs. For example, the fish-safe turbines had a mortality rate of 0%, meaning they were completely safe for American Eel, which is the best-case scenario. The conventional alternative had a fish screen guidance efficiency of 95%, which represents a best-case scenario with proper screen design for American Eel [81], as described later, but the conventional propeller turbine mortality rate was 85% to reflect a worst-case-scenario based on anecdotal evidence from recent small hydropower developments. The effects of the other modules were minimized with zero mortality rates for the spillways and 100% guidance efficiency for the whitewater park. The sluice gate was assumed to provide safe passage, but the small design flow and high operating flow were expected to have minimal impact on the effective mortality.

These baseline conditions were simulated for each of the four configurations using the Advanced Greedy method. The effective mortality for the fish-safe designs (Eco-innovation and Fish-safe Unit Addition) was zero since there were no sources of mortality. The Conventional Unit Addition configuration had an effective mortality rate of 3.1%, with a 1.7% loss in energy generation compared to the Fish-safe Unit Addition. The Eco-restoration configuration (FS + Weir + VS) had an effective mortality rate of 3.2%, with a similar loss in energy generation. The mortality rates for these designs were low, given the high guidance efficiency of the fish screen. However, the fish model inputs had considerable uncertainties, so further sensitivity analyses were conducted to understand the effect of these relationships on effective mortality.

The first downstream passage sensitivity analysis looked at the effect of the number of generation modules on effective mortality. This analysis used the same methodology as the generation optimization section. The fish-safe configurations had zero mortality using the baseline conditions, so only the fish screen configurations were assessed. The Eco-restoration and the Conventional Unit Addition configurations were simulated with module counts between 1 to 30. The results for both configurations were almost equal, so only one curve is illustrated in Figure 45. There was a positive polynomial relationship between the number of modules and effective mortality, reminiscent of the annual generation curve in Figure 44. The relationship was driven by the amount of flow allocated to the turbine and the combined guidance efficiency and mortality of the screen-turbine configuration (95% guidance with a mortality rate of 85% represents an expected mortality of 4.2%). Despite having high generation flows at higher modules counts, the modules were not operated during the low-flow downstream passage season, resulting in effective mortalities of only 6% at extremely high powerhouse design flows. Even for configurations without screens and high turbine mortality rates, turning modules off during the low flow season could limit mortality without considerable generation losses.

The next analysis looked at the screen's combined guidance efficiency and the turbine's mortality rate. The screen guidance efficiency depends on the shape and behaviors of the target species and the screen's hydraulics, angle, and spacing [81]. A study of bar rack and louver guidance efficiencies for American Eel resulted in efficiencies ranging between 33-95% for different design configurations [81]. The most important factor in the study was the angle of the screen, as the max guidance efficiency for the 45-degree angle to flow was 72%, and the max for the 15-degree angle to flow was 95% [81]. The angle of the Bosher fish screen, based on the ratio of the screen area to the turbine array width, was approximately 40 degrees from the direction of turbine flow, but the angle from the inflow was unclear from engineering drawings. Therefore, the baseline guidance efficiency of 95% was selected as the highest recorded guidance efficiency, assuming that the screen was placed at the proper angle to inflow. Sensitivity analysis highlighted the range of effective mortalities based on different guidance efficiencies to account for the angle and approach velocities uncertainties. The guidance efficiencies were varied between 35%-100% with 5% increments to reflect the ranges found in the literature [81].

In this sensitivity analysis, the turbine mortality was also varied to account for uncertainties in the conventional turbine mortality rates, which differ based on the species, turbine, and flow characteristics [79]. A study of turbine mortality for American Eel at five hydropower plants on the Shenandoah River found turbine mortality rates between 15.8-40.7% for the five sites [163]. These resulted in project-specific (effective) mortality rates of 3-14.3% [163]. A review of turbine mortality rates found Kaplan mean mortality rates of 25.7% for American Eel (*Anguillidae Anguilla*) with a standard deviation of 10.6% [165]. However, the baseline mortality rate of 85% was selected to represent a worst-case scenario based on experience from recent small hydropower developments. It is also important to note that turbines may have different mortality rates for different species with different physiologies and swimming behaviors. The sensitivity

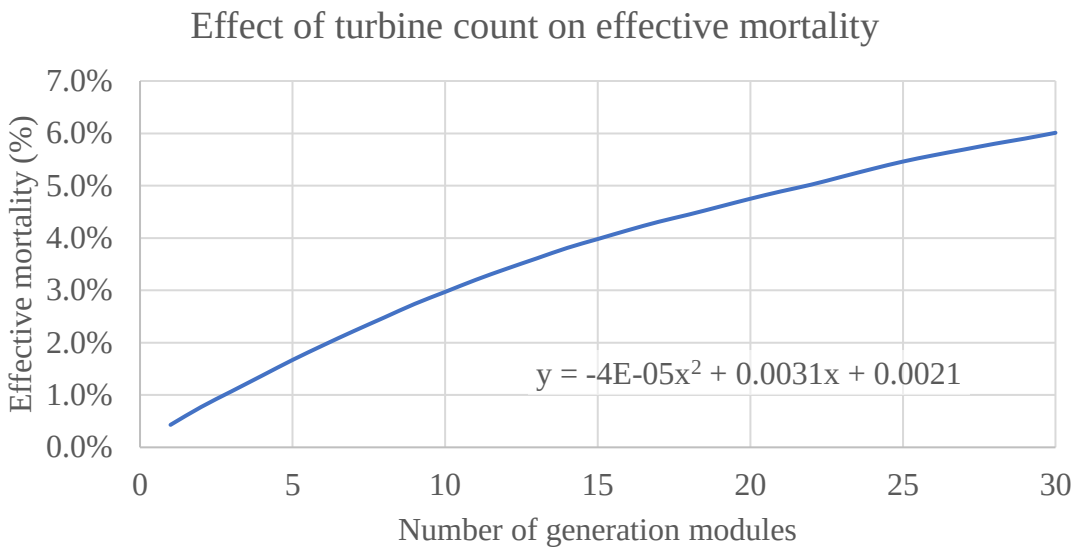

Figure 45. The relationship between turbine count and effective mortality for Bosher fish screen configurations.

analysis of the Conventional Unit Addition configuration varied the turbine mortality rates between 30-100% with increments of 15% to illustrate the range of possibilities for different species-screen-turbine combinations. The Peak Ramping dispatch method was used for all simulations.

The combined guidance and mortality sensitivity analysis results are illustrated in Figure 46. The relationships between guidance efficiency and effective mortality were negative polynomial relationships. At high guidance efficiencies and low mortality rates, the effective mortality went to zero as all fish were excluded from the main source of mortality. For example, the baseline condition of 85% turbine mortality had an effective mortality of about 3% at a 95% guidance efficiency and 21% at a 35% guidance efficiency. For a turbine mortality rate of 30% that better reflects the rates found in the literature [81], the effective mortalities went from 1% to 8% across the same guidance efficiency range. At the lowest guidance efficiency (35%) and highest mortality rate (100%), the effective mortality was only about 25%, which shows the role of flow allocation in the model. Higher turbine mortalities led to higher effective mortalities, and the effect of the mortality diminished as screen guidance increased, as expected. However, a turbine mortality of 100% does not imply a 100% effective mortality since the turbine operation and flow allocation affect how the fish are distributed across the facility. In the case of Bosher, the low flow season and minimum flow requirements inherently limit the impact of turbine mortality. It is important in conversations with resource agencies to address the selected technologies and how the plant is operated during the downstream passage season. Overall, this analysis validated that the model worked as intended and highlighted the impact of the proportional fish to flow allocation assumption in the model.

The next analysis looked at the mortality rate of the fish screen. Fish impingement, or the physical contact of a fish on a barrier under velocities too high for the fish to escape, is a risk when including fish exclusion structures. The risk of impingement depends on the screen spacing, the target species, and the approach velocity [166]. If the species are too large to fit between the spaces and the velocities are too strong, the fish cannot swim away safely. The effective mortality model factors in impingement via the mortality rate of the fish screen. The 0.75in screen used in this case study was designed with a 2ft/s approach velocity, the recommended maximum approach velocity to avoid impingement [167]. Thus, the baseline mortality rate for the fish screen was set to zero. However, it is beneficial to understand the effect of impingement on effective mortality if improperly designed for non-target species or certain hydraulic conditions. For example, a fish passage study at a small hydropower facility on the Mississippi River estimated that approximately 14% of local species were large enough to be at risk for impingement [167]. Using this number as a reference, a sensitivity analysis was conducted on the Eco-restoration configuration with the Peak Ramping dispatch model by varying the screen mortality between 0-15% with 3% increments. The results were linear with a regressed equation of $M_{eff} = 0.0054M_{screen} + 0.0306$. This means that each 1% increase in screen mortality led to a 0.005% increase in effective mortality, which is very low

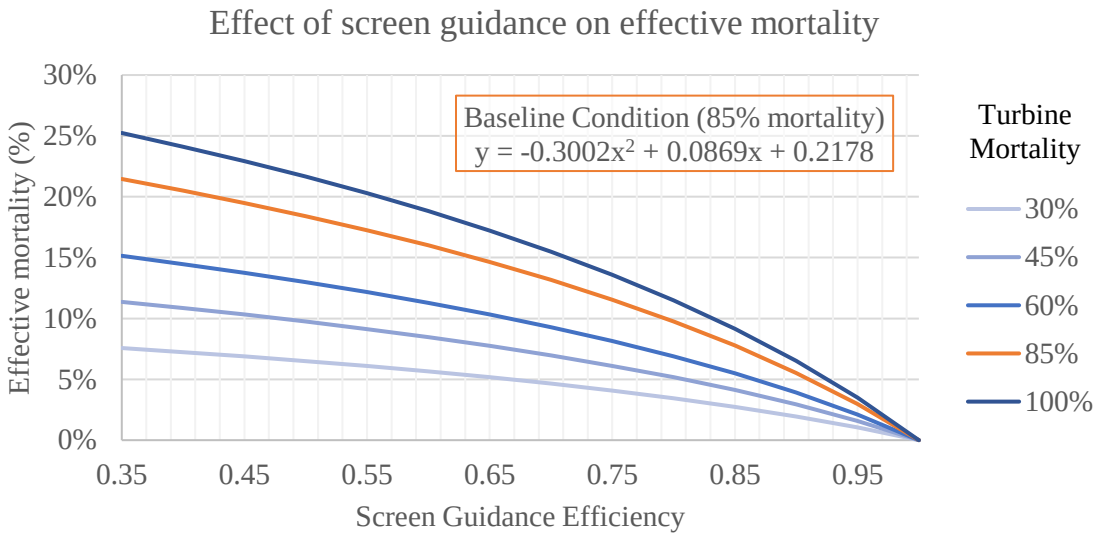

Figure 46. The relationships between screen guidance, turbine mortality, and effective mortality for the Conventional Unit Addition configuration of the Bosher case study site.

because the screen mortality was considered in the model after the 95% guidance efficiency was applied. So, only fish that were not successfully guided away could be impinged in this case. The 3.06% constant in the linear equation reflects the baseline condition with a 0% mortality screen and an 85% turbine mortality. This highlighted a current limitation in the screen tree approach to downstream fish passage. Since the fish flow is determined using the ratios of relative discharge times guidance efficiency, the effect of impingement is only considered after the fish flow allocation step. The impact of impingement or other factors like refusal and delays could be included by using a prior step that only uses the flow allocation and not the guidance efficiency. Alternatively, the input guidance and mortality rates could be adjusted to account for the expected impingement. Overall, the impingement sensitivity analysis was inconclusive and highlighted a current limitation of the downstream fish passage approach.

Another area of uncertainty was the mortality rate of the existing weir. Fish were expected to pass over the weir and fall into the tailwater with minimal injuries. Based on the height of the drop and the flow velocity, injuries could occur from a collision with the weir or riverbed, impact with the receiving water, or other hydraulic interactions with the weir flow (e.g., hydraulic rollers). The weir crest elevation was set at 16.2ft from the bed datum. The minimum recorded tailwater elevation was approximately 3.4ft, resulting in a drop height of 12.8ft at low flow conditions. The US Fish and Wildlife Service's Fish Passage Engineering Design Criteria recommend plunge pools (the tailwater depth in the model) to be equal to 25% of the drop height (3.2ft) with a minimum of 4ft [168]. The tailwater did not meet the minimum 4ft threshold at low flow conditions, although it did meet the 25% recommendation. Therefore, it was pertinent to evaluate scenarios where weir mortality rates were non-zero. Sensitivity analysis was conducted for weir mortality rates between 0-20% with 4% increments to illustrate the relationships between weir mortality and effective mortality. Simulations were run using the Conventional Unit Addition configuration and the Peak Ramping dispatch model. The runs resulted in a linear relationship between weir mortality and effective mortality with an equation of $M_{eff} = 0.8479M_{weir} + 0.0297$. This means that each 1% increase in weir mortality led to a 0.85% increase in effective mortality. The constant of 2.97% reflects the mortality caused by the screened turbines. Since the weir had a guidance efficiency of zero, the linear relationship was expected. The slope reflects the average relative discharge during the downstream passage months, which was substantial for the concrete weir. As such, NSD projects, even for low-head sites, should ensure adequate plunge pools downstream of the spillways to limit mortality. Since high spillway mortality could have a large impact on effective mortality, future research could better assess the risk of spillway mortality for innovative low-head spillway designs and existing NPDs.

The last area of uncertainty studied in this case study was the turbine mortality rates. Considerable research and investment have gone into developing and validating fish-safe turbines. Despite this testing, innovations without field-scale deployment present a risk to decision-makers. So, it is important for the stakeholders who are taking the risk to understand these risks in terms of likelihood and potential costs (fish mortality). The

baseline mortality rate used for the fish-safe turbines was 0%, whereas the baseline for the conventional turbines was 85%. Using the Eco-restoration and Eco-innovation configurations with the Peak Ramping dispatch model, the sensitivity analysis varied the fish-safe turbine mortality rate between 0-100% in 5% increments. The results of the analysis are illustrated in Figure 47. In the model, turbine mortality is applied after the allocation of fish flow, so the relationships between turbine mortality and effective mortality were linear. The difference in slopes between the two curves highlights the impact of the fish exclusion screen. The baseline conditions for the two configurations (marked by dots in Figure 47) were 0% for fish-safe turbines and 3% for the conventional screen design. However, at higher turbine mortalities, the fish-safe configuration increased effective mortality at a rate of 0.32% per 1% increase in turbine mortality, and the conventional screen design increased at a rate of 0.036% per 1% increase in turbine mortality. The slope for the fish-safe design only reflects the average relative discharge of the generation modules, while the other scenario also considers the effect of the screen guidance efficiency. As such, the generation modules receive approximately 32% of the total inflow during the downstream passage months. The difference between the lines indicates the percent of fish saved by the fish screen. Thus, as turbine mortality rates decrease through innovative designs, the value of the fish screen diminishes. In the worst-case scenario, the 95% effective fish screen would save a maximum of 28% of fish during the peak downstream passage months. With a more reasonable mortality of 30% for a conventional turbine, the fish savings is only 9%.

These downstream passage sensitivity analyses were based on the assumptions in the model and will differ in practice for different sites; however, they help put the value proposition of fish screens into perspective. Resource agencies typically require fish screens for fish protection, but the costs may largely outweigh the benefits, especially compared to potential alternatives. In this case study, the fish screen had a capital cost of $12.5M and an annual operating cost of $31,000. Along with the 1.7% decrease in energy generation from head losses, these costs increased LCOEs by about $63/MWh compared to the fish-safe turbine alternative. Assuming that fish flow is proportional to flow, the maximum possible fish mortality reduction was 28% in a worst-case scenario, although expected fish savings are much lower for realistic mortality rates for American Eel. However, fish-safe turbines could eliminate mortality. As such, regulators and designers need to decide whether these reductions in fish mortality are worth these costs, which could make a project infeasible. These results incentivize investment into alternatives like fish-safe turbines and seasonal operation schemes rather than positive exclusion devices.

Upstream passage - Vertical slot fishway vs. Rock Ramp

Upstream fish passage is critical to project success but often requires different mitigation measures than downstream passage. Upstream mitigation measures for low-head projects focus primarily on volitional fishways meant to attract and transport upstream migrants across the facility safely. Nature-like volitional fishways use natural materials to improve fish passage while reducing costs and improving the site's aesthetics. In addition to high relative capital costs [11], fish passage mitigation measures like these can detract from

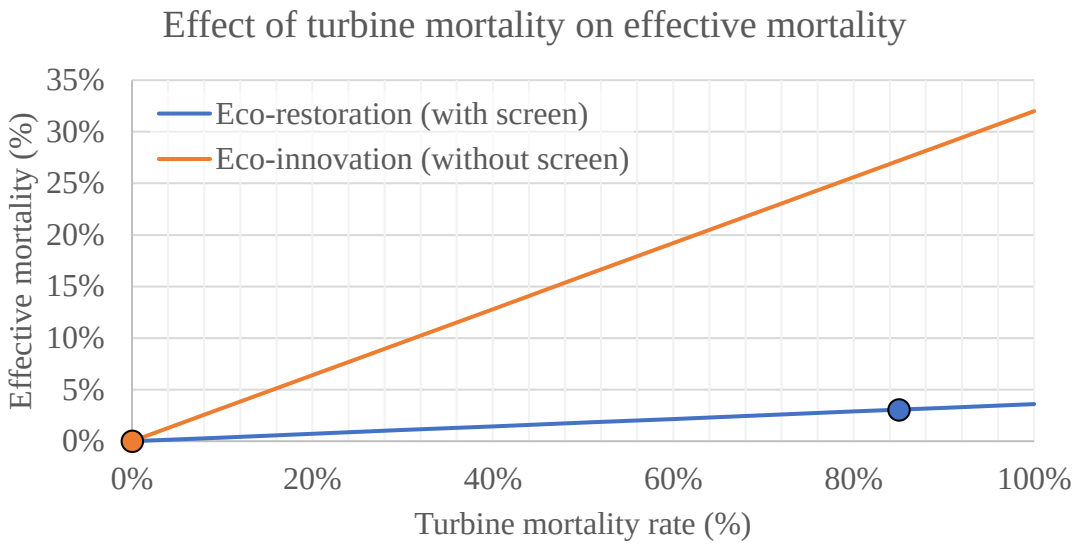

Figure 47. The result of the turbine mortality sensitivity analysis for the Eco-restoration and Eco-innovation configurations. The dots indicate the baseline turbine mortality rates.

energy generation by using flows that could be allocated to turbines. Furthermore, the performance of fishways can be difficult to predict, quantify, and monetize since the value of these environmental technologies is non-monetary and biological processes are complex. For example, improper entrance locations or insufficient attraction flows can lead to low passage efficiencies [95]. Improved fishway performance is generally tied to higher design flows and lower slopes, but these are also associated with higher costs and less generation [95].

The Bosher case study has two alternatives for upstream fish passage. The site has an existing vertical-slot (VS) fishway that uses 225cfs on average to attract and pass fish through a series of slots and pools specifically designed for the target species' swimming behaviors [162]. Additionally, an innovative rock ramp (RR) design was proposed that acts as a nature-like fishway and an uncontrolled spillway. The rock ramp has a low-flow notch of 250cfs that contributes to the attraction flow and a minimum spillway flow requirement of 1320cfs. The upstream fish passage model, described in Chapter Three, uses three components (the attraction efficiency, entrance efficiency, and passage efficiency) to determine the facility-wide effective upstream passage. The attraction efficiency is a function of the module relative discharge because fish are assumed to be attracted to higher flows that indicate the main stem. The entrance and passage efficiencies are module-specific metrics that proportionally affect the effective upstream passage, although the entrance efficiency also affects the distribution of fish across the facility. The waterSHED model used this upstream passage model and the other generation and economic models to quantify the cost-benefit tradeoffs of these two designs.

The baseline conditions for the upstream passage model parameters, listed in the Model Setup section, were based on a review of fish passage studies from Bunt, Casto-Santos, and Haro [95] that provided cross-species passage and attraction efficiency averages for various fishway types. However, the review grouped the effects of attraction and entrance efficiency into a singular metric, meaning the effects of low attraction flows were incorporated as the reported attraction efficiency. Vertical-slot fishways were reported to have a mean attraction efficiency of 63% (median 80%) with a range of 0-100% and a mean passage efficiency of 45% (median 43%) with a range of 0-100% [95]. For nature-like fishways, the review determined a mean attraction efficiency of 48 % (median 50%) and a mean passage efficiency of 70% (median 86%), both with ranges of 0-100% [95]. Technical fishways, like vertical-slot fishways, were shown to have higher entrance efficiencies than nature-like fishways, like the rock ramp; however, these efficiencies varied significantly based on slope and design flow. Nature-like fishways reported better passage efficiencies than technical fishways due to the reduced slopes, making the climb easier for poorer swimmers. However, nature-like fishways also reported worse entrance efficiencies due to the lack of attraction flows and poor entrance siting. Given that the rock ramp was the largest hydraulic feature at the site with a width of 820ft and had minimum flow requirements and notch flows to provide consistent attraction, the rock ramp was not expected to face issues with fish attraction or entrance efficiencies. To

better compare the expected performance of the rock ramp and VS fishway, the baseline entrance efficiencies for both modules were set as 80%. The passage efficiencies of the VS fishway and rock ramp were set to 45% and 70%, respectively, which were the reported means for each type. Additionally, as described in the Model Setup section, the attraction efficiency function was tuned to a relative discharge threshold of 2.3% (a = 0.3, b = 0.03) based on the assumption vertical slot fishway was designed for sufficient attraction at the Q_{30}. Finally, the upstream passage months for American Eel were February to June based on a study from Eyler [163], meaning the effective upstream passage was only calculated during these months. These months correspond to the high flow season at Bosher dam, making it difficult to provide sufficient relative discharges.

The first step in analyzing upstream passage performance was to run the baseline conditions for the Eco-innovation and Fish-safe Unit Addition configurations. These simulations were run with the Advanced Greedy dispatch model, and the results are documented in Table 21. The Eco-innovation configuration had an LCOE about 1.7 times larger than the Fish-safe Unit Addition configuration ($83.23/MWh) due to the cost of the rock ramp ($9.6M). However, the rock ramp had an effective upstream passage rate of 56% compared to 33% for the VS fishway. The 56% effective passage is equal to the product of the entrance and passage efficiencies for the rock ramp, meaning that the rock ramp did not have any attraction efficiency losses. The expected effective passage for the VS fishway based on the product of these efficiencies would be 36%, so the attraction efficiency component contributed to a 3% loss in effective passage. In terms of generation, the Fish-safe Unit Addition configuration produced 0.3% more energy (65MWh) than the Eco-innovation configuration due to the difference between the VS fishway design flow (225cfs) and the rock ramp notch flow (250cfs).

Two additional runs were conducted with the Fish-safe Unit Addition configuration, one with seasonal operation of the VS fishway and another with the VS fishway as a new construction, as shown in Table 21. By limiting the operation of the VS fishway only to the peak upstream migration months (February to June), the project may generate more energy with limited impacts on passage. In the simulation with seasonal operation, even though the fishway was operated seasonally, the minimum spillway flow was kept at 1095cfs because the minimum spillway flow could not be set for each month. This was expected to slightly increase generation in the seasonal operation scenario compared to the realistic scenario where the minimum spillway flow would be adapted during those months. The simulation showed that seasonal VS fishway operation increased energy generation by 2.8% (478MWh), resulting in an LCOE reduction of $2.30/MWh with no reduction in upstream passage. However, there would be no pathways for upstream passage during the rest of the year. Another simulation was run to simply compare the economic performance if the VS fishway had to be constructed since most NPDs do not include fishways. As previously described, the estimated cost of a new VS fishway, based on an escalation of the actual Bosher dam construction costs, was $2.9M, which increased the LCOE of the Fish-safe Unit Addition configuration from $83.23/MWh to $96.79/MWh. Comparing the construction of a new VS fishway versus the rock ramp

Table 21. Results of baseline conditions for the Bosher upstream passage analysis.

Configuration name	Module shorthand	LCOE ($/MWh)	Total Cost	Annual Energy Generation (MWh)	Effective upstream passage (%)
Fish-safe Unit Addition	FS + Weir + VS	$83.23	$11,439,700	16843	33%
Eco-innovation	FS + RR + WW	$141.43	$23,304,700	16778	56%
Seasonal VS Operation	FS + Weir + Seasonal VS	$80.93	$11,439,700	17321	33%
New VS addition	FS + Weir + New VS	$96.79	$14,484,700	16843	33%

(with no whitewater park), the VS fishway would increase LCOE from the Fish-safe Unit Addition baseline by $13.56/MWh with an effective passage of 33%. On the other hand, the rock ramp would add $49.60/MWh with an effective passage of 56%. In other words, the VS fishway costs $0.41/MWh per 1% of effective passage, while the rock ramp costs $0.89/MWh. Again, the LCOEs incorporate the capital costs, operating costs, and energy losses of each design. The VS fishway is the more cost-effective option; however, the value of the 23% difference in passage may affect stakeholder decisions.

Two sensitivity analyses were conducted to explore the model relationships further and highlight areas of uncertainty. The first area of uncertainty was the entrance and passage efficiencies for the VS fishway and rock ramp. Fishway entrance efficiencies depend on the dimensions and hydraulic design of the entrance and differ between fishway types and the target species. Passage efficiencies similarly depend on how well the hydraulic design supports desired swimming conditions of the target species. Since there was only one upstream pathway in each configuration, the entrance efficiency did not influence the distribution of fish flow. Instead, the effective passage model becomes a linear function of the product entrance and passage efficiencies. This relationship was tested by running sensitivity analysis on the Eco-innovation and Fish-safe Unit Addition configurations with the Peak Ramping dispatch model by iterating between 0-100% passage efficiencies with increments of 5%. The entrance efficiencies were kept constant at 80%. The expected linear results from this sensitivity analysis are illustrated in Figure 48. The rock ramp relationship was a straight line between 0% passage and 80% passage, which was the maximum passage allowed by the entrance efficiency. However, the VS fishway relationship differed due to the attraction efficiency. There was a 3% loss in effective passage at the baseline condition and a 7.2% loss in effective passage at the 100% passage efficiency mark. The loss is a function of the relative discharge of the modules during the upstream passage months. The rock ramp had considerable flows due to the notch flow and minimum flow requirement, so it experienced no losses in attraction. This highlights the model's simplicity for cases of one species and one fish passage module, which is the typical scope. Future research could assess the cross-species effects by parameterizing the model for multiple species or could test cases with multiple fishways.

The next sensitivity analysis focused on the attraction efficiency model, detailed in Chapter Three. Fish attraction is one of the most complicated factors in fish passage literature because hydraulic conditions vary across sites, and swimming preferences vary across species. However, an underlying theme is that low attraction flows from the fishway can limit the ability of migrants to identify the entrance [143]. The effective upstream passage model uses this theme to parameterize attraction efficiency as a function of the relative discharge so that modules with low flows compared to the total facility flow are penalized. Tuning the model presented a challenge and area of uncertainty since little data exists on fishway relative discharges. Studies may include fishway design flows, but they neglect facility flows and their variability over time. As previously described, the baseline condition for American Eel at the Bosher site was tuned to a relative discharge threshold of around 2.3% (a = 0.3, b = 0.03) based on the

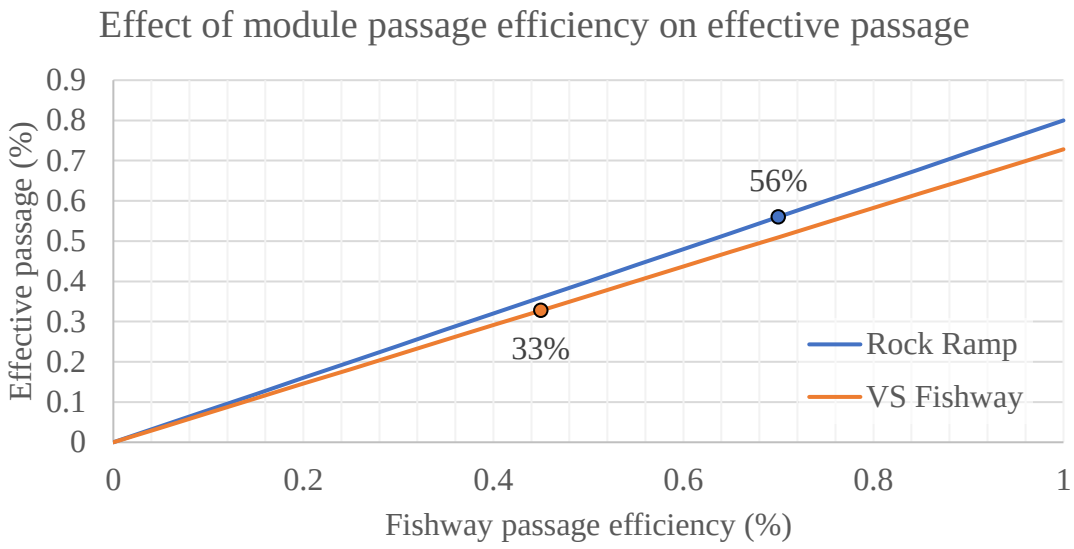

Figure 48. Results of the passage efficiency sensitivity analysis for the Eco-innovation and Fish-safe Unit Addition configurations of the Bosher site. The dots indicate the baseline conditions.

assumption vertical slot fishway (225cfs) was designed for adequate attraction at the Q_{30} (7630cfs). The resulting curve is illustrated by the blue line in Figure 18. The attraction sensitivity parameter (*b*) determines the slope of the sigmoid function, while the relative discharge parameter (*a*) determines where the sigmoid function drops off, which is the more critical of the two parameters. As such, a sensitivity analysis was conducted on the Fish-safe Unit Addition configuration with the Peak Ramping dispatch model by varying the relative discharge parameter between 0.01 to 13.02 in variable increments relating to the scale of the number. In other terms, the relative discharge threshold (the value at which the sigmoid function equals 99%) was varied between 0.08% and 98.9%. Relative discharges above these values were assumed to have minimal attraction losses.

The results of this analysis are illustrated in Figure 49. The relationship resembles an inverse sigmoid curve. The relative discharge for the VS fishway is dependent on the inflow and flow allocation during the upstream passage months, and it does not change based on the attraction function. Thus, the curve reflects the effective passage as the sigmoid attraction function moves across a set average relative discharge. As expected, the curve shows that the effective passage decreases in a shape similar to the attraction function at higher discharge thresholds. The baseline condition of a 2.3% relative discharge threshold led to a 33% effective passage, which is a 3% loss due to attraction. At a relative discharge threshold of 10%, the effective passage dropped to 16%, or a 20% loss due to attraction. The effective passage of about 2% that occurred at a relative discharge threshold of 98.9% is a remnant of the attraction sensitivity factor (*b*).

These upstream passage models and inputs were based on the literature but must be validated with real site data before further application. However, the attraction parameter sensitivity analysis showed that the novel attraction efficiency framework captured the expected trends and could be a valuable tool for early assessments of fishway design flow tradeoffs. To validate the model, site studies would need to capture the fish passage efficiencies, the fishway flow, and the total facility flow to determine the relative discharge. Environmental and hydraulic factors, such as temperature, tailwater depth, and flow velocities, should also be measured over time to determine other potential factors for successful passage. The other analyses showed that the rock ramp was more effective at passing fish while the VS fishway was cheaper per unit of fish passage despite the losses to attraction. However, the rock ramp provides several non-power benefits in addition to the 23% increase in effective passage, including an improvement in site aesthetics and increased safety for recreationalists since the drop from the low-head dam would be alleviated. As such, research and investment into cost reductions for nature-like rock ramps could be a serious boon for low-head NPD development. This could include standardized design practices, expediated construction processes, or incentive programs. Even without NPD generation retrofits, these rock ramps could be an alternative to dam removal by increasing the fish passage characteristics of low-head dams without the loss of dam function.

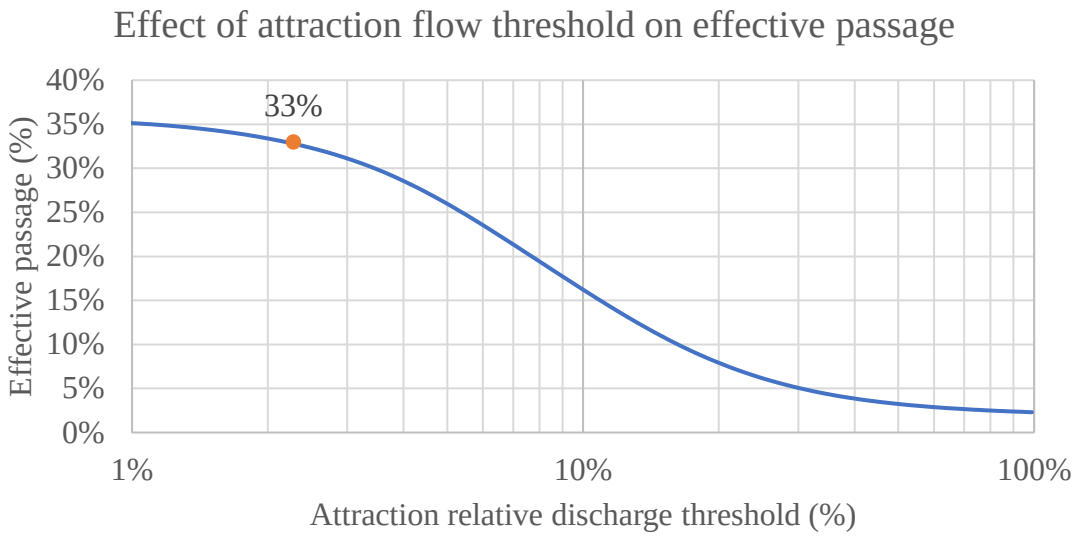

Figure 49. The relationship between the relative discharge threshold (the 99% value of the attraction efficiency sigmoid function) and the effective upstream passage for the Fish-safe Unit Addition configuration of the Bosher site. The dot marks the baseline condition. Note the log-x scale.

Value of recreation

Recreation modules can provide the ability for boats, kayaks, canoes, and other recreationalists to traverse the facility and enjoy recreation features. Whitewater parks and boat chutes are the most common examples currently. The primary performance metric for recreation modules is module availability, which describes how much time the module can operate safely during the year. Several metrics influence this availability, including the design flow and the headwater/tailwater restrictions. While business models will differ between projects, the waterSHED model provides a useful feature that provides revenue to the project based on module availability times the value of recreation, which describes the revenue per hour of availability. This can be considered the price of admission for the recreation feature. Using this feature and the enumeration method, the waterSHED model can determine the breakeven point where the revenue from the module outweighs the capital and operating costs. However, one current limitation of the tool is the daily operation timestep, so modules that only operate for daylight hours must be properly discounted for 24-hour operation. As such, the following analysis was conducted outside of waterSHED using the module availability results of the model.

The proposed Eco-innovation configuration for Bosher included a whitewater park built in place of the existing VS fishway. Based on high-level estimates, the park would cost $1.7M and have an annual operating cost of $3,200. The whitewater park would require between 300-600cfs but would only be operated during daylight hours, about half the day on average throughout the year (Table 17 in the Appendix). As such, the baseline module design flow was set to 300cfs, assuming that the park had enough storage and flexibility to mitigate the impact of variable water needs on the flow allocation. The whitewater park was also assumed not to have headwater or tailwater level constraints. The park was assumed to get recreationalists whenever the combined air and water temperature is above 80˚F, which occurs on a monthly average throughout the year (Table 17 in the Appendix), so the baseline condition was to operate the module year-round. However, a more realistic expectation would be to operate during the typical recreation season between April and October. The whitewater park was placed after generation modules in the passage module priority curve, so the park would be allocated after the generation modules were ramped but before the sluice gate was opened. However, the priority will depend on the project developer and, in some cases, may precede generation modules. Five scenarios of the Eco-innovation configuration were run in waterSHED with the Advanced Greedy dispatch model to understand the tradeoffs between these inputs. These scenarios included:

- Baseline – low priority and year-round operation
- No Whitewater – the Eco-innovation configuration without the whitewater park
- Seasonal – low priority and seasonal (April to October) operation
- Priority – high priority (above generation) with year-round operation
- Seasonal + Priority – high priority and seasonal operation

The recreation module allocation time series, cost, and energy generation results were extracted and input into a separate model that discounted the recreation hours by the average daylight hours for that month (Table 17 in the Appendix). This produced the expected annual hours of operation for the whitewater park. The energy loss from the whitewater park was calculated by subtracting the annual energy of each scenario by the annual energy of the No Whitewater scenario. The annual loss from the whitewater park was calculated by summing the annual O&M costs ($3,200) with the energy loss times the price of energy ($60/MWh). The net present value of the annual loss and the capital cost was computed using the baseline discount rate (7%) and project life (40 years). Finally, the breakeven value of recreation was calculated using a goal seek program that iterated the value of recreation ($/hr) until the net revenue went to zero. The results of the analysis are described in Table 22.

For the baseline conditions, the breakeven value of recreation was $29.18/hr. Costs for kayak rentals typically range between $8 to $15, so this value is reasonable, assuming more than one person can use the module at a time and the park can attract recreationalists throughout the year. Compared to the No Whitewater scenario, the baseline condition had a slight (0.33%) decrease in energy generation. Although low operation priority did not affect the generation allocation, it did impact the flow over the spillway, which indirectly affected the head. However, the baseline condition had relatively low annual availability, with only 140 days of the year in operation or 38% of the time it could be operating. From June to October, which coincides with the low flow seasons, there was not enough flow to turn on the whitewater park after meeting the minimum spillway flow requirement. During the seasonal (low-priority case), this effect was even more noticeable as the module was operated only 65 days a year or 30% of the time it could be operating (214 days in the season), which almost doubled the breakeven costs. Increasing the module priority partially addressed this concern, increasing the year-round operation to 84% and the seasonal operation to 77% availability. However, these lead to energy losses of 6.08% and 3.67% for year-round and seasonal cases. Considering the energy loss, costs, and availability, the most cost-effective option with a breakeven value of recreation of $28.95 was the high-priority, year-round operation, which also provides the highest recreation availability. However, this estimation may overvalue the potential revenue during cold months when attendance may be limited.

Overall, the breakeven value of recreation analysis provided a valuable estimation of how the module interactions impact the true cost of the whitewater park. Future research efforts should integrate an expected attendance distribution over the year to get a more accurate picture of the expected revenue. Surveys of the local population or assessments of similar recreation features in the area could provide useful attendance data. The designers should consider how to operate the facility during months where the low-flow season and the recreation season overlap. The availability could be managed by using a dynamic minimum flow requirement that is proportional to the inflow, which would decrease the required spillway flow while maintaining similar hydrologic patterns. The waterSHED model should also be improved to allow hourly operation of the facility since

Table 22. Results of the breakeven value of recreation analysis for the Eco-innovation configuration of the Bosher site.

Performance metric	Baseline	No Whitewater	Seasonal	Priority	Seasonal + Priority
Annual recreation hours	1684	0	880	3706	2225
Average days on per year	140	0	65	306	165
Percent of possible days available	38%	0%	30%	84%	77%
Annual energy generation (MWh)	16778	16833	16808	15809	16216
Percent energy loss	0.33%	0.00%	0.15%	6.08%	3.67%
Breakeven value of recreation ($/hr)	$29.18	NA	$53.83	$28.95	$37.25

daylight operation of the whitewater park could influence generation. Innovations in recreation modules to reduce costs and flow requirements would also improve the value proposition and decrease the value of recreation. Although the SMH framework is based on functional decomposition, combined recreation and fishway modules could reduce civil works costs for new developments. Like the rock ramp, natural whitewater park designs that leverage local materials could also help reduce costs.

Discussion

This case study aimed to answer research questions involving the cost-benefits tradeoffs of fish-safe designs and recreation modules at the Bosher dam site. These economic and fish passage tradeoffs were quantified through rapid prototyping of several design scenarios. Validating the generation model was an important first step to establishing economic performance. The generation model was validated against a reference flow duration curve model and showed that the waterSHED formulation tended to show a best-case scenario for generation because it assumed 100% availability. The waterSHED model could be improved by adding planned and unplanned outage features to the simulation process. The generation optimization process arrived at similar conclusions to the reference model for the optimal number of generation modules for baseline Eco-innovation configuration (10 versus 11). However, it highlighted the sensitivity of LCOE as an objective metric and the importance of stakeholder perspectives in the design process. For example, although a three-module design was the most cost-effective option for the Fish-safe Unit Addition configuration, it may be beneficial to stakeholders to increase capacity to help meet grid demand despite estimated LCOE increases. The model also showed that the Fish-safe Unit Addition configuration would be relatively feasible with an LCOE of around $84/MWh, although the other configurations would require cost reductions for the non-power modules. Increased power prices or renewable energy incentives could also help improve economic performance.

The downstream passage analysis assessed the cost-benefit tradeoffs of fish exclusion designs versus fish-safe turbines. Compared to a scenario with 0% mortality from fish-safe turbines, conventional fish screen designs would have a higher effective mortality of around 3%, along with a 1.7% loss in generation and a $63/MWh increase in LCOE. The downstream migration season for American Eel coincided with the low flow season resulting in limited powerhouse flows during migration. As such, seasonal turbine operation could be a feasible fish passage mitigation measure for this site. However, further simulations and research would be needed to study the mortality for multiple species and migration seasons. Fish-safe turbines showed considerable value by improving economic and fish passage performance. Continued investment in fish-safe turbine designs and testing, as well as a reexamination of regulatory practices related to fish exclusion, would be beneficial for low-head hydropower development.

The upstream passage analysis assessed the cost-benefit tradeoffs of technical fishways versus nature-like fishways. The rock ramp was expected to perform about 23% better than the VS fishway for upstream passage due to better passage performance and less

attraction loss. The VS fishway was estimated to lose about 3% of effective passage from low attraction during high flow periods. However, the rock ramp was considerably more expensive on a dollar per unit of passage efficiency. Cost reductions for rock ramp designs could be greatly beneficial for NPD rehabilitations and NSD development due to the environmental and social non-power benefits, like improved safety and aesthetics. Standardized processes for design and material collection, modular formwork, and incentive programs could reduce costs and enable economies of scale.

The value of recreation analysis assessed the cost-benefit tradeoffs of a modular whitewater park. Several design scenarios were simulated, including designs with high priority and seasonal operation. Year-round operation with high-priority dispatch showed the lowest breakeven value of recreation of $28.95/hour, although the year-round, low priority design showed a similar breakeven value but with much less annual availability. Future site investigation efforts should survey expected attendance and willingness-to-pay values throughout the year to understand consumer demand. The whitewater park would be worthwhile if the expected average hourly revenue exceeds this benchmark. Additionally, sub-daily dispatch modeling would help understand the operational relationships between park operation and generation dispatch.

It is important to note that these results are site-specific and have several limitations. First, the model is based on the high-level data and assumptions available during this pre-feasibility study, so site investigation is needed before further decision-making. Second, the fish passage models are novel conceptual models based on existing literature, but they are untested and require future validation. In particular, the screen tree framework and the attraction efficiency model could be very useful as the community moves towards standardized measures of facility and basin-wide environmental performance metrics [44]. Finally, these results were assessed using one stakeholder perspective. Different energy price and discount rate assumptions, for example, could greatly impact the economic results. However, the waterSHED model is useful because it is interactive and allows different stakeholders to apply their own preferences and answer their own research questions. As the knowledge base of modular hydropower design grows, the waterSHED provides the framework for quickly applying inter-disciplinary research to real-world design decisions.

CHAPTER FIVE

CONCLUSIONS AND RECOMMENDATIONS

Sustainable and innovative designs are needed for low-head, instream, run-of-river (LIR) projects to continue new hydropower development in the US. The literature review showed that existing hydropower design models are narrowly focused on economic objectives using constant head assumptions that do not apply to low-head sites. In addition, environmental considerations focus on minimum environmental flow requirements that are less relevant for LIR hydropower. The identified areas for improvement included the expansion of model formulations across environmental and social domains, particularly barrier effects caused by the dam structure, and the explicit optimization of these non-power benefits. This research formulated and applied a novel hydropower design model called waterSHED that aimed to incorporate environmental and social objectives into the conceptual design process of modular hydropower projects.

Following the principles of the Standard Modular Hydropower project, the waterSHED model represented hydropower technologies in an object-oriented approach based on module functions. The object-oriented approach expedited the modeling process for two case studies by streamlining the input process for conventional and innovative technologies with a graphical user interface. The virtually created SMH facilities were simulated using daily run-of-river operation to assess high-level performance metrics. A system of models was created by leveraging existing literature to describe the relationships between operation, energy generation, fish passage, sediment passage, recreation, and economic performance. While the sophistication and resolution of the models were limited by the available data and feasibility-stage scope, the system of models represented a clear improvement on existing methods through both the integration of non-power benefits and the object-oriented approach. Two methods were evaluated for optimizing module selection and flow allocation given user-defined technologies and assumptions. The enumeration process was deemed more effective for small solution spaces, like in the case studies. However, a custom genetic algorithm could facilitate larger solution spaces as the number of modular hydropower technologies in the market grows and the system of models becomes more complex. Four different generation dispatch algorithms were created to optimize flow allocation across modules. The Peak Ramping and Advanced Greedy stood out, the former having fast computation times with limited loss to optimality and the latter having the optimal generation dispatch with longer runtimes.

Case studies were conducted to validate the construction of the model and gain insights into the cost-benefit tradeoffs relevant to LIR hydropower plants. The sediment, fish passage, economic, recreation, generation, and dispatch models were tested in the case studies and showed proper performance. Sensitivity analyses were used to explore the model formulations by isolating the effects of select inputs on facility performance. This method enabled the case studies to evaluate the effect of uncertainties and innovations.

Each section discusses the site-specific design recommendations and areas for future research, but the highlights are summarized below.

Case Study A highlighted the need for cost reductions across the module classes, especially in hydropower foundations and generation modules. Various potential innovations, like modular earthen dams and combined recreation and fish passage modules, were proposed to stimulate these cost reductions. Sensitivity analyses were also conducted on the headwater levels and sediment gate parameters to evaluate the tradeoffs between generation, cost, and sediment continuity. They validated the theme in the literature that smaller and more frequent sediment passage events are better for sediment continuity, which presents a stark difference in design thinking from conventional sediment flushing and dredging practices. Additionally, sediment trapping is not expected to be severe at low-head dams, which incentivizes the use of low-flow sediment siphons or the use of spillways for sediment passage. The headwater level analysis represents a significant advancement in hydropower design modeling since most models assume constant heads and cannot account for design changes at different heads. Applying the waterSHED model to other sites and technology sets would help further validate these results and model functionality.

Case Study B assessed the tradeoffs between different module configurations at an existing NPD. The waterSHED model showed that fish-safe turbines have several advantages to conventional fish exclusion designs, including increased generation and reduced fish mortality. Additionally, the nature-like rock ramp design could improve fish passage and human safety, but cost reductions are needed to increase feasibility. Sensitivity analyses were conducted on the fish passage model parameters to explore the effectiveness of the formulations. The screen tree model could be improved to account for screen impingement, refusal, and passage delays. Analyzing the breakeven cost of recreation helped quantify the recreation revenues required to make the whitewater park worthwhile in different operation scenarios. The fish passage and recreation models proved to be useful and novel tools for design decisions; however, further research is needed to validate them in practice.

Recommendations for future research can be categorized as improvements to hydropower design modeling, applications of the model, and improvements in modular facility design research. Several features that could be added to improve the utility and accuracy of waterSHED include sub-daily operation, more detailed assessment of turbine setting and freeboard hydraulics, volumetric sediment passage models, time-based energy price models, and improved civil works models for dam and foundation parameterization. Sub-daily operation modeling especially would help identify operational interactions between recreation modules that only operate during daylight hours, generation modules that prioritize operation during peak loads, and fish passage modules that may target fish with diurnal or nocturnal migration preferences. This sub-daily feature would also help model tradeoffs related to the ROR timescale, like the tradeoff between hydrologic alteration and energy generation or ancillary services. Fifteen-minute flow data is available for a

limited subset of stream gages in the US, but a method of extrapolating daily average inflows into a sub-daily flow time series would be needed for consistent application. In addition, while non-power benefits are integrated through constraints and the tradeoff analyses, explicit optimization of these non-power benefits should be included in the model, per the recommendations in Chapter Two. The current model uses penalty functions to detract from objective functions when the non-power constraint is not met. A weighting factor approach would let the user set preferences for power and non-power benefits and incorporate them into a singular objective function. Case Study A found that capacity selection should also be driven by external factors like the developer's risk preference, so a weighting factor could allow users to select higher or lower capacity points if LCOEs are similar. Expanding the tool to consider networked hydropower systems could be valuable for identifying and optimizing SMH projects built in series to promote economies of scale. Continued updates and expansion of the module library could establish this tool as a cornerstone of modular hydropower design thinking.

Applications of the tool to other case studies and sensitivity analyses would further validate the modeling approach and generate research insights. For example, projects with multiple species, different sized turbines, multiple fishway or recreation modules, and various head values would also be useful for further validating the system of models. Since the case studies in this study used the enumeration method, it is important to test the stability and efficacy of the custom genetic algorithm for large solution spaces. The number of iterations, population size, evolution processes, and convergence criteria must be tuned for the module selection problems of interest. The enumeration method would provide a benchmark for optimality and computation time, and the genetic algorithm could also be compared to other heuristic methods like simulated annealing or tabu search. In addition, the sensitivity analysis capability would be beneficial for quantifying uncertainty across the facility design. Case Study A, for example, examined the uncertainty in foundation costs. Application of the sensitivity analysis procedure to weir coefficient relationships, stage-discharge relationships, inflow, energy price, and module costs could provide useful assessments of uncertainty and, therefore, project risk. These analyses would then help identify the project characteristics that are most important to project outcomes. The case studies identified headwater elevation, foundation depth, and non-power module selection as some of the major cost drivers for the reference sites. These drivers may change for different site conditions and technologies, and the waterSHED modeling framework provides the flexible capabilities needed to identify site-specific drivers.

Further research in the modular hydropower design space can help increase the feasibility of low-head hydropower projects. The case studies highlighted several module innovation areas. In particular, nature-like modular technologies, like rock ramps or modular earthen dams, that leverage low-cost, less dense materials could facilitate construction on top of thick soil foundations by displacing loads across larger footprints and reducing excavation costs. Nature-like designs could also support aesthetics and ecosystem functions like fish passage, as shown by the rock ramp fish passage analysis.

Research would be needed to standardize the construction procedures if using local materials in addition to or in place of prefabricated forms. Advanced manufacturing for hydropower could also facilitate the customization of modular components that could increase performance and reduce costs within a standardized approach. For example, 3D printing molds for turbine runners used within a standardized modular form could add a level of optimization to increase generation. Additionally, since Case Study A showed that head is still a major cost driver at low-head sites, improved reservoir modeling using remote sensing could help identify the maximum headwater level that has limited social impacts rather than using the 100-yr flood level assumption. Research and stakeholder engagement regarding standardized performance metrics across the environmental domains would also benefit future modeling and regulatory efforts.

This work provides a true example of inter-disciplinary research. The waterSHED model and related analyses applied principles of computer science to the field of hydropower using a system of models that spans geomorphic, geotechnical, hydrologic, economic, biological, and social domains. Academic advancements were generated in several areas, and multi-objective optimization was the underlying theme that brought them together. This research also has a broader impact on the hydropower community by creating a user-friendly tool and through case studies conducted with industry stakeholders. While this dissertation compiles a considerable amount of work on modular hydropower plants, there is even more work to be done. The waterSHED model provides a conceptual foundation for future research into the space as it was designed to grow with new research and technologies. With continued development, modular hydropower plants can be an important source of renewable electricity and non-power benefits to help meet sustainability goals worldwide.

LIST OF REFERENCES

[1] “Hydropower Vision: A New Chapter for America’s Renewable Electricity Source,” 2016.
[2] “Hydropower Special Market Report - Analysis and forecast to 2030,” 2021.
[3] R. Uria-Martinez, M. Johnson, and S. Rui, “2021 Hydropower Market Report,” no. January, 2021.
[4] B. Hadjerioua, Y. Wei, and S.-C. Kao, “An Assessment of Energy Potential at Non-Powered Dams in the United States.” Oak Ridge National Lab. (ORNL), Oak Ridge, TN (United States), 2012.
[5] S.-C. Kao *et al.*, “New Stream-reach Development: A Comprehensive Assessment of Hydropower Energy Potential in the United States,” no. GPO DOE/EE-1063. Oak Ridge National Laboratory (ORNL), Oak Ridge, TN (United States), 2014.
[6] C. J. Vörösmarty, M. Meybeck, B. Fekete, K. Sharma, P. Green, and J. P. M. Syvitski, “Anthropogenic sediment retention: major global impact from registered river impoundments,” *Glob. Planet. Change*, vol. 39, no. 1, pp. 169–190, 2003.
[7] T. Patsialis, I. Kougias, N. Kazakis, N. Theodossiou, and P. Droege, “Supporting Renewables’ Penetration in Remote Areas through the Transformation of Non-Powered Dams,” *Energies*, vol. 9, no. 12, 2016.
[8] “U.S. Hydropower : Climate Solution and Conservation Challenge,” 2020.
[9] P. W. O’Connor, S. T. DeNeale, D. R. Chalise, E. Centurion, and A. Maloof, “Hydropower Baseline Cost Modeling, Version 2.” Oak Ridge National Laboratory (ORNL), Oak Ridge, TN (United States), 2015.
[10] C. Hansen, M. Musa, C. Sasthav, and S. DeNeale, “Hydropower development potential at non-powered dams: Data needs and research gaps,” *Renew. Sustain. Energy Rev.*, vol. 145, p. 111058, 2021.
[11] G. A. Oladosu, J. Werble, W. Tingen, A. Witt, M. Mobley, and P. O’Connor, “Costs of mitigating the environmental impacts of hydropower projects in the United States,” *Renew. Sustain. Energy Rev.*, vol. 135, no. February 2020, p. 110121, 2021.
[12] A. Levine *et al.*, “An Examination of the Hydropower Licensing and Federal Authorization Process,” Golden, CO, 2021.
[13] H. I. Jager and M. S. Bevelhimer, “How Run-of-River Operation Affects Hydropower Generation and Value,” *Environ. Manage.*, vol. 40, no. 6, pp. 1004–1015, 2007.
[14] C. Sasthav and G. Oladosu, “Environmental design of low-head run-of-river hydropower in the United States: A review of facility design models,” *Renew. Sustain. Energy Rev.*, vol. 160, p. 112312, 2022.
[15] U. Energy Information Administration, “Levelized Cost and Levelized Avoided Cost of New Generation Resources in the Annual Energy Outlook 2020,” Feb. 2020.
[16] B. T. Smith, A. Witt, K. M. Stewart, K. Lee, S. DeNeale, and M. Bevelhimer, “A Multi-Year Plan for Research, Development, and Prototype Testing of Standard Modular Hydropower Technology.” Oak Ridge National Laboratory (ORNL), Oak Ridge, TN (United States), 2017.
[17] A. Witt, S. DeNeale, T. Papanicolaou, B. Abban, and N. Bishop, “Standard

Modular Hydropower: Case Study on Modular Facility Design." Oak Ridge National Laboratory (ORNL), Oak Ridge, TN (United States), 2018.
[18] K. M. Stewart, B. T. Smith, A. Witt, S. DeNeale, M. Bevelhimer, and J. L. Pries, "Simulation and Modeling Capability for Standard Modular Hydropower Technology." Oak Ridge National Laboratory (ORNL), Oak Ridge, TN, 2017.
[19] A. Witt, B. T. Smith, A. Tsakiris, T. Papanicolaou, K. Lee, and K. M. Stewart, "Exemplary Design Envelope Specification for Standard Modular Hydropower Technology." Oak Ridge National Lab. (ORNL), Oak Ridge, TN (United States), 2017.
[20] B. Dursun and C. Gokcol, "The role of hydroelectric power and contribution of small hydropower plants for sustainable development in Turkey," *Renew. Energy*, vol. 36, no. 4, pp. 1227–1235, 2011.
[21] F. Boustani, "An Assessment of the Small Hydropower Potential of Sisakht Region of Yasuj," *World Acad. Sci. Eng. Technol.*, vol. 57, Sep. 2009.
[22] A. Lee, "U.S. wind generating capacity surpasses hydro capacity at the end of 2016," *U.S. Energy Information Administration*, 2017. .
[23] R. Uria-Martinez, M. Johnson, and R. Shan, "U.S. Hydropower Market Report," 2021.
[24] M. Ho *et al.*, "The future role of dams in the United States of America," *Water Resour. Res.*, vol. 53, no. 2, pp. 982–998, Feb. 2017.
[25] R. Black, B. McKenney, R. Unsworth, and N. Flores, "Economic Analysis for Hydropower Project Relicensing: Guidance and Alternative Methods," 1998.
[26] R. J. Bellmore *et al.*, "Status and trends of dam removal research in the United States," *Wiley Interdiscip. Rev. Water*, vol. 4, no. 2, pp. 4–1164, 2017.
[27] S. G. Roy *et al.*, "A multiscale approach to balance trade-offs among dam infrastructure, river restoration, and cost," *Proc. Natl. Acad. Sci.*, vol. 115, no. 47, pp. 12069 LP – 12074, Nov. 2018.
[28] E. H. Stanley and M. W. Doyle, "Trading off: the ecological effects of dam removal," *Front. Ecol. Environ.*, vol. 1, no. 1, pp. 15–22, Feb. 2003.
[29] T. B. A. Couto and J. D. Olden, "Global proliferation of small hydropower plants – science and policy," *Front. Ecol. Environ.*, vol. 16, no. 2, pp. 91–100, Mar. 2018.
[30] M. M. Johnson, S.-C. Kao, N. M. Samu, and R. Uria-Martinez, "Existing Hydropower Assets." HydroSource, Oak Ridge, TN, 2021.
[31] J. Opperman, G. Grill, and J. Hartmann, "The Power of Rivers: Finding balance between energy and conservation in hydropower development," The Nature Conservancy, Washington, D.C., 2015.
[32] A. Witt, A. Fernandez-McKeown, M. Mobley, S. DeNeale, M. Bevelhimer, and B. Smith, "How Standard Modular Hydropower Can Enhance the Environmental, Economic, and Social Benefits of New Small Hydropower Development." Oak Ridge, TN, 2017.
[33] A. Kuriqi, A. Pinheiro, A. Sordo-Ward, M. Bejarano, and L. Garrote, "Ecological Impacts of Run-of-River Hydropower Plants-Current Status and Future Prospects on the Brink of Energy Transition," *Renew. Sustain. Energy Rev.*, vol. 142, p. 110833, Mar. 2021.

[34] “Hydropower Primer: A Handbook of Hydropower Basics,” 2017.
[35] G. W. Annandale, G. L. Morris, and P. Karki, *Extending the Life of Reservoirs: Sustainable Sediment Management for Dams and Run-of-River Hydropower*. The World Bank, 2016.
[36] K. S. Meijer and S. Hajiamiri, “Quantifying well-being values of environmental flows for equitable decision-making: A case study of the Hamoun wetlands in Iran,” *Int. J. River Basin Manag.*, vol. 5, no. 3, pp. 223–233, Sep. 2007.
[37] W. Summer, W. Stritzinger, and W. Zhang, “The impact of run-of-river hydropower plants on temporal suspended sediment transport behaviour,” *IAHS Publ. Proc. Reports-Intern Assoc Hydrol. Sci.*, vol. 224, pp. 411–420, 1994.
[38] N. L. Poff *et al.*, “The Natural Flow Regime,” *Bioscience*, vol. 47, no. 11, pp. 769–784, 1997.
[39] M. Craig, J. Zhao, G. Schneider, A. Schneider, S. Watson, and G. Stark, “Net revenue and downstream flow impact trade-offs for a network of small-scale hydropower facilities in California,” *Environ. Res. Commun.*, vol. 1, no. 1, p. 11001, 2019.
[40] S. Deneale *et al.*, “Hydropower Geotechnical Foundations : Current Practice and Innovation Opportunities for Low-Head Applications,” Oak Ridge, TN (United States), 2020.
[41] M. Bevelhimer, C. DeRolph, and A. Witt, “Site Classification for Standard Modular Hydropower Development: Characterizing Stream Reaches by Module Need.” Oak Ridge National Lab. (ORNL), Oak Ridge, TN, 2018.
[42] A. Kuriqi, A. N. Pinheiro, A. Sordo-Ward, and L. Garrote, “Flow regime aspects in determining environmental flows and maximising energy production at run-of-river hydropower plants,” *Appl. Energy*, vol. 256, p. 113980, 2019.
[43] E. Parish, B. Pracheil, R. McManamay, S. Curd, C. DeRolph, and B. Smith, “Review of environmental metrics used across multiple sectors and geographies to evaluate the effects of hydropower development,” *Appl. Energy*, vol. 238, p. 101, Mar. 2019.
[44] B. M. Pracheil *et al.*, “A Checklist of River Function Indicators for hydropower ecological assessment,” *Sci. Total Environ.*, vol. 687, pp. 1245–1260, 2019.
[45] D. Anderson, H. Moggridge, P. Warren, and J. Shucksmith, “The impacts of ‘run-of-river’ hydropower on the physical and ecological condition of rivers,” *Water Environ. J.*, vol. 29, no. 2, pp. 268–276, Jun. 2015.
[46] S. Trussart, D. Messier, V. Roquet, and S. Aki, “Hydropower projects: a review of most effective mitigation measures,” *Energy Policy*, vol. 30, no. 14, pp. 1251–1259, 2002.
[47] M. Mattmann, I. Logar, and R. Brouwer, “Hydropower externalities: A meta-analysis,” *Energy Econ.*, vol. 57, pp. 66–77, 2016.
[48] T. Key, L. Rogers, D. Brooks, and A. Tuohy, “Quantifying the Value of Hydropower in the Electric Grid: Final Report,” 2011.
[49] R. S. Winton, E. Calamita, and B. Wehrli, “Reviews and syntheses: Dams, water quality and tropical reservoir stratification,” *Biogeosciences*, vol. 16, p. 1671, 2019.

[50] A. T. Silva *et al.*, “The future of fish passage science, engineering, and practice,” *Fish Fish.*, vol. 19, no. 2, pp. 340–362, Mar. 2018.
[51] C. Sindelar, J. Schobesberger, and H. Habersack, “Effects of weir height and reservoir widening on sediment continuity at run-of-river hydropower plants in gravel bed rivers,” *Geomorphology*, vol. 291, pp. 106–115, 2017.
[52] P. Gibeau, B. M. Connors, and W. J. Palen, “Run-of-River hydropower and salmonids: potential effects and perspective on future research,” *Can. J. Fish. Aquat. Sci.*, vol. 74, no. 7, pp. 1135–1149, Dec. 2016.
[53] C. Nilsson and B. M. Renöfält, “Linking Flow Regime and Water Quality in Rivers,” *Ecol. Soc.*, vol. 13, no. 2, Dec. 2008.
[54] F. Colas, V. Archaimbault, and S. Devin, “Scale-dependency of macroinvertebrate communities: Responses to contaminated sediments within run-of-river dams,” *Sci. Total Environ.*, vol. 409, no. 7, pp. 1336–1343, 2011.
[55] T. Harlan, R. Xu, and J. He, “Is small hydropower beautiful? Social impacts of river fragmentation in China’s Red River Basin,” *Ambio*, vol. 50, no. 2, pp. 436–447, 2021.
[56] G. Mamo, M. Marence, J. Chacon-Hurtado, and M. Franca, “Optimization of Run-of-River Hydropower Plant Capacity,” *Int. Water Power Dam Constr.*, Aug. 2018.
[57] I. A. Niadas and P. G. Mentzelopoulos, “Probabilistic Flow Duration Curves for Small Hydro Plant Design and Performance Evaluation,” *Water Resour. Manag.*, vol. 22, no. 4, pp. 509–523, 2008.
[58] R. Montanari, “Criteria for the economic planning of a low power hydroelectric plant,” *Renew. Energy*, vol. 28, no. 13, pp. 2129–2145, 2003.
[59] S. T. Deneale, G. B. Baecher, K. M. Stewart, E. D. Smith, and D. B. Watson, “Current State-of-Practice in Dam Safety Risk Assessment,” Oak Ridge, TN, 2019.
[60] L. Spitalny, D. Unger, and J. M. A. Myrzik, “Potential of small hydro power plants for delivering ancillary services in Germany,” in *CIRED Workshop*, 2012, no. May.
[61] J. S. Anagnostopoulos and D. E. Papantonis, “Optimal sizing of a run-of-river small hydropower plant,” *Energy Convers. Manag.*, vol. 48, no. 10, pp. 2663–2670, 2007.
[62] N. G. Voros, C. T. Kiranoudis, and Z. B. Maroulis, “Short-cut design of small hydroelectric plants,” *Renew. Energy*, vol. 19, no. 4, pp. 545–563, 2000.
[63] B. D. Richter, J. V Baumgartner, J. Powell, and D. P. Braun, “A Method for Assessing Hydrologic Alteration within Ecosystems,” *Conserv. Biol.*, vol. 10, no. 4, pp. 1163–1174, Aug. 1996.
[64] A. Kuriqi, A. N. Pinheiro, A. Sordo-Ward, and L. Garrote, “Influence of hydrologically based environmental flow methods on flow alteration and energy production in a run-of-river hydropower plant,” *J. Clean. Prod.*, vol. 232, pp. 1028–1042, 2019.
[65] M. Bevelhimer, R. McManamay, and B. O’Connor, “Characterizing Sub-Daily Flow Regimes: Implications of Hydrologic Resolution on Ecohydrology Studies,” *River Res. Appl.*, vol. 31, 2014.

[66] B. Lehner *et al.*, “High-resolution mapping of the world’s reservoirs and dams for sustainable river-flow management,” *Front. Ecol. Environ.*, vol. 9, no. 9, pp. 494–502, Nov. 2011.
[67] G. Grill, C. Ouellet Dallaire, E. Fluet Chouinard, N. Sindorf, and B. Lehner, “Development of new indicators to evaluate river fragmentation and flow regulation at large scales: A case study for the Mekong River Basin,” *Ecol. Indic.*, vol. 45, pp. 148–159, 2014.
[68] G. M. Brune, “Trap efficiency of reservoirs,” *Eos, Trans. Am. Geophys. Union*, vol. 34, no. 3, pp. 407–418, Jun. 1953.
[69] M. Reisenbüchler, M. D. Bui, D. Skublics, and P. Rutschmann, “Sediment Management at Run-of-River Reservoirs Using Numerical Modelling,” *Water*, vol. 12, no. 1. 2020.
[70] R. J. P. Schmitt, S. Bizzi, A. Castelletti, J. J. Opperman, and G. M. Kondolf, “Planning dam portfolios for low sediment trapping shows limits for sustainable hydropower in the Mekong,” *Sci. Adv.*, vol. 5, no. 10, p. eaaw2175, Oct. 2019.
[71] J. C. Schmidt and P. R. Wilcock, “Metrics for assessing the downstream effects of dams,” *Water Resour. Res.*, vol. 44, no. 4, Apr. 2008.
[72] S. A. Brandt, “Classification of geomorphological effects downstream of dams,” *CATENA*, vol. 40, no. 4, pp. 375–401, 2000.
[73] S. A. Brandt, “Prediction of Downstream Geomorphological Changes after Dam Construction: A Stream Power Approach,” *Int. J. Water Resour. Dev.*, vol. 16, no. 3, pp. 343–367, Sep. 2000.
[74] G. E. Grant, J. C. Schmidt, and S. L. Lewis, “A geological framework for interpreting downstream effects of dams on rivers,” *Water Sci. Appl.*, vol. 7, pp. 209–225, 2003.
[75] M. J. Noonan, J. W. A. Grant, and C. D. Jackson, “A quantitative assessment of fish passage efficiency,” *Fish Fish.*, vol. 13, no. 4, pp. 450–464, 2012.
[76] S. J. Cooke and S. G. Hinch, “Improving the reliability of fishway attraction and passage efficiency estimates to inform fishway engineering, science, and practice,” *Ecol. Eng.*, vol. 58, pp. 123–132, 2013.
[77] D. W. Roscoe and S. G. Hinch, “Effectiveness monitoring of fish passage facilities: historical trends, geographic patterns and future directions,” *Fish Fish.*, vol. 11, no. 1, pp. 12–33, Mar. 2010.
[78] C. R. Schilt, “Developing fish passage and protection at hydropower dams,” *Appl. Anim. Behav. Sci.*, vol. 104, no. 3, pp. 295–325, 2007.
[79] A. H. Colotelo, A. E. Goldman, K. A. Wagner, R. S. Brown, Z. D. Deng, and M. C. Richmond, “A comparison of metrics to evaluate the effects of hydro-facility passage stressors on fish,” *Environ. Rev.*, vol. 25, no. 1, pp. 1–11, Jul. 2016.
[80] I. Albayrak, R. M. Boes, C. R. Kriewitz-Byun, A. Peter, and B. P. Tullis, “Fish guidance structures: hydraulic performance and fish guidance efficiencies,” *J. Ecohydraulics*, pp. 1–19, Jan. 2020.
[81] S. V Amaral, F. C. Winchell, B. J. McMahon, and D. A. Dixon, “Evaluation of angled bar racks and louvers for guiding silver phase American eels,” in *American Fisheries Society Symposium*, 2003, vol. 33, pp. 367–376.

[82] R. M. Almeida *et al.*, “Limnological effects of a large Amazonian run-of-river dam on the main river and drowned tributary valleys,” *Sci. Rep.*, vol. 9, no. 1, p. 16846, 2019.
[83] A. Kuriqi, A. N. Pinheiro, A. Sordo-Ward, and L. Garrote, “Water-energy-ecosystem nexus: Balancing competing interests at a run-of-river hydropower plant coupling a hydrologic–ecohydraulic approach,” *Energy Convers. Manag.*, vol. 223, p. 113267, 2020.
[84] G. E. Hauser and W. G. Brock, “Aerating Weirs For Environmental Enhancement of Hydropower Tailwaters,” *Lake Reserv. Manag.*, vol. 11, no. 3, pp. 225–229, Dec. 1995.
[85] E. I. Daniil, J. Gulliver, and J. R. Thene, “Water-Quality Impact Assessment for Hydropower,” *J. Environ. Eng.*, vol. 117, no. 2, pp. 179–193, Mar. 1991.
[86] M. Carolli, G. Zolezzi, D. Geneletti, A. Siviglia, F. Carolli, and O. Cainelli, “Modelling white-water rafting suitability in a hydropower regulated Alpine River,” *Sci. Total Environ.*, vol. 579, pp. 1035–1049, 2017.
[87] B. H. Bakken and T. Bjorkvoll, “Hydropower unit start-up costs,” in *IEEE Power Engineering Society Summer Meeting*, 2002, vol. 3, pp. 1522–1527 vol.3.
[88] V. Koritarov *et al.*, “Pumped Storage Hydropower Valuation Guidebook,” Lemont, Illinois, 2021.
[89] J. S. Gulliver and R. E. A. Arndt, *Hydropower Engineering Handbook*. United States: McGraw-Hall, 1991.
[90] C. C. Warnick, H. A. Mayo, J. L. Carson, and L. H. Sheldon, *Hydropower Engineering*. Englewood Cliffs, New Jersey: Prentice Hall Inc., 1984.
[91] A. Kuriqi, A. Pinheiro, A. Sordo-Ward, and L. Garrote, “Trade-off Between Environmental Flow Policy and Run-of-River Hydropower Generation in Mediterranean Climate,” in *European Water*, 2017, pp. 123–130.
[92] G. A. Oladosu, J. Werble, W. Tingen, A. Witt, M. Mobley, and P. O’Connor, “Costs of mitigating the environmental impacts of hydropower projects in the United States,” *Renew. Sustain. Energy Rev.*, vol. 135, no. February 2020, p. 110121, 2020.
[93] C. Katopodis and J. G. Williams, “The development of fish passage research in a historical context,” *Ecol. Eng.*, vol. 48, pp. 8–18, 2012.
[94] D. Grimardias, J. Guillard, and F. Cattanéo, “Drawdown flushing of a hydroelectric reservoir on the Rhône River: Impacts on the fish community and implications for the sediment management,” *J. Environ. Manage.*, vol. 197, pp. 239–249, 2017.
[95] C. M. Bunt, T. Castro-Santos, and A. Haro, “Performance of Fish Passage Structures at Upstream Barriers to Migration,” *River Res. Appl.*, vol. 28, no. 4, pp. 457–478, May 2012.
[96] M. Ibrahim, Y. Imam, and A. Ghanem, “Optimal planning and design of run-of-river hydroelectric power projects,” *Renew. Energy*, vol. 141, pp. 858–873, 2019.
[97] T. Bøckman, S.-E. Fleten, E. Juliussen, H. J. Langhammer, and I. Revdal, “Investment timing and optimal capacity choice for small hydropower projects,” *Eur. J. Oper. Res.*, vol. 190, no. 1, pp. 255–267, 2008.

[98] J. P. P. G. Lopes de Almeida, A. G. Henri Lejeune, J. A. A. Sá Marques, and M. Conceição Cunha, “OPAH a model for optimal design of multipurpose small hydropower plants,” *Adv. Eng. Softw.*, vol. 37, no. 4, pp. 236–247, 2006.
[99] S. Basso and G. Botter, “Streamflow variability and optimal capacity of run-of-river hydropower plants,” *Water Resour. Res.*, vol. 48, no. 10, 2012.
[100] M. Najmaii and A. Movaghar, “Optimal design of run-of-river power plants,” *Water Resour. Res.*, vol. 28, no. 4, pp. 991–997, 1992.
[101] S. M. H. Hosseini, F. Forouzbakhsh, and M. Rahimpoor, “Determination of the optimal installation capacity of small hydro-power plants through the use of technical, economic and reliability indices,” *Energy Policy*, vol. 33, no. 15, pp. 1948–1956, 2005.
[102] M. Andaroodi and A. Schleiss, “Standardization of civil engineering works of small high-head hydropower plants and development of an optimization tool,” EPFL-LCH, 2006.
[103] R. Peña, A. Medina, O. Anaya-Lara, and J. R. McDonald, “Capacity estimation of a minihydro plant based on time series forecasting,” *Renew. Energy*, vol. 34, no. 5, pp. 1204–1209, 2009.
[104] A. Santolin, G. Cavazzini, G. Pavesi, G. Ardizzon, and A. Rossetti, “Techno-economical method for the capacity sizing of a small hydropower plant,” *Energy Convers. Manag.*, vol. 52, no. 7, pp. 2533–2541, 2011.
[105] I. A. Adejumobi and D. I. Shobayo, “Optimal Selection of Hydraulic Turbines for Small Hydro Electric Power Generation - A Case Study of Opeki River, South Western Nigeria,” *Niger. J. Technol.*, vol. 34, no. 3, pp. 530–537, 2015.
[106] M. M. Munir, A. S. Shakir, and N. M. Khan, “Optimal Sizing of Low Head Hydropower Plant- A Case Study of Hydropower Project at Head of UCC (Lower) at Bambanwala,” *Pakistan J. Eng. Appl. Sci.*, vol. 16, pp. 73–83, 2015.
[107] P. Razurel, L. Gorla, B. Crouzy, and P. Perona, “Non-proportional repartition rules optimize environmental flows and energy production,” *Water Resour. Manag.*, vol. 30, no. 1, pp. 207–223, 2016.
[108] I. Yousuf, A. R. Ghumman, and H. N. Hashmi, “Optimally sizing small hydropower project under future projected flows,” *KSCE J. Civ. Eng.*, vol. 21, no. 5, pp. 1964–1978, 2017.
[109] P. Sarzaeim, O. Bozorg-Haddad, B. Zolghadr-Asli, E. Fallah-Mehdipour, and H. A. Loáiciga, “Optimization of Run-of-River Hydropower Plant Design under Climate Change Conditions,” *Water Resour. Manag.*, vol. 32, no. 12, pp. 3919–3934, 2018.
[110] V. Yildiz and J. A. Vrugt, “A toolbox for the optimal design of run-of-river hydropower plants,” *Environ. Model. Softw.*, vol. 111, pp. 134–152, 2019.
[111] S. Basso, G. Lazzaro, M. Bovo, C. Soulsby, and G. Botter, “Water-energy-ecosystem nexus in small run-of-river hydropower: Optimal design and policy,” *Appl. Energy*, vol. 280, p. 115936, 2020.
[112] J. P. S. Catalão, H. M. I. Pousinho, and V. M. F. Mendes, “Scheduling of head-dependent cascaded hydro systems: Mixed-integer quadratic programming approach,” *Energy Convers. Manag.*, vol. 51, no. 3, pp. 524–530, 2010.

[113] J. L. Gordon, “Hydraulic turbine efficiency,” *Can. J. Civ. Eng.*, vol. 28, no. 2, pp. 238–253, 2001.
[114] M. Mohanpurkar, Y. Luo, R. Hovsapian, E. Muljadi, V. Gevorgian, and V. Koritarov, “Novel Control Strategy for Multiple Run-of-the-River Hydro Power Plants to Provide Grid Ancillary Services,” in *Hydrovision 2017*, 2017.
[115] D. Li, W. Wan, and J. Zhao, “Optimizing environmental flow operations based on explicit quantification of IHA parameters,” *J. Hydrol.*, vol. 563, pp. 510–522, 2018.
[116] S. Mishra, S. K. Singal, and D. K. Khatod, “Optimal installation of small hydropower plant—A review,” *Renew. Sustain. Energy Rev.*, vol. 15, no. 8, pp. 3862–3869, 2011.
[117] O. Paish, “Small hydro power: technology and current status,” *Renew. Sustain. Energy Rev.*, vol. 6, no. 6, pp. 537–556, 2002.
[118] D. K. Okot, “Review of small hydropower technology,” *Renewable and Sustainable Energy Reviews*. 2013.
[119] V. Dadu, A. Dadu, D. Frunza, G. Catarig, F. Popa, and B. Popa, “Innovative Concepts Applied to Recent Small Hydropower Plants,” in *Energy Procedia*, 2017.
[120] D. Anderson, H. Moggridge, P. Warren, and J. Shucksmith, “The impacts of ‘run-of-river’ hydropower on the physical and ecological condition of rivers,” *Water Environ. J.*, vol. 29, no. 2, pp. 268–276, Jun. 2015.
[121] B. T. Smith, H. I. Jager, and P. March, “Prospects for combining energy and environmental objectives in hydropower optimization,” *Waterpower XI*, 2007.
[122] R. Shan, C. Sasthav, X. Wang, and L. M. M. Lima, “Complementary relationship between small-hydropower and increasing penetration of solar photovoltaics: Evidence from CAISO,” *Renew. Energy*, vol. 155, 2020.
[123] I. Fantin-Cruz, O. Pedrollo, P. Girard, P. Zeilhofer, and S. K. Hamilton, “Effects of a diversion hydropower facility on the hydrological regime of the Correntes River, a tributary to the Pantanal floodplain, Brazil,” *J. Hydrol.*, vol. 531, pp. 810–820, 2015.
[124] R. Marcé, E. Moreno-Ostos, J. M. García-Barcina, and J. Armengol, “Tailoring dam structures to water quality predictions in new reservoir projects: Assisting decision-making using numerical modeling,” *J. Environ. Manage.*, vol. 91, no. 6, pp. 1255–1267, 2010.
[125] J. Garrido, Á. Zafra, and F. Vázquez, “Object oriented modelling and simulation of hydropower plants with run-of-river scheme: A new simulation tool,” *Simul. Model. Pract. Theory*, vol. 17, no. 10, pp. 1748–1767, 2009.
[126] “U.S. Department of Energy Announces Groundbreaking Hydro Prize Winners,” *Office of Energy Efficiency and Renewable Energy*, 2021. [Online]. Available: https://www.energy.gov/eere/water/articles/us-department-energy-announces-groundbreaking-hydro-prize-winners. [Accessed: 25-Sep-2021].
[127] J. Chen and A. Engeda, “Design considerations for an ultra-low-head Kaplan turbine system,” *IOP Conf. Ser. Earth Environ. Sci.*, vol. 240, no. 4, 2019.
[128] Q. Fen, K. Zhang, and B. Smith, *Small Hydropower Cost Reference Model*, no.

October. 2012.
[129] J. Therrien and G. Bourgeois, “Fish Passage at Small Hydro Sites,” Quebec City, 2000.
[130] T. Linnansaari, B. Wallace, R. A. Curry, and G. Yamazaki, “Fish Passage in Large Rivers: A Literature Review,” 2015.
[131] M. E. Caisley, F. A. Bombardelli, and M. H. Garcia, “Hydraulic Model Study of a Canoe Chute for Low-head Dams in Illinois (HES 63),” 1999.
[132] R. E. Horton, “Weir Experiments , Coefficients , and Formulas,” Washington D.C., 1907.
[133] G. M. Kondolf *et al.*, “Sustainable sediment management in reservoirs and regulated rivers: Experiences from five continents,” *Earth’s Futur.*, vol. 2, no. 5, pp. 256–280, May 2014.
[134] S. A. P. Dowda, “A System Dynamics Approach to Sediment Management at Small Hydropower Facilities,” no. May, 2020.
[135] S. V Amaral, S. M. Watson, A. D. Schneider, J. Rackovan, and A. Baumgartner, “Improving survival: injury and mortality of fish struck by blades with slanted, blunt leading edges,” *J. Ecohydraulics*, vol. 5, no. 2, pp. 175–183, Jul. 2020.
[136] “Fish Protection at Water Diversions: A Guide for Planning and Designing Fish Exclusion Facilities,” Denver, Colorado, 2006.
[137] A. M. Siyam, “Reservoir sedimentation control.” University of Bristol, 2000.
[138] “REST Web Services,” *U.S. Geological Survey*, 2021. [Online]. Available: https://waterservices.usgs.gov/rest/. [Accessed: 25-Sep-2021].
[139] M. Mallen-Cooper and I. G. Stuart, “Optimising Denil fishways for passage of small and large fishes,” *Fish. Manag. Ecol.*, vol. 14, no. 1, pp. 61–71, Feb. 2007.
[140] C. Katopodis, L. Cai, and D. Johnson, “Sturgeon survival: The role of swimming performance and fish passage research,” *Fisheries Research*, vol. 212. pp. 162–171, 2019.
[141] R. A. Wurbs, *Modeling and Analysis of Reservoir System Operations*. Upper Saddle River, NJ: Prentice Hall Inc., 1996.
[142] J. I. Pérez-Díaz, J. R. Wilhelmi, and J. Á. Sánchez-Fernández, “Short-term operation scheduling of a hydropower plant in the day-ahead electricity market,” *Electr. Power Syst. Res.*, vol. 80, no. 12, pp. 1535–1542, 2010.
[143] J. G. Williams, G. Armstrong, C. Katopodis, M. Larinier, and F. Travade, “Thinking like a fish: A key ingredient for development of effective fish passage facilities at river obstructions,” *River Res. Appl.*, vol. 28, no. 4, pp. 407–417, 2012.
[144] M. Larinier, “Dams and fish migration,” *World Comm. Dams, Toulouse, Fr.*, 2000.
[145] F. J. Bravo-Córdoba, F. J. Sanz-Ronda, J. Ruiz-Legazpi, L. Fernandes Celestino, and S. Makrakis, “Fishway with two entrance branches: Understanding its performance for potamodromous Mediterranean barbels,” *Fish. Manag. Ecol.*, vol. 25, no. 1, pp. 12–21, Feb. 2018.
[146] F. J. Magilligan, M. O. Roberts, M. Marti, and C. E. Renshaw, “The impact of run-of-river dams on sediment longitudinal connectivity and downstream channel equilibrium,” *Geomorphology*, p. 107568, 2020.
[147] A. J. Pearson and J. Pizzuto, “Bedload transport over run-of-river dams, Delaware,

U.S.A.," *Geomorphology*, vol. 248, pp. 382–395, 2015.
[148] G. Tan *et al.*, "Review and improvement of conventional models for reservoir sediment trapping efficiency," *Heliyon*, vol. 5, no. 9, pp. e02458–e02458, Sep. 2019.
[149] M. A. Eizel-Din *et al.*, "Trap efficiency of reservoirs on the Nile River," *River Flow 2010*, pp. 1111–1118, 2010.
[150] N. M. T. K. Revel, L. P. G. R. Ranasiri, R. M. C. R. K. Rathnayake, and K. P. P. Pathirana, "Estimation of Sediment Trap Efficiency in Reservoirs - an Experimental Study," *Eng. J. Inst. Eng. Sri Lanka*, vol. 48, no. 2, p. 43, 2015.
[151] S. E. Lewis *et al.*, "Calculating sediment trapping efficiencies for reservoirs in tropical settings: A case study from the Burdekin Falls Dam, NE Australia," *Water Resour. Res.*, vol. 49, no. 2, pp. 1017–1029, 2013.
[152] P. Lawrence and A. Lo Cascio, "Sedimentation in small dams: Hydrology and drawdown computations," *HR Wallingford*, vol. OD TN 119, no. Rev 0.0, 2004.
[153] T. Sawunyama, A. Senzanje, and A. Mhizha, "Estimation of small reservoir storage capacities in Limpopo River Basin using geographical information systems (GIS) and remotely sensed surface areas: Case of Mzingwane catchment," *Phys. Chem. Earth*, vol. 31, no. 15–16, pp. 935–943, 2006.
[154] M. Elhakeem, A. N. T. Papanicolaou, and A. G. Tsakiris, "A probabilistic model for sediment entrainment: The role of bed irregularity," *Int. J. Sediment Res.*, vol. 32, no. 2, pp. 137–148, 2017.
[155] W. R. Brownlie, "Flow Depth in Sand-Bed Channels," *J. Hydraul. Eng.*, vol. 109, no. 7, pp. 959–990, Jul. 1983.
[156] P. Klingeman, "Analysis Techniques: Flood Frequency Analysis," *Oregon State University*, 2005. [Online]. Available: https://streamflow.engr.oregonstate.edu/analysis/floodfreq/#log. [Accessed: 03-Mar-2022].
[157] "Guidelines for determining flood flow frequency." US Geological Survey Hydrology Subcommittee, Reston, VA, 1982.
[158] G. Oladosu and C. Sasthav, "Hydropower Capital and O&M Costs: An Exploration of the FERC Form 1 Data," Oak Ridge, TN, 2022.
[159] U. S. G. Survey, "National Hydrography Dataset." U.S. Dept. of the Interior, Reston, VA, 2004.
[160] "National Inventory of Dams," *US Army Corps of Engineers*, 2021. [Online]. Available: https://nid.usace.army.mil/ords/f?p=105:1::::::
[161] H. G. Heinemann, "A new sediment trap efficiency curve for small reservoirs," *J. Am. Water Resour. Assoc.*, vol. 17, no. 5, pp. 825–830, Oct. 1981.
[162] A. L. Weaver, M. T. Fisher, B. T. Bosher, M. L. Claud, and L. J. Koth, "Boshers Dam Vertical Slot Fishway: A Useful Tool to Evaluate American Shad Recovery Efforts in the Upper James River," in *American Fisheries Society Symposium*, 2003, pp. 339–347.
[163] S. Eyler, S. A. Welsh, D. R. Smith, and M. Rockey, "Downstream passage and impact of turbine shutdowns on survival of silver American Eels at five hydroelectric dams on the Shenandoah River," *Trans. Am. Fish. Soc.*, vol. 145, no.

5, pp. 964–976, 2016.
[164] Alternate Hydro Energy Centre, “Guidelines for Selection of Turbine and Governing System for Hydroelectric Project,” Alternate Hydro Energy Centre, 2008.
[165] B. M. Pracheil, C. R. DeRolph, M. P. Schramm, and M. S. Bevelhimer, “A fish-eye view of riverine hydropower systems: the current understanding of the biological response to turbine passage,” *Rev. Fish Biol. Fish.*, vol. 26, no. 2, pp. 153–167, 2016.
[166] G. Allen, S. Amaral, and J. Black, “Fish Protection Technologies: The US Experience BT - Operational and Environmental Consequences of Large Industrial Cooling Water Systems,” S. Rajagopal, H. A. Jenner, and V. P. Venugopalan, Eds. Boston, MA: Springer US, 2012, pp. 371–390.
[167] S. V Amaral, B. S. Coleman, J. L. Rackovan, K. Withers, and B. Mater, “Survival of fish passing downstream at a small hydropower facility,” *Mar. Freshw. Res.*, vol. 69, no. 12, pp. 1870–1881, 2018.
[168] (U.S. Fish and Wildlife Service) USFWS, “Fish Passage Engineering Design Criteria,” Hadley, Massachusetts, 2017.
[169] “Climate and Average Weather Year Round in Richmond Virginia, United States,” *Weather Spark*, 2022. [Online]. Available: https://weatherspark.com/y/20906/Average-Weather-in-Richmond-Virginia-United-States-Year-Round#:~:text=The time of year with,temperature of 78°F.
[170] P. Virtanen *et al.*, “SciPy 1.0: Fundamental Algorithms for Scientific Computing in Python,” *Nat. Methods*, vol. 17, pp. 261–272, 2020.
[171] “Modular and Scalable Downstream Passage for Silver American Eel,” *Alden Laboratory*, 2021. [Online]. Available: https://www.aldenlab.com/projects/doe-downstream-fish-passage-american-eel. [Accessed: 25-Sep-2021].
[172] “The Passage Portal,” *Whooshh Innovations*, 2021. [Online]. Available: https://www.whooshh.com/Our-Innovations/Products/Systems/Fish-Passage/Passage-Portal. [Accessed: 25-Sep-2021].
[173] “Kynard Alternating Side Baffle Fish Ladder,” *BK-Riverfish*, 2021. [Online]. Available: https://bkriverfish.com/products/. [Accessed: 25-Sep-2021].
[174] C. DeRolph, M. Bevelhimer, and A. Witt, “SMH Explorer Stream Network Attributes.” Oak Ridge National Laboratory (ORNL), Oak Ridge, TN, 2019.
[175] *Guidelines for Design of Intakes for Hydropower Plants*. American Society of Cvil Engineering (ASCE) Committee on Hydropower Intakes, 1995.

APPENDIX

Additional Figures

Table 23. Dynamic module design variables summary.

Module Class	Design Variable	Intermediate Variables
Non-overflow	Normal operating level	Volume
Foundation	Depth	Volume
Recreation	Mean annual flow Normal operating level	Number of steps
Fish Passage	Mean annual flow Normal operating level	Number of steps
Water Passage	Normal operating level	
Sediment	Mean annual flow	

Table 24. Assumed shear stress coefficients from Elhakeem [154] that are used in the calculation of maximum critical shear stress.

Coefficient	Description	Fine	Coarse
n	Number of particles defining the thickness of the active layer	5	3
C	Volumetric fraction of sediment particles in the active layer	0.6	0.4
a	Constant describing the dynamic fraction angle of sand and gravel (between 0.8 and 1.4)	0.94	0.94
R_r	Relative roughness, or the ratio of mobile particles to bed particles	1	1.5

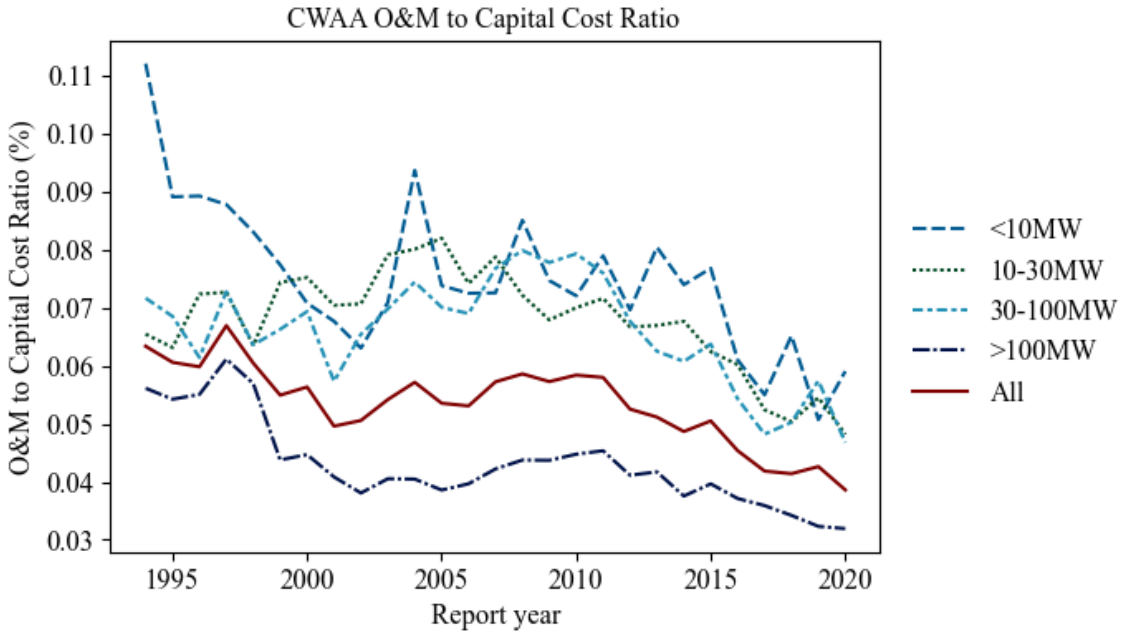

Figure 50. Capacity weighted annual average ratio of operating and maintenance costs to capital costs for FERC regulated hydropower plants by size class.

Table 25. Sediment sluice gate operating flows for each entrainment probability at each reference site.

Probability	Sluice gate operating flow		
	Deerfield	Housatonic	Schuylkill
50%	16044	7754	13343
45%	13570	6774	11975
40%	11251	5974	10692
35%	9188	5155	9472
30%	7267	4363	8292
25%	5642	3583	7131
20%	4256	2837	5882
15%	3065	1989	4704
10%	2030	1273	3554
5%	1107	660	2352
Baseline probability for 6774cfs	28.50%	44.65%	23.465

Table 26. Bosher dam average monthly daylight and temperature conditions via Weather Spark [169].

Month	Hours of Daylight	Daily Average Water Temperature (F)	Daily Average Temperature	Water + Air Temperature
Jan	9.9	43	37	80
Feb	10.8	41	40	81
Mar	12	45	48	93
Apr	13.2	54	58	112
May	14.2	63	66	129
Jun	14.7	72	75	147
Jul	14.4	77	78	155
Aug	13.5	78	76	154
Sep	12.4	74	70	144
Oct	11.2	66	59	125
Nov	10.1	56	49	105
Dec	9.6	49	41	90
Avg	12.2	59.8	58.1	117.9

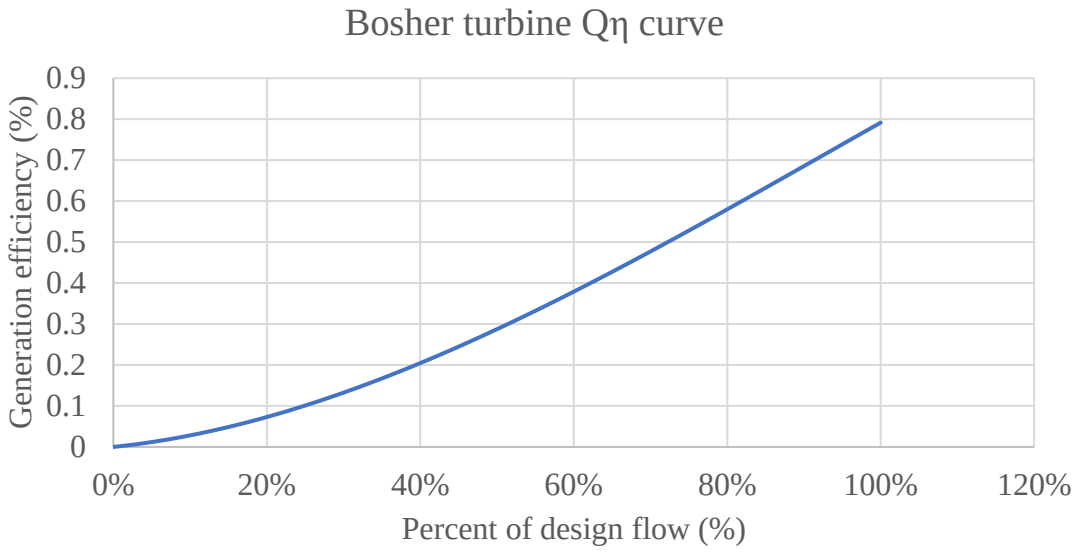

Figure 51. Bosher turbine flow efficiency product curve.

Table 27. Summary of 0.75in fish screen head loss calculations and assumptions.

Metric	**Value**	**Method**
Design flow	4480cfs	Based on total turbine design flow.
Fractional open area	0.5	Given in engineering drawings.
Design approach velocity	2ft/s	Given in engineering drawings.
Screen height	10ft	Given in engineering drawings.
Head loss coefficient	0.975	Assumed based on the approach velocity.
Design flow-through velocity	4ft/s	Approach velocity divided by the fractional open area.
Screen area	2240ft^2	A = Q/V (Area equals the design flow divided by the approach velocity).
Screen width	224ft	W = A/H (width equals the area divided by the height).
Estimated design head loss	0.243ft	Based on Equation 31.

Additional Models and Methods

Custom Genetic Algorithm

Following the discussion in the Solution Methods section, two methods were evaluated for optimal selection of modules. The goal of this optimization problem is to select the number of modules for each module class in the module library that optimizes the selected objective metric, like LCOE and NPV. The enumeration method was created to iterate through small design spaces, like those in the case studies, while a custom genetic algorithm was created for large design species. Genetic algorithms (GAs) are heuristic optimization methods based on evolutionary principles. These algorithms do not guarantee optimality but can efficiently search the design space for complex problems. A custom GA was selected because it works by interchanging bits within a bit string, like interchanging modules within an SMH facility. The GA was created from scratch in Python rather than using a pre-built package to better flexibility in its construction and evolution processes.

Figure 52 describes the overall process flow for the GA. The GA starts by creating a random population of possible solutions where each solution is called an individual. The random facilities are created by randomly selecting at least one of each of the required modules (spillway, non-overflow, and foundation) and one or more passage modules. The initial maximum on the number of each passage module class defaults to 20 modules unless otherwise specified. Then each facility is simulated using the system of models to calculate the objective function value. LCOE is often the best choice for the objective function because it captures initial and annual costs/benefits without energy price assumptions. The objective function value for each facility is ranked accordingly. Then the rankings are used to evolve the population of facilities to create a new set of individuals. Several functions were created to facilitate the evolution process:

- Keep fittest – The top solutions are copied between populations without change.
- Mutation – A random sample of the current population is altered between populations. For each selected facility, a random number of modules within the facility are either duplicated, removed, or redesigned to a new design variable if the module is dynamic.
- Crossover – A random sample of modules from one of the fittest solutions is transferred to another module from the population.
- Randomized – A new random facility is added to the new population.

The user can set the number of each process that occurs during evolution. Once the new population is created, the process iterates again to simulate, rank, and evolve the population. The process ends after a user-specified number of iterations. Constraints are incorporated through a penalty function that impacts the objective function if a constraint is not met. Further research is needed to test solution times, estimate optimality, and understand the most effective number of iterations and evolution processes.

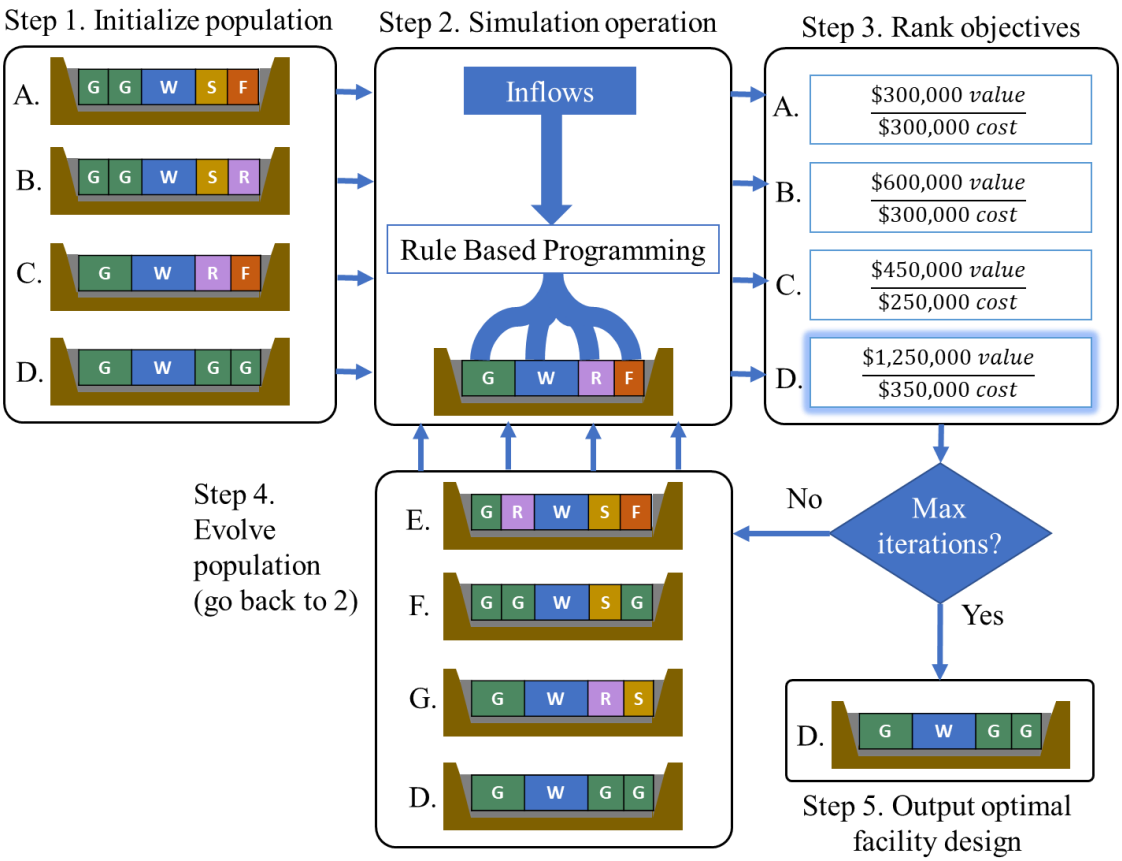

Figure 52. Illustration of genetic algorithm procedure for module selection and evolution

Regression Analysis

Throughout the model, relationships are needed to describe trends in data. For example, stage-discharge data must be turned into a stage-discharge equation for the tailwater elevation model. Additionally, equations are used to describe the outputs of the sensitivity analyses in the case studies. As such, a standardized method of conducting linear regressions was created using tools from Python. The goal of this process was to identify the least complex equation that best matched any exhibited trends in the data. The parameters and methods may have differed slightly based on the use case, but the general process for regressing data is described in this section.

The first step was to identify and remove outliers in the data. A z-score was calculated to determine the number of standard deviations away from the mean for each data point, and any value with a z-score greater than three was considered an outlier. Then, linear regressions were conducted for the equation forms shown in Table 28, listed from top to bottom in increasing polynomial order. The *curve_fit* function from the *scipy* package in Python was used to conduct non-linear least-squares regression of the data [170]. If the resulting regression obtained an R^2 value greater than a specific threshold (0.97 by default), the process returned the regressed equation. This threshold ensured that the least order equation that provided a reasonable fit would be output rather than the highest order equation, which may overfit the data.

A separate but similar process was used for piecewise stage-discharge equations, like in Figure 11 and Figure 38, which had distinct shapes for low-flow and high-flow periods. First, a reference point was visually selected to delineate the transition between the piecewise curves. Second, the data was separated, and linear regression was run on both sides to determine the general equation forms. Third, for power curves with three variables (*a*, *b*, and *c* per Table 28), the constant *c* was selected based on either the minimum data value or the reference point depending on whether the power curve was on the high flow or low flow portion. Fourth, models were set up to calculate the R^2 value for the high flow and low flow portions based on the *a* and *b* coefficients. The coefficient (*a*) was calculated so that for different exponents (*b*) the equation equaled the reference point at the corresponding flow value. Finally, a goal seek optimization was conducted on the exponents (*b*) to minimize the resulting R^2 value of the equation form. The resulting equations created a smooth piecewise curve with R^2 values greater than 0.99 for all curves. This process could be improved by optimizing the reference point or using pre-packaged piecewise regression models, but this process accomplished the desired results quickly and effectively for the small number of stage-discharge curves included in this study.

Table 28. Equation forms available in the waterSHED model.

Equation Type	**Form**
Constant	$y = a$
Linear	$y = ax + b$
Power	$y = ax^b + c$
Polynomial-2	$y = ax^2 + bx + c$

Flood Frequency Analysis

Flood frequency analysis interpolates the flood return period flows using historical peak flow data. The following methodology was used to determine the number of spillway modules needed for the sites in Case Study A and is a functionality within the waterSHED tool. The methodology and assumptions are based on the Case Study Report [17], which designed the Deerfield site to pass a 10-year flood flow and be safely overtopped by a 100-year flood flow. The methodology was adapted from the Oregon State University streamflow evaluations online toolkit [156] as recommended by USGS Bulletin 17B [157].

The annual peak streamflow data was gathered from USGS's National Water Information System, which has data for over 29,000 sites in the US [138]. The peak flows were fit to a Log-Pearson Type III distribution, as shown in Equation 32. In the following formulation, the set of flows (x) is a set of N flows indexed by n. The flows are transformed into log space, and then the mean and standard deviation (described below) are used along with an empirically derived frequency factor to form the distribution. The frequency factor (K) is determined from a discrete table of values [156] based on the skewness coefficient (shown below as C_s) and the flood return period (T_{return}), which is the estimated number of years between flood events of a given size. The table only provides return periods of 1, 2, 5, 10, 25, 50, 100, and 200 years, so linear interpolation was used to determine flood return periods for flows between these years. This allows the model to approximate the flood return period of a spillway design flow. Example results of the flood frequency analysis for the Schuylkill reference site are illustrated in Figure 53. The linear interpolation may introduce error into the process, but the 10-year and 100-year flood flows are the primary benchmarks for the case studies. The method could be improved by creating continuous models for the frequency factor and selecting the distribution type based on hydrologic regions, but this served as a sufficient approximation for this study.

Log-Pearson Type III Distribution

$$\log(x) = \overline{\log(x)} + K\sigma_{logx} \qquad \text{Equation 32}$$

Mean

$$\overline{\log(x)} = \frac{\sum_n^N \log(x_n)}{N}$$

Standard deviation

$$\sigma_{logx} = \sqrt{\sum_n^N \frac{\left(\log(x_n) - \overline{\log(x)}\right)^2}{N-1}}$$

Frequency factor

$$K = f(C_s, T_{return})$$

Skewness coefficient

$$C_s = \frac{N\sum_n^N \left(\log(x_n) - \overline{\log(x)}\right)^3}{(N-1)(N-2)\left(\sigma_{logx}\right)^3}$$

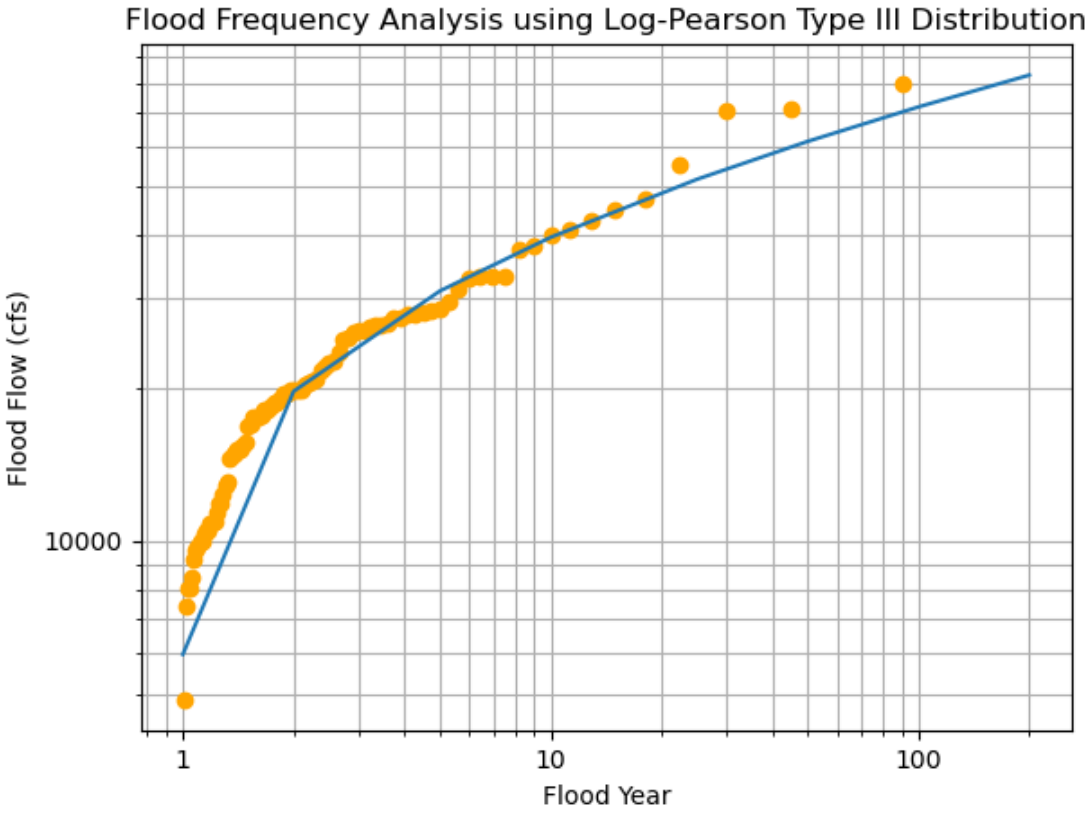

Figure 53. Example results of the flood frequency analysis for the Schuylkill sites.

Object-Oriented Class Attribute Definitions

The following sections present the definitions and descriptions of the classes and class attributes for the object-oriented framework for modular hydropower design. This can serve as a glossary for the variables within the system of models. Each attribute has a definition, and, if needed, they also have additional descriptions, units, and variable notations. The classes are categorized in a module class section and a simulation class section. The module classes include the Foundation, Non-overflow, Generation, Water Passage, Sediment, Fish Passage, Recreation, and Screen classes. The simulation classes include the Site, Cost Table, Preference, and Species classes.

Module Classes

SMH modules are technologies that can be placed within an SMH facility. The structure of the module classes employs properties of inheritance as illustrated in Figure 8. The SMH Module class is the overarching parent class for all modules and includes the following five attributes that are common across all the child module classes.

- ***Name*** – The name used to identify the module in figures.
- ***Capital cost*** – The capital cost for a module should include all fixed, one-time costs to prepare a module for operation. These can include material, equipment, installation, transportation, etc. ($C_{cap,m}$ - $)
- ***Annual operating cost*** – The annual operating costs for a module are the annualized expected costs for maintaining and operating the module. ($C_{op,m}$ - $/year)
- ***Width*** – The module dimension along the dam axis from bank to bank, perpendicular to streamflow. (Y_m - ft)
- ***Length*** – The module dimension parallel to streamflow. (X_m - ft)

There are two classes, Foundation and Non-overflow modules, that are direct inheritors of the SMH module class and only contain these attributes, although they are treated differently in the model. **Foundation modules** connect modules to the streambed, providing structural support, watertight seals, and safe operation of the facility. Modular foundations for hydropower are currently in early innovation stages [126] but could include technologies like precast concrete and anchored floating powerhouses [40]. The number of foundation modules is based on the facility footprint (total facility footprint divided by the foundation module area). Foundation costs can also be set via the additional capital cost, additional non-capital cost, and excavation rate attributes in the Cost Table object.

Non-overflow modules inhibit the flow of water past the facility. These modules are analogous to conventional dams, which are typically custom-designed for each site using earthfill, rockfill, or concrete designs [40]. Innovative modular technologies could include pre-cast concrete structures shipped to the site to reduce construction time and costs. The number of non-overflow modules is determined by dividing the open stream width (stream width minus the width of instream passage modules) by the width of one

non-overflow module. The Non-overflow module can also include the cost of abutments. However, low-head dams may not include non-overflow sections and instead create weirs or spillway structures that span the facility.

The **Passage Module class** is a subclass of the SMH Module class that can pass flow. The Passage Module class is inherited by the Generation, Water Passage, Aquatic Species Passage, Sediment Passage, and Recreation classes. Since these modules pass flow, they can interact with upstream and downstream fish passage and be parameterized by the metrics used in the fish passage models described in Chapter Three. However, the fish passage attributes are optional and not needed for simulation. As such, the Passage Module class has the following attributes:

- ***Design flow*** –The flow rate through the module at design conditions. The applications of the design flow differ slightly between Passage Module subclasses. For Generation modules, the design flow is the set point used to indicate the peak Qη flow and is used in the dispatch models. The generation modules can be operated at any flow between the minimum and maximum operating flow. For controlled or uncontrolled spillways, the design flow reflects the maximum design flood, where flows exceeding the design flood will be considered overflow. These spillway modules can be allocated any flow less than or equal to the design flow. For the other modules, the design flow represents the flow allocated to the module during operation. For the module to turn on, the flow available must exceed the design flow, and only the design flow can be allocated to the module. ($Q_{des,m}$ - cfs)
- ***Operating months*** – The months during which the module is on and is allocated flow. During the operating months, modules are modeled to operate continuously. (T_m - months)
- ***Instream or diversion*** – Instream modules will be placed along the dam axis and count towards the dam width. Diversion modules are placed on the banks in the facility schematic and can represent bypasses. This impacts the number of required non-overflow modules.
- ***Downstream guidance efficiency*** – The percentage of species individuals entrained in the flow allocated to the module safely excluded from flow into the module. A guidance efficiency of 0% means all fish that attempt to enter the module will enter, while an efficiency of 100% means that all fish will be excluded and guided to another structure. This metric is normally measured for fish guidance structures like bar racks and louvers and is parameterized for each species. The value depends on many factors, including species physiology, structure dimensions, and flow velocity. Efficiencies can vary between 0% to 100% depending on the technology. Modules without upstream fish guidance structures should assume a guidance efficiency of 0%. ($G_{m,s}$ - %)
- ***Downstream mortality rate*** – The percentage of species individuals killed or unable to reproduce after passage through the module. A mortality rate of 0% means that no fish that pass through the module are harmed, while a mortality rate of 100% means that no fish can safely pass. This metric is normally measured for turbines and

spillways and is parameterized by species. The value depends on many factors, including species physiology, technology dimensions (e.g., blade length), and flow characteristics. Rates can vary between 0% to 100% depending on the technology. ($M_{m,s}$ - %)

- ***Upstream entrance efficiency*** – The percentage of species individuals that can successfully enter the module after being attracted to the entrance. An entrance efficiency of 0% means that no fish can enter the module, while an entrance efficiency of 100% means that all fish can enter safely. This metric is normally measured for volitional fishways and is parameterized by species. The value depends on the swimming preferences of species of interest and the hydraulics of the entrance. Efficiencies can vary between 0% to 100% depending on the technology. ($E_{m,s}$ - %)
- ***Upstream passage efficiency*** – The percentage of species individuals that can successfully ascend the module after entering. A passage efficiency of 0% means that no fish can ascend, while a passage efficiency of 100% means that all fish can ascend safely. This metric is normally measured for volitional fishways and is parameterized by species. The value depends on the swimming preferences of the species of interest and the hydraulics of the passageways. Efficiencies can vary between 0% to 100% depending on the technology, although 100% passage rates can be difficult to achieve. Modules without species passage capabilities should assume an efficiency of 0%. ($P_{m,s}$ - %)

The following paragraphs specify the remaining class attributes for the module classes. **Recreation modules** provide a safe passageway for recreation crafts, such as boats, kayaks, and canoes. Recreation modules can provide social values to stakeholders and maintain connectivity between recreational areas. Examples of recreation modules include boat chutes [131] and the proposed whitewater park design in Case Study B. **Fish passage modules** facilitate the passage of aquatic species across the facility in upstream and downstream directions. The Fish Passage module class was designed with volitional fishways in mind because they are more common at low-head sites than non-volitional or trap-and-truck schemes that can be more expensive. These volitional technologies require continuous flows to attract species and create hydraulic conditions conducive to safe passage. Technical fishways, like Denil and vertical slot fishways, are often modular because they use repeatable series of pools, slots, and other structures to create the desired hydraulic conditions. Examples of innovative aquatic species passage modules include Alden Laboratory's modular Silver American Eel Passageway [171], Whooshh Innovation's Passage Portal [172], and BK-Riverfish's Kynard Alternating Side Baffle Fish Ladder [173].

The Recreation and Fish Passage module classes share similar module attributes but are treated differently in the performance models. For example, only recreation modules can provide recreation revenue during the calculation of annual benefits. The following parameters relate to the headwater and tailwater operating constraints, based on the Case Study Report [17]. At each timestep, the modules can only be operated if the headwater and tailwater levels meet these constraints. Depending on the technology, recreation

modules may require sufficient tailwater depths to provide safe drop-offs or sufficient headwater levels to provide safe hydraulics. Similarly, fish passage modules may require adequate head and tailwater levels to provide the desired entrance and exit hydraulics. For ease of input, the following headwater constraint attributes were parameterized in relation to the normal operating headwater level, while the tailwater constraint attributes were parameterized in relation to the bed elevation.

- ***Maximum headwater drop*** – The maximum decrease in headwater elevation with respect to the normal operating headwater level allowed during module operation. ($H_{head,min,m}$ – ft)
- ***Maximum headwater rise*** – The maximum increase in headwater elevation with respect to the normal operating headwater level allowed during module operation. ($H_{head,max,m}$ -ft)
- ***Minimum tailwater level*** – The minimum tailwater elevation required for module operation. ($H_{tail,min,m}$ -ft)
- ***Maximum tailwater level*** – The maximum tailwater elevation allowable for module operation. ($H_{tail,max,m}$ -ft)

Generation modules use flow to produce electrical power and include all the electro-mechanical equipment and water conveyance structures required to produce that power. Modular turbines are emerging as viable low-head options, although deployment is relatively limited in the US [16]. The following attributes were based on hydropower plant and turbine design manuals [89], [90], and the existing RHDM literature described in Table 4.

- ***Minimum operating flow*** – The minimum flow required to operate the module. ($Q_{min,m}$ – cfs)
- ***Maximum operating flow*** – The maximum flow that can be allocated to the module. If the turbine-overrun option is allowed, the excess flow will be allocated to increasing allocated flow above the design flow before spill allocation. The design flow acts as the maximum allocated flow if the turbine-overrun option is off. ($Q_{max,m}$ – cfs)
- ***Minimum operating head*** – The minimum gross head required to operate the module. ($H_{min,m}$ – ft)
- ***Design head*** – The gross head at which the module operates at peak efficiency. This is used with the head efficiency equation to calculate head turbine efficiency. ($H_{des,m}$ – ft)
- ***Maximum operating head*** – The maximum gross head allowable during module operation. ($H_{max,m}$ – ft)
- ***Flow efficiency equation*** – The power output efficiency coefficient as a function of the relative discharge, which is the flow allocated to the module divided by the design flow (i.e., design flow = 100%). This efficiency curve should include all loss

components along the powertrain, except for head losses. ($\eta_{Q,m}\left(\frac{Q_{m,t}}{Q_{des,m}}\right)$ - % as a function of %).

- ***Head efficiency equation*** – The power output efficiency coefficient as a function of the relative head, which is the gross head across the module divided by the design head (i.e., design head = 100%). ($\eta_{H,m}\left(\frac{H_t}{H_{des,m}}\right)$ - % as a function of %)
- ***Max power*** – The maximum possible power output of the unit. This value is used to calculate generation capacity factors and is used to cap power output during the simulation. If the calculated power output is higher than the designated max power during a given timestep, the output is set to the max power. This attribute is optional and can account for the capacity limitations of the generator or other electrical equipment. If an input is not given, the max power is set to the calculated power at the maximum operating head and flow. ($P_{max,m}$ – kW)
- ***Cost of start-stops*** – The attributed cost of damages for one ramping cycle of the turbine. A ramping cycle consists of turning the module on and off. Turbines often accumulate damage during these cycles as the flow rate passes through cavitation ranges. More frequent start/stops reduce the expected life of the turbine, which can increase maintenance costs. This attribute is optional and calculates turbine operating costs as a function of operation rather than as static annual module or annual plant O&M costs. ($C_{ss,m}$ – $/start-stop)

Water passage modules control or enable the flow of water from upstream to downstream. These modules can operate quite differently based on the operating mode attribute, which can be either continuous, uncontrolled spillway, or controlled spillway. Continuous operation resembles the operation of the recreation or fish passage modules where the module is either on or off and can only be allocated the design flow. This could reflect minimum flow bypasses or flows for aesthetic or water quality purposes. Uncontrolled spillways are parameterized by a weir coefficient and a crest height that controls the relationship between flow and headwater elevation, as described by Equation 2 in the Operational Models section. Controlled spillways can regulate the headwater level with different flow allocations, creating a constant headwater level. The uncontrolled and controlled spillways can be allocated flow up to the design flow, which reflects the maximum design flood. Weirs are a common example of uncontrolled spillways. Overshot and radial gates are common examples of controlled spillways. Each facility must have one type of spillway module and can only have one type of spillway module. The following Water Passage module attributes depend on the operation mode, with the crest height and weir coefficient only applying to uncontrolled spillway operation.

- ***Operating mode*** – The operating mode determines the flow allocation procedures and the effect of module flow on the headwater elevation. Water passage modules can operate in one of three modes:

    - Continuous: these modules pass a constant discharge during the simulation timestep.
    - Controlled Spillway: these modules can regulate the flow through the module to maintain a constant headwater elevation.
    - Uncontrolled Spillway: these modules pass flow but cannot actively regulate the headwater elevation (e.g., weirs).
- ***Weir coefficient*** – A constant based on the shape of the weir. This input is only required in uncontrolled spillway mode. (C_{spill} – $ft^{1/2}/s$)
- ***Crest height*** – The height of the top of the weir in reference to the bed elevation. The crest height should be equal to the normal operating level. (Z_{spill} – ft)

Sediment passage modules pass bedload and suspended load sediments through the facility. Like water passage modules, these modules can operate differently based on the operating mode attribute, which can be either continuous, sluicing, or flushing. Continuous sediment modules, also called bypasses, act like recreation or fish passage modules where the module is either on or off and can only be allocated the design flow. Examples include tunnels, siphons, and canals that use a continuous flow to divert sediments around the dam. Sluicing sediment modules are parameterized by an operating flow, which is the inflow threshold that must be met to allocate the design flow to the module. Low-level gates or outlets can sluice sediments using high velocity flows to pass sediment-laden water during high flow events. Flushing modules are parameterized by a flushing frequency and the flushing duration, which determine when flushing events occur in the simulation. During a flushing event, all flow is routed through the sediment module as the reservoir is drawn down to scour accumulated sediments. Various low-level outlets and gate designs, like slide gates, can be operated in flushing mode. For the following parameters, the operating mode is required, while the others can be optional depending on the operating mode.

- ***Operating mode*** – The operating mode determines the conditions under which the module is allocated flow. Sediment modules can be operated in one of three modes.
    - Continuous: these modules operate at consistent design flows throughout the operating months.
    - Sluicing: these modules operate whenever a designated inflow threshold is met.
    - Flushing: these modules are used for drawdown flushing during specified flushing events where the headpond level is decreased and sediment is passed through low-level outlets at high velocity.
- ***Operating flow*** – The minimum inflow threshold required to mobilize bed-load sediments and open the sluice gate. Sediment sluices will only be allocated flow if the total inflow is greater than the operating flow. This input is only used in the sluicing operating mode. ($Q_{op,m}$ – cfs)
- ***Flushing duration*** – The number of timesteps (days) required to flush the reservoir. This input is only required when the module operates in flushing mode. During

flushing events, all passage modules except for spillway and sediment modules are turned off. ($T_{dur,m}$ – days)

- ***Operating frequency*** – The number of flushing events per year. This input is only required when the module operates in flushing mode. During flushing events, all passage modules except for spillway and sediment modules are turned off. Flushing events occur at the first available time step and at equal intervals afterward. Flushing events outside of the simulation time are not considered. ($T_{freq,m}$ – flushes/year)

The **Screen class** represents technologies that are placed in series with SMH modules. Examples can include trash racks, fish exclusion screens, and booms. These technologies are typically designed to protect other technologies and species from damage by excluding them from the flow. The Screen class was not included in the SMH EDES [19] and is not a subclass of the SMH Module parent class. The Screen class required greater design flexibility than standardized modules since screen technologies are often sold by screen area rather than discrete modules. Thus, screens were created as a dynamic class, which provides several options for parameterizing the module. Screen objects can be created with constant attributes that do not change with the facility design or with attribute functions that change the costs and dimensions according to controlling variables like screen area and design flow. In addition to the following attributes, the Screen class also has the downstream guidance efficiency ($G_{m,s}$) and downstream mortality rate ($M_{m,s}$) attributes with the same definitions previously list for the Passage Modules class. The mortality rate can be used to factor in screen impingement; however, the mortality rate is currently applied after the guidance step. For example, a 10% mortality rate on an 80% guidance efficiency screen means that the 10% mortality rate only applies to the 20% of fish that make it through the screen. The Screen class has the following attributes:

- ***Name*** – The name used to identify the screen.
- ***Capital cost*** – The capital cost should include all fixed, one-time costs to prepare the screen for operation. These can include material, equipment, installation, transportation, etc. The capital cost can be constant or parameterized as a function of the total area or design flow. ($C_{cap,m}$ - $)
- ***Annual operating cost*** – The annual operating costs for a screen are the annualized expected costs for maintaining and operating the screen. The annual operating cost can be constant or parameterized as a function of the total area or design flow. ($C_{op,m}$ - $/year)
- ***Head loss equation*** – The equation that determines the total head loss to the covered modules as a function of either the active area (the submerged screen area times the fractional open area), the operating flow (the flow allocated to the covered modules), or a combination of both. ($H_{loss,m}$ - % as a function of ft^2 or cfs)
- ***Incline*** – The angle of the screen from horizontal in the streamwise direction. At a 90 degree incline, the module would be perpendicular to the streamwise direction, while

a 0-degree angle would be flat along the bed. The incline is used to determine the active area. ($X_{angle,m}$ - degrees)

- ***Height*** – The screen dimension in the vertical dimension to streamflow. This height can be constant or a function of the normal operating level. (Z_m – ft)
- ***Bottom elevation*** – The vertical distance from the bed to the bottom of the screen. This can account for raised screens and impact the active area. ($Z_{bot,m}$ - ft)
- ***Width*** – The module dimension along the dam axis from bank to bank, perpendicular to streamflow. The width can be constant or parameterized as a function of the stream width or the width of the covered modules. (Y_m - ft)
- ***Fraction open area*** – The percentage of the total screen area that flow can pass through (i.e., the total screen area minus the material area). ($A_{frac,m}$ - %)
- ***Covered modules*** – The set of SMH passage module objects in series with the screen. The design flow of the screen and other parameters will be determined by the number of covered modules in the facility. ($M_{covered,m}$ – set of module names)

Since the Screen is a dynamic module that resizes depending on the site conditions, several internal processes must redesign the screen before each simulation. The redesign process occurs once the facility is constructed but before operation. The following redesign steps only apply if the inputs are parameterized as functions and are not constant. First, the screen height is calculated based on the normal operating level and the provided height equation. Second, the screen width is calculated by summing the widths of covered modules in the facility, if necessary, and applying the provided width equation. In Case Study B, the width equation uses a screen angle of 40degrees to convert the module width to the screen width. Third, the total screen area is calculated by multiplying the screen height and width. Fourth, the design screen flow is calculated by summing the design flows of the covered modules. Finally, the capital and operating costs are calculated using the relative variables and equations.

Several processes are also conducted during the simulation to determine screen head losses based on the flow allocation. The head loss equation can be set as a function of the screen operating flow and or the active area. The operating flow is the flow through the screen and to the covered modules during a given time step. The active area is the total area of the flow passing through the screen, which can be calculated as the submerged screen area times the fractional open area. To calculate the active area, the model calculates the submerged screen height by subtracting the headwater elevation at the timestep by the bottom elevation and multiplying it by the sine of the incline ($Z_{submerged} = \sin(X_{angle,m}) \times (Z_{head,t} - Z_{bot,m})$). The active area then becomes a product of the submerged height, the screen width, and the fraction open area, which accounts for the width of the bars ($A_{active} = X_m Z_{submerged} A_{frac,m}$). Like the model in Equation 31 used in Case Study B, this allows the head loss to be calculated according to the velocity through the screen.

Simulation Classes

The simulation classes include all the additional variables needed to characterize the project. These include the Site, Cost Table, Preferences, and Species classes. The following paragraphs describe the attributes of each class.

The **Site class** is the collection of hydrologic and hydraulic characteristics describing the stream reach of interest. Sites can be found using the SHM explorer tool [174] and the NPD DamCAT tool [10]. Information to inform the following attributes can be found using public GIS tools and USGS databases [138], [159].

- ***Stream width*** – The distance between the left and right banks along the dam axis at the height corresponding to the defined normal operating level. This value is used as a minimum for the total width of instream modules. (Y_{river} – ft)
- ***Bed elevation*** – The bed elevation above mean sea level at the dam axis (used for graphics purposes). (Z_{bed} – ft amsl)
- ***Stream slope*** – The average stream slope of the stream-reach before development. This attribute is used in several places, including the sediment entrainment and reservoir volume model support tools. (S_{river} – ft/ft)
- ***Trap efficiency parameter*** – A dimensionless sedimentation factor (β) used with the Siyam [137] formulation of the Brune model to reflect the reduction in reservoir storage capacity due to sedimentation. A value of 1 resembles a mixer tank where all sediment is kept in suspension, while a value close to 0 resembles a desilting basin where all sediment falls out of suspension. Thus, smaller values indicate a greater likelihood of sedimentation, resulting from many factors like larger sediment sizes. The original Brune curve illustrated upper, median, and lower curves with values of 0.0055, 0.0079, and 0.015, respectively [68]. (β – unitless)
- ***Inflows*** – The mean daily discharge time series data used as facility inflows during the simulation. These can be historical data from stream gages, modified historical data, or predicted future flows. ($Q_{in,t}$ – cfs)
- ***Peak flood flows*** – The time series of peak flood events used in the flood frequency analysis to calculate the spillway design flood flow return period. The flood frequency analysis procedure is described in the Flood Frequency Analysis section. ($Q_{flood,t}$ – cfs)
- ***Stage-discharge equation*** – The tailwater depth as a function of inflow. Stage-discharge data from the site can be regressed into a stage-discharge equation, assuming that the tailwater maintains similar hydraulic characteristics before and after development. ($Z_{stage}(Q)$– ft as a function of cfs)
- ***Stage-storage equation*** – The reservoir volume as a function of the headwater elevation. This equation is used to calculate the sediment trapping efficiency. ($V_{res}(Z)$ – ft^3 as a function of ft)

The **Cost Table class** is the collection of parameters used to convert module performance into simulated cost and benefit outcomes. The cost model structure was based on

previous cost assessments of a reference SMH facility but was designed to be flexible for different use cases. The use of these inputs is described in the Economic Models section. Some of the following attributes are optional and depend on the allocation of costs across modules. For example, foundation costs can be attributed to foundation modules or integrated into the excavation costs attribute. In addition, several attributes can be incorporated as fixed values or as a percentage of the initial cost of capital (ICC).

- ***Energy price*** – The average price of energy per MWh. The energy price determines the generation revenue and is assumed constant throughout the simulation to reflect a constant PPA price. (R_{kwh}- \$/MWh)
- ***Additional capital costs*** – The one-time, fixed expenses incurred on capital assets that are not covered by the module capital costs. This can be used to include the costs for buildings, property, electrical equipment, etc., that do retain value after commissioning. This cost category is included in the ICC calculation. (C_{cap}- \$)
- ***Additional non-capital costs*** – The one-time expenses incurred during the development process that do not involve capital assets. This can include the costs for the care of water, parking, recreational features, etc., that do not retain value after commissioning. This cost category is not included in the ICC calculation. (C_{non}- \$)
- ***Excavation rate*** – The cost to excavate overburden material as a function of the dam foundation area. This is one option for pricing excavation. The cost to excavate is this value times the total area of all modules. (C_{exc}- \$/ft^2)
- ***Overhead cost*** – The cost of overhead activities such as licensing and administration. (C_{ov}- \$ or % of ICC)
- ***Engineering cost*** – The cost of engineering activities. (C_{eng}- \$ or % of ICC)
- ***Contingency allowance*** – The cost of unexpected expenditures. This can include costs from construction delays, material cost increases, and capital reserves. (C_{con}- \$ or % of ICC)
- ***Annual O&M cost*** – The annual cost to operate and maintain the facility. This is one option for including annual operating costs that are not incorporated into the module O&M costs. (C_{om}- \$ or % of ICC)
- ***Value of recreation*** – The revenue associated with each recreation module as a function of availability, which is the number of hours per year that recreation modules are on. (R_{rec}- \$/hr)
- ***Flood cost*** – The cost per unit of flow exceeding the facility's hydraulic capacity during a given timestep. Any flow exceeding the flow capacity of all modules will be called over-flow and incur a flood cost equal to this value times the excess flow. (C_{flood}- \$/cfs)
- ***Discount rate*** – The rate used to discount future cash flows and determine the present value of those cash flows. (d- %)
- ***Project life*** – The expected duration of project operation before plant retirement. This value is used in the calculation of the net present value. (T_{life}- years)

The **Preferences class** is the collection of design and simulation parameters used to evaluate the performance of a facility. The following attributes represent design choices about how the facility is tested and operated rather than the selection or design of modules.

- ***Normal operating headwater level*** – The headwater elevation with respect to the bed elevation at the dam axis that is maintained during normal operation. If the spillway is controlled, the headwater level is assumed constant at the normal operating level. If the spillway is uncontrolled, the crest height must be at least as high as the normal operating level, and any flow allocated to the spillway causes the headwater level to increase. (Z_{op} – ft)
- ***Test data start date*** – The start date for the simulation period within the inflow time series data. (T_{start} – date)
- ***Test data end date*** – The end date for the simulation period within the inflow time series data. The recommended length of the simulation is at least one year; however, all performance metrics are annualized, so running simulations with shorter or longer simulation times are possible. (T_{end} – date)
- ***Generation dispatch model*** – The method used to allocate flows across the generation modules. The four dispatch models are:
    - Design Ramping - turbines are ramped from smallest to largest. When flow is available, modules are ramped to the design flow before turning on the next module. This method is the fastest and is best used when peak efficiencies occur at the design flow.
    - Peak Ramping - turbines are ramped from smallest to largest. When flow is available, modules are ramped to the peak efficiency flow before ramping the next module. Once all modules are ramped to the peak efficiency, they are ramped to the design flow. If turbine overrun is allowed, they are also ramped to the max operating flow from smallest to largest. This method is similar in speed to the Design Ramping and should be used for turbines where the peak efficiency is not close to the design flow (e.g., Kaplan turbines).
    - Simple Greedy - a greedy algorithm is used to determine the distribution of flows across modules. As the turbines are ramped, the algorithm sequentially allocates the next unit of flow to the turbine with the largest increase in power output. This method should be used over the Design Ramping method when using modules of different sizes.
    - Advanced greedy - this method combines the Peak Ramping and Simple Greedy models. Modules are first ramped to the peak efficiency flow. Then flow is allocated to turn on modules if flow is available. Then a greedy algorithm allocates the remaining flow between turbines that are on. This method is most likely to find the optimal dispatch of modules but takes more time than the peak ramping approach, which has similar performance for most turbines.
- ***Allow turbine over-run***– This determines whether the generation modules can be allocated flow greater than the design flow when excess flow is available. If over-run

is allowed, all modules will first be allocated their design flow and then ramped up to their max flow if flow is available, depending on the dispatch model. This may allow the modules to generate more power but at lower efficiencies. If over-run is not allowed, the module cannot be allocated flow above the design flow.

- ***Spillway notch flow*** – The flow allocated to the spillway before passage module allocation that does not affect the headwater level. This value is optional and can represent cuts or notches in weirs or spillways. (Q_{notch} – cfs)
- ***Spillway minimum flow*** – The flow requirement for the spillway that must be met before passage module allocation. This value does affect the headwater level. This value is optional and can be used to meet minimum flow requirements, which are flows that must be passed downstream without passage through turbines. The value can be set as a constant flow or a percentage of the inflow. Any notch flows also count towards this minimum flow constraint. ($Q_{min,spill}$ – cfs)
- ***Operational priorities*** – This is module class priority ranking used to determine the order of modules in the rule curve. Module classes are ranked from 1 (highest priority) to 5 (lowest priority). As described in the Operational Models section, the modules with the highest priority are allocated flow first, and modules with lower priorities are then allocated flow if sufficient flow remains to turn on the module. Non-power module types within the same class are prioritized from smallest design flow (highest priority) to largest design flow (lowest priority). Generation modules are dispatched based on the selected dispatch model.

The **Species class** represents a species of interest in the fish passage performance models described in the Fish Models section. Fish passage systems are often designed with targeted species in mind, which have species-specific swimming behaviors, migratory patterns, and biomechanics. The fish passage performance models enable the calculation of cross-species metrics that average values for multiple species. This class is not required for simulation of the facility but is required to measure fish passage performance. Examples of common North American species found at small hydropower sites can be found in Table 1 in the International Energy Agency report on fish passage at small hydropower sites [129]. However, further study is needed to characterize the following attraction parameters for different species.

- ***Species name*** – The name used for species in calculations and figures.
- ***Relative discharge parameter*** – The coefficient used in the attraction efficiency function to set the relative discharge threshold required to prevent attraction efficiency losses. The higher the value, the higher the module flow must be to attract fish. The midpoint of the attraction efficiency curve is calculated by multiplying the relative discharge parameter by the attraction sensitivity parameter. For example, a relative discharge parameter of 0.2 and an attraction sensitivity parameter of 0.1 create a curve with close to 100% attraction at 3% relative discharge, a 50% attraction at 2% relative discharge, and close to 0% attraction at 1% relative discharge. (a_s – unitless)

- ***Attraction sensitivity parameter*** – The coefficient used in the attraction efficiency function to set the slope of the attraction efficiency function. Higher values tend to create steeper step functions so that smaller changes in relative discharge will lead to larger changes in attraction. The midpoint of the attraction efficiency curve is calculated by multiplying the relative discharge parameter by the attraction sensitivity parameter. For example, a relative discharge parameter of 0.2 and an attraction sensitivity parameter of 0.1 create a curve with close to 100% attraction at 3% relative discharge, a 50% attraction at 2% relative discharge, and close to 0% attraction at 1% relative discharge. (b_s – unitless)
- ***Upstream migration months*** – The months during which the species travels upstream across the facility (from tailwater to headwater). The upstream effective passage for the species is only calculated during these months. ($T_{up,s}$ – months)
- ***Downstream migration months*** – The months during which the species travels downstream across the facility (from headwater to tailwater). The downstream effective passage for the species is only calculated during these months. ($T_{down,s}$ – months)

Module Attributes

Case Study A

Table 29. Kaplan turbine module attribute determination.

Attribute	Generation module attribute
Name	Kaplan Turbine
Capital cost	Adapted from Fen, Zhang, and Smith [128], using the cost for dual regulated axial flow turbines with a fixed $50,000 to account for the variable component of the reference switchyard and interconnection costs. A scaling factor of 3.76 adjusts the module costs to match the Deerfield reference costs and accounts for inflation ($2010 to $2021) and additional non-electromechanical costs, such as gates, modular formwork, intakes, and outlets. In the equation below, P_m is the nominal power output at design head and flow and $H_{des,m}$ is the design head of the module. $$C_{cap,m} = (1536 H_{des,m}^{-0.193} P_m^{0.982} + 50{,}000) \times 3.76$$
Annual operating cost	Zero; included as part of the assumption that annual O&M costs are 6% initial cost of capital.
Width (dam-axis)	Following the Case Study Report [17], the width of the generation module is based on the expected turbine runner diameter. The diameter as a function of flow was estimated using a regression of 126 Kaplan turbines. The diameter equation from the Case Study Report [17] is adapted to provide the width in feet. The width of the module is assumed to be three times the size of the runner diameter. $$Diameter\ (ft) = 0.5\left(Q_{des,m} \times \left(\frac{0.0283 cms}{1 cfs}\right)\right)^{0.457} \times \left(\frac{1 ft}{0.3048 m}\right)$$ $$Y_m = 3 \times Diameter$$
Length (streamwise)	The same methodology for the module width (above) is used for the module length, except the length is assumed to be seven times the size of the runner diameter. $$X_m = 7 \times Diameter$$
Design flow	Varied during optimization; the baseline design flow is 338cfs per the optimal design in the Case Study Report [17].
Operating months	Assumed to be operated during all months.
Instream or Diversion	Assumed to be an instream module.
Minimum operating flow	Based on the Guidelines for Selection of Turbine and Governing System for Hydroelectric Project report [164]. $$Q_{min,m} = 0.40 \times Q_{des,m}$$

Table 29 continued.

Attribute	Generation module attribute
Maximum operating flow	Based on the Guidelines for Selection of Turbine and Governing System for Hydroelectric Project [164]. Generation modules are only operated above the design flow when turbine over-run is allowed. $$Q_{max,m} = 1.05 \times Q_{des,m}$$
Minimum operating head	Based on the "Propeller – Adjustable blade turbine" from Table 1.1 in the Guidelines for Selection of Turbine and Governing System for Hydroelectric Project [164]. $$H_{min,m} = 0.65 \times H_{des,m}$$
Design head	Varied during optimization; The baseline design head is 10.4ft for the Deerfield, Housatonic, and Schuylkill sites. This value was selected in the Case Study Report [17] as 95% of the gross head at the Q_{50}.
Flow efficiency curve	Gordon [113] provides empirical models for efficiency curves of common hydraulic turbine designs. The general form used for the Kaplan turbines (shown below) uses two separate functions for curves before the design flow and after the design flow. The equation is parameterized by the speed-no-load flow (Q_{snl}), the peak efficiency flow (Q_{peak}), and the peak efficiency (E_{peak}) along with empirical coefficients. $$\eta_Q(Q) = \begin{cases} E_{peak} - E_{peak}\left(1 - \frac{Q_{snl}}{Q_{peak}}\right)^{-k}\left(1 - \frac{Q}{Q_{peak}}\right)^{k}; Q < Q_{peak} \\ E_{peak} - \left(\frac{Q}{Q_{peak}} - 1\right)^{1.5}; Q \geq Q_{peak} \end{cases}$$ The Case Study Report [17] used this model and assumptions about the speed and diameter relationships to generate an efficiency curve. However, this method resulted in low design efficiencies for low-head turbines. The method was adapted to form the following piecewise equation with several assumptions about the efficiency breakpoints and adjusting it to be a function of relative discharge. The speed-no-load flow is assumed to occur at 20% of the design flow and the peak efficiency flow at 80% [113]. The parameter k accounts for the age of the turbines, so it was assumed to be 7.2, which is reflective of new turbines. Finally, the peak efficiency was assumed to be 83%, similar to the Case Study Report [17] calculation and on the higher end of low-head turbine efficiencies, which typically range from 70-85%. Simplifying the previous form creates the following model. $$\eta_{Q,m}\left(\frac{Q_{m,t}}{Q_{des,m}}\right) = \begin{cases} 0.83 - 6.65(1 - 1.25x)^{7.2}; x < 0.8 \\ 0.83 - (1.25x - 1)^{1.5}; x \geq 0.8 \end{cases}$$

Table 29 continued.

Attribute	Generation module attribute
Maximum operating head	Based on the "Propeller – Adjustable blade turbine" from Table 1.1 in the Guidelines for Selection of Turbine and Governing System for Hydroelectric Project [164]. $$H_{max,m} = 1.25 \times H_{des,m}$$
Head efficiency curve*	Based on the head efficiency equation from Gordon 2001 [113], this formulation depends on the relative head and not on the turbine type or flow conditions, which are integrated into the flow efficiency equation. $$\eta_{H,m}\left(\frac{H_t}{H_{des,m}}\right) = -0.5x^2 + x + 0.5$$
Max Power*	Automatically calculated using the module power output equation (Equation 3).
Cost of start-stops*	Assumed to be zero.

Table 30. Obermeyer spillway attribute determination.

Attribute	Water passage module attribute
Name	Obermeyer spillway
Capital cost	Capital costs for a 13.5ft tall Obermeyer spillway gate configuration were provided for the three reference designs. These were parameterized into 20ft long gate sections with a design flow of approximately 5,500cfs. The 13.5ft gates were assumed appropriate for any NOLs lower than 13.5ft, and the piecewise equation below shows this with a constant cost during this range. For higher NOLs, it is assumed that precast concrete would be added to raise the gate to match the NOL. A model was created to calculate the amount of concrete added based on the reference designs. With a precast concrete cost of \$975/m^3, the costs were computed for different NOLs and converted into a linear equation that scales on the normal operating level. Both parts of the piecewise equation are equal at 13.5ft, and cost scales linearly above 13.5ft. $$C_{cap,m}(Z_{nol}) = \begin{cases} 387{,}833\,; x \leq 13.5 \\ 14200x - 196133; x > 13.5 \end{cases}$$
Annual operating cost	Zero; included as part of the assumption that annual O&M costs are 6% initial cost of capital.
Width (dam-axis)	Assumed to be 20ft based on engineering drawings.
Length (streamwise)	Assumed to be 29ft based on engineering drawings.
Design flow	Calculated as 5,500cfs by parameterizing the reference spillway design flows by the spillway widths in the engineering drawings.
Operating months	Assumed to be operated during all months.
Instream or diversion	Assumed to be an instream module.
Operating mode	Controlled Spillway; The gate is pneumatically actuated to raise and lower according to a set headwater level.
Weir coefficient*	N/A; Not needed because this is a controlled spillway.
Crest height*	N/A; Not needed because this is a controlled spillway.

Table 31. Sediment sluice gate attribute determination.

Attribute	Sediment passage module attribute
Name	Sediment sluice gate
Capital cost	$288,000; Based on reference cost estimates. The same gate design is used throughout all sites.
Annual operating cost	Zero; included as part of the assumption that annual O&M costs are 6% initial cost of capital.
Width (dam-axis)	15ft; Based on the reference engineering drawings.
Length (streamwise)	30ft; Based on the reference engineering drawings.
Design flow	Varied during scenario; The baseline design is assumed to be 20% of the operating flow per the assumption in the Case Study Report [17].
Operating months	Assumed to be operated during all months.
Instream or diversion	Assumed to be an instream module.
Operating mode	Sluicing
Operating flow*	Varied during scenarios; The baseline operating flow is 6774cfs, which corresponds to the 50% probability of entrainment for a d_{50} of 24.6mm at the Deerfield site.
Flushing duration*	N/A; This module is not in flushing mode.
Operating frequency*	N/A; This module is not in flushing mode.

Table 32. Boat chute attribute determination.

Attribute	Recreation module attribute
Name	Boat chute
Capital cost	The cost of the boat chute was parameterized on a per-step basis from the reference cost tables. The fixed component accounts for the control building, gate, and miscellaneous safety equipment, while the variable cost accounts for the concrete used per step. $$C_{cap,m} = 86{,}286\ N_{steps} + 306{,}000$$
Annual operating cost	Zero; included as part of the assumption that annual O&M costs are 6% initial cost of capital.
Width (dam-axis)	21ft; Based on the reference drawings.
Length (streamwise)	The length of the boat chute is determined based on the number of steps required to descend the facility safely. Based on the reference drawings, the length of each step in the boat chute is 29.5ft. $$X_m = 29.5\ N_{steps}$$ The procedure for calculating the number of steps is adapted from the methods in the Case Study Report [17] and Caisley, Bombardelli, and Garcia [131]. In the following equation, 1.3ft is the maximum allowed drop height, 1.5ft is the initial submergence below the NOL, and 1.9ft is the minimum tailwater depth. The resulting value is rounded down to account for discrete steps values and optimized step designs that may reduce the total length. $$N_{steps} = \frac{Z_{nol} - (1.5 + 1.9)}{1.3}$$
Design flow	50.5cfs; The Case Study Report [17] designed the boat chute to operate between the Q_{95} and the Q_{50} from May to November. The design flows were determined by scaling this flow range by the ratio of the module width to the river width, resulting in an operating range of 29-72cfs. The selected design flow of 50.5cfs is the average of this range.
Operating months	May to November; Based on the Case Study Report [17].
Instream or diversion	Assumed to be an instream module.
Max headwater drop*	N/A; The reference sites used a controlled spillway.
Max headwater rise*	N/A; The reference sites used a controlled spillway.
Min tailwater level*	1.9ft; Based on the Case Study Report [17] and Caisley, Bombardelli, and Garcia [131].
Max tailwater level*	N/A; The maximum tailwater depth indicated in the Case Study Report [17] for the Deerfield design is 2.6ft, but this drastically limited availability, so it was assumed that the design was adapted to provide safe passage in high tailwaters.

Table 33. Vertical-slot fishway attribute determination

Attribute	Fish passage module attribute
Name	Vertical slot fishway
Capital cost	The cost of the fishway was parameterized on a per step (i.e., pools) basis from the reference cost tables. The number of steps calculation is described below. The fixed component accounts for the rack and slide gate, while the variable cost accounts for the concrete used per step. $C_{cap,m} = (15844\ N_{steps} + 50{,}000)$
Annual operating cost	Zero; included as part of the assumption that annual O&M costs are 6% initial cost of capital.
Width (dam-axis)	11.3ft; Based on the reference drawings.
Length (streamwise)	The length of the fishway is determined based on the number of steps required to maintain suitable hydraulic conditions for fish passage. Based on the reference drawings, the length of each pool/step is 13.63ft. $X_m = 13.63\ N_{steps}$ The procedure for calculating the number of steps is presented in the Case Study Report [17]. In the following equation, 1.5ft is the initial submergence below the NOL, and 0.055 is the slope needed to meet the hydraulic conditions. The resulting value is rounded down to account for discrete steps values and optimized pool designs that may reduce the total length. $N_{steps} = \frac{Z_{nol} - 1.5}{0.055 \times 13.63}$
Design flow	34.5cfs; The Case Study Report [17] designed the boat chute to operate between the Q_{95} and the Q_5 during the migratory months of March to June. The design flows for vertical slot fishways depend on the module slope and the design velocity. The module was designed for several species, including American Shad and Alewife. The maximum velocity through the slot of 5.25ft/s was designed for Striped Bass.
Operating months	March to June; Based on the migratory months assumed in the Case Study Report [17].
Instream or diversion	Assumed to be an instream module.
Max headwater drop*	N/A; The reference sites used a controlled spillway.
Max headwater rise*	N/A; The reference sites used a controlled spillway.
Min tailwater level*	2.1ft; Based on the tailwater during the Q_{95} for the aquatic species months used to design the module steps.
Max tailwater level*	4.9ft; Based on the tailwater during the Q_5 for the aquatic species months used to design the module steps.

Table 34. Precast foundation attribute determination.

Attribute	Foundation module attribute
Name	Precast foundation
Capital cost	The reference cost tables were parameterized on a square meter basis as a function of the depth to bedrock (Z_{fou}). The fixed cost component accounts for 0.5m of site clearing, 0.5m of leveling concrete, and 4.5m anchor rods. The variable cost component accounts for the excavation costs and the cost of concrete needed to fill the foundation from the bedrock level to the bed datum. The scaling factor (F_{scale}) helped match the foundation costs to the reference cost tables and account for the additional foundation modules needed upstream and downstream of the module footprints to provide stability and erosion protection. The scaling factors for Deerfield, Housatonic, and Schuylkill were 1.82, 1.2, and 1.4, respectively. $$C_{cap,m} = \left(247.7\, Z_{fou} + 810\right) \times F_{scale}$$
Annual operating cost	Zero; included as part of the assumption that annual O&M costs are 6% initial cost of capital.
Width (dam-axis)	Assumed to be 3.28ft.
Length (streamwise)	Assumed to be 3.28ft.
Depth (vertical)	Varied during sensitivity analysis; based on assumptions from the Case Study Report [17], the baseline foundation depth was 5ft.

Table 35. Precast non-overflow attribute determination.

Attribute	Non-overflow module attribute
Name	Precast non-overflow
Capital cost	The capital cost is based on a volumetric estimate for a 1m wide non-overflow module, as shown in the equation below. The fixed cost component accounts for handrail costs based on the reference cost tables. The variable component accounts for the shape of the module and the ratios/respective costs of precast and filling concrete. The scaling factor of 0.87 helps match the Deerfield reference costs and accounts for the reduction in concrete needed for abutment modules. $C_{cap,m} = (19.97\, X_m Y_m Z_m + 500) \times 0.87$
Annual operating cost	Zero; included as part of the assumption that annual O&M costs are 6% initial cost of capital.
Width (dam-axis)	3.28ft; Based on a 1m parameterization. ($Y_m = 3.28$)
Length (streamwise)	The length of the module is calculated using the equation below, which assumes a constant length to height ratio of 0.86 to provide additional stability as the height increases. This ratio is based on the reference drawings. $X_m = 0.86\, Z_m$
Height (vertical)	The height of the module is equal to the normal operating level plus 0.5ft of freeboard. $Z_m = Z_{nol} + 0.5$

Case Study B

Table 36. Fish-safe propeller and conventional turbine attribute determination. These modules have similar attributes, so they are included in the same table.

Attribute	Generation module attribute
Name	Fish-safe propeller (FS) and conventional turbine (Screen)
Capital cost	The capital cost was calculated by modifying an empirical cost equation from Fen, Zhang, and Smith [128] for an axial, single regulation propeller turbine, as shown below. The design head was 11ft, and the nominal capacity was 316kW. A scaling factor of 1.6 was used to account for inflation and additional modular equipment. The module cost also includes the cost for the powerhouse foundations on a per unit basis, which adds $328,000 to create a total module cost of $1,032,000. $C_{cap,m} = 1.6 \times \left(18872 H_{des,m}^{-0.546} P_m^{0.761}\right) + 328000$
Annual operating cost	Assumed equal to 5% of the capital cost or $51,600/year.
Width (dam-axis)	17ft based on engineering drawings.
Length (streamwise)	66ft based on engineering drawings.
Design flow	448cfs based on provided designs.
Operating months	Assumed to be operated during all months.
Instream or Diversion	Assumed to be an instream module.
Minimum operating flow	300cfs based on provided designs.
Maximum operating flow	448cfs; the module cannot be over-run.
Minimum operating head	5.94ft based on provided head efficiency information.
Design head	11ft based on provided designs.
Maximum operating head	12.98ft based on provided head efficiency information.
Flow efficiency curve	The flow efficiency attribute uses an empirical model, shown below, to parameterize provided flow efficiency information. Inherent to this curve are several efficiency assumptions, including a peak turbine efficiency of 88%, a generator efficiency of 95%, a drive efficiency of 96%, and electrical losses of 2%. This curve represents a conceptual turbine technology for a low-head application and does not reflect the performance of specific products on the market. $\eta_Q(Q) = -0.3325x^{0.932} + 0.1921$
Head efficiency curve*	Assumed a constant 96% based on provided head loss information. This component includes any draft tube and intake losses.
Max Power*	Automatically calculated using the module power output equation (Equation 3).
Cost of start-stops*	Assumed to be zero.

Table 37. Existing concrete weir and rock ramp attribute determination. These modules have similar attributes, so they are included in the same table.

Attribute	Water passage module attribute
Name	Existing concrete weir (Weir) and ramp rock (RR)
Capital cost	Weir: Assumed to be zero since it is an existing structure. RR: [$9,600,000] based on provided cost estimates.
Annual operating cost	Weir: Assumed to be zero. RR: [$96,000] based on a 1% capital cost assumption.
Width (dam-axis)	820ft based on engineering drawings.
Length (streamwise)	16ft based on engineering drawings.
Design flow	Assumed to be 280,000cfs to operate similarly to the rock ramp.
Operating months	Assumed to be operated during all months.
Instream or diversion	Assumed to be an instream module.
Operating mode	Uncontrolled Spillway.
Weir coefficient	Assumed to be 3.087, which is the theoretical weir coefficient for a broad-crested weir. The notch flow from the rock ramp is excluded from the headwater level calculation, so the concrete weir and rock ramp are treated as broad-crested weirs with similar weir coefficients.
Crest height	16.2ft based on engineering drawings.

Table 38. Sluice gate attribute determination.

Attribute	Sediment module attribute
Name	Sluice gate
Capital cost	$194,000 based on provided cost estimates.
Annual operating cost	$9,700 based on a 5% of capital cost assumption.
Width (dam-axis)	20ft based on engineering drawings.
Length (streamwise)	60ft based on engineering drawings.
Design flow	500cfs based on the provided information.
Operating months	Assumed to be operated during all months.
Instream or diversion	Assumed to be an instream module.
Operating mode	Sluicing
Operating flow	The operating flow was set to 6,100cfs to turn on at flows large enough to turn on the 10 generation modules, the recreation module, and the minimum flow. This value is the Q38 and is roughly equal to a 62% entrainment probability for a d50 of 1.4mm very coarse sand.

Table 39. Whitewater park attribute determination.

Attribute	Recreation module attribute
Name	Whitewater park (WW)
Capital cost	[$1,700,000] based on provided cost estimates.
Annual operating cost	[$3,200] based on provided cost estimates.
Width (dam-axis)	60ft based on engineering drawings.
Length (streamwise)	300ft based on engineering drawings.
Design flow	300cfs, which is the minimum of the provided flow range (300-600cfs) and accounts for only partial operation during the day.
Operating months	Varied during analysis. This baseline condition is year-round operation because recreationalists are expected whenever the combined average water and air temperature is above 80˚F, which occurs year-round, as illustrated in Table 17. The seasonal condition is April to October, based on the assumptions in the Case Study Report [17].
Instream or diversion	Assumed to be an instream module.
Max headwater drop*	N/A. The module was assumed to have sufficient operational flexibility to accommodate high-flow and low-flow conditions.
Max headwater rise*	N/A. The module was assumed to have sufficient operational flexibility to accommodate high-flow and low-flow conditions.
Min tailwater level*	N/A. The module was assumed to have sufficient operational flexibility to accommodate high-flow and low-flow conditions.
Max tailwater level*	N/A. The module was assumed to have sufficient operational flexibility to accommodate high-flow and low-flow conditions.

Table 40. Existing vertical-slot fishway attribute determination.

Attribute	Fish passage module attribute
Name	Existing vertical slot fishway (VS)
Capital cost	Varied during analysis. The baseline condition was zero because the structure already exists at the site. When treated as a new structure, the capital cost was $2,900,000. The reported cost by Weaver [162] was 1.5M in 1999, so an escalation factor of 1.94 was applied, and the final value was rounded.
Annual operating cost	An annual operating cost of $18,000 was determined from the ORNL environmental mitigation database [11]. The cataloged upstream fish passage measures were filtered to projects under 50ft of head, and visual outliers were removed. The 14 entries (one outlier) had an average annual O&M cost of $17,623, which was rounded to $18,000.
Width (dam-axis)	56ft based on engineering drawings.
Length (streamwise)	210ft based on engineering drawings.
Design flow	225cfs based on the minimum flow reported in Weaver [162].
Operating months	Varied during analysis. The baseline condition was year-round operation because American Eels have been shown to pass upstream and downstream throughout each month [152]. The fishway flow is considered part of the minimum flow requirement.
Instream or diversion	Assumed to be an instream module.
Max headwater drop*	N/A. The module was assumed to have sufficient operational flexibility to accommodate high-flow and low-flow conditions.
Max headwater rise*	N/A. The module was assumed to have sufficient operational flexibility to accommodate high-flow and low-flow conditions.
Min tailwater level*	N/A. The module was assumed to have sufficient operational flexibility to accommodate high-flow and low-flow conditions.
Max tailwater level*	N/A. The module was assumed to have sufficient operational flexibility to accommodate high-flow and low-flow conditions.

Table 41. 0.75in fish screen attribute determination.

Attribute	Screen attribute
Name	0.75in Fish Screen (Screen)
Capital cost	The capital cost for the screen covering one generation module is approximately $1,250,000. This was determined using a cost estimate from an engineering contractor parameterized as $2792/cfs. Each generation module had a design flow of 448cfs, so the baseline total screen cost for ten generation modules was approximately $12,500,000.
Annual operating cost	The annual operating cost for the screen covering one generation module was approximately $3127. This was determined with the ORNL environmental mitigation database [11]. The database was filtered to fish screen entries, and visual outliers were removed, which resulted in 18 entries with one outlier. The average annual operating cost for fish screens was approximately $27,500. After considering inflation and parameterizing the costs on a per-module basis, the O&M costs were assumed to be 0.25% of the screen capital costs or $3127 for the 448cfs modules. This cost accounts for screen cleaning and repair.
Head loss equation	The head loss equation was modified from the general equation provided by USBR [136] by calculating velocity from the allocated flow and the open area. The assumed head loss coefficient *k* was 0.975, the value recommended by the American Society of Civil Engineers [175] parameterized based on the through-screen velocity. The design head loss for ten generation modules at full design flow was 0.243ft. $$H_{loss,m}(Q_{covered}) = \frac{0.975}{2g}\frac{Q_{covered}^2}{A_{open}^2}$$
Incline (streamwise)	90 degrees, meaning the screen is completely vertical.
Height (vertical)	10ft based on engineering drawings.
Bottom elevation	0ft, meaning the screen is not raised and is completely submerged below headwater levels of 10ft.
Width (dam-axis)	The screen width for one module was based on the generation module width and a screen angle of approximately 40 degrees, per the equation below. The baseline screen width for a screen spanning ten modules was 224ft. $$Y_m(Y_{covered}) = \frac{Y_{covered}}{\cos(40)}$$
Fractional open area	0.5 based on engineering drawings.
Covered modules	The screen covers the conventional turbine modules.

VITA

Colin Sasthav is an interdisciplinary engineer with a passion for sustainability and renewable energy. Colin decided to pursue a career in sustainability after taking a trip to Mumbai, India, with his family. There, he witnessed the stark contrast between the smog-ridden metropolis and the lush rural jungles just south of the city. He wanted to understand why society had altered the environment so drastically and how he could instigate systemic change to make access to clean air and water a human right.

Desiring to learn more, he attended The Ohio State University to get a Bachelor of Science degree in Biological Engineering. The basic principles of nature became an integral part of how he thought about sustainability, problem-solving, and life in general. Nature relies on diverse and interdependent systems, and climate-related problems require interdisciplinary solutions. His undergraduate engineering education provided many technical skills, from hydraulics and thermodynamics to plant science and economics. Colin also received a minor in environmental economics, where he learned about the importance of quantifying environmental benefits and the tradeoffs between multiple objectives. Colin participated in several internships and consulting projects related to energy and sustainability during his undergraduate education. Most notably, Colin spent two summers on the distributed generation team at American Electric Power, learning how behind-the-meter resources can help reduce electricity bills and support grid function.

To become a leader in renewable energy, Colin joined the Energy Science and Engineering Ph.D. program within the Bredesen Center for Interdisciplinary Research and Graduate Education at the University of Tennessee. This program allowed him to take classes specializing in optimization and water resources while conducting research at Oak Ridge National Laboratory. Colin's main research project was the Standard Modular Hydropower (SMH) project, which aimed to reduce costs and improve environmental performance for low-head hydropower projects. His dissertation research created a novel hydropower design model that turned SMH from a concept to a user-friendly tool that academia and the hydropower industry can use to evaluate environmental tradeoffs. At Oak Ridge, Colin supported several other research efforts, including work on non-powered dams, cost modeling, hydropower foundations, and a hydropower test facility. Outside of work hours, Colin showed initiative by competing in and winning two case study competitions involving energy economics and hydropower innovation.

Colin is driven by a desire to improve his community and the environment. Colin plans to use his interdisciplinary background and research on environmental tradeoffs to enhance decision-making in the energy industry. Throughout his collegiate experience, Colin also saw the need to improve sustainability education across grade levels. Sustainability is inherently interdisciplinary, making it difficult to place within a specific major or curriculum. A doctoral degree would enable Colin to progress towards leadership in the field and advance sustainability education for future generations.